New Developments in Chromatographic NMR

Guillermo Lucena Alcalde

Submitted for the qualification of PhD

University of Sussex

July 2017

I hereby declare that this thesis has not been and will not be submitted in whole or in part to another University for the award of any other degree.

Signature……

University of Sussex

Guillermo Lucena Alcalde

Thesis submitted for the qualification of PhD

New developments in Chromatographic NMR

Summary

Analysis in chemistry has always been hindered by the presence of impurities in samples or mixtures that are difficult to separate. Nuclear magnetic resonance has proven to be one of the most powerful analysis techniques to enable the study of mixtures by pseudoseparation using molecular parameters such as the diffusion coefficient through the application of the DOSY technique. In order to extend the application of this technique, an improvement has been proposed know as matrix-assisted DOSY (MAD-DOSY) or chromatographic NMR. This technique is based on the addition of a sample modifier that will interact differently with the molecules, varying and separating their diffusion coefficients, or even changing slightly the chemical shifts.

To extend the application of chromatographic NMR, size exclusion stationary phases have been combined with DOSY experiments. These studies have been applied to analyze mixtures modifying the diffusion coefficient in terms of size exclusion behavior and to increase the understanding of the interactions between the analytes and the stationary phase. These studies have been published in Magnetic Resonance in Chemistry.

One of the main issues when using DOSY is spectral overlapping, which is the main cause of poor resolution. In addition to this problem, a consequence of using stationary phases is the appearance of increased broadening of the signals due to differences in magnetic susceptibility. Thus, to achieve the aim, the study of diffusion properties have been performed under HR-MAS conditions which can help to remove susceptibility effect, but has complicating effects on the DOSY experiment. A method to obtain reliable diffusion measurements under HR-MAS have been developed using a D_2O sample. Different conditions have been investigated including different pulse sequences, variation of parameters of the pulse sequence (diffusion delay or gradient strength), spinning rate and synchronization of the pulse sequence with the sample spinning. Also improvements in sample preparation as the addition of spacers in different locations of the sample rotor, to both reduce radial field variations and the sample volume, in order to obtain the most accurate diffusion values. This method have been published in Magnetic Resonance in Chemistry. The method have been applied to a wide range of molecules to extend the understanding of diffusion under HR-MAS conditions.

In order to extend the range of application of NMR chromatography, a complementary study of the analysis of a mixture of different enantiomers including ethylenediamine cobalt complexes, aminoacids and some other organic small molecules adding to the sample a chiral stationary phase as a sample modifier is included in the final chapter of this thesis.

Acknowledgements

I would like to first sincerely thank my supervisor, Dr Iain J. Day, for giving me the opportunity to work and learn from him, and for the support that he has given to me during the last three and a half years of research, as well as for infinite patience shown during and after the multitude of corrections in the preparation of this thesis.

I would also like to thank all the past members of the Day group, especially Jonathan Katz for the help provided to learn how to use new software and for the patience while explaining details about diffusion NMR pulse sequences.

Much of the work done during the experiments with cobalt complexes required long synthetic processes to obtain pure enantiomers, I would like to thank Dr Iain Crossley and his group, especially Matt Leech for helpful tips to obtain higher yields.

Thanks must also go to my secondary supervisor Dr Mark Osborne for showing his support and availability to discuss any problem that could arise during this three and a half year. As well as all the people that have shared an office with me. Especially Aidan Fisher who has shared with me the process of doing a Ph. D. and writing a thesis.

In concluding these acknowledgements I need to thank my family and closest friends, and my basketball and salsa family for all their continuous support, especially those that have lift me up when I needed it the most and helped me to keep focus during the process of writing: Borja Heredia, Irene Maluenda, Bruno Chin, Patricia Ochoa and Isabelle Cannon.

Contents

1 Introduction..... 1

1.1 Nuclear magnetic resonance..... 1

1.1.1 NMR theory..... 2

1.1.1.1 Chemical shift..... 6

1.1.1.2 Relaxation..... 7

1.1.2 Diffusion NMR..... 9

1.1.2.1 The Stokes-Einstein equation..... 9

1.1.2.2 Importance of magnetic field gradients in diffusion NMR..... 10

1.1.2.3 Measuring the diffusion coefficient by NMR..... 11

1.1.2.4 Improved diffusion pulse sequences..... 14

1.1.2.5 Diffusion ordered spectroscopy (DOSY)..... 16

1.1.3 High resolution magic angle spinning (HR-MAS)..... 17

1.2 Chromatography..... 19

1.2.1 Uses of chromatography..... 20

1.2.2 Types of chromatography..... 20

1.2.2.1 Ion exchange chromatography..... 20

1.2.2.2 Size exclusion chromatography..... 21

1.2.2.3 Chiral Chromatography..... 22

1.3 Combination of diffusion NMR, chromatography and MAS..... 22

1.3.1 Diffusion NMR and stationary phases..... 23

1.3.2 Chromatographic NMR and HR-MAS..... 23

1.4 Charged polymers diffusion in solution..... 25

1.5 Thesis Outline…… 26

2 Materials and Methods…… 28

2.1 Materials…… 28

2.1.1 Chemicals…… 28

2.1.2 Solvents…… 30

2.2 Sample preparation…… 30

2.2.1 Stationary phases and polymers…… 30

2.2.2 Synthesis of the cobalt complexes…… 31

2.2.2.1 $[(+)Co(en)_3]Cl_3$ and $[(-)Co(en)_3]Cl_3$…… 31

2.2.2.2 $[Co(diphenen)_3]Cl_3$…… 33

2.2.2.3 $[Co(meten)_3]Cl_3$…… 34

2.3 NMR…… 35

2.3.1 ^1H proton spectra…… 35

2.3.2 Diffusion NMR experiments…… 35

2.3.3 Magic angle spinning…… 36

2.3.3.1 Reduction of the active volume of glass rotor…… 36

2.4 Other physical techniques…… 37

2.4.1 Optical rotation…… 37

3 Mixtures analysis by diffusion NMR enhanced with Size Exclusion Stationary phases: SEC-DOSY…… 38

3.1 Selection of candidates: Appropriate molecules for a proof of concept…… 39

3.1.1 Selection of candidates: Parameter optimization…… 40

3.1.2 First candidates: Electrostatic problems…… 41

3.1.3 A solution for the Electrostatic problems: Neutral polymers…… 45

3.1.4 Final candidates…… 54

3.2 SEC-DOSY of polymer mixtures..... 59

3.3 Conclusions..... 63

4 Optimizing diffusion studies by HR-MAS NMR..... 65

4.1 Proteins and polymers under MAS..... 67

4.1.1 Parameters of study..... 69

4.1.2 Experiments with proteins..... 71

4.1.3 Experiments with polymers..... 74

4.2 Optimization of DOSY under MAS conditions..... 77

4.2.1 The discovery of a bug in the code of the NMR pulse sequence..... 77

4.2.2 The pulse sequence selected for HR-MAS studies..... 81

4.2.3 Improvements in sample preparation for DOSY-NMR under MAS..... 83

4.2.4 Sedimentation effects under MAS..... 87

4.3 Conclusions..... 89

5 Extending the understanding of diffusion NMR studies under magic angle spinning..... 91

5.1 Experiments with polymers..... 91

5.1.1 Experiments with neutral polymers..... 92

5.1.1.1 Diffusion properties without stationary phase under MAS..... 92

5.1.1.2 Experiments with stationary phases..... 96

5.1.2 Experiments with Poly (Styrene Sulfonate)..... 97

5.1.2.1 The Lorentz force hypothesis..... 99

5.1.3 Understanding of diffusion under the Lorentz force hypothesis..... 100

5.1.3.1 Effect of size and viscosity..... 101

5.1.3.2 Effect of the spin rate..... 103

5.1.3.3 Effect of the charge..... 104

5.1.4 Study of the Lorentz force with a set of PSS polymers..... 108

5.1.4.1 Charged ion concentration in solution…… 110

5.1.4.2 Effect of the spin rate at different concentrations…… 113

5.1.4.3 Variation of the diffusion delay…… 115

5.2 Experiments with small molecules…… 116

5.2.1 Experiments in static conditions…… 117

5.2.2 Experiments under MAS conditions…… 118

5.2.3 Separation in the diffusion domain without stationary phases…… 124

5.3 Conclusions and future work…… 125

6 Size exclusion chromatographic NMR applied to the separation of enantiomers…… 126

6.1 Cobalt complexes…… 127

6.1.1 Tris(ethylenediamine)Cobalt (III) chloride: $[Co(en)_3]Cl_3$…… 128

6.1.2 Tris(1,2-Diphenylethylenediamine)Cobalt (III) chloride: $[Co(diphenen)_3]Cl_3$ 131

6.1.3 Tris(1,2-diaminopropane)Cobalt (III) chloride: $[Co(meten)_3]Cl_3$…… 132

6.2 Chiral Chromatography combined with NMR…… 133

6.2.1 DOSY-NMR studies with Sephadex G50…… 134

6.2.2 DOSY-NMR studies with Sephadex G10…… 137

7 Final thoughts…… 140

7.1 Experiments into a 5 mm tube in static conditions…… 140

7.1.1 Size exclusion chromatography phenomena…… 141

7.1.2 Chiral chromatography phenomena…… 141

7.2 Experiments under magic angles spinning…… 142

7.2.1 Optimization of diffusion measurements under MAS…… 143

7.2.2 Understanding diffusion under MAS…… 143

Bibliography…… 145

Appendix A Calculations…… 159

Appendix B Publications…… 161

B.1 Size-exclusion chromatographic NMR of polymer mixtures…….. 162

B.2 Size-exclusion chromatographic NMR under HR-MAS……..166

List of Figures

1.1 Net magnetization (M_0) of a nuclei in the presence of a magnetic field (B_0)

1.2 Net magnetization (M_0) after the application of a 90° RF pulse in presence of a magnetic field (B_0)

1.3 Pathway followed by two different size molecules passing through a size exclusion resin.

1.4 Schematic illustration of the dependence of T_1 and T_2 on the rotational correlation time τ_c.

1.5 Nuclear spins after the application of a 90° pulse and a magnetic field gradient applied. The arrows represent the magnetic moments of the nucleus in that layer of the sample along the z axis.

1.6 Spin echo and stimulated echo pulse sequences.

1.7 Vector representation of magnetization during a spin echo sequence. a) and b) show the magnetization flipped by a 90° pulse, c) and d) show the spins dephasing during the time period τ due to the different precessing frequencies, e) shows the application of a 180° pulse, finally f) and g) show the refocusing of the spins during the period of time τ.

1.8 Gradient compensated stimulated spin echo (GCSTE) and bipolar pulse pair stimulated spin echo (BPPSTE) pulse sequences. The diffusion delay (Δ) is the time between the midpoints of the two diffusion encoding period.

1.9 The Oneshot pulse sequence, the diffusion delay (Δ) is the time between the midpoints of the two diffusion encoding period and τ that between the midpoints of the antiphase field gradient pulses within a given diffusion encoding period.

1.10 0.1mM mixture of 10 kDa PVP and 50 kDa PEO in D_2O. The straight lines show the diffusion coefficient of the signals of interest. Red for PEO and blue for PVP.

1.11 Magic angle spinning experimental set, where B_o is the applied magnetic field, θ_R is the magic angle 54.74°, θ is the angle between B_o and the principal z axis and β is the angle between principal z axis of the tensor and the spinning axis.

2.1 Enantiomers Δ (left) and Λ (right) of the complex tris(ethylenediamine)cobalt (III).

2.2 Structures of $[Co(Meso\text{-}1,2\text{-}diphenen)_3]^{3+}$.

2.3 Structure of $[Co(meten)_3]^{3+}$.

2.4 Oneshot sequence, arrows indicate the incrementation of gradients.

3.1 Poly (allylamine) (Paa) and Poly (Styrene Sulfonate) (PSS) repeating units.

3.2 ^{1}H-NMR spectrum 0.1 % w/w of 70 kDa Poly (Styrene Sulfonate) and 15 kDa Poly (allylamine) in D_2O with 25 mM NaCl buffer.

3.3 Diffusion coefficients of separated 0.1 % w/w 15 kDa Poly (allylamine) (1.95 ppm) and 70 kDa Poly (Styrene Sulfonate) (7.48 ppm) polymers in presence of different concentrations of NaCl buffer in D_2O.

3.4 DOSY-NMR spectrum of 0.1 % w/w of 15 kDa Paa in 25 mM NaCl buffer in D_2O, the protons next to the N appear at 3ppm, the proton from the ramification of each monomer appear at 1.98ppm and the aliphatic protons from the main chain appear at 1.5 ppm.

3.5 Poly (2-Ethyl-2-Oxazoline) (PEO) and Poly (Vinyl Pirrolidone) (PVP) repeating units.

3.6 Superimposed ^{1}H-NMR spectrum of 0.5 mM 10 kDa PVP (red) and 0.5 mM 50 kDa PEO (blue) in D_2O.

3.7 Diffusion coefficients of 10 kDa Poly (Vinyl Pirrolidone) (PVP) and 50 kDa Poly (2-Ethyl-2-Oxazoline) (PEO) when they are not in a mixture and varying their concentrations in D_2O.

3.8 Diffusion coefficients without Sephadex G50 of a mixture of 10 kDa PVP (1.95 ppm) and 50 kDa PEO (1.06 ppm) varying their concentrations in D_2O.

3.9 0.1 mM mixture of 10 kDa PVP and 50 kDa PEO in D_2O. The straight lines show the diffusion coefficient of the signals of interest. Red for PEO and blue for PVP.

3.10 Diffusion coefficients of a mixture of 10 kDa PVP (1.95 ppm) and 50 kDa PEO (1.06 ppm) varying their concentrations in D_2O in presence of Sephadex G50. Two data points not shown due to low concentration that impeded correct recording of the diffusion coefficient.

3.11 0.3 mM mixture of 10 kDa PVP and 50 kDa PEO in D_2O in presence of Sephadex G50.

3.12 ^{1}H-NMR spectra of a mixture 0.3 mM each polymer 50 kDa PEO + 10 kDa PVP with Sephadex G50, Superdex 75 and Superdex 200.

3.13 Poly (Methacrylic Acid) (PMA) and Poly (Styrene Sulfonate) (PSS) repeating units.

3.14 Diffusion coefficients of 33 kDa PMA (0.98 and 0.88 ppm) varying their concentrations in 150 mM NaCl + 50 mM Na_3PO_4 buffer.

3.15 Diffusion coefficients for some PMA molecular weight reference standards in the presence and absence of Sephadex G50 (top) and Superdex 75 (bottom).

3.16 Diffusion coefficients for paired mixtures of PMA and PSS in the presence and absence of Sephadex G-50. The straight lines are the result of fitting Equation (3.2) to the experimental data.

3.17 ^{1}H NMR spectra of a mixture of 20.3 kDa PMA and 63.9 kDa PSS in the absence and presence of the Sephadex G-50 stationary phase. DOSY spectrum of the same mixture in the absence of the Sephadex G-50 stationary phase.

3.18 Diffusion coefficients for mismatched mixture 20 kDa PMA + 63 kDa PSS in the presence and absence of Sephadex G-50.

4.1 ^{1}H-NMR spectra of 60 kDa PMA and 63.9 kDa PSS with sephadex G-50 without HR-MAS conditions and same sample under HR-MAS with a spin rate of 2 kHz * mark the spinning sidebands from HOD and ** mark the spinning sidebands of the stationary phase.

4.2 Difference in the chemical shift of spinning sidebands in a 63.9 kDa PSS sample spun at 1.8 KHz and 2.2 KHz. * mark the spinning sidebands from HOD.

4.3: DOSY-NMR spectra of 14.1 kDa Bovine α-lactalbumin and 63,9 kDa PSS in D_2O at spin rate 2 kHz.

4.4: Variation of the temperature inside the NMR rotor of a sample of ethylene glycol at increasing spinning rates.

4.5 Diffusion of proteins in buffer at 2 kHz spin rate with and without Sephadex G50.

4.6 Diffusion of set of PSS polymers in buffer at spin rate 2 kHz with and without Sephadex G50.

4.7 Diffusion of set of PSS polymers in buffer at spin rate 1.8 kHz (left) and 2.2 kHz (right) with and without Sephadex G50.

4.8 Observed variation in the measure diffusion coefficient of HOD with spin rate using the Agilent-supplied pulse sequences. a) and b) are for the GCSTE, c) and d) for the BPPSTE and e) and f) for the Oneshot sequence. a), c) and e) are the pulse sequences as supplied in the Agilent library while b), d) and f) use complete rotor synchronization of the RF-pulses, gradient duration and delays before the correction of the bug in the analysis software.

4.9 Observed variation in the measure diffusion coefficient of HOD with spin rate using the Agilent-supplied pulse sequences. a) and b) are for the GCSTE, c) and d) for the BPPSTE and e) and f) for the Oneshot sequence. a), c) and e) are the pulse sequences as supplied in the Agilent library while b), d) and f) use complete rotor synchronization of the RF-pulses, gradient duration and delays.

4.10: Schematic representation of the MAS rotor without sample volume restriction (left), with axial volume restriction restriction (middle) and radial volume restriction (right)

4.11 Observed variation in the measured diffusion coefficient of HOD with spin rate recorded using the Oneshot sequence and a diffusion encoding time Δ of 100 ms. (a) Shows the sample confined to a diameter of 1.5 mm by the inclusion of a Teflon spacer, (b) shows the sample

restricted to a height of 2.6 mm using a pair of 1 mm Teflon discs above and below the sample and (c) is the combination of both sample restriction methods.

4.12 Concentration profiles for various poly (styrene sulfonate) samples in a 4 mm (outer diameter) high-resolution MAS rotor spinning at a speed (ν_r) of 2 kHz. The grey horizontal line indicates the static concentration. The curves were calculated using the method of Bertini *et al*. from sedimentation equilibria. Image taken from Day and co-workers publication.

5.1 Diffusion coefficients of a set of concentrations of 10 kDa PVP and the residual signal of HOD in D_2O at different spinning rates using the fully rotor synchronised Oneshot sequence varying the gradient length.

5.2 Diffusion coefficients of a set of concentrations of 50 kDa PEO and the residual signal of HOD in D_2O at different spinning rates using the fully rotor synchronised Oneshot sequence varying the gradient length.

5.3 Diffusion coefficients of the polymers 10 kDa PVP and 50 kDa PEO and the residual HOD signal in separated samples made of 0.8 mM polymer concentration in D_2O with and without Sephadex G50 at 2.5 kHz spinning rate varying the gradient length.

5.4 Diffusion coefficients of a set of concentrations of 70 kDa PSS and the residual signal of HOD in D_2O with a phosphate buffer at 2.5 kHz spinning rate using the fully rotor synchronised Oneshot sequence varying the gradient length.

5.5 Diffusion coefficients of the polymers shown in table 5.4 and their corresponding HOD residual signal in a static sample in D_2O and phosphate buffer for the charged polymers.

5.6 Diffusion coefficients of the polymers shown in table 5.4 and their corresponding HOD residual signal at 0.7 kHz in D_2O and phosphate buffer for the charged polymers.

5.7 Diffusion coefficients of 10 kDa PVP and 50 kDa PEO and their corresponding HOD residual signal in D_2O at three different spin rates varying the gradient length.

5.8 Diffusion coefficient of the polymers in table 5.3 and their corresponding residual HOD at different spin rates in D_2O for neutral polymers and phosphate buffer for the charged ones. The dips in the diffusion coefficients shown in the figure at 10 and 50 kDa correspond to the neutral polymers PVP and PEO which is in agreement with both the Lorentz force and the effect of charged particles in diffusion.

5.9 Diffusion coefficient of 50 kDa PEO and the residual HOD with and without buffer at different spinning rates.

5.10 Diffusion coefficient of a set of PSS polymers with different molecular weights and their corresponding residual HOD signal at different concentrations (presented in table 5.4) that ensure the same amount of monomer in solution in presence of 150 mM NaCl and 50 mM Na_3PO_4 buffer in D_2O at two different spin rates.

5.11 Diffusion coefficient of 65 kDa PSS, 20 kDa PSS and their corresponding residual signal of HOD at different concentrations and spin rates with and without phosphate buffer (150 mM NaCl + 50 mM Na_3PO_4) in D_2O.

5.12 Diffusion coefficient of 65 kDa PSS at different concentrations varying the spinning rate in D_2O. HOD residual signal it is not presented as it showed the same pattern.

5.13 Diffusion coefficient of 65 kDa PSS at 0.8 mM concentration varying the spinning rate with and without buffer in D_2O. HOD residual signal it is not presented as it showed the same pattern.

5.14 Diffusion coefficients of 20 kDa and 65 kDa PSS at different spin rates varying the diffusion delay in D_2O.

5.15 Diffusion coefficients of the molecules summarised in table 5.5 and their corresponding HOD residual signal with and without buffer in D_2O in static conditions.

5.16 Diffusion coefficients of the molecules presented on table 5.5 that show the expected diffusion behaviour at different spin rates with and without buffer.

5.17 Diffusion coefficients of tartaric acid, Me_4NCl, p-styrene sulfonate and their corresponding HOD residual signal varying the spinning rate with and without buffer.

5.18 Diffusion coefficients of lidocaine and $[Co(en)_3]Cl_3$ their corresponding HOD residual signal varying the spinning rate with and without buffer.

5.19 Static diffusion coefficients of the molecules presented in figure 5.16 compared to the average diffusion coefficient at different spinning rates with and without buffer.

6.1 Enantiomers Δ and Λ of the complex tris(ethylenediamine)cobalt (III).

6.2 Stacked spectrum of 10mM $[Co(en)_3]Cl3*2H_2O$ for comparison between purchased (top) and 10mM synthetized (bottom).

6.3 Structures of $[Co(Meso\text{-}1,2\text{-}diphenen)_3]^{3+}$ and $[Co((1R,2R)\text{-}(+)\text{-}diphenen)_3]^{3+}$.

6.4 Spectrum of the 32 possible isomers of the complex $[Co(meten)_3]Cl_3$ and structure of the expected racemic mixture of the complex.

6.5 Diffusion coefficient of racemic mixture and enantiomers at 50mM in absence of stationary phase. 1-ph1-propanol and menthol are dissolved in D_2O:MeOD, tyrosine is dissolved in D_2O:HCl and $[Co(en)_3]Cl_3$ in D_2O.

6.6 DOSY-NMR spectrum of 50 mM Menthol in a mix 2:1 of D_20:MeOD.

6.7 Diffusion coefficient of racemic mixture and enantiomers in presence of Sephadex G50 at 50mM. 1-ph1-propanol and menthol are dissolved in D_2O:MeOD, tyrosine is dissolved in D_2O:HCl and $[Co(en)_3]Cl_3$ in D_2O.

6.8 DOSY-NMR spectrum of 50 mM $[Co(en)_3]Cl3*2H_2O$ in presence of Sephadex G-50 in D_2O.

6.9 Diffusion coefficient of racemic mixture and enantiomers in presence of Sephadex G10 at 50mM. 1-ph1-propanol and menthol are dissolved in D_2O:MeOD, tyrosine is dissolved in D_2O:HCl and $[Co(en)_3]Cl_3$ in D_2O.

6.10 DOSY-NMR spectra of 50 mM tyrosine in presence of Sephadex G-50 and 50 mM tyrosine in presence of Sephadex G-10 both in D_2O with 3 drops of DCl.

List of Tables

2.1 Properties of stationary phases.

2.2 Summary of proteins used with their corresponding molecular weight.

2.3 Summary of the small molecules used with their corresponding molecular weights.

3.1 Parameters returned from fitting equation (3.2) to the data in Figure 3.8 the data for PSS are from Joyce and Day.

3.2 Parameters returned from fitting equation (3.2) to the data in Figure 3.9.

4.1 Summary of diffusion coefficients of samples of 2 mM proteins varying of molecular weights in buffer with and without urea 8 M at 2 kHz spinning rate.

4.2 Summary of proteins used for HR-MAS NMR chromatography.

5.1 Comparison of the diffusion coefficients of the 10 kDa PVP polymer and 50 kDa PEO and their corresponding HOD residual signals at different spinning rates of a sample 0.8 mM polymer concentration in D_2O.

5.2 Comparison of the diffusion coefficients of different polymers and their corresponding HOD residual signals at different spinning rates in a sample 0.8 mM polymer concentration in D_2O and buffer for the charged polymer.

5.3 Summary of polymers and concentrations used to perform DOSY NMR studies under MAS conditions.

5.4 Summary of the molecular weight, polydispersity and concentrations of the set of PSS polymers used to perform DOSY NMR studies under MAS conditions.

5.5 Summary of the diffusion coefficient of PSS polymers in the presence and the absence of a buffer at different spin rates

5.6: Summary of the small molecules, molecular weights, concentrations and charges used to record their diffusion coefficient in static conditions with and without phosphate buffer in D_2O

6.1 Summary of $[Co(en)_3]Cl3*2H_2O$ diffusion data – D_2O.

6.2 Different isomers from the complex $[Co(meten)_3]Cl_3$. First row refers to the position of the methyl group on the ligand, second row refers to the two possible enantiomers of the octahedral complexes and third and fourth rows refers to the chiral center configuration.

6.3: Summary of compounds with their corresponding molecular weights used to perform chiral DOSY NMR.

Abbreviations

BPPSTE: Bipolar pulse pair stimulated spin echo

BSA: Bovine serum albumin

DLS: Dynamic light scattering

DOSY: Diffusion Ordered SpectroscopY

FID: Free induction decay

GCSTE: Gradient compensated stimulated spin echo

HR-MAS: High Resolution Magic Angle Spinning

LED: Longitudinal eddy current delay

LSR: Lanthanide shift reagents

MAD: Matrix Assisted DOSY

NMR: Nuclear Magnetic Resonance

NUS: Non Uniform Sampling

OR: Optical rotation

PAA: Poly (acrylic acid sodium salt)

Paa: Poly (allylamine)

PEG: Poly Ethylene Glycol

PEO: Poly (2-Ethyl-2-Oxazoline)

PMA: Poly (Methacrylic Acid)

PSS: Poly (Styrene Sulfonate)

PVP: Poly (Vinyl Pirrolidone)

RF: Radiofrequency

SDS: Sodium Dodecyl Sulfate

SE: Spin echo

SEC: Size Exclusion Chromatography

STE: Stimulated spin echo

Chapter 1
Introduction

The study of molecular diffusion by different techniques has had great interest over the last decades as it can offer information on a wide range of physical properties including molecular size [1], shape [2], complexation, aggregation [3, 4], encapsulation, and hydrogen bonding. The study of diffusion has been made by different methods such as radioactive tracer studies [5], dynamic light scattering (DLS) [6] or fluorescence correlation spectroscopy [7]. However, the work presented in this thesis will be focused on an alternative that does not require specialised handling of radioactive isotopes, is non-invasive, does not require prior separation and that allows to make fast measurements over a range of temperatures. It was suggested in the 1960s and has been improved since then, it is diffusion NMR. The experiments in this thesis were made to enhance the diffusion NMR method with the use of size exclusion stationary phases to perform chromatographic NMR and high resolution magic angle spinning (HR-MAS).

In this chapter a brief description of the basic NMR theory and a full discussion on the main methods to record diffusion coefficients using a NMR spectrometer and which are the main advantages of using magic angle spinning (MAS) in NMR will be presented. This will be followed by a brief introduction about the method of chromatography focusing on size exclusion and highlighting the importance of diffusion in this method. The chapter will be concluded with a discussion about the combination of both chromatography and diffusion NMR, and how MAS can enhance this combination.

1.1 Nuclear magnetic resonance

Nuclear magnetic resonance (NMR) is a non-invasive technique that enables one to obtain very diverse molecular information, such as atomic connectivity, diffusion coefficients, spatial geometry, molecular aggregation and much more. In this section, the basic principles of NMR are introduced, followed by a deeper insight in the basic principles of diffusion NMR and an

explanation of the most common diffusion pulse sequences. Finally there will be a brief explanation of the high resolution magic angle spinning technique (HR-MAS).

1.1.1 NMR theory

There is a wide range of spectroscopic techniques that are used by chemists to analyse their samples and obtain useful information [8, 9]. Most of these techniques allow to obtain information through the study of the transitions between different energy levels by electrons that are excited with electromagnetic radiation. However, nuclear magnetic resonance spectroscopy obtains the information through the study of the transitions between different energy levels of the nuclear spin instead of the electrons.

Nuclei possess an intrinsic angular momentum (I) that it is called spin, the value of the spin is greater or equal to zero and a multiple of ½. Those nuclei that possess spin $I = 0$ are consider non-magnetic and cannot be observed by NMR. The spin angular momentum is a vector *I* whose direction and magnitude are quantized. The magnitude of the vector is described in equation 1.1 [10], and the allowed projections of the vector into an arbitrarily chosen axis are given by $I = m\hbar$ where *m*, is the magnetic quantum number and has $2I + 1$ values between $+I$ and $-I$ (i.e. m = $-I$, $-I + 1$,….$I - 1$, $+I$). These projections are degenerate in the absence of a magnetic field. The nucleus that it is measured in the work presented in this thesis is ^{1}H which possesses a spin $I = ½$. Therefore, it has two possible energy levels. Nucleus that possess a spin higher than ½ are called quadrupolar nuclei and due to the larger amount of energy levels their study by NMR is more complicated. However, as all the nucleis measured in this thesis have a spin $I = ½$, quadrupolar nuclei will not be discussed any further in this thesis.

$$I = \sqrt{I(I+1)} \times \hbar \tag{1.1}$$

Where ħ is the reduced plank constant. Another property of the nucleus is the nuclear magnetic moment $\boldsymbol{\mu}$ (another vector quantity) which is related to the spin as it is shown in equation 1.2 [10].

$$\boldsymbol{\mu} = \gamma \boldsymbol{I} \tag{1.2}$$

Where Υ is the gyromagnetic ratio of the nucleus. Therefore the larger the gyromagnetic ratio the larger is the magnitude of the magnetic moment. The magnetogyric ratio of the ^{1}H is 26.752 × 10^7 $T^{-1}s^{-1}$ and the natural abundance is 99.98% [10]. The energy degeneracy of the energy levels described by $2I + 1$ is lifted if a strong magnetic field is applied. The energy of the magnetic moment in a magnetic field can be described as a scalar product of the two vectors as it is shown in equation 1.3.

$$E = -\boldsymbol{\mu} \cdot \boldsymbol{B_0} \tag{1.3}$$

Where E is the energy of the level and $\boldsymbol{B_0}$ is the magnetic field applied. If equation 1.2 is combined with the allowed projections of I in the z axis (along the magnetic field), then the energy can be described as it is shown in equation 1.4.

$$\Delta E = -m\hbar\gamma B_0 \tag{1.4}$$

The $2I + 1$ energy levels formed are all equally spaced with an energy gap $\hbar\Upsilon B_0$. In the case of the nucleus ^{1}H, there are only two energy levels as it has spin value ½, which are +½ and -½ and are sometimes referred as α and β states respectively (see figure 1.1). At thermal equilibrium the population of these two states is described by the Boltzmann distribution shown in equation 1.5 [11].

$$\frac{n_\beta}{n_\alpha} = e^{\left(-\frac{\Delta E}{k_B T}\right)} \tag{1.5}$$

Where n_α and n_β are the populations of the α and β states, ΔE is the energy gap between the two states (calculated by equation 1.4), k_B is Boltzmann constant (1.381×10^{-23} JK^{-1}) and T is the absolute temperature in $_{Kelvin}$. As it can be seen on the equation 1.5 the difference in populations depends on the strength of the magnetic field applied and the temperature. At thermal equilibrium there is a slight preference for the α state where the magnetic moments are aligned with the magnetic field. This preference creates a net magnetization along the z axis (same direction as the magnetic field, see figure 1.1), whereas there is no net magnetization in the plane (x, y) as all the magnetic moments are randomly distributed along these directions and average the magnetic moment to zero [12].

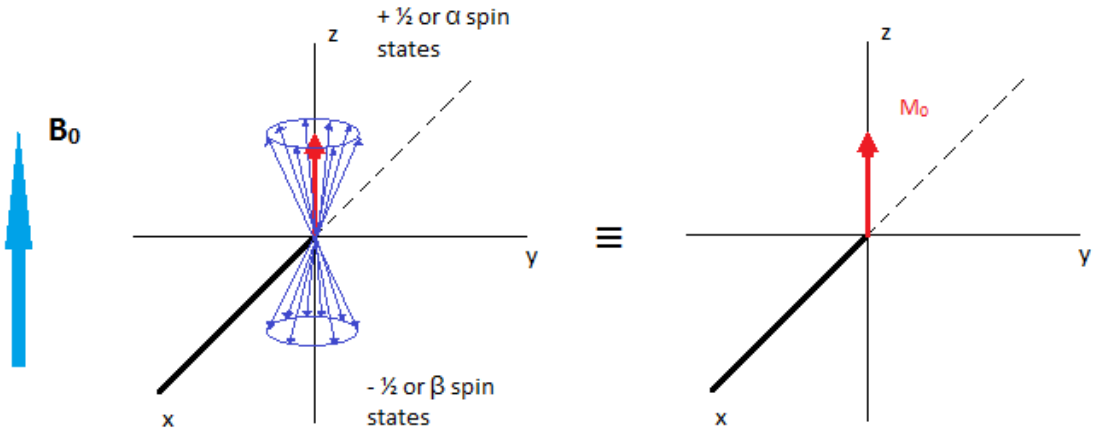

Figure 1.1: Net magnetization (M_0) of a nuclei in the presence of a magnetic field (B_0)

The selection rule for NMR spectroscopy is Δm = ± 1 so that the allowed transitions occur between adjacent levels. Therefore the resonance frequency is [10]:

$$\Delta E = h\nu \;\rightarrow\; \nu_{NMR} = \frac{\gamma B_0}{2\pi} \tag{1.6}$$

In order to achieve the transition between two different levels (from state α to β), it is needed to irradiate the sample with energy that meets the resonance frequency. In the case of ^{1}H in a 14.1 T magnetic field (as it is the used in this work) the frequency needed is 600 MHz, which is within the radio frequency range of the electromagnetic spectrum. This means that NMR lies at the low frequency region compared to most of the spectroscopic techniques that require higher energies to achieve transition between energy levels. Therefore, the difference of population between the two levels is very small compared to other techniques, as it is proportional to the difference in energy between the energy levels, ΔE (see equation 1.5). This is one of the biggest drawbacks of the technique. The sensitivity of the technique depends on the difference in the populations, as the number of transitions between the two energy states determine the intensity of the signals that appear in the spectrum. Hence, the small difference between the two energy levels makes NMR not very sensitive due to a very small difference in the populations of both levels. Therefore, larger magnetic fields also involve larger differences between the energy levels, thus higher sensitivity. For these reasons ^{1}H is one of the most observed nucleus by NMR, as if two different nucleus are in presence of the same magnetic field, the one with largest gyromagnetic ratio will have a larger ΔE (see equation 1.4). Then since ^{1}H has a very large gyromagnetic ratio and a high natural abundance the gap between the energy levels is larger than the gap of other nucleus.

The individual magnetic moments of the spins in the presence of a magnetic field are spinning around the z axis (direction of the magnetic field). This motion is called the Larmor precession and when the rate of this precession matches the resonance frequency it is called the Larmor frequency and can be described in either Hz or rad s^{-1} the conversion is shown in equation 1.7 [12]. Therefore, it depends for every nucleus, as they have different resonance frequencies. The direction of the motion depends on the sign of the gyromagnetic ratio and can be clockwise or anticlockwise.

$$\omega_0 = -\gamma B_0 \text{ in rad s}^{-1} \quad \text{or} \quad \nu_0 = \frac{-\gamma B_0}{2\pi} \text{ in Hz} \tag{1.7}$$

The NMR phenomena occurs when the nucleus changes the spin state due to the absorption of a quantum of energy [12]. As it has been mentioned above, in NMR the energy necessary for this to happen is achieved through the application of radio-frequency pulses perpendicular to the main static magnetic field. This creates an oscillating magnetic field in resonance with the Larmor precession, which causes the net magnetization to move away from the z axis [11] (see

figure 1.2). The total angle that the magnetization is moved away depends on the length of the pulse applied, see equation 1.8 [12].

$$\theta = \omega t_p = \gamma B_1 t_p \quad (1.8)$$

Where θ is the tip angle, ω is the frequency of the radio-frequency (RF) pulse applied, t_p is the duration of the pulse in seconds and B_1 is the magnetic field of the RF pulse.

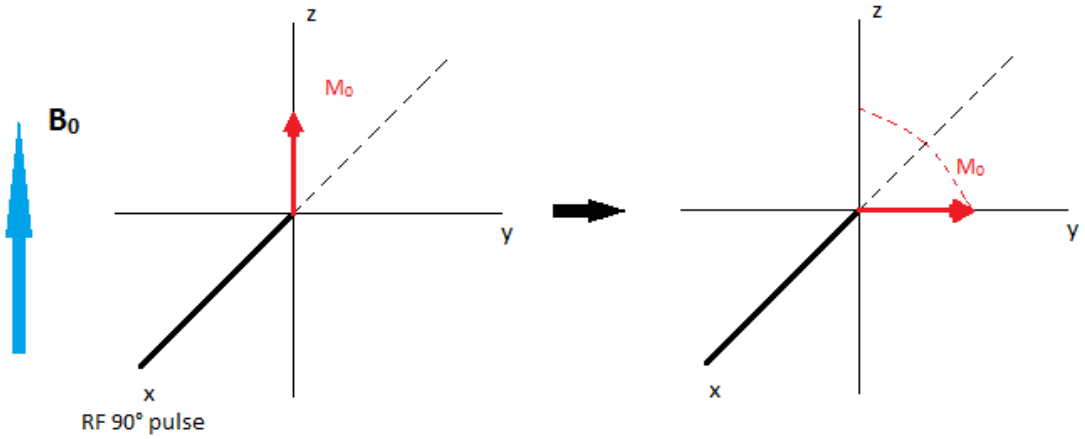

Figure 1.2: Net magnetization (M_0) after the application of a 90° RF pulse in presence of a magnetic field (B_0)

To help to understand the effect of the RF pulse, it is convenient to consider a reference frame that rotates around the z at the transmitter frequency of the spectrometer (ω_1). This way the RF field appears static and the apparent frequency of precession is the difference between the Larmor frequency and the transmitter frequency, known as the offset (Ω) which is shown in equation 1.9 [11].

$$\Omega = \omega_0 - \omega_1 \quad (1.9)$$

After a RF pulse is applied along the x axis the net magnetization will rotate from the z axis to the – y axis. Then the magnetization will rotate about the z axis with an observed frequency Ω in the rotating frame. The precession of the net magnetization about the z axis produce a current on the RF coil detecting in the x-y plane. Every time that the magnetization induces a voltage in the RF coil a current is induced known as the free induction signal which is detected in an NMR experiment. All the signals detected until the net magnetization is restored in the z axis form the free induction decay (FID) that has the form of equation 1.10 [11].

$$S(t) = S_0 e^{i\Omega t} \times e^{-R_2 t} \quad (1.10)$$

Where R_2 is the transverse relaxation rate that determines the rate at which the transverse magnetization decays back to zero. The FID is a function of time. However, it is possible to convert the signal to a function of frequency through a Fourier transformation. The Fourier

transformation is a mathematical operation that produces a spectrum with a peak of intensity S_0 at a frequency Ω and a width depending on the relaxation rate R_2, the line profile is a lorentzian. The Fourier transformed version of equation 1.10 is described in equation 1.11.

$$S(\omega) = S_0 \left(\frac{R_2}{R_2^2 + (\omega - \Omega)^2} - \frac{i(\omega - \Omega)}{R_2^2 + (\omega - \Omega)^2} \right) \quad (1.11)$$

In which, typically the displayed spectrum is the real part. In the case of several resonances the time domain signal is the sum of each of the resonances and the Fourier transform yields the frequency domain spectrum [11].

1.1.1.1 Chemical shift

It has been presented in the previous section that the resonance frequency of a particular nucleus depends on the gyromagnetic ratio of the nucleus Υ and the external field applied B. However, it does not depend only on those two factors, it also depends on the local electronic distribution in the molecules [10]. This is one of the reasons that makes NMR such an attractive technique for the chemist, as it is possible to differentiate between two identical nuclei located in different parts of a molecule or just with a different electron distribution around. This effect is known as the chemical shift, and it arises because the actual magnetic field experienced by a particular nucleus differ slightly from the external field B_0, which is the magnetic field that would be experienced by a nucleus without electrons. However, B_0 produces motion on the electrons around the nucleus, this motion creates a small magnetic field B'. Therefore, the nucleus is said to be shielded, and the actual magnetic field experienced B is the one described by equation 1.12 [10]. B_0 and B' are related as B' depends on the strength of B_0.

$$B = B_0 - B' = B_0 \times (1 - \sigma) \quad (1.12)$$

Where σ is the constant of proportionality between B' and B_0, and it is known as the shielding constant ($\sigma = B'/B_0$). Therefore, the Larmor frequency for a particular nucleus can be described by the equation 1.13 [10].

$$\nu = \frac{\gamma \times B_0}{2\pi} \times (1 - \sigma) \quad (1.13)$$

The shielding constant σ is not a very convenient way of expressing the chemical shift as it depends on the external magnetic field. Instead, the chemical shift is commonly expressed as the difference between the Larmor frequency of nucleus of interest ν_0 and that of a reference nucleus ν_{ref} (typically tetramethylsilane (TMS) is used as reference compound) using a dimensionless parameter δ expressed in ppm. This parameter is described by equation 1.14 [10].

$$\delta = 10^6 \frac{\nu_0 - \nu_{ref}}{\nu_{ref}} \quad (1.14)$$

The chemical shift δ is independent of the magnetic field strength applied and the nucleus that have more electrons around are more shielded, this means that they appear at lower chemical shift (i.e aliphatic functional groups for ^{1}H nuclei), while if the nucleus is less shielded it will appear at larger chemical shifts (i.e aromatic protons for ^{1}H nuclei).

1.1.1.2 Relaxation

After the application of a RF pulse to an NMR sample the magnetic moment is shifted from the +z axis and the following process that returns the bulk magnetization to the thermal equilibrium conditions is known as relaxation. This process is of vital importance in NMR as it will not only influence the sensitivity of the measurement but will also determine the amount of time that can be used to manipulate the spins after their initial excitation [12]. The relaxation process in NMR is considerably longer than other spectroscopic techniques, as an example the lifetime of an excited electronic state is less than nanoseconds while an excited nuclear state can take from seconds to minutes to achieve a complete relaxation. This is caused because the energy gap between an electronic excited state and the non-excited is much larger than in the case of nuclear states. Therefore, the transitions takes place faster to recover the minimum energy state. The relaxation process can be separated into two components, spin-lattice and spin-spin relaxation.

The spin-lattice relaxation is also called longitudinal relaxation and it corresponds to the recovery of the Boltzmann distribution of spin populations between the two energy states (for a spin ½) at thermal equilibrium in presence of a magnetic field. The spin-lattice relaxation is characterized by the relaxation time T_1. In terms of the vector model used to describe so far the bulk magnetization, it is the time it takes to place the bulk magnetization along the z axis back into the +z axis. The relaxation mechanism that affects the most to the spin-lattice relaxation, occurs through an exchange of energy, which generates small amounts of heat, from the nuclear spin system to the surroundings. This exchange is facilitated by the dipolar couplings, this meaning the interaction of the spin with small local magnetic fields that are oscillating at the Larmor frequency. Usually these local magnetic fields are generated by spins in the surrounding areas, that through molecular agitation (more frequently intramolecular spin-spin dipolar interactions and rotational diffusion) can oscillate at frequencies close to the Larmor frequency [13]. The rate constant of longitudinal relaxation (T_1^{-1}), depends on the probability that the local fields are oscillating at the Larmor frequency (ω_0). Therefore, it is proportional to the spectral

density $J(\omega_0)$. It is also proportional to the mean square value of the local fluctuating fields $\langle B^2 \rangle$ and to the gyromagnetic ratio γ. The predicted relaxation rate is described in equation 1.15 [10].

$$\frac{1}{T_1} = \gamma^2 \ \langle B^2 \rangle J(\omega_0) \tag{1.15}$$

The spin-spin relaxation is also called the transverse relaxation and it corresponds to the process where all the spins that are precessing around the z axis with phase coherence after the application of a 90° pulse, start fanning out due to small changes in the precession frequency. This is caused by the experience of different small local fields. In terms of the vector model this means that spin-spin relaxation is the time that the bulk magnetization that is transferred from the +z axis to the x-y plane after a 90° pulse takes to disappear from the transverse plane. The transverse relaxation is characterized by another time constant T_2. The transverse relaxation process occurs due to two different reasons, the first one is from inhomogeneity in the main field (which is the main cause for spin ½), and the second arises from intramolecular and intermolecular interactions in the sample. The relaxation time constant from the two sources combined is designated T_2^* and is described in the equation 1.16 [12].

$$\frac{1}{T_2^*} = \frac{1}{T_2} + \frac{1}{T_{2(\Delta B_0)}} \tag{1.16}$$

Where T_2 refers to contribution from genuine relaxation processes and $T_{2(\Delta B_0)}$ to that from field inhomogeneity. T_2^* is inversely proportional to the line width (see equation 1.17 [12]), short T_2 values means fast decay of the net magnetization in the transverse plane and broader peaks.

$$\Delta\nu_{1/2} = \frac{1}{\pi T_2} \tag{1.17}$$

Where $\Delta\nu$ is the relaxation-induced linewidth.

The local fields that induce longitudinal relaxation can also affect T_2 and since it is not possible to restore completely the magnetization while there is still a transverse component, then $T_2 \leq T_1$ for spin ½ [11]. Therefore, the rate of transverse relaxation depends not only on local fields oscillating at the Larmor frequency (same as T_1) but also, due to the loss of phase coherence of the spins. These two factors are expressed in equation 1.18. The latter contribution is dependent on the spectral density at zero frequency because random motion at any frequency reduces the efficiency of the relaxation mechanism.

$$\frac{1}{T_2} = \frac{1}{2}\gamma^2 \langle B^2 \rangle J(\omega_0) + \frac{1}{2}\gamma^2 \langle B^2 \rangle J(0) \tag{1.18}$$

The fast motion of the molecules (molecular tumbling) produces an averaging of the local magnetic fields, as a result T_2 becomes longer as there is a reduction in the dephasing of the spin

coherence [11]. J(ω) has been described in equation 1.15 as the spectral density function and it is assumed to be affected by the molecular motion as shown in equation 1.19 [10].

$$J(\omega) = \frac{2\,\tau_c}{1 + \omega^2\tau_c^2} \tag{1.19}$$

Where τ_c is the rotational correlation time, which is the average time that a molecule needs to rotate one solid radian. This time increases if the molecule is larger or the sample is more viscous, and decreases when the temperature is raised [10]. The dependence of both T_1 and T_2 with the rotational correlation time is presented in figure 1.2.

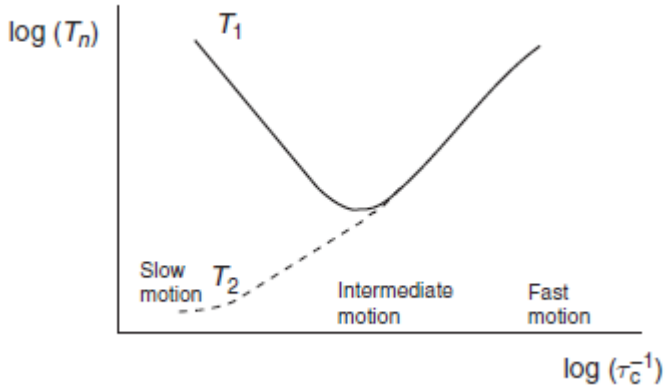

Figure 1.3: Schematic illustration of the dependence of T_1 and T_2 on the rotational correlation time τ_c. T_1 is described as log(eq1.15) and T_2 as log(eq1.18) [12]

The graph above shows that T_1 hits a minimum value. This value is when the correlation time (τ_c) is equal to the inverse Larmor frequency ($\tau_c = 1/\omega_0$), meanwhile T_2 decreases when the motion decreases. This means that T_2 is shorter for larger molecules, and as T_2 is related to the linewidth of the peaks as described in equation 1.17, larger molecules show broader signals.

1.1.2 Diffusion NMR

1.1.2.1 The Stokes-Einstein equation

When a stationary phase or a sample modifier is not present in the sample, the diffusion coefficient of the molecule dissolved is related to the size by the Einstein-Sutherland relation shown in equation 1.20 [14].

$$D = \frac{k_b \times T}{f} \tag{1.20}$$

Where k_b is the Boltzmann constant, T is the absolute temperature and f represents the hydrodynamic friction coefficient or frictional factor, a term that reflects the size and shape of

the molecule. If the molecules are related to the Stokes radius of the sphere (r_s) in a medium of viscosity (η), then f can be described through the Stokes equation (equation 1.21):

$$f = 6\pi\eta r_s \tag{1.21}$$

When equations 1.20 and 1.21 are combined, it is obtained the Stokes-Einstein equation, presented in equation 1.22 [14].

$$D = \frac{k_b \times T}{6\pi\eta r_s} \tag{1.22}$$

In which, it is demonstrated that the size is inversely related to the diffusion coefficient and the viscosity. Thus for larger molecules, smaller diffusion coefficients will be obtained [12].

The measurements of diffusion coefficients through the use of NMR have been possible ever since the discovery of spin echoes by Hahn [15]. Later on, in 1954 the effect of diffusion in free precession in NMR was studied using the spin echo suggested by Hahn, this effect was described by Carr and Purcell [16]. They determined the self-diffusion coefficient of water in the presence of a continuous field gradient. However, this technique presented several limitations due to the use of a steady magnetic field gradient, such as an increase of the linewidths due to the presence of the magnetic field gradient during the acquisition [17], which hindered the analysis of multiple peaks. This issue was solved by Stejskal and Tanner that proposed the use of pulsed field gradients in place of the steady field gradient used by Carr and Purcell [18]. In addition, as pulsed field gradients do not affect the linewidth it was possible to use larger gradients without increasing the RF power, which allowed the measurement of smaller diffusion coefficients [17], [19].

1.1.2.2 Importance of magnetic field gradients in diffusion NMR

Magnetic field gradients have a vital importance in the study of diffusion by NMR as they introduce a spatial dependence to the magnetic field strength, described in equation 1.23 [20]. The gradients in a NMR z-axis probe are applied along the z axis, increasing the magnetic field strength from down to top of the sample.

$$B(r) = B_0 + \boldsymbol{g} \cdot \boldsymbol{r} \tag{1.23}$$

Where *B(r)* is the magnetic field strength depending on the spatial position $\boldsymbol{r}$, B_0 is the strength of the static magnetic field produced by the NMR magnet and $\boldsymbol{g}$ describes the magnetic field gradient. The magnetic gradients can be applied in different directions as it is done in magnetic resonance imaging (MRI). However, for the work presented in this thesis all the gradients were applied homogenously in space producing a linear change along the z axis [17].

As it was discussed before the Larmor frequency is dependent on the magnetic field strength (equation 1.7), if equation 1.7 and 1.23 are combined, the application of a magnetic field gradient introduces spatial dependency to the Larmor frequency, as it is described in equation 1.24.

$$\omega(r) = -\gamma B(r) = -\gamma(B_0 + gr) = \omega_0 - \gamma(gr) \quad (1.24)$$

The magnetic field gradient is always applied after transferring the magnetization to the x-y plane through the application of a 90° pulse. The magnetic field gradients then give a position-dependent phase angle (ø) to the nuclei described in equation 1.25 [21]. In order to visualise the effect of a pulse field gradient, the magnetic moments of the nuclei in different spatial location generate a helix (Figure 1.3)

$$\emptyset = -\gamma g \delta z \quad (1.25)$$

Where g is the strength of the gradient applied and δ is the duration of the pulse field gradient.

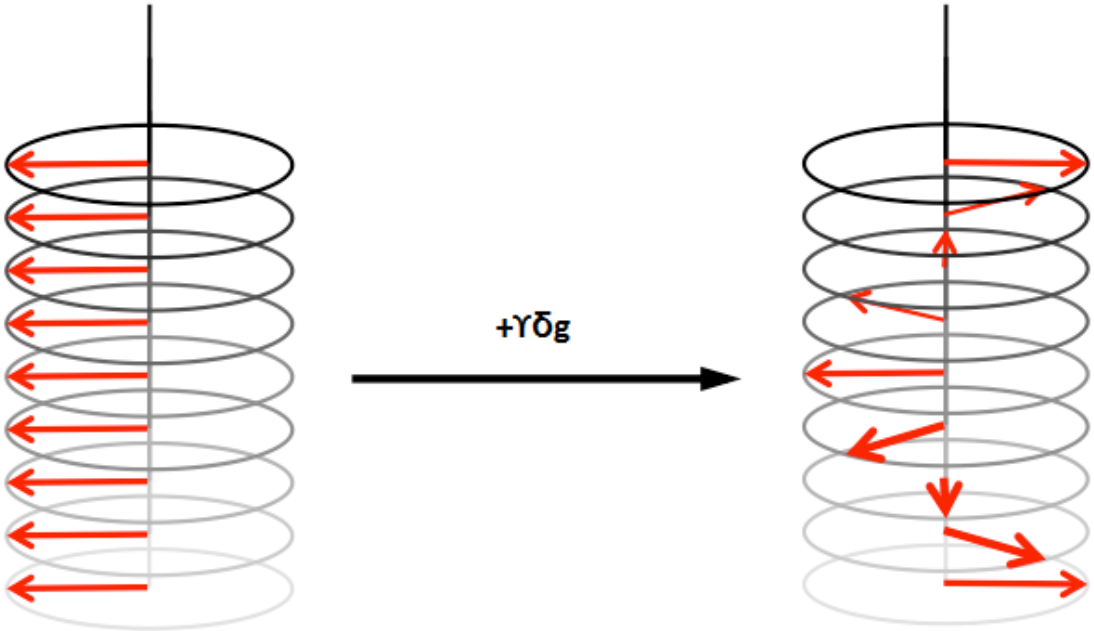

Figure 1.4: Nuclear spins after the application of a 90° pulse and a magnetic field gradient applied. Red arrows represent the magnetic moments of the nucleis in that layer of the sample along the z axis. Figure adapted from [22]

1.1.2.3 Measuring the diffusion coefficient by NMR

To measure diffusion coefficients in NMR the pulse sequences applied are based on the use of pulsed field gradients and the spin echo. The effect of the pulsed field gradient have already been described in the previous section. In the pulse sequences, two field gradients will be applied, separated by a diffusion delay (Δ), which is the period of time between the two pulsed

field gradients. The first pulsed field gradient will encode the spatial position, and the second one will refocus the spatial encoding.

The spin echo (figure 1.4 a) is the application of a series of RF pulses that will flip the bulk magnetization from the z axis to the x-y plane, then the spins will be induced to fan out due to the dephasing experienced, caused by different precession frequencies (as part of the T_2 relaxation process explained before, due to main field inhomogeneity or slightly different magnetic local fields and due to the magnetic gradients applied). After a period of time (τ) a 180° pulse is applied that will flip the magnetization and the spins will be induced to refocus during another τ period of time and form an echo (see figure 1.5). The two main pulse sequences to perform these experiments are the spin echo and the stimulated echo both based on Hahn studies [15], the sequences are represented in figure 1.4.

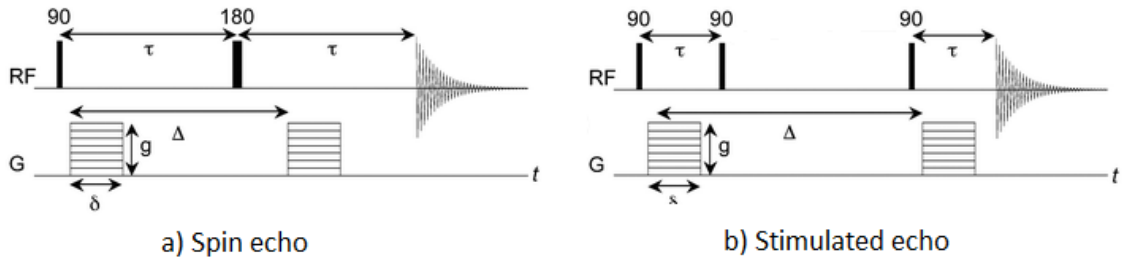

Figure 1.5: Spin echo and stimulated echo pulse sequences where g is the gradient strength, δ is the gradient length and Δ is the diffusion delay. Image adapted from [23]

The pulse field gradient stimulated echo (PFG-STE figure 1.4 b) is an improved version of the spin echo (SE figure 1.4 a). The main difference between both pulse sequences is that the magnetization is stored in the z direction (through the use of three 90° RF pulses instead of a 90 and a 180° pulses) and is only transverse to the main field during the periods of labelling with gradients. Thus it is less affected by J-modulation and although 50% of the signal is lost, the signal-to-noise ratio could be better due to less J-modulation and less T_2 loss. In addition the magnetization lost is dictated by the potentially slower relaxation T_1 instead of T_2 [21].

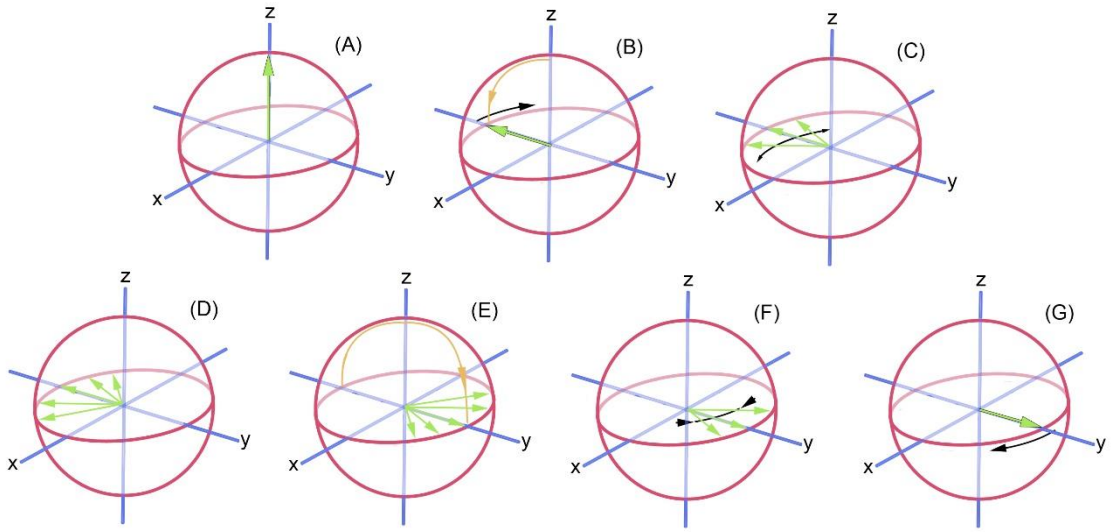

Figure 1.6: Vector representation of magnetization during a spin echo sequence. A) and B) show the magnetization flipped by a 90° pulse, C) and D) show the spins dephasing during the time period τ due to the different precessing frequencies, E) shows the application of a 180° pulse, finally F) and G) show the refocusing of the spins during the period of time τ. Image adapted from [24]

The attenuation caused by the pulsed field gradients is only noticeable if the molecules move during the diffusion delay (Δ). If this happens the strength of the magnetic field that a molecule will experience in the decoding pulsed field gradient would be different to the strength of the encoding pulsed field gradient and the refocusing would not be complete. All the molecules in solution are following a random motion produced by the collision with fast solvent molecules known as the Brownian motion [25]. Therefore the phase shift experienced by diffusing spins after the pulsed field gradients have been applied is random and when averaged it results in signal attenuation. This attenuation is related with the diffusion coefficient of the spin by the equation 1.26 described by Stejskal and Tanner [18].

$$I_G = I_0 \, e^{\left[-(\gamma\delta g)^2 \times D \times \left(\Delta - \frac{\delta}{3}\right)\right]} \tag{1.26}$$

Where I_G is the intensity of the signal after the gradients applied, I_0 is the intensity of the signal without any gradient applied, γ is the gyromagnetic ratio of the nucleus, δ is the length of the gradient applied, D is the diffusion coefficient, g is the strength of the gradient applied and Δ is the length of diffusion delay. This equation is adjusted for the use of square shaped gradients.

1.1.2.4 Improved diffusion pulse sequences

In this thesis, three different pulse sequences that are adaptations from the STE and the PFG-SE sequences have been used to measure the diffusion coefficient of molecules, which are the gradient compensated stimulated spin echo (GCSTE), bipolar pulse pair stimulated spin echo (BPPSTE) [26] and the Oneshot sequence [27]. These sequences will be briefly introduced in this section.

Both GCSTE and BPPSTE sequences (figure 1.6) have been previously compared with other sequences by Pelta et al. [28]. The aim of these improved pulse sequences is to reduce or remove unwanted effects produced by the application of pulsed field gradients such as Eddy currents, other elements can be added to remove J-modulation [29], [30] or convection [31] which can vary the apparent diffusion coefficient of a molecule [21].

Eddy currents are generated in conducting surfaces that are close to the gradient coils due to the rapid rise and fall of the gradient pulses what leads to distortions such as phase changes or gradient induced broadening in the spectra [32]. The two main additions to the pulse sequences to remove the effect of Eddy currents are the longitudinal eddy current delay (LED not shown) and the bipolar pulse pairs (BPP). The LED is an additional delay at the end of the STE sequence to let the eddy currents decay while the magnetization is stored in the z axis. The BPP is the split of the pulsed field gradients in a pair of two opposite signed pulsed field gradients with half of the pulse length and with a 180° RF pulse in between [33]. The 180° RF pulse makes that the two gradients have an additive effect. However, it does not affect eddy currents producing a cancellation effect between the currents produced after each pulse. The BPPSTE sequence introduced by Wu is presented in figure 1.6 b) [26]. The GCSTE sequence does not need the use of a 180° pulse as it places both of the antiphase pulse field gradients into the diffusion delay period [28].

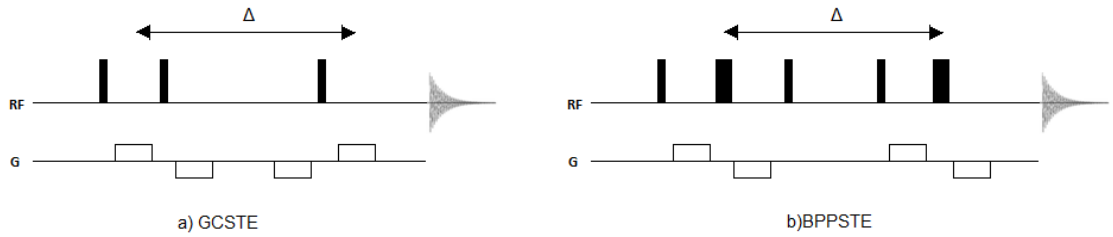

Figure 1.7: Gradient compensated stimulated spin echo (GCSTE) and bipolar pulse pair stimulated spin echo (BPPSTE) pulse sequences. The diffusion delay (Δ) is the time between the midpoints of the two diffusion encoding period. Thin black bars represent 90° pulses, while thick bars represent 180° pulses.

Another of the main issues when measuring diffusion is the effect of J-modulation. This occurs when scalar coupling exists between nuclei, then the precession frequency of the spin is influenced by the magnitude of the coupling constant (J) [32]. Homonuclear J-modulation effects cannot be refocused with the spin echo. Therefore, the only way to minimise the effect of J-modulation is to try to store the magnetization along the z axis and keep it away from the transverse plane. This is another advantage of the stimulated spin echo type sequences compared to the spin echo. The pulse sequence that has been used the most to perform the experiments presented in this thesis is the Oneshot sequence described by Pelta et al. [27]. This sequence derives initially from the BPPSTE sequence, and the main advantage is that it allows diffusion measurements in a single shot mode without a significant loss of resolution in neither the spectral nor the diffusion domain [27]. To do so this pulse sequence uses bipolar field gradient pulse pairs with extra unbalancing and balancing gradient pulses, the unbalancing gradients allow the selection of the coherence pathways removing the need for phase cycling, after this the lock signal needs to be refocussed. Hence, some extra balancing gradients are added to refocus the lock signal. A last element to supress J-modulation is added, this is the use of a 45° pulse right before the signal acquisition that removes antiphase terms which cause phase distortion, as demonstrated by Botana et al. in the description of Oneshot45 [30]. The pulse sequence used in this thesis is presented in figure 1.7 and has been adapted from the sequence described by Pelta et al. [27].

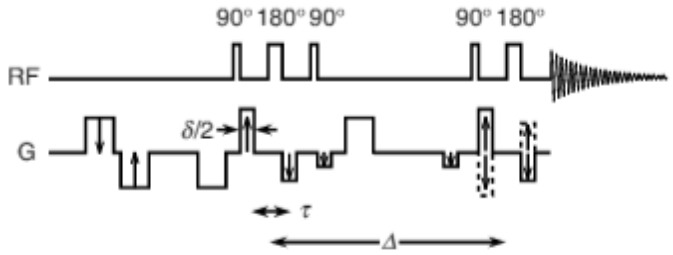

Figure 1.8: The Oneshot pulse sequence, the diffusion delay (Δ) is the time between the midpoints of the two diffusion encoding periods and τ that between the midpoints of the antiphase field gradient pulses within a given diffusion encoding period [27]

1.1.2.5 Diffusion ordered spectroscopy (DOSY)

In the previous sections, it has been described how to record the diffusion coefficient of molecules and some of the problems that have to be overcome to obtain accurate measurements. Diffusion ordered spectroscopy (DOSY), is the most usual method to display the data obtained after performing a diffusion NMR experiment. DOSY is a pseudo two dimensional presentation of the diffusion data, which shows the chemical shift domain (^{1}H-NMR spectrum) in the x axis and the diffusion coefficient (diffusion domain) in the y axis [34]. To obtain this display of the data, the signal attenuation of each peak in the spectrum is fitted to an exponential decay such as the Stejskal-Tanner equation (equation 1.26) [35]. Then each peak can be presented in the diffusion domain as a Gaussian centered on the diffusion coefficient that was obtained after fitting the signal attenuation to the exponential equation. Finally the width will be determined by the residual error of the fit [36]. It is worth mentioning that in the case of two overlapping peaks the diffusion coefficient will be an average of the components that appear under that peak. Hence, resolution of similar overlapped species is difficult. In order to represent this pseudo-2D spectra, there exist a wide range of complex mathematical procedures that allow processing the data like DECRA [37], CONTIN [34], SPLMOD [34] and some others that if the reader wants to have a deeper insight could read different sources [17], [21].

The diffusion data could also be presented in one dimension or in three dimensions (if a 3D experiment is performed). However, this particular method is very useful to present the data of a mixture, as it is possible to see each component of the mixture along the diffusion axis. An example of the DOSY plot is shown in figure 1.8, two polymers with significantly different sizes dissolved in D_2O

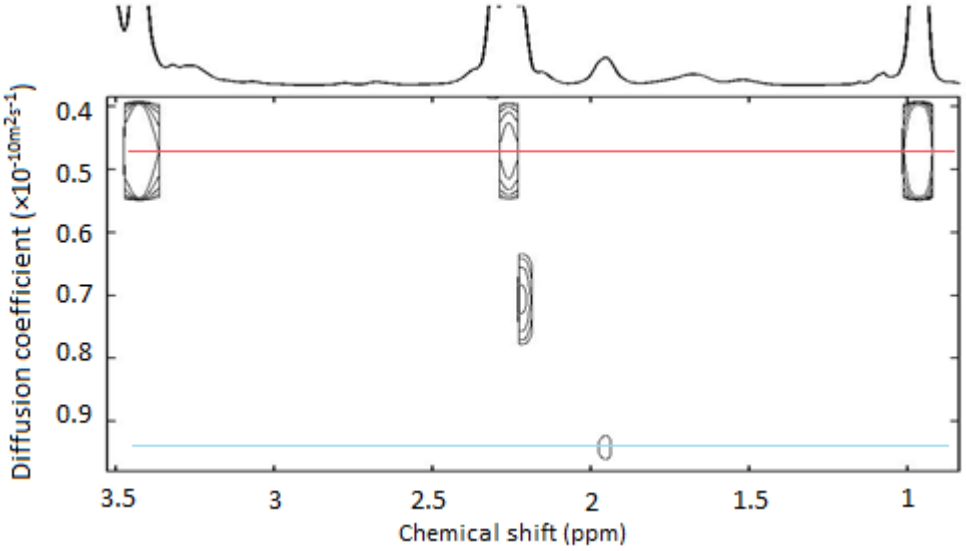

Figure 1.9: 0.1mM mixture of 10 kDa PVP and 50 kDa PEO in D_2O. The straight lines show the diffusion coefficient of the signals of interest. Red for PEO and blue for PVP

1.1.3 High resolution magic angle spinning (HR-MAS)

In section 1.1.1.3, the different relaxation mechanisms of the bulk magnetization after the application of a RF pulse were discussed. For a particular spin of a molecule in solution there are some interactions that are dependent of the orientation of the molecule with respect to the applied magnetic field, they are said to be anisotropic. Such as the orientation and distance of all the local magnetic fields produced by spins in the surroundings. However, the rapid isotropic tumbling of the molecule when it is in solution averages the molecular orientation dependence. This causes that this particular spin will show a signal with the exact same chemical shift as all the other corresponding spins of the molecules with the same structure in solution. Therefore, in general when a liquid sample is studied by NMR the peaks of the spectrum are sharp and clear.

In a solid sample the mobility of the molecules is significantly reduced. Therefore, all these interactions are no longer averaged anymore. Hence, the spins that in liquid samples show the same signal from one molecule to another possess now a slightly different precession frequency, which causes a significant broadening in the signals of the spectrum. Consequently, it is necessary to apply techniques to achieve high resolution spectra when solids are present in the sample.

One of the most common techniques that could be applied to remove or reduce the anisotropic interactions is Magic Angle Spinning (MAS). In this technique the sample will be spun very fast about an axis inclined at an angle of 54.74° with respect to the applied magnetic field (B_0). This will make the signals of the spectrum appear sharper and with better resolution because the

effects of chemical shielding anisotropy and heteronuclear dipolar couplings are averaged. It has been proved to be a very useful technique enabling the study of solid samples and liquid samples that contain a solid phase as in NMR chromatography. For example, in a sample setup like the one represented in figure 1.9, it is suffice to say that the molecular orientation dependence is of the form shown in equation 1.27 [38]:

$$H(\theta) \propto 3cos^2\theta - 1 \qquad (1.27)$$

Where θ is the angle which describes the orientation of the spin interaction tensor with respect to the main magnetic field. If the sample is a solid the angle θ takes on all possible values because it depends on the orientation of the molecule which is fixed and different from one to another, due to the restricted mobility of the molecules in the solid state.

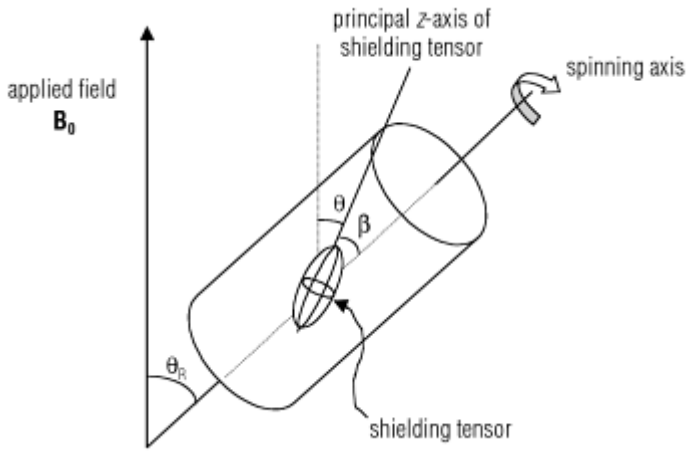

Figure 1.10: Magic angle spinning experimental set, where B_o is the applied magnetic field, θ_R is the magic angle 54.74°, θ is the angle between B_o and the principal z axis of shielding tensor and β is the angle between principal z axis of the tensor and the spinning axis. Adapted from [39]

When we spin the sample at an angle θ_R respect to the applied magnetic field, then θ varies with time because the molecules are rotating with the sample. In this situation the average of the orientation dependence of the nuclear spin can be described as follow in equation 1.28 [40]:

$$< 3cos^2\theta - 1 > = \frac{1}{2}(3cos^2\theta_R - 1)(3cos^2\beta - 1) \quad (1.28)$$

Both angles β and θ vary for every molecule and are fixed in a solid sample due to the restricted mobility. However, the angle θ_R can be set by the experimenter and if it is set at 54.74 then $3cos^2\theta_R - 1 = 0$ and so the average $< 3cos^2\theta - 1 >$ = 0. So if the sample spins fast enough (faster than the strength of the interaction) then ϑ is averaged rapidly and it is possible to recover the liquid like shape of the peaks in the spectrum. For a deeper insight the reader can consult both of the books of Duer [40, 41].

The possibility of recovering the liquid like line shape of the peaks in the spectrum has made magic angle spinning become a very useful technique with multiple applications. Such as structural biology, from studies of dynamics to solving the 3D structure of proteins [42, 43], studies of molecular motions in solids [44], studies of porous material like zeolites [45] and some other useful applications that the reader can consult in the literature [41]. However, in this thesis the experiments performed, included in many cases a solid stationary phase, but the analyte were still molecules in solution. Therefore, the broadening of the signals is caused by differences between the magnetic susceptibility of the stationary phase and the solvent, since the magnetic susceptibility also contains terms which have a $3cos^2\theta - 1$ dependence. MAS technique also averages these differences and reduce the broadening produced by the addition of the stationary phases. Hence, the combination of diffusion NMR under MAS and the use of stationary phases, can be of great interest in order to perform diffusion studies where the loss of resolution is minimum and there is the possibility to modulate the diffusion properties of molecules.

1.2 Chromatography

Chromatography is a technique that involves a diverse and important group of methods that enable the separation of closely related components in complex mixtures. In this technique a mobile phase, which has the sample dissolved and is usually a gas or a liquid, has to pass through a stationary phase, which is usually either a solid or a liquid fixed to a solid. While the solution is passing through the stationary phase the molecules of the sample will be retained due to different interactions (ionic, hydrophobic, polar and others) with the stationary phase. At the same time the continuous flow of the solvent will keep moving the analytes in solution. Finally the stronger these interactions are the slower the molecules will pass through the stationary phase. There are different types of chromatography not only because of the interactions that take place between phases, but also due to the dependence on the physical state of the phases. See [46], [47] for further details.

1.2.1 Uses of chromatography

Chromatography can usually have two purposes, preparative and analytical. Preparative chromatography tries to separate the components usually to purify and continue using these components [48, 49], while analytical uses very little quantities just to determine what compounds there are in the sample and in which specific quantities. The studies presented in this thesis lay into the analytical part of chromatography, as there is not a physical separation of the components in the sample, but a modification of the diffusion coefficient of the molecules dissolved, that enable the analysis of a sample without the need of a physical separation.

1.2.2 Types of chromatography

Chromatography is a technique that can be classified in many different ways depending if the categories come from the bed shape, such as planar or column chromatography, physical state of the mobile phase (such as gas, liquid or supercritical fluid chromatography) or the type of interaction that takes place between the analyte and the stationary phase (separation mechanism). The separation mechanism is what it is going to be the main topic of discussion in this section. There are many types of separation mechanisms,the more relevant ones being ion exchange [50], size exclusion [51] and chiral chromatography [52].

1.2.2.1 Ion exchange chromatography

Ion exchange application is a technique that is widely used to analyse or purify a wide range of molecules, and it is particularly useful to separate neutral from charged molecules. Depending on the charge of the analytes, the stationary phase can be either cationic exchange (the stationary phase has negative charge) or anionic exchange (the stationary phase has positive charge). The molecules that are eluting in the mobile phase have different polarities. The elution process occurs in presence of a polar stationary phase. Therefore, the more polar molecules experience a larger interaction with the stationary phase than those that are less polar and this causes the separation. There are two types depending on the polarity of the eluting phase. If the eluting phase is less polar than the stationary phase, it is known as normal phase chromatography. However, if the eluting phase is substantially more polar than the stationary phase, then it is known as reverse phase chromatography.

Some of the improvements that are the aim of research of chapters 4 and 5 could be applied to enhance chromatographic NMR with stationary phases based on an ion exchange separation mechanism. However, the main focus of this thesis is on size exclusion chromatography.

Therefore if the reader is interested in this particular technique, there are a wide range of interesting articles and books that can be consulted in the literature [53, 54].

1.2.2.2 Size exclusion chromatography

Size exclusion is the mechanism of separation that has been chosen to perform most of the experiments presented in this work. The technique is also known as gel filtration or gel permeation chromatography. The stationary phase used in this type of chromatography is formed by a porous material (usually dextrans such as Sephadex, agarose such as Sepharose or polyacrylamide such as Bio-Gel [55]). The molecules that pass through the porous material are separated by sizes, being the largest molecules the fastest to elute, while the smallest ones experience a larger interaction with the stationary phase and stay retained for longer. However, to achieve the right effect, it is needed to select the right pore size or grade of retention of the stationary phase. The smallest molecules will elute last because they will fit into the pores of the stationary phase. Hence, they will explore it following a longer pathway than the largest molecules that move around the beads of the stationary phase to elute. This behaviour is represented in figure 1.10.

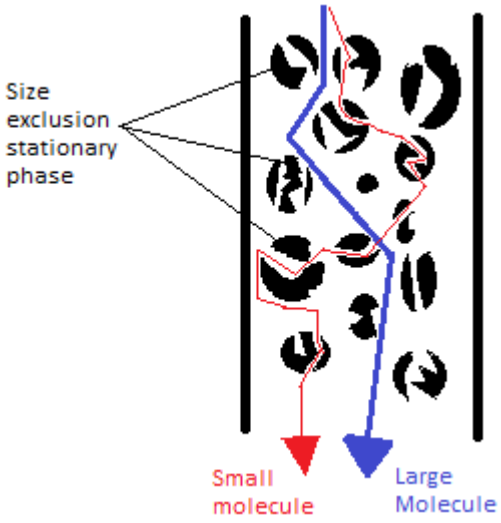

Figure 1.11: Pathway followed by two different size molecules passing through a size exclusion resin

Nevertheless, the pore size is particularly important in NMR, if the pore size is not selected correctly, and the pores are either too big or too small, both molecules will follow similar pathways and will only be separated by their speed of diffusion. This technique is mainly used for the separation of large biomolecules such as proteins [57, 58], separation of polymers [58], separation of carbon nanotubes [59] as well as to estimate the molecular weight of an unknown

protein [60] or to determine the distribution of molecular weights in a polymer sample [61]. See [51, 63] for further details.

1.2.2.3 Chiral Chromatography

Chiral chromatography began to be used by chemists in the mid-1960s in both liquid and gas chromatography. The aim was to try to separate optically active isomers (enantiomers). Usually, the silica stationary phases that are used for ion exchange chromatography were coated with a polymeric material to which was bonded an optically active isomer [63]. This addition produced a diastereomeric complex with one of the enantiomers of the racemic mixture, which means that one of the enantiomers is more retained in the stationary phase and the separation is possible. It is also possible to find size exclusion stationary phases made of chiral molecules such as Sephadex stationary phases.

The separation mechanism that is used to perform the studies presented in chapter 6 is chiral separation, and it is made with the use of two Sephadex stationary phases with different pore sizes.

1.3 Combination of diffusion NMR, chromatography and MAS

Diffusion NMR is an incredibly useful technique. It has been developed to be used in many different fields of chemistry, and have allowed to obtain valuable information to measure kinetics and mechanism of reaction [64], increase the understanding on aggregation phenomena [66, 67], and extend knowledge in many other areas of food research [67], biology or medicine such as the study of diffusion in mucosal systems produced by mucosal cells [68]. Nevertheless, the techniques shows major limitations when the diffusion coefficients of the analytes studied are close in the diffusion domain, or if they overlap in the spectral domain. Therefore, one of the ways to overcome that limitation, is the use of sample modifiers that enable the modulation of diffusion properties, such as chromatographic stationary phases.

1.3.1 Diffusion NMR and stationary phases

In the previous section it has been shown that the diffusion coefficient is affected by size, viscosity and temperature through equation 1.27. However, the diffusion coefficient is not only dependent on these factors, the modulation of diffusion properties can be achieve through the use of chromatography and analysed by NMR. There are several studies that combine these techniques and that have named the method as NMR chromatography, a technique of

enhancing the study of NMR diffusometry by adding a stationary phase that extend the range of diffusion of molecules by the change of their diffusion coefficients [69]. The first examples of this method were developed by Caldarelli and co-workers in 2003. In their studies they combined common silica based HPLC stationary phases with NMR, introducing the stationary phase into a HR-MAS rotor with the dissolved sample, and obtained a separation in the diffusion domain for a mixture of ethanol, naphthalene and dec-1-ene in ethanol-d_6 and a mixture of ethanol, dichlorophenol and heptane in cyclohexane-d_{12}, which showed the same diffusion modulation that is shown in HPLC [70]. However, this method has been gaining more importance during the last decade, and several advances have been published. For instance, Caldarelli and co-workers extended their studies with silica based experiments in 2008 showing that it was possible to perform NMR chromatography in a mixture with different deuterated solvents such as the separation of a mixture of alcohols in D_2O and a mixture of aromatic compounds in $CDCl_3$ into a HR-MAS rotor, in order to deal with the broadening produced on the signals by the addition of the stationary phase [71]. Other silica based NMR chromatography studies without the use of HR-MAS were developed by Hoffman and co-workers in 2008. In these studies, they managed to obtain separation using a silica based stationary phase. However, to reduce the overlapping produced due to the addition of a solid stationary phase, they found a mixture of solvents that matched the magnetic susceptibility of the solvent and the stationary phase, such as a mixture of $CDCl_3$ and CH_2I_2 [72]. Later in 2011 they continued developing their studies, and showed, that it was possible to predict the reduction in the diffusion coefficient experienced by molecules in presence of the silica based stationary phase, depending on the nature of the binding between the analyte and the stationary phase [73]. A good review of analytical applications of NMR chromatography was published in 2012 by Krishnan and co-workers for those more interested [74]. As it was mention in section 1.2 of this chapter, there are different types of chromatography depending on the type of interaction between the stationary phase and the analyte. Therefore, the modulation produced in the diffusion coefficient also depends on electrostatic interactions (silica based stationary phase) as the studies performed by Caldarelli and Hoffmann [71, 74], size can be used to modulate the diffusion (size exclusion stationary phase) [3, 76] or simply spatial distribution (chiral stationary phases) as the studies presented in chapter 6.

1.3.2 Chromatographic NMR and HR-MAS

The study of samples by NMR that contain a solid, has shown to be challenging due to the presence of anisotropic interactions as it was discussed in section 1.1.3 of this chapter. The slow tumbling rate of the molecules increases the importance of these type of interactions. Hence,

very large molecules in solution such as polymers also suffer this effect. Moreover, the addition of a stationary phase produce differences between the magnetic susceptibility of the solvent and the stationary phase that also broaden the peaks in the spectrum, as it has been seen in previous studies [1, 76]. This issue reduced notably the resolution of the spectra and the application of chromatographic NMR, as it is quite difficult to find analytes that would not overlap either with the stationary phases or the other analytes present in the sample. For all these reasons, it seem to be very convenient to extend the studies performed in chromatographic NMR with HR-MAS conditions.

The application of magic angle spinning to diffusion NMR experiments in presence of stationary phases had been suggested before by Caldarelli and co-workers [71, 72]. However, due to the "little attention that had been devoted so far to delimiting the role of the extra force field induced by sample rotation on the significance and reliability of self-diffusivity measurements" [76] Caldarelli and co-workers extended their studies in presence of HR-MAS and found that it is not a straightforward task. However, they found that smaller volumes in the rotor, led to more accurate diffusion coefficients and also reported a range of spinning rates that would be suitable for the performance of these studies [76]. The advantages of the use of MAS conditions in reducing the broadening of the signals has been proven, also Parella and co-workers have reported the fact that sample rotation can avoid undesirable convection effects due to temperature gradients in tube NMR [77]. However, there are some difficulties with the use of the MAS technique. Some of the major problems had been reported by Caldarelli and co-workers in 2013, such as the appearance of spinning sidebands or the presence of bubbles inside the rotor sample that can, not only affect to the accuracy of the diffusion measurements but also affect to some delicate samples when they are under high spinning rates [78]. However they showed that by optimizing the sample preparation these effects can be reduced. Another problem that appears with the use of MAS have been reported by Goldman and Tekely, and is the appearance of radial field sidebands produced by the radial component of the RF field at the edges of the coil. Therefore they have shown that "for a sample placed in a rotor of length exceeding the solenoid coil or for a small volume sample placed at the edge of the coil, the radial-field effect may contribute significantly to the intensity of the -1 spinning sideband of rotor-modulated internal interaction" [79]. During the timeline of the work presented on this thesis, some experiments have already been published proving that HR-MAS can be an effective way to develop chromatographic NMR [80]. However, the presence of high spin rates produced effects that are not completely understood.

1.4 Charged polymers diffusion in solution

A large amount of the theories that are presented and discussed in these thesis are based on the diffusion of neutral and charged polymers in solution. For this reason, a basic insight to polymer diffusion in solution is given in this section. All of the discussion carried in this section, is going to be focus on polymers in a very dilute environment. This is because as we are interested in the self-diffusion of large molecules in solution without the influence of other polymers. The concentration where the diffusion coefficient is affected by neighbouring polymers, is known as overlap concentration [81]. Therefore the discussion will be focus on the diffusion that occurs below that concentration.

Diffusion is the process that is responsible for the movement of a molecule from one part of a system to a different part of the system. Without the application of external factors is due to random molecular motions known as Brownian motion. The basic model of self-diffusion, has been discussed previously in section 1.1.2.1 and is described by the Stokes-Einstein equation presented in equation 1.22, which shows that the self-diffusion coefficient is dependent on the size of the molecule.

For most of the small molecules the size does not suffer huge variations. However, charged polymers can show very different sizes depending on the media, the intramolecular interactions or external interactions. Most of these variations are due to the presence of charges when the polymer is in solution, these molecules are known as polyelectrolytes if the charges are all of the same sign or polyampholytes if the charges have different sizes [82,83].

There are several models to explain the conformation of a polymer chain in solution such as the flory model, where the chain has an ellipsoid conformation filled by the polymer chain, or the scaling model where the conformation is achieved by the formation of a chain of electrostatic blobs filled by polymer chain [83] (See figure 1.12). However, what is important is that when the polymer is a poly electrolyte the conformation varies due to the repulsion experienced by the charged groups in the chains. This fact, along other chromatographic advantages made vital the use of a buffer that will act as a counter ion and enable the conformation of the polymer to be stable and therefore, be able to obtain reproducible diffusion measurements.

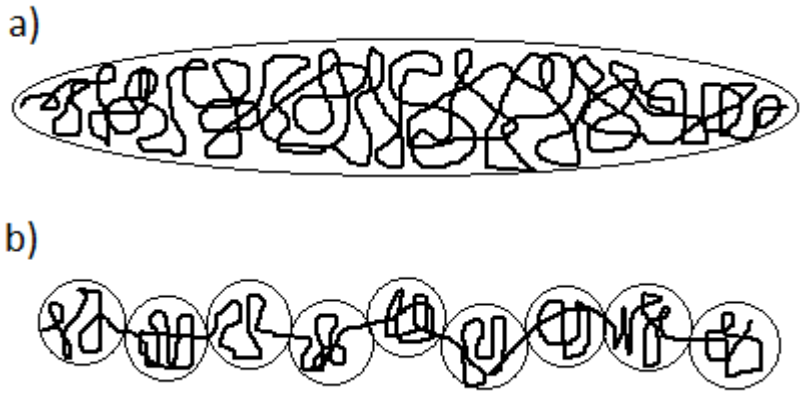

Figure 1.12: Schematic representation of a polyelectrolyte chain in an ellipsoid conformation a) and as a chain of electrostatic blobs b)

1.5 Thesis Outline

This thesis aim, is to extend the range of available methods to analyse mixtures by NMR through the measurement of diffusion coefficients. As well as, to extend the understanding of the interactions that happen between the analytes and the stationary phases used. In order to facilitate this aim, it is necessary to extend the understanding of diffusion under high spinning rates, which will allow to implement the advantages that arise from the combination of MAS and chromatographic NMR studies.

Chapter 2 will outline the experimental methods and materials used in this thesis.

Chapter 3 will focus on the development of size exclusion stationary phases to analyse mixtures under NMR in static conditions, described as SEC-DOSY. The diffusion coefficient of mixtures containing two different polymers will be recorded with and without Sephadex stationary phases, to see if it is possible to modulate the diffusion properties of the polymers through their size and increase the understanding of the interactions between the polymers and the stationary phase.

Chapter 4 and 5 will focus on the application of MAS to diffusion NMR. In chapter 4 the diffusion coefficient of some proteins and polymers are measured under MAS in presence and absence of stationary phase. After some confusing results, a method to obtain accurate diffusion coefficients of water under MAS is described. In chapter 5 a wide range of experiments are performed with different molecules (large, such as polymers and small molecules such as aminoacids and some others) dissolved in presence and absence of a phosphate buffer to try to

understand the effects that arise when MAS is implemented and have an effect in the diffusion of the molecules in solution.

Chapter 6 will focus in the study of enantiomers in the presence of a size exclusion stationary phase with chiral properties (Sephadex) to see if it is possible to modulate the diffusion properties of two enantiomers and differentiate the two enantiomers on a mixture by NMR chromatography.

Chapter 2
Materials and methods

This chapter will detail all the materials used to perform the experiments and their sources, methods of sample preparation and methods of data acquisition and analysis throughout this work.

2.1 Materials

2.1.1 Chemicals

For the NMR experiments performed in chapters 3, 4 and 5, all the polymers used were acquired from Sigma Aldrich, except the poly (styrene-4-sulfonate) and the poly (methacrylic acid) molecular weight reference standards which were from Kromatek.

All the size exclusion stationary phases that were used to perform the diffusion NMR experiments, were acquired from Sigma Aldrich. Sephadex is comprised of a crosslinked polydextrans matrix with epichlorohydrin and it is supplied as a powder [84]. Superdex consists of dextran covalently attached to highly cross-linked agarose, and it was supplied as suspensions in 20% aqueous ethanol. Sephadex G10 was “medium” and Sephadex G50 was “superfine” with particle sizes of 20 - 120 µm and the Superdex were “prep grade” with particle sizes of 22 - 44 µm [85]. Other pertinent information such as the fractionation range for the stationary phases that were used to perform this work are detailed in table 2.1.

Stationary phase	**Bead size (µm)**	**Fractionation range (kDa)**		**Swelling factor (mg/ml)**
		Globular proteins	**Dextrans**	
Sephadex G10	40-120	0 - 0.7	0 - 0.7	2 - 3
Sephadex G50	20 - 50	1.5 - 30	0.5 - 10	9 – 11
Superdex 75	22 – 44	3 - 70	0.5 - 30	-
Superdex 200	22 - 44	10 - 600	1 – 100	-

Table 2.1: Properties of stationary phases

Other chemicals used in chapter 4, including the wide range of proteins listed in table 2.2 were supplied by Sigma Aldrich.

Proteins	Molecular weight (kDa)
Bovine serum albumin	66.5
Albumin Chicken Egg	44.3
α-Chymotrypsinogen A	25.6
β-Lactoglobulin	18.4
Bovine α-Lactalbumin	14.2
Cytochrome C	12

Table 2.2: Summary of proteins used with their corresponding molecular weight

All the small molecules used in chapter 5 and listed in table 2.3 were obtained from Sigma Aldrich except sodium p-styrene sulfonate hydrate which was supplied by TCI.

Molecule	Molecular weight (Da)
$[Co(en)_3]Cl_3$	345.59
Thiamine hydrochloride	337.26
EDTA	292.24
Lidocaine	234.3
p-Styrene sulfonate	206.2
Tyrosine	181.2
Pyridoxine hydrochloride	169.2
Tartaric acid	150
Nicotinamide	122.1
4-Fluorophenol	112.1
Me_4NCl	109.6

Table 2.3: Summary of the small molecules used with their corresponding molecular weights

Finally all the chemicals that need to be used to synthetize the cobalt complex and all the pure enantiomers used to perform the experiments in chapter 6 were obtained from Sigma Aldrich, except D-(-) tartaric acid which was supplied by TCI.

2.1.2 Solvents

Most of the experiments were performed in deuterium oxide, which was obtained from Goss Scientific with a purity of 99.94%D. Some of the pure enantiomers that were used to perform the experiments in chapter 5 were dissolved in methanol-d_4 99.8%D, and some of the D_2O soluble enantiomers to make them dissolve needed drops of deuterium chloride 35% wt in D_2O with a purity 99%D. Both of them were obtained from Sigma Aldrich. Ethanol, methanol and chloroform were "analytical grade" and acquired from Fisher Scientific. The water used to prepare samples was always distilled water.

In order to prepare polyelectrolyte samples, a phosphate buffer solution (150 mM NaCl and 50 mM Na_3PO_4) was prepared using dibasic sodium phosphate (Na_2HPO_4) and sodium phosphate monobasic dihydrate ($NaH_2PO_4 \cdot 2H_2O$), both of them were supplied by Sigma Aldrich with purities ≥98%. The buffer was prepared mixing 29.6 mg of $NaH_2PO_4 \cdot 2H_2O$ + 115 mg of Na_2HPO_4 + 438.4 mg NaCl in 5 ml D_2O that was later diluted by a factor of 10 to use it in the samples.

2.2 Sample preparation

2.2.1 Stationary phases and polymers

Following the specifications of the supplier [86], Sephadex G10 was prepared for use by swelling the powder for ≈24 hours in 3 ml of solvent per gram of dry stationary phase, after this time more solvent was added to form a 240 mg ml^{-1} suspension. This suspension was then washed 2 – 3 times with the required solvent to remove residual impurities of other solvents. The amount of 240 mg ml^{-1} was found to be the minimum concentration to cover with stationary phase the RF coil region when it is settle in a 5 mm NMR tube. The process of preparation of Sephadex G50 was similar, but in this case the specifications of the supplier were 11 ml of solvent per gram of dry stationary phase [87], and the concentration that covered the RF coil region when the stationary phase was let to settle was 60 mg ml^{-1}.

Superdex 75 and 200 stationary phases were obtained as 20% aqueous ethanol suspensions. Therefore, the stationary phases were re-suspended in the bottle and the required volume was removed by pipette. In order to remove the unwanted ethanol, the suspension was washed no less than three times with the same volume of the required solvent. After leaving the suspension to settle under gravity the volume of the stationary phase was ≈75% of the total volume.

For the experiments performed in NMR tube along the chapters 3 and 6, the samples of stationary phases with analyte were prepared following the procedure described by Joyce [66]. 200 µl of the supernatant from the 1 ml samples of settled stationary phase was replaced by 200

µl of analyte stock solution. The stationary phase was then re-suspended by vortexing to ensure thorough mixing of the analyte and the stationary phase and transferred into an NMR tube. The suspensions were allowed to settle for at least 30 minutes before NMR acquisition.

For the experiments performed under MAS conditions in chapter 4, the samples with stationary phase were prepared filling the 40 µl rotor pipetting 60 µl of re-suspended sample, after letting the stationary phase to settle for at least 30 minutes, 15 µl of supernatant were removed by pipette. Then the rotor was slowly sealed with a Teflon plug drying carefully the extra 5 µl supernatant that ensure that no bubble was left into the rotor. Finally the drive ring was attached.

2.2.2 Synthesis of the cobalt complexes

In this section the synthesis of the cobalt complexes used in chapter 6 is described. The literature describes this synthesis through the use of a base [88], or through the use of HCl [89]. Due to the easier synthetic process (less steps and less laboratory handling were required) all the synthesis described in this section are adapted from the method described by Krause et al. [89].

2.2.2.1 $[(+)Co(en)_3]Cl_3$ and $[(-)Co(en)_3]Cl_3$

The synthesis of this complex is divided in two parts. The first part is the synthesis of the racemic mixture of the cobalt complex $[Co(en)_3]Cl_3$ (see figure 2.1) and it is described below:

Figure 2.1: Enantiomers Δ (left) and Λ (right) of the complex tris(ethylenediamine)cobalt (III)

A solution was made with 6 g of $CoCl_2 \cdot 2H_2O$ in 20 ml of distilled water and was placed into a beaker. Due to the strong smell and fumes produced by the anhydrous ethylenediamine, 4.5 ml were added using a disposable pipet in the fume hood to 10 ml of distilled water into a 250 ml Erlenmeyer flask. This solution was cooled in ice, while it was still in the ice bath 4 ml of 6M HCl were added slowly to keep the temperature low. While it was still in the ice and with continuous magnetic stirring, the initial cobalt solution was added carefully (drop by drop). Immediately after, 10 ml of 30% H_2O_2 were added slowly with continuous swirling. The solution was then

removed from the ice bath and the flask was kept under stirring until the effervescence ceased. The mixture was then placed in a hot plate and boiled gently to reduce the volume.

Once the volume had been reduced to about 30 ml, another 30 ml of concentrated HCl was added, followed by 60 ml of ethanol. The suspension was cooled in ice for at least 3 hours and suction filtered. Finally the powder obtained was washed with ethanol and ether, then let air dry for at least 6 hours, after this time a ^{1}H-NMR spectra was recorded to ensure that the complex is the expected one and compare to a readily available commercial complex supplied by Sigma-Aldrich.

The second part of the experiment is the procedure followed to obtain the pure enantiomers separated from the racemic mixture synthesized before. The process is described below:

From the racemic mixture obtained above, 3.3 g were placed with 1.8 g of L-(+)-tartaric acid in a 100 ml beaker. Then 15 ml of distilled water were added followed by 1 g of NaOH. The beaker was then covered with parafilm and placed on a stirring plate until the solids dissolve completely (the heat produced by the NaOH should be enough, if not warm very gently). After this step the mixture was left cool to room temperature overnight after removing the parafilm, otherwise the amount of solvent is too high, this way a slow crystallization is achieved. The dark orange crystals were collected by suction filtration and after removing the filtrate washed with 20 ml of 1:1 water and acetone, followed by 20 ml of pure acetone. Finally let air dry overnight.

The optical rotation of the crystals was then measured in order to check purity to continue with the synthesis using a polarimeter following the procedure described in section 2.4.

If the purity is not high enough (> 90%) the crystals must be recrystallized. Otherwise, 2 g of the crystals are placed in a 50 ml beaker and broken to smaller pieces. Then 1 pellet of NaOH (approx. 0.3 g) was added with 15 ml of very cold distilled water. The mixture was stirred until the solids dissolve (the heat produced by the NaOH should be enough, if not warm very gently and never longer than 5 minutes). Then 1.5 g of NaCl were added to the mixture under continuous stirring and let to dissolve for 5 minutes. Finally the mixture was let cool on an ice bath for 2 hours and the crystals were collected by suction filter. The crystals were washed with a an ice cold solution of 1.5 g NaCl in 10 ml distilled water to remove the tartrate, followed by 10 ml ethanol and then 10 ml acetone. The crystal were let air dry overnight and their optical activity was measured to check purity.

The other isomer should be obtained from the filtrate separated after the synthesis of [(+)Co(en)$_3$][(+)tart]Cl. However, it was not possible to obtain a pure enough sample with the

method found in the literature. Therefore, the synthesis described in part two was repeated exactly the same but with the use of D-(-)-tartaric acid. Every step of the synthesis was followed by the recording of a ^{1}H-NMR spectrum to ensure that the compounds obtained were the expected ones. Also every step of this synthesis was performed with yields higher or equal to 75%.

2.2.2.2 $[Co(diphenen)_3]Cl_3$

The synthesis of these complex followed exactly the same procedure as the method described for $[Co(en)_3]Cl_3$. However, the ligand diphenylethylediamine is not very soluble in water due to the two phenyl groups (see figure 2.2). In addition, the enantiopure ligands were extremely expensive. Therefore, the synthesis was done with the amounts of chemicals and sovents described below:

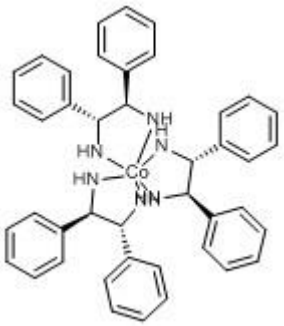

Figure 2.2: Structures of $[Co(Meso\text{-}1,2\text{-}diphenen)_3]^{3+}$

A solution was made with 0.1 g of $CoCl_2 \cdot 2H_2O$ in 5 ml of distilled water and was placed into a beaker. Through the use of a disposable pipet in the fume hood, 0.3 g of diphenylethylendiamine were dissolved in the minimum amount of distilled water possible (≈ 15 - 20 ml) into a 250 ml Erlenmeyer flask. This solution was cooled in ice, while it was still in the ice bath 0.5 ml of 6M HCl were added slowly to keep the temperature low. While it was still in the ice and with continuous magnetic stirring, the initial cobalt solution was added carefully (drop by drop). Immediately after, 0.3 ml of 30% H_2O_2 were added slowly with continuous swirling. The solution was then removed from the ice bath and the flask was kept under stirring until the effervescence ceased. The mixture was then placed in a hot plate and boiled gently to reduce the volume.

Once the volume had been reduced to about 10 ml, then 0.5 ml of concentrated HCl was added, followed by 10 ml of ethanol. The suspension was cooled in ice for at least 3 hours and suction filtered. Finally the powder obtained was washed with ethanol and ether, then let air dry for at least 6 hours.

The reaction worked with the racemic mixture of the meso ligand but not with the pure enantiomers, this was due to a steric effect, as with the pure ligands the phenyl groups are all in the same side of the molecule clashing each other in the space, while when the meso was used the phenyl groups are one on each side of the molecule as described in figure 2.2. Therefore, the synthesis of the pure enantiomers of the complex was not completed.

2.2.2.3 $[Co(meten)_3]Cl_3$

The synthesis of these complexes (see figure 2.3) followed exactly the same procedure as the method described for $[Co(en)_3]Cl_3$. However, due to the high price of the enantiopure ligands the amounts used were substantially smaller.

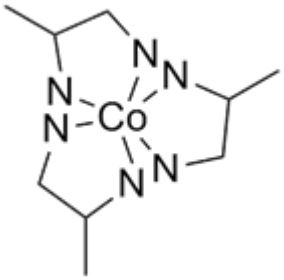

Figure 2.3: Structure of $[Co(meten)_3]^{3+}$

A solution was made with 0.1 g of $CoCl_2 \cdot 2H_2O$ in 0.33 ml of distilled water and was placed into a beaker. Through the use of a disposable pipet in the fume hood, 0.11 ml of 1,2-diaminopropano were added to 0.22 ml of distilled water into a 250 ml Erlenmeyer flask. This solution was cooled in ice, while it was still in the ice bath 0.1 ml of 6M HCl were added slowly to keep the temperature low. While it was still in the ice and with continuous magnetic stirring, the initial cobalt solution was added carefully (drop by drop). Immediately after, 0.22 ml of 30% H_2O_2 were added slowly with continuous swirling. The solution was then removed from the ice bath and the flask was kept under stirring until the effervescence ceased. The mixture was then placed in a hot plate and boiled gently to reduce the volume.

Once the volume had been reduced to about 0.5 ml, another 0.5 ml of concentrated HCl was added, followed by 2 ml of ethanol. The suspension was cooled in ice for at least 3 hours and suction filtered. Finally the powder obtained was washed with ethanol and ether, then let air dry for at least 6 hours.

The amount of different isomers that this reaction produced was impossible to separate. Therefore, the synthesis of the enantiopure cobalt complex was not completed.

2.3 NMR

All experiments along this thesis were performed on a Varian VNMRS 600 spectrometer (Agilent technologies) using VnmrJ software (version 3.2 revision A). Two probes were used in these experiments, the acquisition of standard liquid experiments was done using a 5 mm X{^{1}H} broadband probe equipped with an actively-shielded z-gradient coil capable of producing 0.72 T m^{-1}. The experiments that required the use of magic angle spinning were acquired with a 4 mm HR-MAS ^{1}H{X} probe equipped with a magic angle gradient coil with a maximum gradient of 1.38 T m^{-1} (NanoProbe^{TM}). For all the experiments performed the sample temperature was set to 298 K unless those that were specified otherwise.

2.3.1 ^{1}H proton spectra

All the one dimensional proton NMR spectra were acquired at a frequency of 599.7 MHz with a spectral width of 9615 Hz, 32768 data points and up to 128 transients.

1D spectra were processed using MestreNova (version 10.0.2-15465). Diffusion data were analysed using DOSY Toolbox (version 1.0) [36].

2.3.2 Diffusion NMR experiments

The pulse sequence that has been used the most to record the diffusion coefficient of molecules along this thesis, was the Oneshot sequence, which has been developed by Pelta et al. [27]. The Oneshot sequence is based on the bipolar pulse pair stimulated echo (BPPSTE) sequence [26], [28]. The Oneshot sequence has the bipolar pulse pairs unbalanced through the gradient strength, this dephases the magnetization not refocused and remove the need of phase cycling. In order to keep the lock signal balancing pulses are added to the beginning and end of the diffusion delay. The pulse sequence can be seen in figure 2.4. To calculate the diffusion coefficient, the equation that describes the signal attenuation that is produced by the diffusion of the molecules, is called the Stejskal-Tanner equation (see equation 1.22). In the Oneshot sequence, this equation is modified to correct the difference in the finite gradient pulse duration and signal attenuation caused by the introduction of additional gradients and unbalancing the bipolar gradients. Equation 2.1 shows the modified equation [27].

$$\frac{I(g)}{I(0)} = e^{\left(-(\gamma\delta g)^2 \times D \times \left[\Delta + \frac{\delta(\alpha^2-2)}{6} + \frac{\tau(\alpha^2-1)}{2}\right]\right)} \qquad (2.1)$$

Where Υ is the gyromagnetic ratio of the observed nucleus, g is the strength of the applied gradient, which in the case of this sequence is the average amplitude of the four dimension-

encoding gradients, D is the diffusion coefficient, δ is the length of the diffusion-encoding gradients (in this sequence each pulse has a duration $\delta/2$), Δ is the diffusion delay, τ is the time between the midpoints of the pulse pairs within each diffusion-encoding period and α is the factor by which the gradient strength of the bipolar pulse pairs are unbalanced.

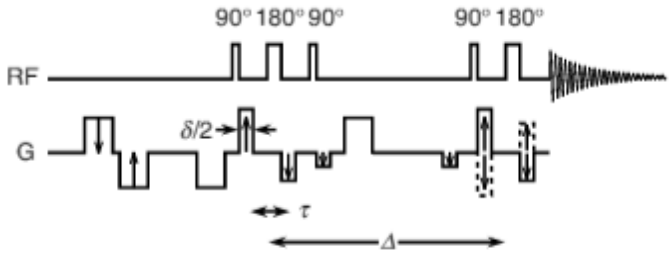

Figure 2.4: Oneshot sequence, arrows indicate the incrementation of gradients [27]

For some of the experiments performed in chapter 4, two different and more simple pulse sequences were used: the gradient compensated stimulated spin echo (GCSTE) and the bipolar pulse pair stimulated spin echo (BPPSTE) [21, 26].

The acquisition parameters for the static experiments were optimized for each set of experiments. Usually with values of 50 ms for the diffusion delay (Δ), 2 ms for the gradient pulse length (δ) and sixteen gradient strength from 0.0452 to 0.5650 T, in equal increments with respect to g^2. The usual values for experiments performed under MAS conditions were fifteen gradient strength arrayed from 0.0500 to 0.3337 T also in equal increments with respect to g^2.

2.3.3 Magic angle spinning

All NMR magic angle spinning experiments were performed using glass rotors with a sample volume of 40 µl. The magic angle in the HR-MAS probe is factory set and was not adjusted in any of these experiments. The range of spin rates used varied from 0.7 to 3 kHz. This range was selected in order to minimise overlap of the spinning sidebands with analyte signals or to see the effect of the spin rate on the diffusion coefficient measurements.

2.3.3.1 Reduction of the active volume of glass rotor

Some of the experiments performed in chapter 4 required modifications in the active sample volume or size of the glass rotors. To reduce the active volume of the glass rotor, teflon was used in three different ways. Firstly, with the addition of two 1 mm thick and 3.1 mm diameter discs inside the rotor, on the top and on the bottom of the glass rotor to achieve axial reduction. The second method was the introduction of cylindrical Teflon spacer into the sample rotor to

reduce the inner diameter from 3.1 to 1.5 mm causing radial reduction. The final method was the combination of the two previous methods.

2.4 Other physical techniques

2.4.1 Optical rotation

Optical rotation (OR) measures were used to determine the purity of the enantiomers of the cobalt complexes that were synthetized, separated and purified for the experiments performed in chapter 6. For the measurements 0.1 g of cobalt complex were dissolved in 2 cm^3 of distilled water. This solution was transferred by pipette to a clean and thoroughly dry 0.5 dm long cuvette and place in the polarimeter at 293 K to measure the specific rotation. The instrument used was an ADP 400 polarimeter from Belligham + Stanley. The light source was a light emitting diode with interference filter producing light with a 589 nm wave length. The value of $[\alpha]_{589}$ was recorded directly from the instrument.

Chapter 3

Mixtures analysis by diffusion NMR enhanced with size exclusion stationary phases: SEC-DOSY

The analysis of mixtures is one of the most common procedures in the day to day work of analytical chemists [64, 88]. Therefore, a large amount of resources are invested every day to separate the components of mixtures [91] and to analyze them with a wide range of different techniques [92]. Therefore, any improvement in this process not only will save a lot of money and chemicals but also a big amount of time.

Consequently, an improvement that would be useful, would be to develop new techniques that enable the analysis of mixtures without prior separation, making the process greener, time saving and reducing the loss of desired compounds due to purification processes [93]. In order to achieve this improvement, NMR and the possibility of measuring the diffusion coefficient of compounds can be the key of the process. Diffusion NMR studies, have already been developed and shown to be very useful in different type of studies, such as extending the understanding of molecular aggregates [4, 66] or characterization of protein-ligand interactions [94]. Also they have shown that it is possible to extend the studies of diffusion coefficients to use diffusion NMR as one of the techniques that will allow the study of mixtures [21]. Moreover, recently a method known as either Matrix Assisted DOSY (MAD) or Chromatographic NMR has become a very popular way to modulate the diffusion properties of molecules and affect their pseudo-separation [70, 93]. A very wide range of sample modifiers had been studied to develop this technique such as the use of different solvents [71], the addition of surfactants such as SDS, PEG and micelles [96]–[100] and through the use of different silica based chromatographic stationary phases [73] or size exclusion stationary phases SEC [1, 3, 71, 93]. The latter ones will be the main focus of this study. However, the addition of a solid stationary phase to a liquid NMR sample studied by a liquids NMR probe, will lead to a significant broadening of the signals in the spectrum due to differences in the magnetic susceptibility between the solvent and the

solid media. The main application of this method is that provides spectral separation of the components in the mixture as well as increase the understanding of molecular interactions between the analyte and the stationary phase used.

In this chapter different polymer mixtures were analyzed in presence of size exclusion chromatographic phases by DOSY-NMR, with the aim of completing previous studies [1], which provided a first insight in how useful can this technique be to improve resolution in the diffusion domain and to understand the interactions that are taking place between the analyte and the chromatographic stationary phase. This may allow a demonstration of the changes observed which can be understood in terms of size exclusion behavior.
Also some of the major limitations and drawbacks of this technique will be discussed, such as peak overlap or the broadening of signals in presence of the stationary phases as well as some methods for their circumvention.

3.1 Selection of candidates: Appropriate molecules for a proof of concept

One of the major limitations when performing DOSY studies are overlapping peaks [21, 93]. It is such a limiting issue when trying to perform successful DOSY experiments that not only additions have been made to the DOSY pulse sequences to try to solve this issue such as pure shift [101]–[105] but also methods to preprocess the data collected have been developed to enable the optimization of the spectrum obtained [104, 105]. However, some of the improvements such as pure shift NMR come at a high cost, in order to reduce the broadening of the signals the J-coupling information is removed and the sensitivity is greatly reduced [99, 100].
Therefore, in order to avoid using the techniques presented in the previous paragraph unless is strictly necessary, it is important to try to select the right molecules for a proof of concept for SEC-DOSY studies. Hence, it is of vital importance to keep in mind the overlapping peaks limitation. In addition, the interactions that are meant to vary the diffusion coefficient of molecules in this chapter must be related to the size of the molecules. Thus, in this section the experiments that provided an optimum selection of candidates and properties are described and presented.
Since the aim of the studies are to investigate SEC-DOSY, it is needed that the variation of the diffusion coefficient of the analytes is related to the different sizes of the molecules when they are in presence of a size exclusion stationary phase. Therefore, it is important that the molecules used, are large, have similar inter and intramolecular interactions and can be found in a wide range of different sizes. Therefore, polymers which are molecules formed of repeating units

(monomers), are the perfect molecules to show large molecules with a wide range of sizes keeping similar inter and intramolecular interactions and one polymer can be found in readily attainable different sizes.

Finally the last limitation imposed when selecting candidates for the study is that they must be soluble in water and this is due to two different reasons. Firstly most of the size exclusion stationary phases are designed to work in water as a solvent which is an important issue as it reduces the range of solvents that can be used for investigating SEC-DOSY and the amount of molecules that could be used for the studies due to solubility problems. Secondly, during the past thirty years, the awareness of the damage that the humans cause to the environment in the society where we are living have been growing. This fact have led the chemical industry to follow the green chemistry movement in order to reduce their impact in the environment [108]. Thus, water is the greenest of solvents because it does not produce any contamination and it is not necessary to be treated for its disposal. In addition, it is the most common solvent in natural processes. Therefore, for the two reasons discussed among this paragraph, a characteristic of all the candidates used to perform the experiments along this chapter to investigate SEC-DOSY, was to be soluble in deuterated water (D_2O). This constraint, limited greatly the eligible candidates as the most sensitive nucleus to be studied by NMR is ^1H and most of the molecules that possess a great amount of ^1H nucleus are molecules with an organic scaffold. Hence, due to their low polarity large organic molecules are not very soluble in water.

3.1.1 Selection of candidates: Parameter optimization

The preparation of samples for diffusion studies can be a challenging process. In addition to the size of the molecules, there are different factors that need to be considered which can strongly vary the diffusion coefficient of polymers, such as concentration, viscosity, temperature and shape of polymers [109]. Most of these factors will be varied in the different experiments presented on this chapter in order to find which ones are optimum for the studies. The temperature is the only factor that will remain the same in all the experiments 298K.

In reference to the characteristics of a DOSY NMR experiment, different pulse sequences can be used. However, the general way to obtain the diffusion coefficients is achieved through the study of the attenuation produced in the signals after varying some parameters of the pulse sequence. A set of ^1H-NMR experiments is acquired varying some of the parameters that appear in equation 3.1. Using the attenuation along the set of experiments the diffusion coefficient is calculated by fitting the equation 3.1 to the experimental data.

$$I_g = I_0\, e^{\left[-(\gamma\delta g)^2 \times D \times \left(\Delta - \frac{\delta}{3}\right)\right]} \quad (3.1)$$

Where I_g is the intensity of the signal, I_0 is the intensity of the signal without any gradient applied, γ is the gyromagnetic ratio of the observed nucleus, δ is the duration length of the gradient applied, D is the diffusion coefficient, g is the strength of the gradient applied and Δ is the diffusion labelling time.

The NMR pulse sequence used to perform the studies along this chapter was Oneshot [27]. There are three parameters which can be varied to measure the diffusion coefficient. First the range of applied gradient strength which was chosen to be 16 increments increased linearly by g^2 from 0.0452 to 0.5650 T. Secondly, the diffusion delay (Δ) which is the period that the molecules used to diffuse freely between the two spatial encoding gradients. If Δ time period is long the attenuation of the signal due to T_1 is increased. Therefore, in order to reduce influence of T_1 on the attenuation of the signal, and ensure that the attenuation is caused by the diffusion of the molecules, it is preferable to use short diffusion delays (Δ). Thus, this parameter was set to be 50ms. Finally, the gradient length (δ) which is the time that the gradient pulses are applied for. Long gradient lengths produce a big error in the diffusion coefficient measured, due to a faster decay and consequently, poor signal to noise ratio. Therefore, this time was set to be 2ms. The combination of these parameters was useful because allowed a limited reduction in the intensity of D_2O (used to reference the spectrum) in the first increments and a good signal decay for the studied polymers along the 16 increments. All these parameters were set following the experiments previously performed by Joyce and Day [66].

3.1.2 First candidates: Electrostatic problems

As mentioned above one of the major issues when performing DOSY-NMR experiments is the overlapping peaks. The diffusion coefficient of molecules is obtained through an attenuation of the NMR signal in the spectrum after an evolution period, so, if there are two or more overlapping signals in the spectrum, the diffusion coefficient obtained will be an average diffusion coefficient of the molecules that are showing the overlapping signals. In order to prevent this problem it is useful to choose candidates (figure 3.1) that show signals in different parts of the spectrum. Therefore, the first polymers selected to perform a well resolved DOSY experiment in the spectral dimension were an aromatic polymer like Poly (Styrene Sulfonate) (PSS) (signals shown between 6-8 ppm) that had already shown ability for SEC studies [1] and a polymer with an amine functional group such as Polyallylamine (Paa) (signals shown between 1-

3 ppm) which their ^{1}H-NMR spectrums are shown in figure 3.2. Both of these polymers show additional signals due to the CH_2 backbone of the polymer. However, these signals have no interest in the performed studies as the signals produced by the backbones of the two different polymers will appear on the same region of the spectrum and they will probably show overlapping between them.

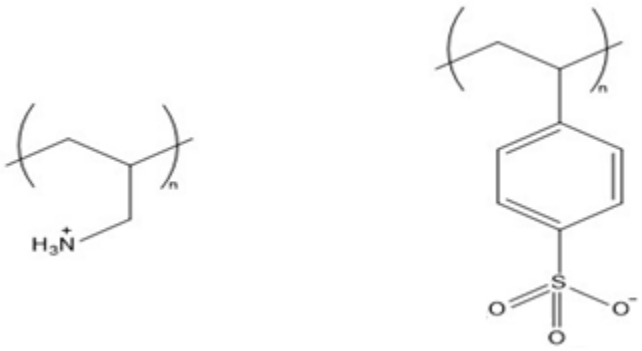

Figure 3.1: Poly (allylamine) (Paa) (left) and Poly (Styrene Sulfonate) (PSS) (right) repeating units

Following the studies done previously by Joyce and Day [1], the diffusion modulating effects that are studied in this chapter are expected to be explained through the interactions between the molecules and the stationary phase, and how different are these interactions when the particles have different sizes. However, the possibility of the molecules to explore the stationary phase depends on the size of the pores of the stationary phase (see table 2.1) and the size of the molecules. Hence, to simplify as much as possible the first results, one of the candidates will fit into the pores but will still be big enough to show interaction with the stationary phase. Therefore, should be strongly affected by the stationary phase and vary its diffusion coefficient, while the other candidate will not fit into the pores and the interaction with the stationary phase should be minimum, which should be shown by either no variation or a very slight variation in the diffusion coefficient. Therefore, the molecular weights of the chosen candidates differ significantly (PSS Molecular weight: 70,000 Da and Paa Molecular weight: 15,000 Da). In addition to the molecular weight, concentration and temperature, the diffusion coefficient of the polymer will also be determined by the shape of the molecule [109]. Since both of these polymers are charged when dissolved in water, a high ionic strength buffer solution was needed to be added to eliminate chain expansion effects due to the polyelectrolyte in solution [108, 109].

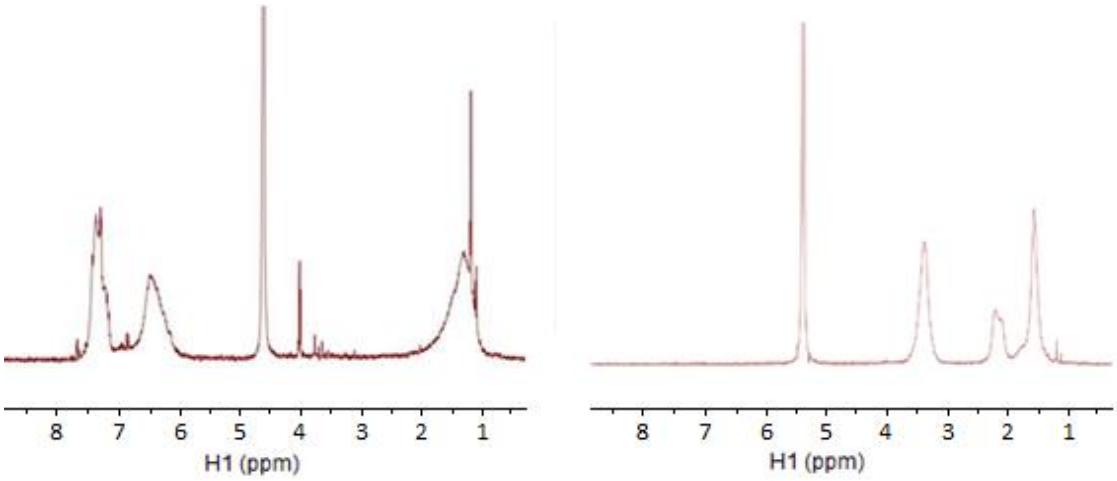

Figure 3.2: ^{1}H-NMR spectrum 0.1 % w/w of 70 kDa Poly (Styrene Sulfonate) (left) and 15 kDa Poly (allylamine) (Right) in D_2O with 25mM NaCl buffer

The diffusion coefficient of each polymer was measured at 25°C through a DOSY-NMR experiment (figure 3.4) in a set of samples with 0.1 % w/w of polymer and a range of NaCl concentrations 25, 50, 75, 100 and 150 mM, the results are shown in figure 3.3.

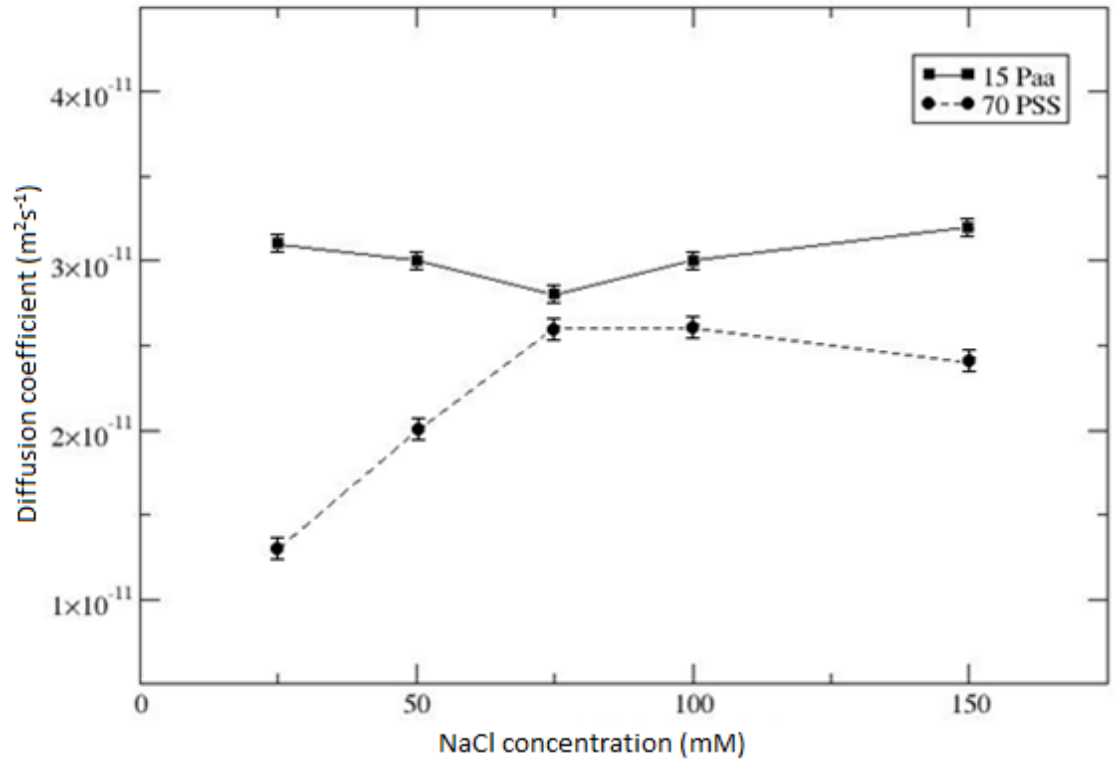

Figure 3.3: Diffusion coefficients of separated 0.1 % w/w 15 kDa Poly (allylamine) (1.95 ppm) and 70 kDa Poly (Styrene Sulfonate) (7.48 ppm) polymers in presence of different concentrations of NaCl in D_2O

Looking at figure 3.3 the candidates seem to behave as it would be expected by two molecules of significant different sizes, because the smaller molecule moves faster than the bigger one which suggest that they could be good candidates to perform SEC studies. However, it can be observed that while Paa diffusion coefficient remains very similar at the different NaCl concentrations, PSS diffusion coefficient increases until the concentration is up to 75 mM. This is probably due to changes in the shape caused by intramolecular electrostatic forces, only when the concentration of salts is high enough the molecules are completely surrounded by counter ions that ensure a uniform shape of the molecules. Therefore, suitable conditions for the experiment are 0.1 % w/w of polymer and NaCl concentration above 75 mM in D_2O. To make sure that the candidates are suitable for the study it is needed to see their diffusion coefficients when they are in a mixture to make sure that there is no entangling or interaction between them that will interfere with their diffusion. The behaviour should be very similar, possibly a bit slower due to the presence of both polymers and changes in the viscosity. For this reason, it is advisable to put an upper limit to the concentration of polymer used.

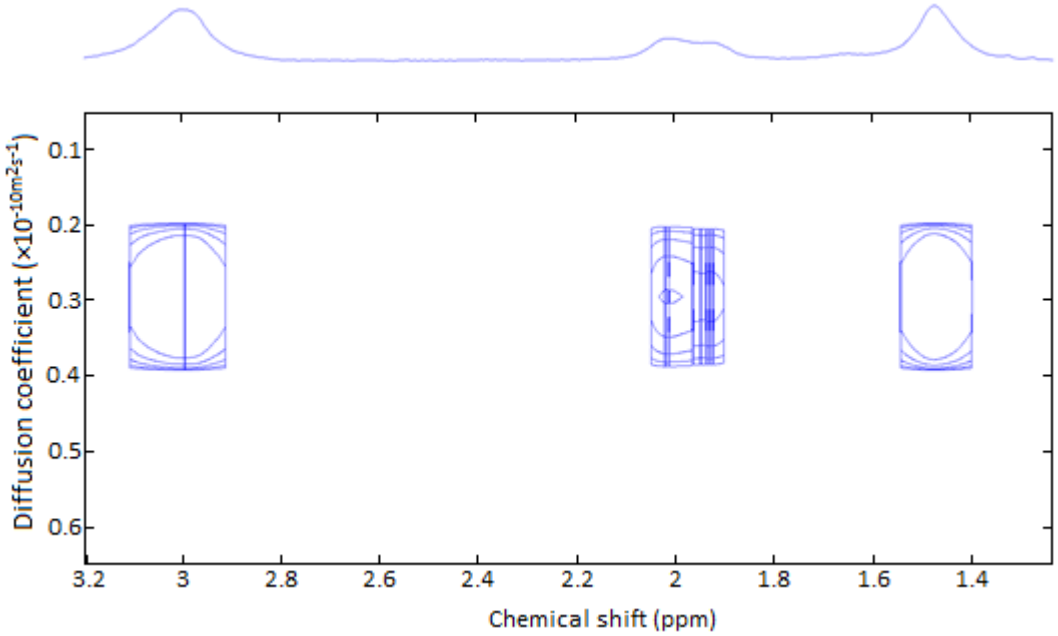

Figure 3.4: DOSY-NMR spectrum of 0.1 % w/w of 15 kDa Paa in 25 mM NaCl buffer in D_2O, the protons next to the N appear at 3ppm, the proton from the ramification of each monomer appear at 1.98ppm and the aliphatic protons from the main chain appear at 1.5 ppm

When the mixture of the two polymers was prepared, a white solid was formed in all the samples and only the Paa was observed in the NMR spectra. In order to know whether the two polymers precipitate because of the difference in their charges or only the PSS was in the formed solid, similar experiments were repeated with an excess of PSS. This time the same white solid was formed but PSS appeared now in the NMR spectra of the mixture. This result suggested that both polymers are soluble when they are free in D_2O. However, when they are in a mixture with

a polymer that has a chain with a net charge of different sign both polymers form an aggregate that is not soluble in D_2O. The results are in agreement with the work done with polyampholytes, that are polymers that carry positively as well as negatively charged groups, by Everaers et al. [112] and Dobrynin et al. They discussed:

> "The solubility of polyampholytes and the composition of solutions at finite concentration. For ordinary polyelectrolytes, which carry charges of only one sign, the water-solubility is mostly due to the gain in translational entropy of the counter-ions in the water phase. The polymers are dissolved in spite of their high electrostatic self-energies, which they minimize by adopting stretched conformations. In contrast, polyampholyte samples can be self-neutralizing, thus resembling mixtures of oppositely charged polyelectrolytes. One can, therefore, expect the formation and precipitation of neutral complexes at finite concentrations."[113].

In the case of our studies the combination of two polyelectrolytes with a net charge of opposite sign in solution seem to reproduce the behaviour seen in polyampholytes where a neutral complex is form. In order to solve this issue higher concentrations of buffer were tried up to 3 M to see if the buffer could act as an electrostatic screen and if it was possible to prevent the polymers from interacting with each other. However, it was impossible to obtain a mixture where both of them remained in solution at the same time. For this reason these polymers are not suitable for proof of concept for SEC studies in a mixture together.

3.1.3 A solution for the electrostatic problems: Neutral polymers

The use of neutral polymers presents a great number of advantages compared to charged polymers when SEC studies are tried. The main advantage is the reduction of possible electrostatic interactions as there are no charges that will have an influence not only in the shape of the polymers in solution but also can vary the diffusion coefficient. Instead, the electrostatic interactions will be caused by dipole-dipole interactions between the electric dipoles formed by the different functional groups in each polymer. Dipole-dipole interactions are much weaker than the interaction produced between electrolytes and they diffusion coefficient will be less affected by them. The reduction in the interaction between the polymers makes easier to explore the interaction between the stationary phase and the molecules. Another small advantage is that no buffer is needed reducing the amount of chemicals needed to prepare the samples.

However, there is a major disadvantage when neutral polymers are used. This disadvantage is their solubility in water. Due to their organic nature it is hard to find candidates that are soluble

and do not show signals that will not overlap as the signals shown by each of the polymers will likely appear showing similar chemical shifts. After looking at the already available commercially neutral polymers, the suitable polymers chosen are shown in figure 3.5.

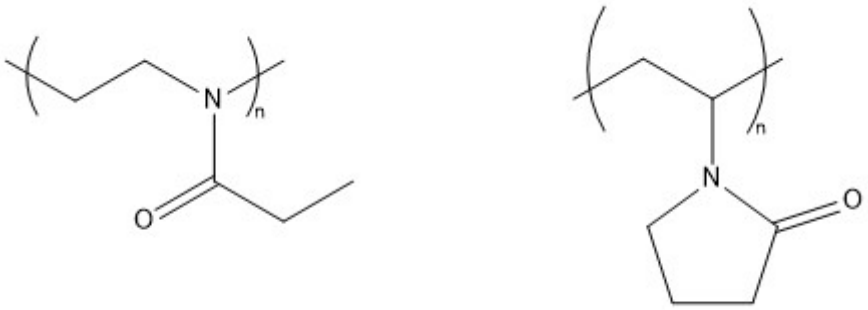

Figure 3.5: Poly (2-Ethyl-2-Oxazoline) (PEO) (left) and Poly (Vinyl Pirrolidone) (PVP) (right) repeating units

These polymers are good candidates because they show signals in different regions of the spectrum (figure 3.6) and because it was possible to find weights that differed significantly from each other such as 10 kDa PVP and 50 kDa PEO.

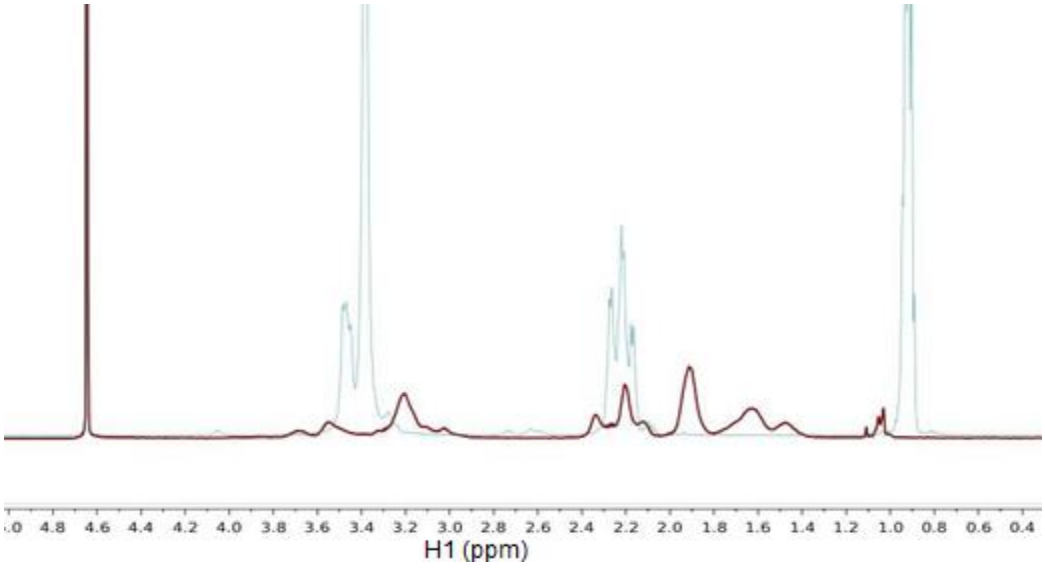

Figure 3.6: Superimposed ^{1}H-NMR spectrum of 0.5 mM 10 kDa PVP (red) and 0.5 mM 50 kDa PEO (blue) in D_2O

As it was mentioned above, the shape of the polymers is going to depend mainly on intermolecular interactions such as dipole-dipole and van der waals forces and concentration.

Therefore, the diffusion coefficients of the polymers where measured at different concentrations in D_2O but not in a mixture to see if the behavior when they are in solution is the expected one to perform SEC-DOSY studies. The diffusion coefficient of these polymers is shown in figure 3.7.

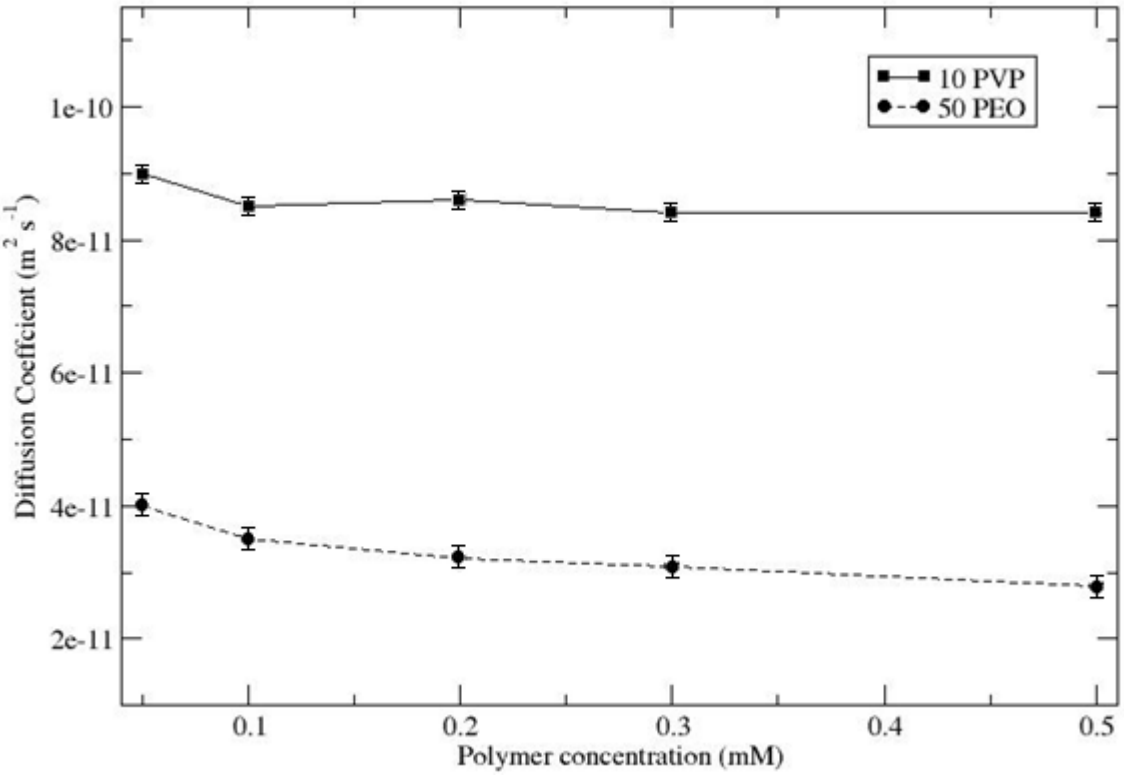

Figure 3.7: Diffusion coefficients of 10 kDa Poly (Vinyl Pirrolidone) (PVP) (from analysis of signal at 1.95 ppm) and 50 kDa Poly (2-Ethyl-2-Oxazoline) (PEO) (from analysis of signal at 1.06 ppm) when they are not in a mixture and varying their concentrations in D_2O

The data presented in figure 3.7 showed exactly what was expected. Firstly, the larger polymer diffuses more slowly than the smaller one which is consistent with the Stokes-Einstein relationship as the radius of the molecule is inversely proportional to the diffusion coefficient. Secondly both polymers show a major decrease in the diffusion coefficients from 0.05 to 0.1 mM when the concentration increased from the polymers barely interacting with each other when the overlap concentration of the polymer has not been reached yet, to a continuous interaction after this point, where the overlap concentration has been reached and therefore the diffusion coefficient decreases slowly with the increase of concentration. Although the same behavior was expected for both polymers, it can be seen that PEO seemed to be more affected by the concentration increase than PVP. This fact suggests, that apart of the gradual reduction produced in the diffusion coefficient when the concentration is increased after the reach of the

overlap concentration of the polymer, where molecules reduce their diffusion coefficient due to a large intermolecular interaction produced by a crowded solution, there is another factor contributing to the reduction of the diffusion coefficient as it was experiencing a much larger reduction compared to the PVP polymer. This factor was the viscosity of the solution. It was observed that higher concentrations of PEO increase the viscosity significantly, the change could be estimated by eye while filling the tube. In contrast this change could not be appreciated when PVP concentration increased. Nevertheless, this issue was not a problem because the aim is to study the diffusion of both polymers when they are in a mixture. Hence, the viscosity that each of the polymers will experience when they are in a mixture in the same solution will be the same, as they are in the same solution, and when the concentration of the polymer varies both polymers will be affected by the same viscosity as opposed to measurements when they are separated where the increased of concentration would suppose a larger viscosity for one compare to the other.

After discarding the lowest concentration because of signal intensity problems when recording the diffusion coefficient, it was needed to make sure that there was not any entanglement or interaction between the polymers when they are on a mixture and verify that a possible peak broadening of the signals would not cause overlap or there would be at least one peak of each polymer not showing any overlap (Figure 3.6).

The diffusion coefficient was now measured for the same range of concentrations in a mixture of the polymers in D_2O, the data collected are show in figure 3.8.

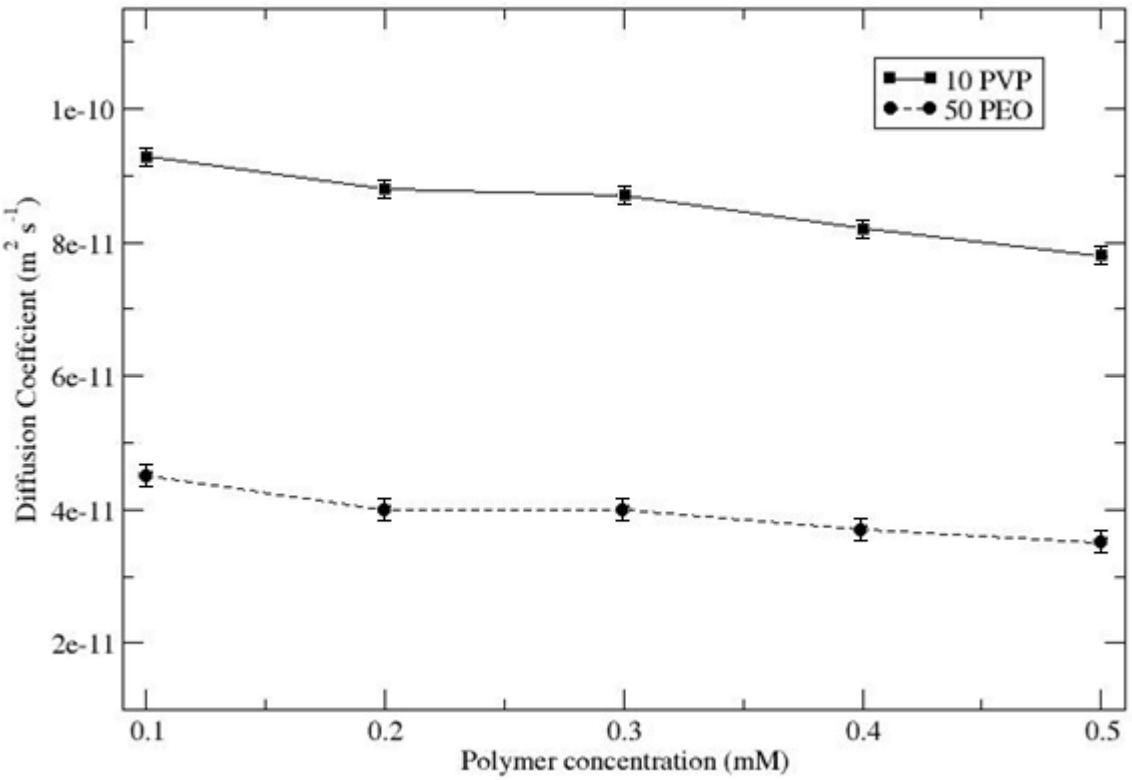

Figure 3.8: Diffusion coefficients of a mixture of 10 kDa PVP (from analysis of signal at 1.95 ppm) and 50 kDa PEO (from analysis of signal at 1.06 ppm) varying their concentrations in D_2O

The behaviour of the polymers when they are in a mixture is similar than when they are free in solution. The small variations observed in each of the polymers when they are compared to the diffusion coefficient out of the mixture, can be explained by the different viscosity experience when they are in a mixture as it was discussed previously. Therefore, when samples of 10 kDa PVP not in a mixture were prepared, there could not be observed major changes in the viscosity while the concentration increased. Conversely, the samples containing 50 kDa PEO experienced a very noticeable increase of their viscosity, notice by eye while filling the tube, when the concentration was increased. Therefore, when both polymers are in a mixture the viscosity experience by the polymers is different to the one they experienced when they were separated, being larger for PVP and smaller for PEO, this changes are even more noticeable at higher polymer concentrations. When the concentration of polymers was low the viscosity in the mixture was similar to the viscosity experienced by each polymer when they were not in mixture. However, at higher concentrations the viscosity that the PVP experienced was higher in the mixture than separated and vice versa for the PEO polymer. For this reason PVP diffusion coefficients are lower at high concentrations in a mixture and PEO diffusion coefficients are larger than out of the mixture. As it was mentioned previously the changes in viscosity were so noticeable that could be estimated by eye when filling the tube.

The previous experiments suggested that these candidates are a good choice in order to perform SEC-DOSY studies. Their diffusion behaviour is the expected one and if there is any type of interaction between them it does not seem to interfere with the size exclusion principles. Last but not least the requirements of overall signal intensity and non-overlap of the signals to develop a successful DOSY experiment are met so far (figure 3.9) Hence, the next step was the addition of a stationary phase to perform the SEC-DOSY experiments.

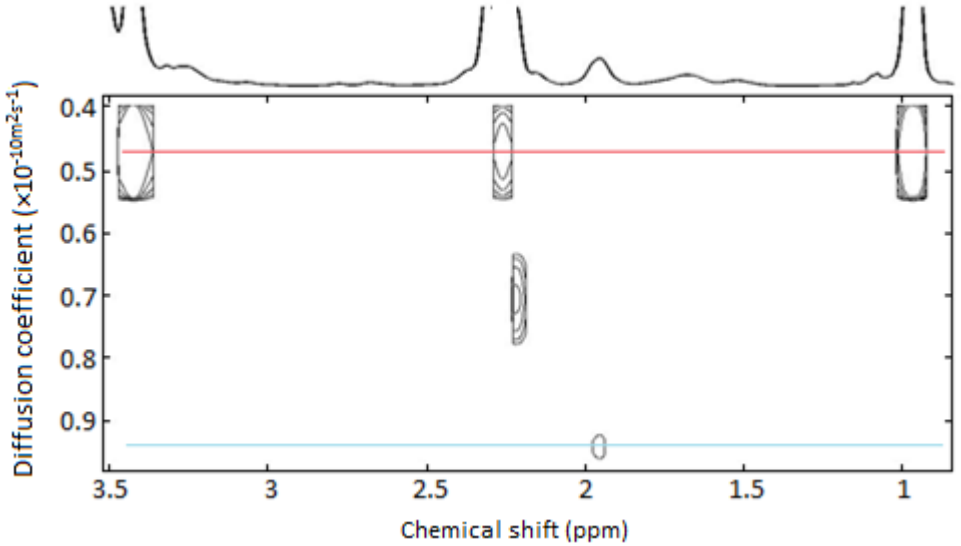

Figure 3.9: 0.1mM mixture of 10 kDa PVP and 50 kDa PEO in D_2O. The straight lines show the diffusion coefficient of the signals of interest. Red for PEO and blue for PVP

The stationary phase chosen was Sephadex G-50 which is comprised of crosslinked polydextrans [84]. The reason of choosing this stationary phase is that it is water-compatible and designed for water to be used as the mobile phase, also their pore size range allow molecules from 1.5 to 30 kDa, which will allow PVP (10 kDa) to interact efficiently with the stationary phase but will not be big enough for a good interaction with PEO (50 kDa). Therefore, a big change in diffusion coefficient would be expected for PVP while a very small change would be expected for PEO.

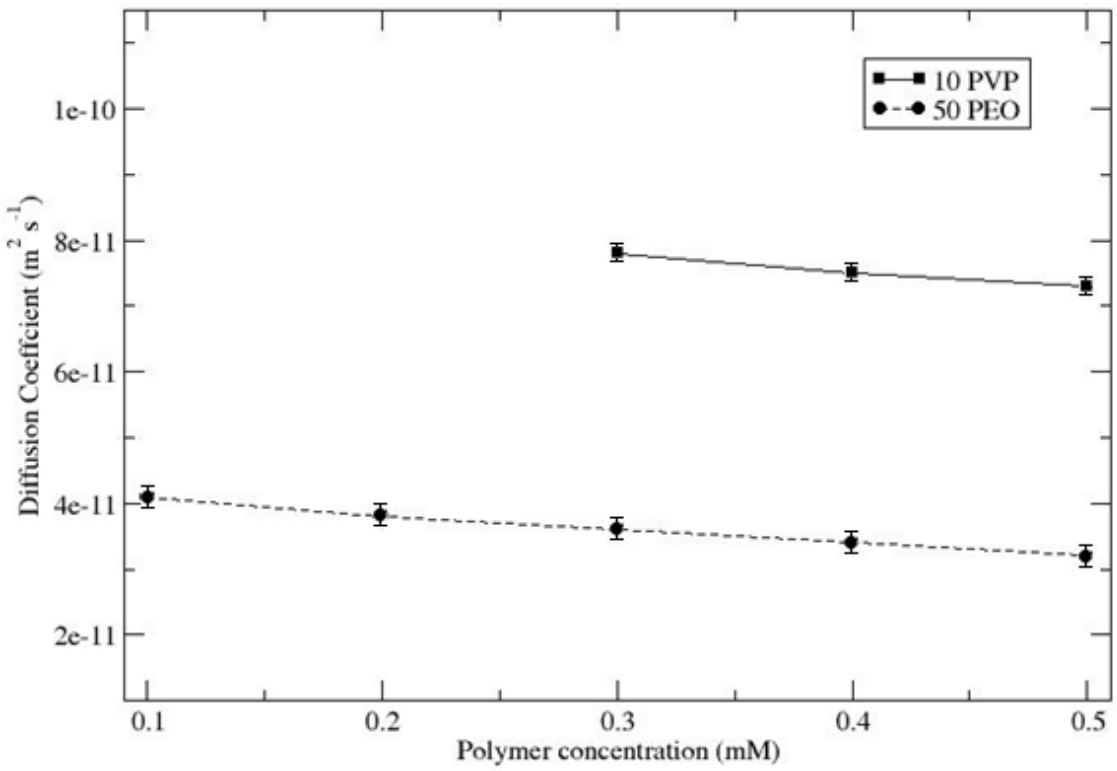

Figure 3.10: Diffusion coefficients of a mixture of 10 kDa PVP (1.95 ppm) and 50 kDa PEO (1.06 ppm) varying their concentrations in D_2O in presence of Sephadex G50. Two data points not shown due to low concentration that impeded correct recording of the diffusion coefficient

Sephadex G50 was added to the mixture and the diffusion studies were repeated to see if it is possible to reproduce the successful SEC-DOSY results in free polymers [3] when the sample is formed by a mixture. The results of these experiments are shown in figure 3.10.

The addition of a stationary phase to the samples produces not only overlapping signals between the particles and the stationary phase, but also as happens in solid state NMR due to the slow tumbling of the molecules, the molecules in the mixture in presence of the stationary phase experienced a limitation in the free motion as well as differences in the magnetic susceptibility [39] which affected the relaxation of the magnetic moments of the nucleus causing broadening in all the signals. Therefore, looking at figure 3.10, the first requirement to develop the studies is that in order to have the signal intensity required after the broadening of signals, the concentration must be kept higher than 0.3 mM otherwise the diffusion measures are not accurate enough because the intensity of the signals is very low.

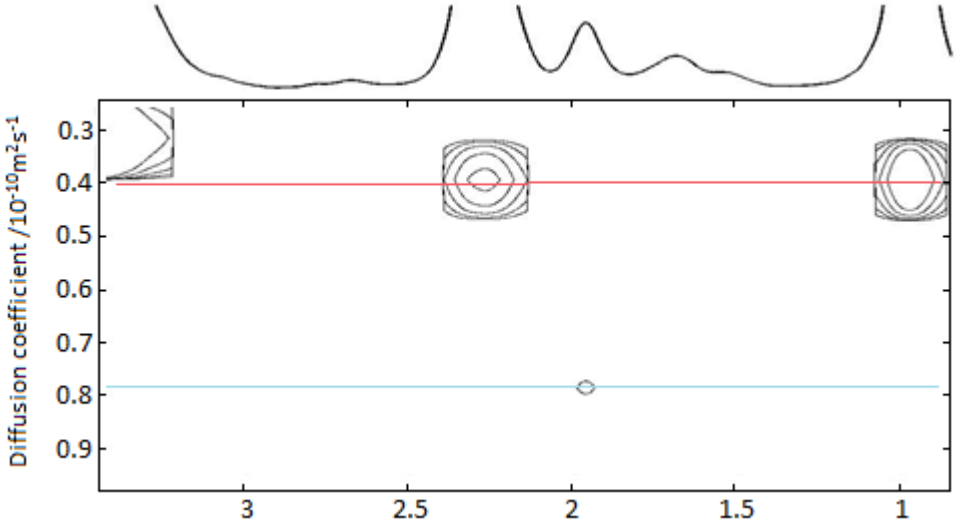

Figure 3.11: 0.3 mM mixture of 10 kDa PVP and 50 kDa PEO in D_2O in presence of Sephadex G50. The straight lines show the diffusion coefficient of the signals of interest. Red for PEO and blue for PVP

Once the concentration issue discussed above is solved by keeping it above 0.3 mM, the results fit with what it is expected from a SEC study. Firstly the diffusion of both polymers (PVP and PEO) has decreased. In addition, the reduction in the diffusion coefficient experienced by the polymers is big enough to conclude that there is an interaction with the stationary phase although is not a huge reduction. This fact means that the interaction that seems to be happening is due to the size and not to other stronger dipole-dipole interaction caused by the functional groups of the polymers. Secondly, the smaller polymer diffuses faster than the bigger one both with and without stationary phase. However, it fits better on the pores of the stationary phase and the interaction between this polymer and the stationary phase is more effective than the interaction between the larger polymer and the stationary phase. This fact lead to a major reduction in the diffusion coefficient for the smaller polymer than for the larger one as it is expected in size exclusion.

So far these candidates have been suitable for the studies and have given a proof of concept to the possibility of performing SEC-DOSY studies on mixtures.

The last step to see if they are suitable candidates and if they will be the chosen ones to carry one with more complete SEC studies using the same polymer structures but with a set of polymers that will have a range of different molecular weights is to repeat the experiments to analyse the mixture in presence of different stationary phases. This way we will make sure that the diffusing behaviour observed before is not due to an anomaly with the Sephadex G50 but that is also possible with other stationary phases that have different pore size and slightly

different chemical structure, and therefore, that will interact slightly different with the molecules in solution.

The Stationary phases chosen for these experiments are Superdex 75 and Superdex 200 which consist of dextran covalently attached to highly cross-linked agarose [85]. This stationary phases were chosen because they were used in previous studies [1] and would be good to compare results. The difference between the two stationary phases are the size and amount of pores in the stationary phase (see table 2.1).

As it was described in the methods section the stationary phases are set under gravity. In order to have accurate and reproducible results it is needed that the stationary phase is set always following the same procedure to ensure that there is always the same ratio solvent-stationary phase in the sample. Unfortunately, although these phases were used before, this time after the two Superdex stationary phases were let to set under gravity they allowed a smaller amount of solvent into the pores than Sephadex G-50, possibly because the use of different polymers made the solvent show different viscosity. This difference made impossible to obtain a correct shimming of the sample. Therefore, this issue led to major overlapping and broadening of the signals. Consequently, it was impossible to perform the SEC-NMR experiments and record trusty measurements of the diffusion coefficient of the polymers, see figure 3.12.

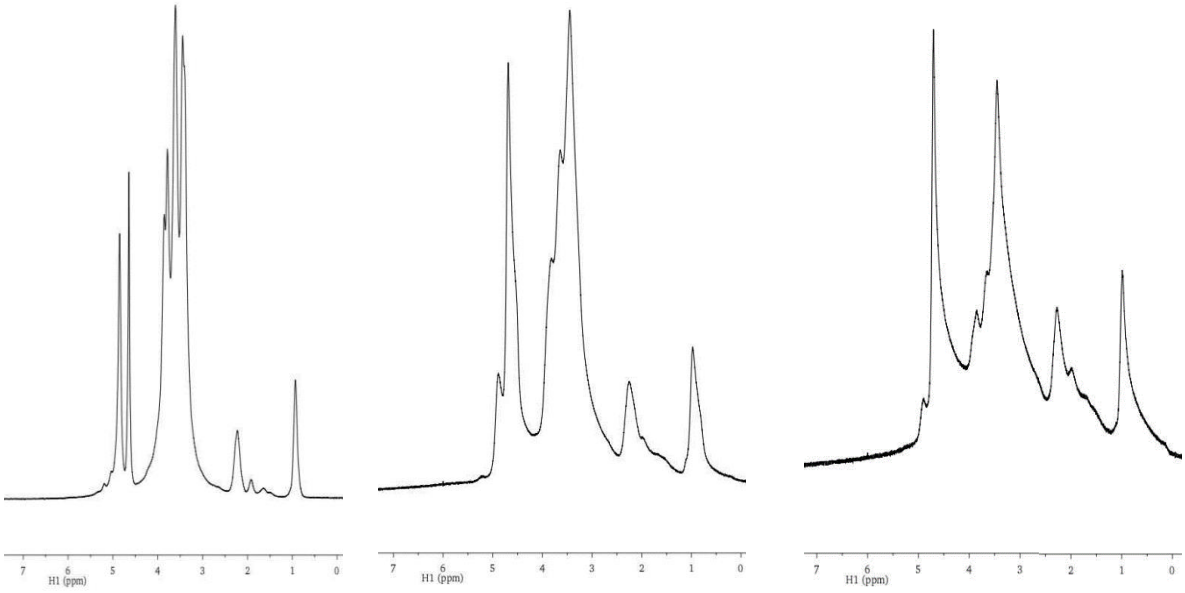

Figure 3.12: ^{1}H-NMR spectra of a mixture 0.3 mM each polymer 50 kDa PEO + 10 kDa PVP with SephadexG50 (left), Superdex75 (middle) and Superdex200 (right)

3.1.4 Final candidates

The neutral polymers used so far have shown that it is possible to perform successfully SEC-DOSY. Unfortunately, Sephadex G50 was the only stationary phase that yielded suitable data. In addition, the subset of readily available commercial neutral polymers that were tested in these studies showed signals that will overlap either with the stationary phase or the other polymer. Therefore, in order to avoid the two polymers precipitating due to the presence of opposite charges, polymers with the same overall electrostatic charge were chosen.

The polymers chosen were Poly (Methacrylic Acid) (PMA) and Poly (Styrene Sulfonate) (PSS) which are shown in figure 3.13. Series of polymer molecular weight reference standards of known polydispersity of PSS had been studied before by Joyce and Day using DOSY-NMR and in presence of Sepahdex G50 [1]. The variations produced in the diffusion coefficient could be understood in terms of size exclusion behavior and gave a proof of concept for SEC-DOSY studies. Another advantage of the polymer PSS is that shows signals in the aromatic region of the spectrum which is far away from the signals shown by the stationary phases. PMA was chosen not only because similarly to PSS it is negatively charged and avoids the issues seen previously when two polymers of net opposite charge were studied, but also because due to the methyl group will show signals in the low chemical shift aliphatic region of the spectrum which is also well separated from both the stationary phases and PSS.

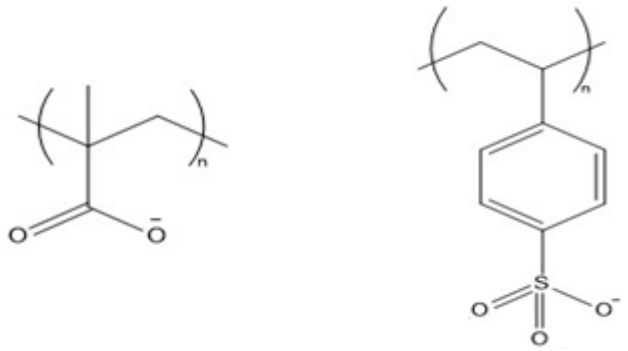

Figure 3.13: PMA (left) and PSS (right) repeating units

As it was discussed with the first candidates the presence of charge on the polymers can determine the shape and the interactions of the polymers with each other and the stationary phases. Therefore, a buffer was needed so that the polymers will always have the same shape and ensure that the electrostatic interactions will always be very similar [114]. Therefore, the buffer chosen was 150 mM NaCl and 50 mM Na_3PO_4 (prepared as described in chapter 2). This buffer was chosen for two different reasons, Firstly, because it was suggested by literature [110], [111] and secondly because it has already been used by Joyce and Day with successful results

[1]. In addition, for size exclusion chromatography salt buffer is recommended to reduce ionic interactions between the analytes and stationary phase [115]. In addition, when the ionic strength is increased in the solution, the chain expansion of polyelectrolytes decreases [110], if the solution is neutral, such as D_2O, the ions on the charged polymer backbone experience Coulomb repulsion producing chain expansion and a decrease in the diffusion coefficients due to the larger polymer size. To make sure which was the most suitable polymer concentration to perform SEC studies the diffusion coefficient of the polymer was measured at a range of concentrations varying from 0.1 mM to 0.5 mM in presence of buffer (150 mM NaCl and 50 mM Na_3PO_4) at 25ºC. The results are shown in Figure 3.14.

As it was expected there was a slight decrease in the diffusion coefficient due to changes in the shape of the polymers when the concentration increases until the point in which molecules started interacting with each other where the diffusion coefficient decreased significantly. Therefore, the best conditions to carry the SEC-DOSY experiments is keeping the concentration at 0.2 mM to make sure that the molecules of the polymers are not hindering themselves and they are not saturating the pores of the stationary phase.

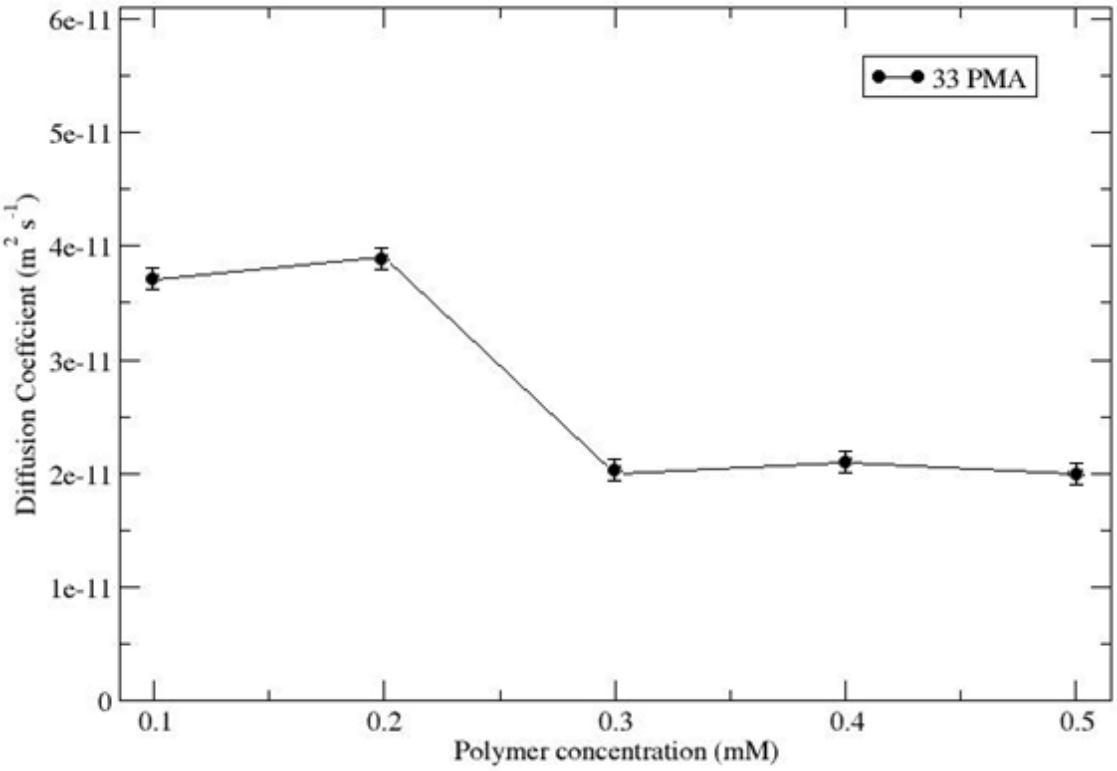

Figure 3.14: Diffusion coefficients of 33 kDa PMA (0.98 and 0.88 ppm) varying their concentrations in 150 mM NaCl + 50 mM Na_3PO_4 buffer

In order to carry SEC-DOSY studies and ensure that no other effect different than the size is causing the variation in the diffusion domain, it is needed to perform the experiments using one

polymer with a range of molecular weights and low polydispersity. This will show two advantages, first the use of the same polymers varying the size will ensure that any effect that the polymers will experience will be the same in the other samples with the exception of the size and second in polymer chemistry, polydispersity is a measure of the distribution of molecular weights present in the sample [116]. Hence, low polydispersity will ensure more accurate diffusion measurements as the polymers that the sample contain have all similar sizes. Therefore, as Joyce and Day [1] did in their previous work with PSS, where they measured the diffusion coefficients of a set of PSS polymer with different molecular weight with and without sephadex G50, a set of polymers of different molecular weight of PMA was selected to study their behavior in presence of the stationary phase but keeping the molecular weight between the two sets of PMA and PSS in a similar range.

In the previous proof of concept studies made by Joyce and Day [1], PSS diffusion properties were modulated using three different stationary phases, Sephadex G50, Superdex 75 and Superdex 200. When one assumes infinite dilution for a spherical molecule, the Stokes-Einstein equation (see equation 1.22) shows how the diffusion coefficient is inversely proportional to the size of the molecule. Hence, as it was expected, the results showed a size-dependent effect with smaller molecules diffusing faster than bigger molecules without stationary phases. This behavior could also be observed when the stationary phases were added. However, smaller molecules varied their diffusion coefficient more than the bigger ones, as would be expected in size exclusion due to the longer time that small molecules spend exploring the pores of the stationary phase. Therefore, the same experiments were repeated with the PMA set of polymers.

The results of the diffusion experiments with the PMA samples with and without Sephadex G50 and Superdex 75 are shown in figure 3.15. The data clearly show similar trend to the PSS samples studies previously by Joyce and Day [1]. Without stationary phase the diffusion coefficients is larger for smaller molecules and decrease while increasing the molecular weight in agreement with the Stokes-Einstein equation (see equation 1.22). After the addition of stationary phase a decrease in the diffusion coefficient can be noticed with larger changes in the smaller the molecules. This behavior is consistent with the size exclusion principles, where in presence of the stationary phases the smaller molecules will spend a longer time in the pores interacting with the stationary phase and this fact will be shown by a reduction in the diffusion coefficient (see figure 1.1). Meanwhile, the bigger molecules would not fit into the pores and will experience less interaction with the stationary phase. Therefore, the diffusion coefficient is more affected in smaller molecules than in the larger ones.

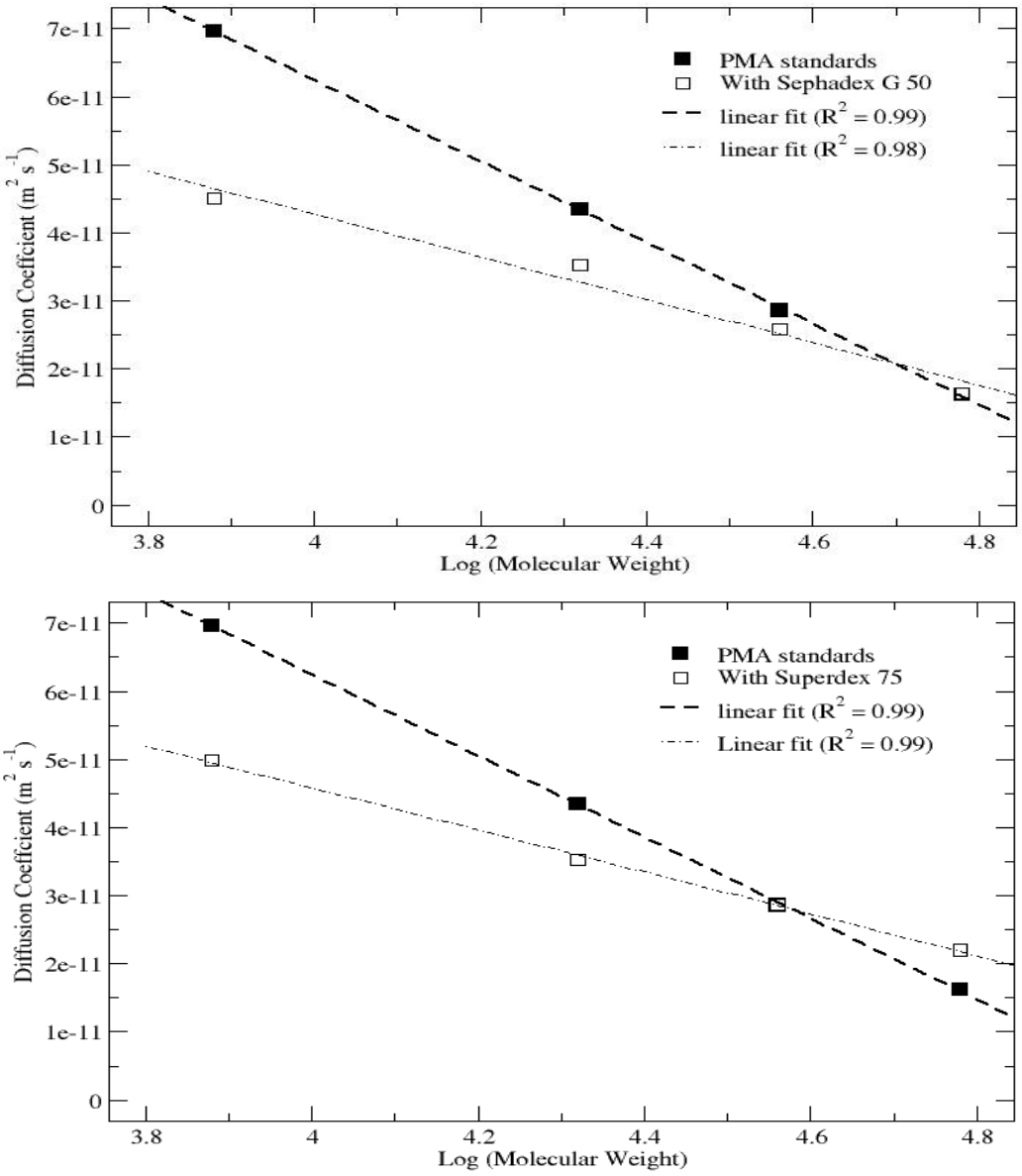

Figure 3.15: Diffusion coefficients for some PMA molecular weight reference standards in the presence and absence of Sephadex G50 (top) and Superdex 75 (bottom). The straight lines are the result of fitting Equation (3.2) to the experimental data

Following the studies that were done before [1] the data were interpreted in terms of an empirical equation similar to the one used by Anderson and Stoddart [115, 116] and Determann and Michel [119]. The equation is as follows:

$$\log Mw = a_0 - a_1 D \tag{3.2}$$

where M_w is the weight-average molecular weight and D the measured diffusion coefficient. The data were fit to a phenomenological straight line given in equation 3.2.

The results of fitting the PMA data from figure 3.15 to the previous equation (3.2) are presented in table 3.6, as well as the results of PSS that were determined in previous studies [1] for comparison.

Sample	**a_0**	**$a_1/10^{-10}$ s m^{-2}**	**R^2**
PMA only	5.05	1.68	0.99
PMA Sephadex G50	5.36	3.19	0.98
PMA Superdex 75	5.49	3.25	0.99
PSS only[1]	5.11	1.50	0.96
PSS Sephadex G50[1]	5.30	2.52	0.94

Table 3.6: Parameters returned from fitting equation (3.2) to the data in Figure 3.10 the data for PSS are from Joyce and Day [1]

Both set of polymers PMA and PSS contain molecules that could be paired between each set as they have similar sizes and similar polydispersities (e.g. 60 kDa PSS and 63.9 kDa PMA). Hence, the results shown in table 3.6 are very similar both in presence and without stationary phase also a_0 remains very similar when adding the stationary phase while a_1 changes significantly, all these facts are in agreement with the expected size exclusion behaviour, a_1 represents the slope of the line described by equation 3.2. Therefore, large variations in the slope means larger interactions between some of the molecules than others, otherwise a_0 would vary but a_1 would remain similar. The small variations in the parameters of the equation 3.2 among the polymers can be explained by the differences in the interactions between the stationary phase and the aromatic (PSS) or the alkyl chains (PMA) [119 – 122]. This means that although both sets seem to show a size dependent change on the diffusing behaviour, the behaviour of both sets is not exactly the same, as the rest of the interactions (not size related) that are taking place between the stationary and the polymers are different. However, these variations are small compared to the main change of behaviour that is caused by the size.

The previous experiments have been repeated in presence of the stationary phase Superdex 200. However, as happened before with the neutral polymers, there were some issues when this stationary phase was present in the samples (see figure 3.12). Some of the samples could not be measured or were inaccurate due to a combination of bad shimming caused by the low amount of solvent allowed into the stationary phase after letting it set under gravity, low intensity of the signals of the polymers with low molecular weight and overlapping between the

signals of the polymers and the signals of the stationary phase. These issues did not affect that much when the larger polymers were used, as their signals were more intense.

The results presented so far suggested that PMA seemed to be a polymer that will allow performing SEC-DOSY in a mixture with PSS, because they showed signals in different regions of the spectrum that will not overlap, they are both polymers negatively charged in solution and therefore they will not precipitate when they are in a mixture, they are both compatible with Sephadex G-50 and their behavior with and without the stationary phase is in accordance with size exclusion principles, and they are readily available commercial polymers. Therefore, the next section will show experiments performed with a mixture of PMA and PSS.

3.2 SEC-DOSY of polymer mixtures

Most of the experiments performed so far, have shown that it is possible to change the diffusion coefficients of molecules through the use of size exclusion stationary phases when they are free in solution, as long as a good shimming of the sample is possible (some stationary phases made it hard) and there is no overlapping signals. However, if SEC-DOSY is expected to become a useful mixture analysis technique for chemist who perform routine lab analysis of mixtures, it is needed to explore if the changes of behaviour experienced by the polymers when a stationary phase is added are the same when the sample is a mixture of the polymers and therefore, if they are in accordance with size exclusion principles. Thus, in this section it will be investigated whether the presence of multiple species will have any influence in the ability of size exclusion stationary phases to modulate the diffusion properties of the molecules involved. To do so, the experiments performed in section 3.1 were repeated with an equimolar mixture of PSS and PMA paired by similar weight. For example 60 kDa PMA with 63.9 kDa PSS etc. The experiments were performed for each of the four pairs with and without Sephadex G50, the results are presented in figure 3.16.

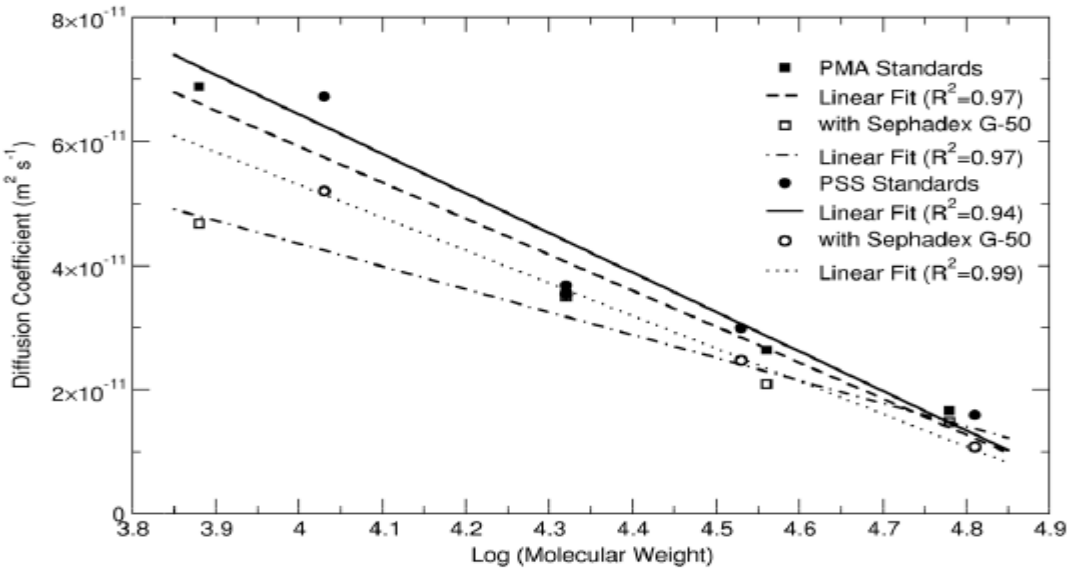

Figure 3.16: Diffusion coefficients for paired mixtures of PMA and PSS in the presence and absence of Sephadex G-50. The straight lines are the result of fitting equation (3.2) to the experimental data. Image adapted from reference [75]

In the absence of the stationary phase the diffusion coefficients observed were very similar to that obtained for the individual polymers at same concentrations, this fact suggest that there is not any entanglement or interaction between the different polymers that affect their diffusion at the concentrations studied. In order to compare the behaviour of the polymers in a mixture to the behaviour as individual polymers, the data shown in figure 3.16 were fitted using equation 3.2, the parameters obtained are shown in table 3.7 and can be compared with the parameters shown in table 3.6.

Sample	**a_0**	**$a_1/10^{-10}$ s m^{-2}**	**R^2**
PMA free	5.02	1.72	0.99
PMA Sephadex G50	5.18	2.72	0.97
PSS free	5.01	1.57	0.94
PSS Sephadex G50	5.00	1.90	0.97

Table 3.7: Parameters returned from fitting equation (3.2) to the data in Figure 3.16. Diffusion is free when is in the absence of stationary phase

Small differences could be noticed comparing the parameters a_0 and a_1 when they are in a mixture or as individual polymers in absence of the stationary phase, such as a_0 varies from 5.05

for PMA as an individual polymer to 5.02 for PMA as part of the mixture, there was a similar variation for a_1 from 1.68 to 1.72. This is probably due to some kind of interaction between the polymers such as the Coulomb repulsion between the charges, or due to slight differences in the viscosity of the sample [121, 122].

When the stationary phase was added, a significant change of the diffusion coefficients of the polymers was shown and as expected from size exclusion behavior the smaller polymers were more affected than the bigger ones. This means that the mixture did not affect the gross modulation effects in diffusion produced by Sephadex G50. When a_0 and a_1 values were compared between the mixture and the individual polymers, variations were not as big when they were on a mixture than with the individual polymers, in both cases a_0 stayed very similar with and without the stationary phases (e.g. a_0 for individual PMA varied from 5.05 without stationary phase to 5.36 with stationary phase and it varied from 5.02 to 5.18 in the case of the mixture). However, a_1 experienced a very big variation when analyzing the individual polymers and a smaller one when the polymers were in a mixture (e.g. a_1 for individual PMA varied from 1.68 without stationary phase to 3.19 with stationary phase and it varied from 1.72 to 2.72 in the case of the mixture). This can be explained by differences in the interaction between polymers and the stationary phase [119 – 122] as well as changes in the viscosity, which in traditional on flow SEC can be removed by calibration methods [125]. This time neither Superdex 75 nor Superdex 200 gave results for a whole data set for any of the polymers due to the shimming problems discussed in the previous section. Therefore, only the data with and without Sephadex G50 were fitted to equation 3.2.

To conclude this section, in order to further generalize the results presented, one last experiment was performed with a sample containing two different polymers with two different molecular weights. The sample was prepared with 20.3 kDa PMA and 63.9 kDa PSS. It was also prepared in a similar way to the samples used before keeping same concentrations and using the same buffer. A DOSY-NMR spectrum without the stationary phase is shown in figure 3.17 (right). Diffusion coefficients of both polymers can be seen in the aromatic and aliphatic regions of the spectrum. However, in between some signals show overlapping [126]. Hence, they show a diffusion coefficient in between of both polymers.

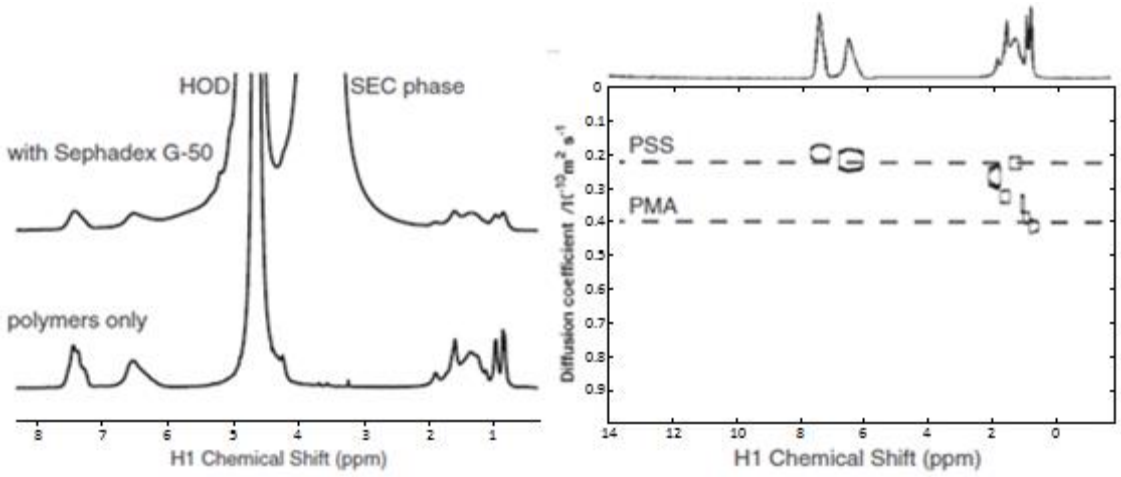

Figure 3.17: [1]H NMR spectra of a mixture of 20.3 kDa PMA and 63.9 kDa PSS in the absence and presence of the Sephadex G-50 stationary phase (left). DOSY spectrum of the same mixture in the absence of the Sephadex G-50 stationary phase (right) image adapted from reference [75]

A ^{1}H-NMR spectrum in presence of the stationary phase is also shown in figure 3.17. It can be observed that although the addition of the stationary phases broad the signals it is still possible to collect a well resolved spectrum.

A DOSY-NMR experiment of the mismatched mixture was performed free and in presence of the three different stationary phases: Sephadex G50, Superdex 75 and Superdex 200. However, as happened previously only Sephadex G50 allowed the necessary amount of solvent into its pores to obtain a good shimming and do not show overlapping between signals that will enable the recording of accurate results.

The results of the diffusion coefficients measured both free in solution and in presence of Sephadex G-50 are shown in figure 3.18. As it was expected, it can be observed that in absence of the stationary phase the values of the diffusion coefficients are very similar to the expected for the individual polymers although for PSS is slightly larger than the observed before. With the addition of the stationary phase, the diffusion coefficient of PMA experience a significant reduction while PSS slightly alter its value, broadly in line with the effects observed in figure 3.15. In agreement with SEC principles, the smaller polymer experienced a much larger reduction in the diffusion coefficient, due to a more effective interaction with the stationary phase. This is caused because it is hindered more by the pores of the stationary phase than the larger polymer. Overall the same effects that were observed with the weight-matched pairs polymers sample are observed now. However, the PSS polymer that is used here (63kDa) has a weight that is larger than the limit size that can be fitted into the pores of Sephadex G-50 (see table 2.1). Hence, the diffusion coefficient should barely be affected by the stationary phase. In

this case the reduction experienced by PSS is slightly larger than the observed in previous experiments for single polymers [1] or weight-matched pairs experiments. This could be caused by some kind of interaction between the polymers or due to restricted space for self-diffusion due to the addition of the stationary phase. It is currently unclear why this effect is seen here and it was not shown before.

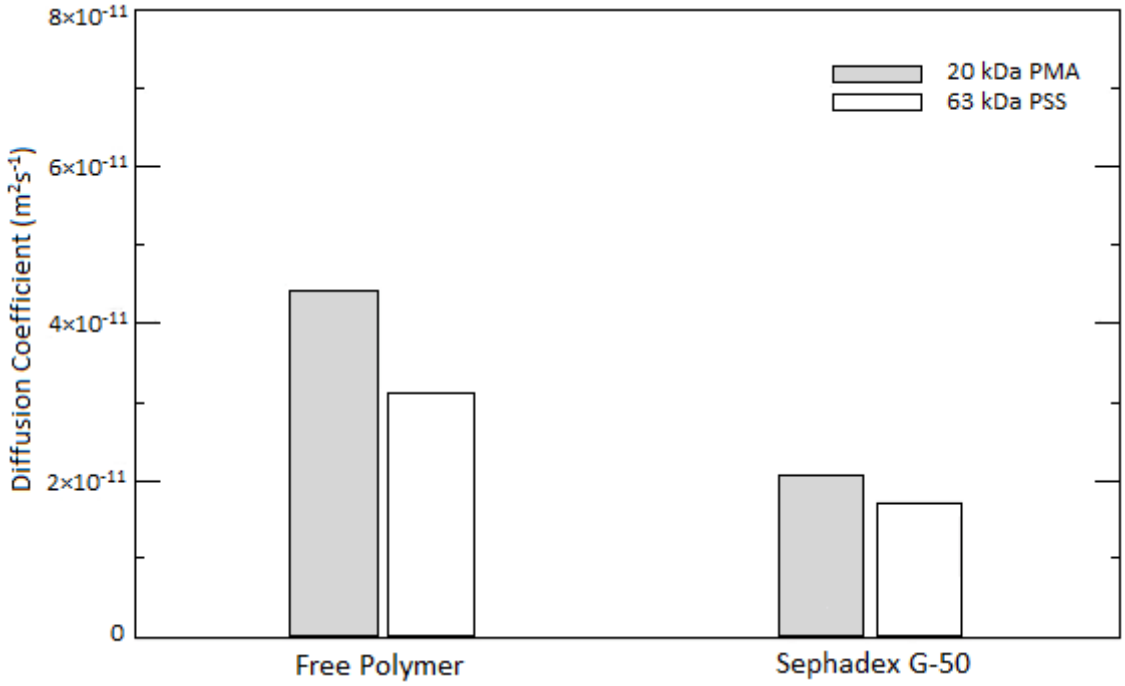

Figure 3.18: Diffusion coefficients for mismatched mixture 20 kDa PMA + 63 kDa PSS in the presence and absence of Sephadex G-50. Image taken from [75]

3.3 Conclusions

In this chapter it has been demonstrated that it is possible to perform SEC-DOSY using different molecules with different characteristics. Nevertheless, in order to perform SEC-DOSY to a mixture in an NMR spectrometer, so it can become a useful addition to all the other MAD-NMR techniques [69, 75], it is needed to improve some of the characteristics that have shown not to be compatible with the technique, such as the use of molecules that can precipitate when they are together in solution or the use of molecules that show overlapping peaks due to broadening produced by the stationary phase. It has also been observed that the use of a buffer have a vital importance for the method when charged molecules are used. However, there are many limitations in the technique so far. The main limitations are firstly, the necessity of a stationary phase that allow enough solvent into its pores to obtain a correct shimming. And secondly, the appearance of overlapping peaks. Hence, in order to make this method useful so it could be implemented as a routinary chemical analysis technique some improvements need to be made to solve or reduce the limitations of the technique. There are several ideas that could reduce

the limitations of the technique and extend its use, such as the use of different solvents that will allow not only to dissolve more molecules, although other stationary phase would be needed as Sephadex G50 is unstable in most of the common organic solvents. The use of different stationary phases will give the experimenter the ability to select more regions of the spectrum, as they will probably show signals in different areas than Sephadex G50. In addition, another of the techniques that could be a great addition to SEC-DOSY without changing the solvent is the use of HR-MAS. This technique would allow to recover the liquid like shape of the signals after the addition of the stationary phase through the reduction on the difference on the magnetic susceptibility of the solvent and the stationary phase. However, the details of this technique will be explored in the subsequent chapters.

Chapter 4

Optimizing Diffusion Studies by HR-MAS NMR

Nuclear magnetic resonance (NMR) is a very important analytical technique that allow chemists to obtain a great amount of different molecular information, such as verification of molecular structures [12], measurements of diffusion coefficients [127], information about formation of aggregates [4] and more. Information at an atomic level can be obtained through the use of a huge number of different pulse sequences [128]. However, most of these experiments are more useful when they are performed in pure samples as the presence of impurities or a mixture of compounds can make the interpretation of the results difficult due to spectral complexity. Nevertheless, this problem can be overcome by separation or purification of the sample by traditional chromatographic methods either online or offline [129, 130]. A different way to address this issue without needing a prior separation is by a pseudoseparation through the use of molecular parameters such as diffusion coefficient [21], or the generation of a maximum-quantum spectrum [131, 132].

The use of the diffusion coefficient to facilitate the analysis of mixtures have been thoroughly studied [21, 133]. However, this method has major limitations when there are overlapping signals in the spectrum (main problems observed in chapter 3), as the diffusion coefficient shown from two overlapping signals is an average of the two true coefficients. For this reason, it has been enhanced by the addition of substances that modify the diffusion properties of molecules to the NMR samples. This method combined with DOSY NMR studies led to the appearance of a technique known as chromatographic NMR or Matrix Assisted DOSY [95]. Different groups have worked developing this technique varying the substances that modify the diffusion properties of the analytes. The range of diffusion modifiers varies from surfactants that form micelles [97, 98] and nanoparticles [134, 135] to polymers [136] and all type of different stationary phases such as silica based stationary phases [73, 70] or size exclusion stationary

phases [1]. However, most of them are affected by the same problems when they are performed, which are broadening signals caused by the matrix added, overlapping and crowded spectra. The addition of a solid material to the NMR sample can cause differences in the magnetic susceptibility between the solvent and the solid media [137, 70] which produce signal broadening that leads to lower sensitivity and larger chances of overlapping between the signals not only of the analytes but also due to the appearance of the signals of the diffusion modifier used.

Different methods have been developed to try to reduce the problems described above such as the use of vanishing surfactants, which are co-solutes that by using solution conditions can form very large structures with fast T_2 relaxation, Nilsson and co-workers have described DOSY pulse sequences that incorporates significant transverse relaxation weighting that allow to filter out matrix signals [138], perdeuterated surfactant micelles [139] or fluorinated surfactants [140] that will not show signals in the spectrum and therefore will reduce the chances of overlapping due to a crowded spectrum. However, many of the common matrixes used in chromatographic NMR stay in the NMR sample as a solid suspension, such silica [73] or size exclusion stationary phases [75]. The use of this sample modifiers have an added problem compared to the previously mentioned micelles and surfactants. The addition of a solid media to the sample can produce broadening to the peaks due to susceptibility-induced line broadening not matching the magnetic susceptibility of the solvent. In order to address this issue, a method have been developed by Hoffmann et. al. which it is usually applied in an empirical manner, minimising the line width through the adjustment of the solvent composition [72]. However, one of the disadvantages of this method is that it is required a stationary phase such as silica that remain stable in the solvent mixture used and is able to tolerate a wide range of solvents. Unfortunately, this is not the case of the stationary phases used in typical size exclusion stationary phases such as Sephadex G50. A different way of dealing with differences in the magnetic susceptibility is through the combination of DOSY NMR with magic angle spinning (MAS) at moderate spin rates between 2-4 kHz [70, 72, 141, 142]. Through the application of this method, liquid like line shapes are restored at the cost of the appearance of spinning sidebands and the potential for vortexing [76, 143].

Since all of the studies performed in chapter 3 were in presence of a size exclusion stationary phase, the method of high resolution magic angle spinning (HR-MAS) was chosen to perform again the experiments presented in the previous chapter, in order to address the problem caused by differences between the magnetic susceptibility of the solvent and the stationary phases. The results of these experiments are presented in this chapter. The focus is in the use

of Size Exclusion Chromatographic (SEC) stationary phases. Although there have been recent investigations to developed fluorinated silica stationary phases [144, 145], these are not commercially available yet and are not applicable to size exclusion chromatography. Therefore, it seem that the most convenient procedure to enhance the method of SEC-DOSY is through the combination of SEC DOSY NMR studies with Magic Angle Spinning (MAS).

Magic angle spinning is a technique used to perform solid state NMR [146] and HR-MAS liquids experiments that consist of applying high spinning rates to the sample orientated at an angle of 54.74° with respect to the direction of the main magnetic field. The addition of this technique makes the signals in the spectrum narrower because it reduces anisotropic contributions. This effect is produced because MAS averages out the $P_2(\cos\theta)$ terms in the spin Hamiltonian. In addition, MAS also reduces the broadening in the analyte signals caused by the slow tumbling rates of the large molecules that are usually studied in SEC such as polymers and proteins. Nonetheless, the use of high spinning rates could have complicating effects when studying diffusion properties such as the appearance of sedimentation and vortexing forces. Therefore, in this chapter, effective conditions to record accurate diffusion coefficients when using MAS will be presented.

4.1 Proteins and polymers under MAS

Most of the experiments that were performed in the previous work done by Day and co-workers [75] to demonstrate that SEC-DOSY on mixtures is possible, lacked some resolution due to the large size of molecules and the presence of a solid stationary phase in the NMR sample. This lack of resolution was caused by the factors discussed at the end of the previous section, which produced broadening in the signals and made more difficult to successfully record diffusion coefficients through the use of DOSY NMR. Hence, to improve the resolution and therefore the range of possible molecules that could be studied using SEC-DOSY a ^{1}H-NMR spectrum was recorded for both polymers PMA and PSS separated but in presence of Sepahdex G50 under MAS conditions and compared with a ^{1}H-NMR of the same sample without MAS. The spectra are shown in figure 4.1.

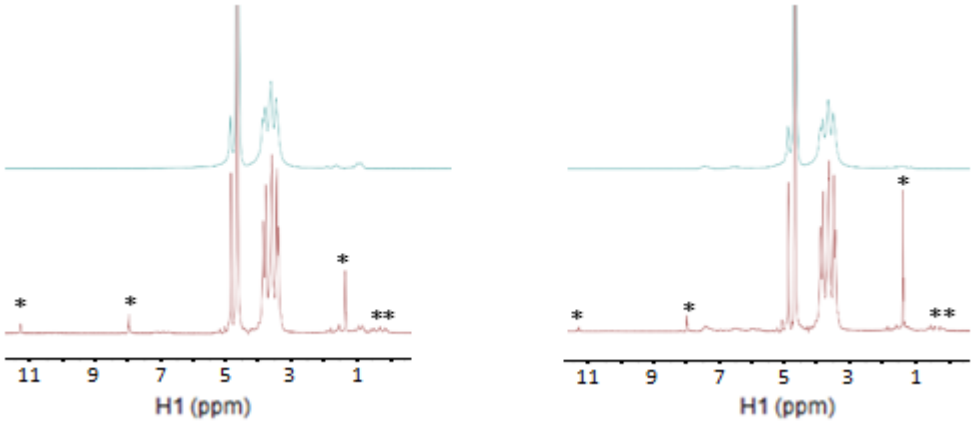

*Figure 4.1: ^{1}H-NMR spectra of 60 kDa PMA (left) and 63.9 kDa PSS (right) with Sephadex G-50 without HR-MAS conditions (Blue) and same sample under HR-MAS with a spin rate of 2 kHz (Red). * mark the spinning sidebands from HOD and ** mark the spinning sidebands of the stationary phase*

The use of MAS increased significantly the resolution of the polymer signals and the stationary phase making them sharper (figure 4.1). Therefore, the line width of the signals is smaller and the signals show less overlapping between them. Consequently, it is worth to continue performing more experiments with the addition of MAS as it seem that it could increase the potential utility of chromatographic NMR. However, the use of MAS produce additional NMR signals known as spinning side bands. This signals could hinder the diffusion studies if they appear overlapping with the signals of interest. However, the position of the spinning sidebands depend on the spin rate of the experiment. Therefore, they should not be a problem when DOSY-NMR is performed as it is easy to avoid any overlapping just varying slightly the spin rate. An example of the variation of chemical shift of the spinning sidebands is shown in figure 4.2.

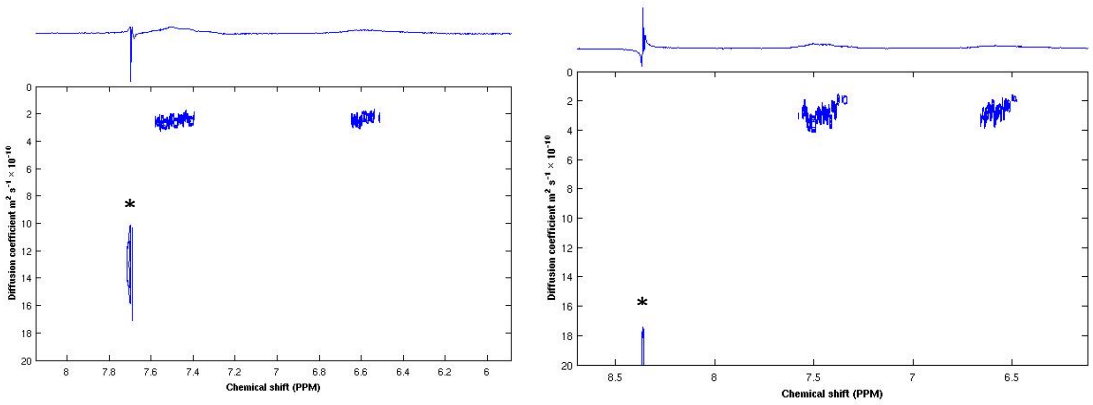

*Figure 4.2: Difference in the chemical shift of spinning sidebands in a 63.9 kDa PSS sample spun at 1.8 KHz (left) and 2.2 KHz (right). * mark the spinning sidebands from HOD*

4.1.1 Parameters of study

To measure diffusion under MAS there are several parameters that should be chosen to obtain accurate measurements such as spin rate, pulse sequence and characteristic parameters of the pulse sequence. The selection of these parameters will be discussed in this section.

The first parameter that was varied was the spinning rate. High spinning rates could cause problems that would hinder the study of diffusion such as vortexing forces [76], sedimentation effects [147] or it can cause damage to the sample depending on its nature [148]. Hence, it is necessary to try to keep the spinning rate as low as possible, which is not a problem with the nanoprobe used for these studies as it has a maximum spin rate of 4 kHz. However, experiments under low spinning rates are more likely to show the previously mentioned spinning sidebans, the lower the spinning rate is the more likely is that the sidebands will appear on the region of the spectrum where the signals of the molecules are. In figure 4.2 it can be seen that the spinning sidebands of HOD when the sample was spun at 1.8 kHz were nearly overlapping with one of the signals, meanwhile at 2.2 kHz spinning rate the sidebands shifted far enough from the polymer signals. Therefore, in order to ensure that there is no overlapping between the spinning sidebands and the molecules of interest a DOSY-NMR spectrum was recorded for a sample of the polymer 63,9 kDa PSS and one of the protein Bovine α-lactalbumin (14.1 kDa) at 2 kHz spinning rate. The DOSY spectrum of each molecule are presented in figure 4.3.

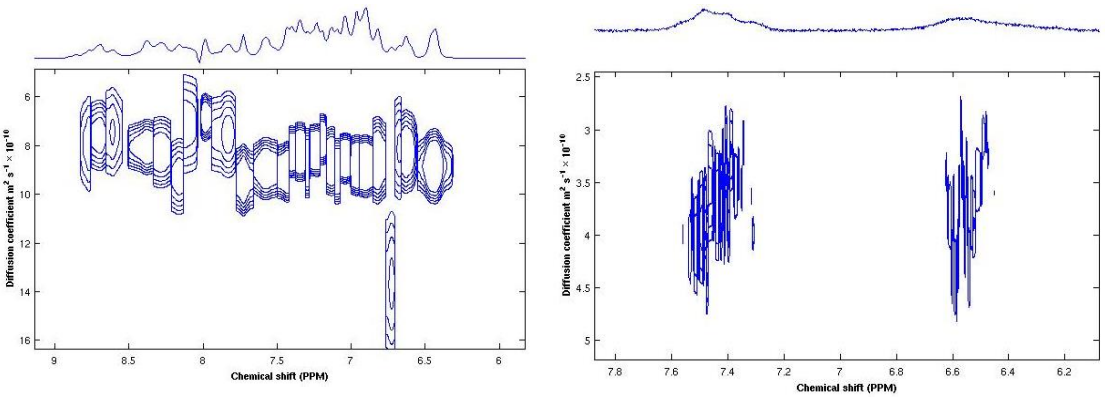

Figure 4.3: DOSY-NMR spectra of 14.1 kDa Bovine α-lactalbumin (left) and 63,9 kDa PSS (right) in D_2O at spin rate 2 kHz

Looking at figure 4.3 it can be seen that 2 kHz is a spinning rate that will allow to perform diffusion studies as there was no overlapping with the spinning sidebands and the region of the spectrum of interest for the polymers studied, and only some of the signals of the protein will show overlapping with the sidebands as proteins show a large amount of signals. However, it can be observed that the diffusion coefficients observed for the molecules have increased

significantly (5-10 times higher) compared to the studies in static samples (the diffusion coefficient varied from 0.3×10^{-10} m^2s^{-1} in static conditions to 3.5×10^{-10} m^2s^{-1} for 63.9 kDa PSS). This effect could be because of the temperature that molecules experience at a high spinning rate, as temperature is directly proportional to the diffusion coefficient as is shown in the Stokes-Einstein equation (see equation 1.22). Although the temperature had been set at 25°C to be the same as all the studies performed previously with static samples [1, 75], the high spinning rate could cause heating on the sample due to friction between the rotor and the air as the rotor spins through it. Therefore, to know exactly what is the temperature that is being experienced by the molecules inside the rotor an ^{1}H-NMR spectrum of a sample of ethylene glycol which can be used as an internal thermometer [149], was recorded at different spin rates to see the variation of the temperature when the spinning rate is increased. The results are shown in figure 4.4.

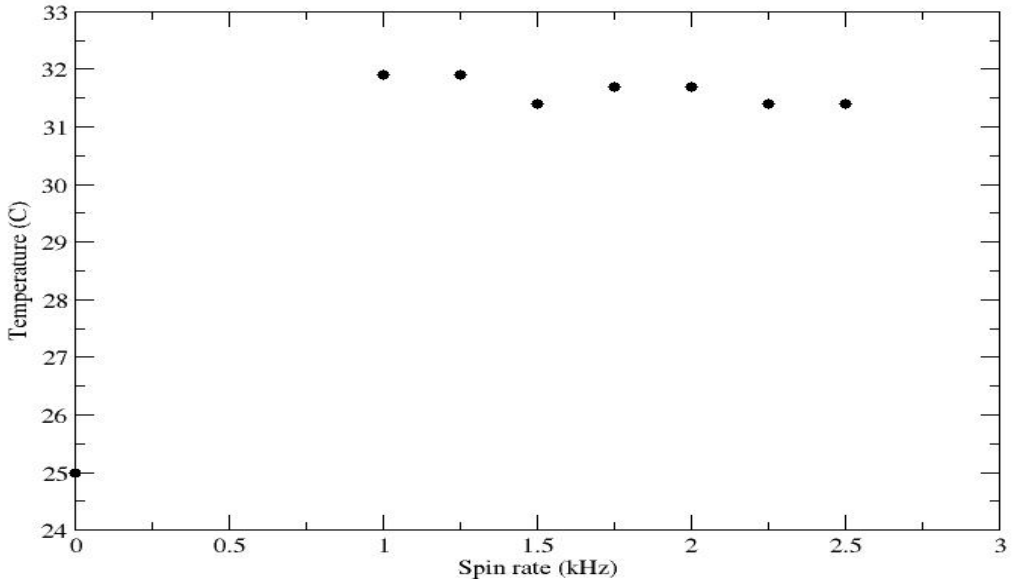

Figure 4.4: Variation of the temperature inside the NMR rotor of a sample of ethylene glycol at increasing spinning rates

The data in figure 4.4 show that the variation of temperature is large when the sample goes from static to moderate spinning rates. However, there is not a significant variation on the temperature after that initial increase. The temperature remained constant when the spinning rate variations happened at an already spinning sample. Therefore, the significant change produced in the diffusion coefficients measured under MAS conditions could be due to an increase in the kinetic energy of the molecules due to the spinning rate or due to the appearance of other forces such as vortexing forces [76].

Finally the pulse sequence that was selected to perform this studies was the Oneshot sequence [27], and the parameters of the sequence were chosen following previous studies made in the group by Anderson [150]. The parameters for the study were 2 ms gradient length δ, 50 ms diffusion delay Δ and the range of arrayed gradient strength was 15 increments increased linearly by g^2 from 0.0500 to 0.3337 T. This allowed a limited reduction in the intensity of D_2O (used to reference the spectrum) in the first increments and a good signal decay for the studied molecules along the 15 increments.

4.1.2 Experiments with proteins

In the previous chapter it was discussed that not only the molecular weight, but also the shape of the molecules is important when performing SEC studies. This issue is of great importance when studying proteins. Proteins are formed by sequences of monomers called amino acids that undergo condensation reactions releasing water and forming a peptide bond. To be able to complete their biological functions this sequences fold into different spatial conformations driven by different intermolecular forces such as hydrogen bonds or van der Waals forces, the final spatial conformations vary from tubular proteins to globular ones [151]. Therefore, it is possible that a protein with a lower molecular weight could diffuse slower because of a larger spatial conformation.

In order to appreciate this effect the diffusion coefficients of a group of different proteins were recorded with high concentrations of urea and without urea at a 2 kHz spinning rate. Urea is an organic compound that in concentrations between 8 and 10 M is a powerful protein denaturant as it disrupts the noncovalent interactions in proteins [152]. Therefore, proteins unfold and increase their effective hydrodynamic size reducing their diffusion coefficient. The results are shown in table 4.1

Proteins Concentration 2mM	Molecular weight kDa	Diffusion coefficient (D) × 10^{-10} m^2 s^{-1}	
		Buffer	Urea 8 M
Bovine serum albumin	66.5	5	4.5
Albumin Chicken Egg	44.3	8.5	6
α-Chymotrypsinogen A	25.6	6.5	4.5
β-Lactoglobulin	18.4	7.5	6
Bovine α-Lactalbumin	14.2	8.25	7
Cytochrome C	12	5.5	4.5

Table 4.1: Summary of diffusion coefficients of samples of 2 mM proteins of varying molecular weights in buffer with and without urea 8 M at 2 kHz spinning rate

Looking at the table above, the data is consistent with the statement that urea can disrupt the noncovalent interactions and expand the spatial conformation of the proteins increasing their effective radius and consequently decreasing the diffusion coefficient. In addition, the result are also in agreement with the importance of protein conformation after the folding process that was mentioned before. This conformation can affect to the diffusion as it is shown by one of the largest proteins of the studied set, the albumin from chicken egg, which it is also the fastest one.

Although the proteins used in this experiments have similar weights to the polymers used in previous studies [75] the diffusion coefficient that they show were larger than the polymer ones which were diffusing between 3.5 and 4.5 × 10^{-10} m^2 s^{-1}. This is in agreement with the fact that polymers show larger sizes than proteins due to the protein folding, as the results became more similar when the urea was used. However, the concentration used for the proteins was much lower than the used for the polymers which could contribute to a slower diffusion coefficient for the polymers.

Nonetheless, the result were not exactly in agreement with the range of velocities expected because the proteins diffused 10x faster than the polymers in static conditions. Therefore, as it was mentioned before, the high spinning rate is increasing the diffusion coefficient probably due to an increase of the kinetic energy. However, for the proteins studied, the diffusing behaviour of the proteins followed the expected pattern. Therefore, they seem as good candidates to carry on with the diffusion studies under MAS conditions.

Finally, in order to compare the proteins results with the polymer results of similar molecular weights, the chosen proteins to continue the studies were the proteins shown in table 4.2 because they have similar weight to the polymers that were used in our previous studies [75].

Protein	Molecular weight (Da)
Bovine Serum Albumin (BSA)	66500
α-Chymotrypsinogen A	25600
β-Lactoglobulin	18400
Bovine α-Lactalbumin	14178

Table 4.2: Summary of proteins used for HR-MAS NMR chromatography

The diffusion coefficients of the proteins were recorded under 2 kHz MAS conditions from samples of 2mM concentration in buffer with and without Sephadex G50. In order to fill the whole rotor with stationary phase the samples were prepared as described in chapter 2. The protein diffusion results are shown in figure 4.5.

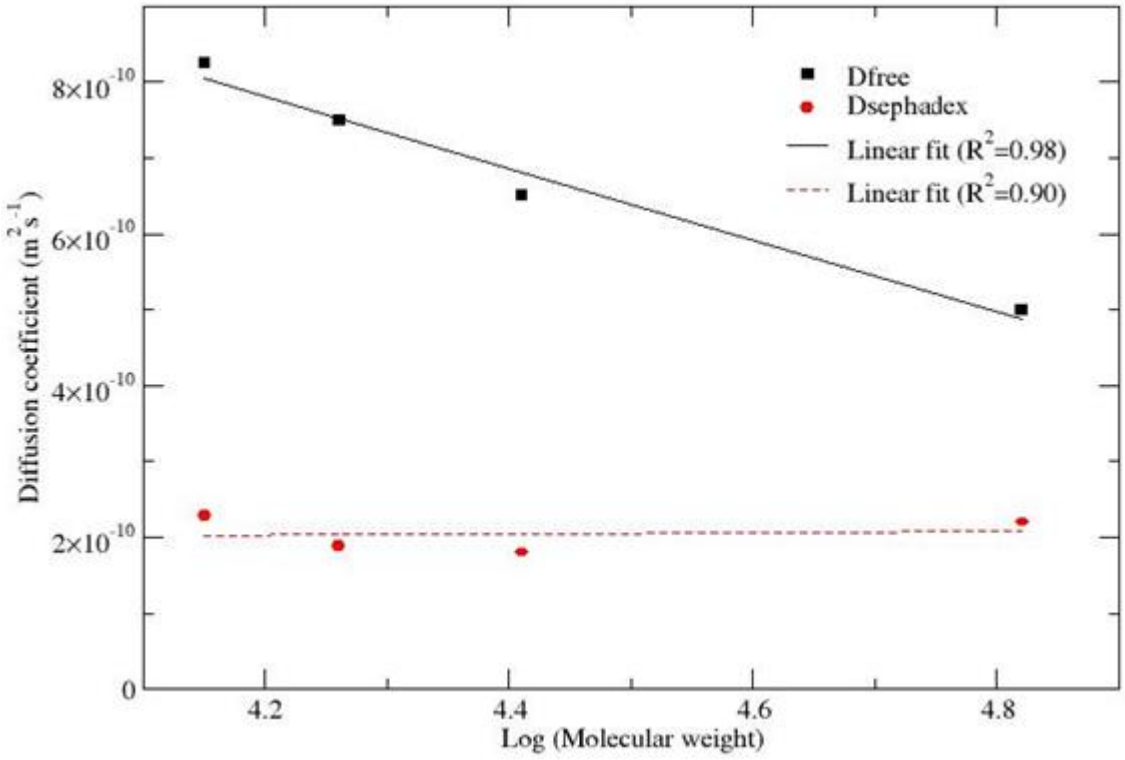

Figure 4.5: Diffusion of proteins in buffer at 2 kHz spin rate with and without Sephadex G50

Without the presence of stationary phase, the results shown by the proteins followed the expected pattern, which is, the larger the protein the slower the diffusion coefficient is. The only not expected results is the high speed of the diffusion coefficient compared to the tube results.

When the stationary phase was added, the diffusion coefficient of the smaller molecules was reduced more than the larger ones. This observation is in agreement with size exclusion principles, as the smaller the molecule is the one that can explore more the pores of the stationary phase allowing a greater interaction between the molecule and the stationary phase. It could also be observed that all the proteins presented a very similar diffusion coefficient in presence of the stationary phase. Although this result could be possible it was unexpected that even the molecules that would not fit in the pores and therefore their diffusion coefficient should barely vary, presented and large variation in the diffusion coefficient (BSA varied from 5.5 to 2.1 × 10^{-10} m^2 s^{-1} when the pore size max is 30 kDa for globular proteins and this protein is 66.5 kDa see tables 2.1 and 4.2). These two facts together suggested that what the molecules were experiencing was not a size exclusion effect but hindered diffusion due to the large centrifugal force generated in the solution that prevented the molecules from diffusing freely may be due to interferences between them and also with the stationary phase. Therefore, the possible explanation is the fact that such a high spin rate could cause sedimentation effects when the stationary phase was present in the sample, which prevented the molecules of diffusing normally in the solution. However, further studies must be done to support this idea such as putting the sample under high centrifugal forces and see if there is a gradient of concentrations generated.

4.1.3 Experiments with polymers

Due to the unexpected results when SEC-DOSY was performed under MAS for protein samples, a new set of similar experiments were performed using polymers. In order to reduce the possibility of sedimentation or saturation of the pores of the stationary phase, the concentration of the samples was reduced to 0.2 mM. Therefore, the diffusion coefficients of a set of PSS polymers were recorded under 2 kHz MAS conditions from samples of 0.2 mM concentration in buffer with and without Sephadex G50. The set of polymers used is the same as in chapter 3 and in our previous studies [1, 75]. The polymer diffusion results are shown in figure 4.6.

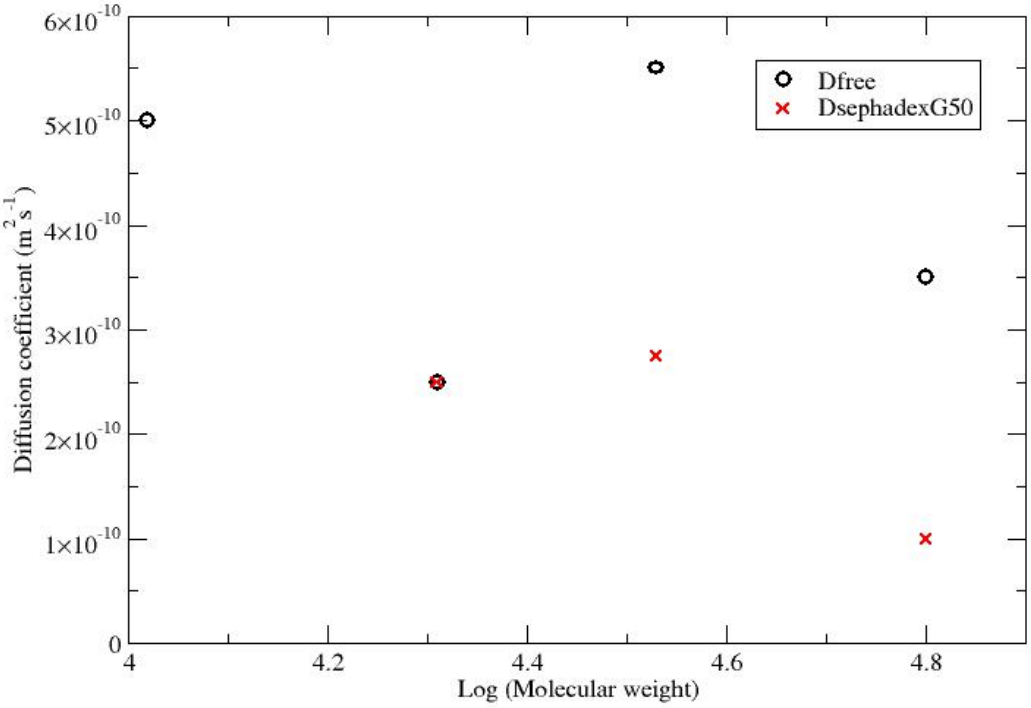

Figure 4.6: Diffusion of set of PSS polymers in buffer at spin rate 2 kHz with and without Sephadex G50

Looking at the diffusion coefficients of the polymer samples shown in figure 4.6, the results were perplexing they did not follow any pattern either when they were in presence of the stationary phase or not. Due to the very low polymer concentration used this time and the broadening caused in the signals by the stationary phase (even with the improvements of the use of MAS), the diffusion coefficient of the smallest polymer could not be recorded in the presence of the stationary phase. In any case all diffusion coefficients that were possible to be measured seemed to show random values which is in total disagreement with the static results presented before in chapter 3 and in the previous studies made on the group [1, 75]. In addition, when the behaviour of the polymer was compared between the free diffusion and the diffusion in presence of stationary phase was not the expected if the molecules where following the behaviour described by the Stokes-Einstein equation (see equation 1.22) where the larger molecules diffuse slower that the smaller molecules. Moreover, the addition of the stationary phase varied only some of the values of the diffusion coefficient, and the value that did not vary (21PSS) was the value that was supposed to suffer the greater variation if a size exclusion phenomena were happening, as it was the polymer that was mean to fit into the pores of the stationary phase. Instead the larger polymers, which should not fit into the stationary phase and therefore should not show variation in the diffusion coefficient, experienced a major decrease.

Nevertheless, there was one conclusion that could be obtained in these results consistent with the data shown by the experiments performed with proteins, the value of the diffusion coefficient is much faster than the tube result and match with the values presented by the proteins with similar sizes, this fact is in agreement with the appearance of a modulating diffusion effect that is not yet understood, such as the possibility of an increase of the kinetic energy experienced by the molecules when they are under fast MAS conditions or the appearance of vortexing forces.

Due to the completely unexpected results, the previous experiments were repeated under two different spinning rates for two reasons. First, although there was no overlapping with the water spinning sideband there could be some overlapping with the spinning sidebands of the other signals of the polymer that were not noticed before due to their low intensity (the possibility of the overlapping with the spinning sidebands of the stationary phase was discarded because the unexpected diffusing behaviour was also observed when the stationary phase was not present). Second, to see if the spinning rate had any influence in the diffusion coefficient. Hence, the experiments were repeated at 2.2 and 1.8 kHz, the results to these experiments are shown in figure 4.7.

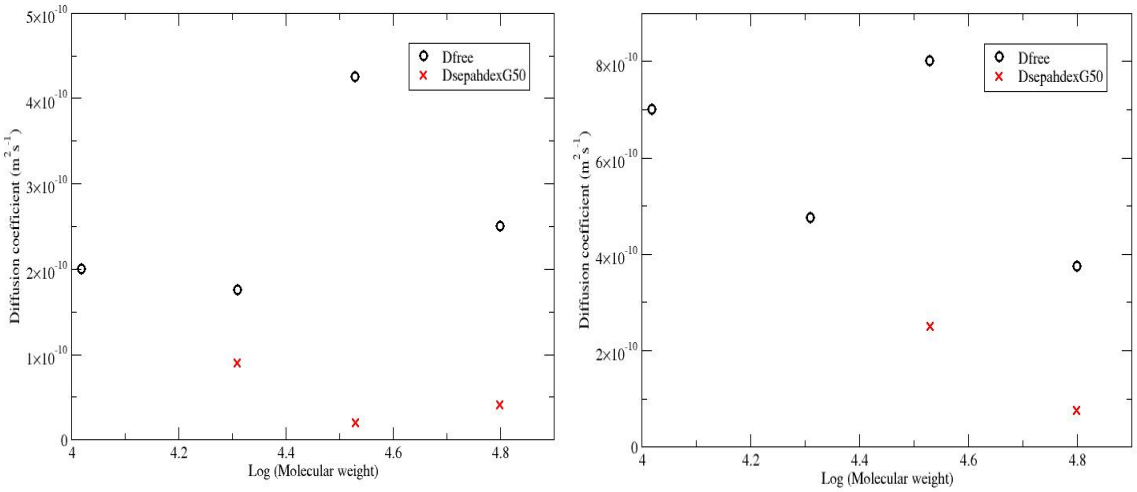

Figure 4.7: Diffusion of set of PSS polymers in buffer at spin rate 1.8 kHz (left) and 2.2 kHz (right) with and without Sephadex G50

The results at different spinning rates were in agreement with the experiments performed at 2 kHz, the diffusion coefficients did not follow any pattern and did not seem to be driven by the size of the molecules as the smaller polymers diffused slower than the larger ones. In terms of size exclusion, the results were also expected as they were similar to the results performed at 2 kHz.

Still, there was an interesting result, the diffusion coefficient seemed to vary a lot depending on the spinning rate. This fact was extremely unexpected as suggests that the spinning influence the diffusion coefficient somehow. However, it could be useful if one were able to understand how the diffusion of molecules is being influenced by the spinning rate, then size exclusion chromatography might still be possible. For these reasons, a step back needed to be taken in order to study the diffusion under MAS in the simplest possible conditions which are just with D_2O samples, where the only influences on the diffusion are due to the pulse sequence or the spinning rate and the physical forces or effects produced by it such as the already mentioned vortexing forces or sedimentation.

4.2 Optimization of DOSY under MAS conditions

The experiments that have been performed so far to study the possibility of size exclusion chromatography under MAS have been either inconclusive or a failure due to a lack of understanding of diffusive behaviour of molecules when they are under a moderate spinning rate as the one provided by the MAS nanoprobe. Therefore, to be able to continue with this studies is necessary to extend the understanding of the diffusion properties when MAS is applied.

In the next section the results of the investigation of the best conditions to obtain accurate diffusion coefficient measurements will be presented, including not only different pulse sequences and selection of parameters such as spinning rate, but also sample preparation and manipulation of the sample with the advantages and drawbacks shown by each method of sample preparation.

4.2.1 The discovery of the bug in the code of the NMR pulse sequence

Following what was commented at the end of the previous section, in order to fully understand what is affecting to the diffusion coefficients under MAS conditions, the simplest way is to try to record the diffusion coefficient of a molecule whose diffusion coefficient is well known and had been studied through different methods, including PFG NMR [153, 154]. In addition, it is important to reduce the possible interactions that the molecule could have with any solvent or other agents present in the sample. Hence, the chosen molecule was HOD which could be studied by NMR as the residual signal of a D_2O sample. Therefore, it does not need a solvent and only interacts with the rest of the water molecules and can be easily measured by DOSY-NMR. Also it has a well-known diffusion coefficient which is around 20×10^{-10} m^2s^{-1} [153, 154].

A DOSY experiment of a sample of D_2O was measured under MAS increasing the spin rate from 1 kHz to 2.5 kHz with intervals of 0.25 kHz. The sequences used were the gradient compensated stimulated echo (GCSTE), bipolar pulse stimulated echo (BPPSTE) [26] and the Oneshot sequence [27]. The series of diffusion coefficients were recorded using different gradient lengths and a 100 ms diffusion delay (Δ). To obtain accurate diffusion coefficients literature suggest the use of rotor synchronised pulse sequences in both their duration and interpulse timing [143, 155, 156]. However, Viel et al. suggested that the synchronization may not be necessary as they did not employ it in their studies and still obtained accurate results [76]. In the Agilent library supplied versions of these pulse sequences, the total area of the diffusion encoding gradients applied is rotor synchronised, but other parameters such as the interpulse spacing are not synchronised with the sample rotation. Hence, this means that the diffusion decoding gradient can end up being applied at a different point of the rotor cycle compared to the diffusion encoding gradient. Therefore, figure 4.8 show the results of recording the diffusion coefficient of HDO with the pulse sequences as they are in the Agilent library (a, c and e) and with the pulse sequences fully synchronised (b, d, f).

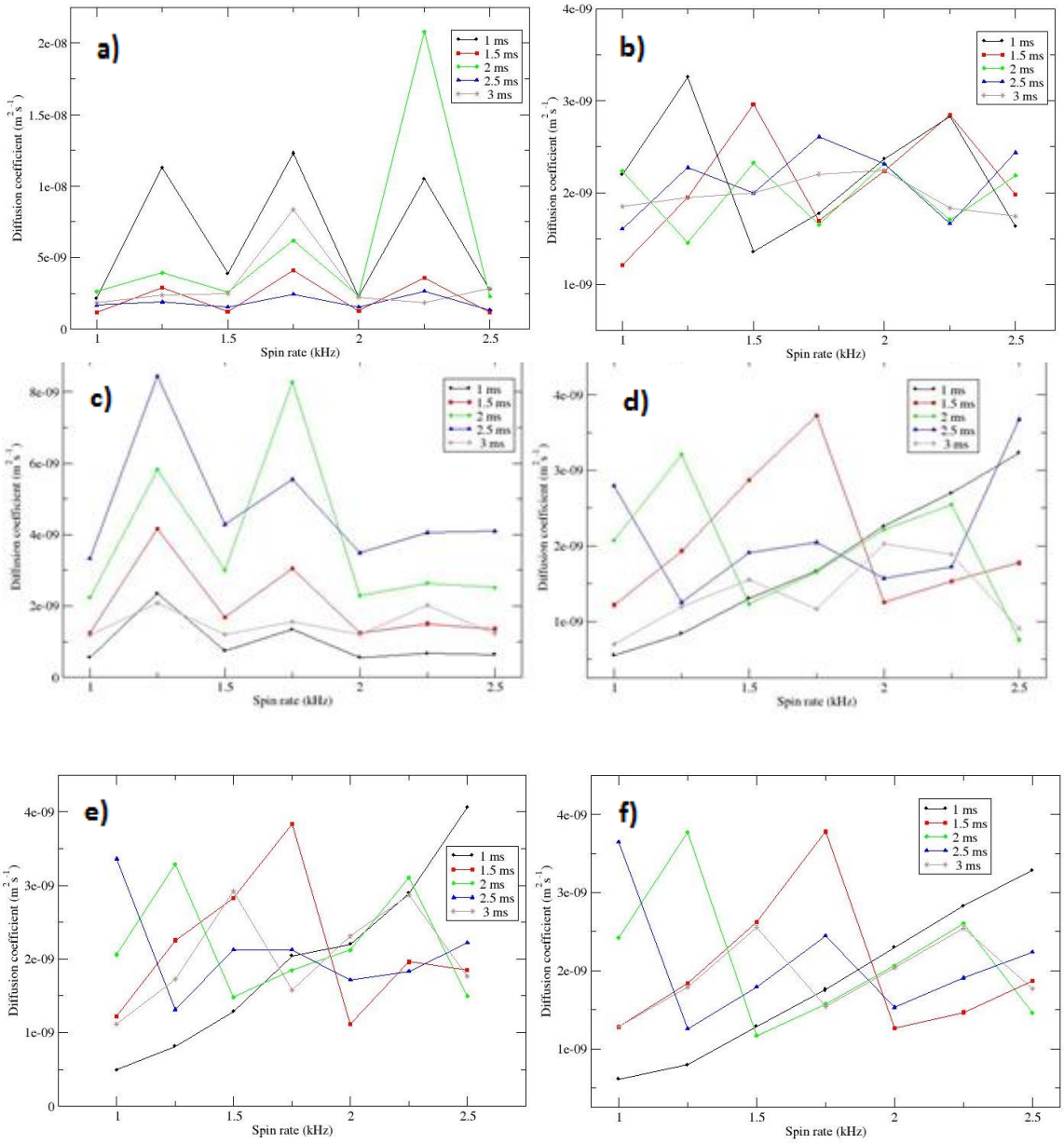

Figure 4.8: Observed variation in the measured diffusion coefficient of HOD with spin rate using the Agilent-supplied pulse sequences. a) and b) are for the GCSTE, c) and d) for the BPPSTE and e) and f) for the Oneshot sequence. a), c) and e) are the pulse sequences as supplied in the Agilent library while b), d) and f) use complete rotor synchronization of the RF-pulses, gradient duration and delays before the correction of the bug in the analysis software

The results shown in figure 4.8 were perplexing again. First because in the results performed with a 5 mm tube, the diffusion coefficient of D_2O was around 18 - 19 × 10^{-10} m^2s^{-1}. Therefore, every diffusion coefficient with a correct signal decay was expected to be faster or similar to this value depending on how affected are they by the effects arising after the application of MAS. Instead the result varied from 5 to 200 × 10^{-10} m^2s^{-1} if they were measured with GCSTE, which

was the worse sequence and from 5 to 40 × 10^{-10} m^2s^{-1} with the Oneshot sequence, which was the sequence that showed the smallest spread of results.

Second there were two possible behaviors that would be easily explained, the first one was to obtain diffusion coefficients that will increase while the spin rate is increased, as these will be experiencing more the effects that arise after the application of MAS, and that caused acceleration in both polymer and protein samples. However, the spin rate variation is not very large so a slight increase of the diffusion coefficient is expected. This behavior could be observed in only one of the series, the one with 1 ms gradient length, but only in 3 of the different pulse sequences. Nonetheless, the diffusion coefficient varied from 5 to 30 × 10^{-10} m^2s^{-1} in the figure that showed the most narrow range of diffusion coefficients (the fully synchronized Oneshot, see figure 4.8f), and the values expected were around 20 × 10^{-10} m^2s^{-1} and not any lower than 18 × 10^{-10} m^2s^{-1} as all the signals decays were correct. The second behaviour which was the one expected was that all the diffusion coefficients would be around 20 × 10^{-10} m^2s^{-1} showing a straight line while the spin rate was increased, as small variations in the spin rate should not affect significantly the diffusion coefficients of the molecules measured.

It could be observed that the full synchronization of the pulse sequences notably reduced the range of observed diffusion coefficients for both the GCSTE and the BBPSTE (range without synchronization goes from 2 to 200 × 10^{-10} m^2s^{-1} and with synchronization goes from 5 to 38 × 10^{-10} m^2s^{-1}) but did not vary significantly the results of the Oneshot sequence (range with and without synchronization goes from 5 to 40 × 10^{-10} m^2s^{-1}). However, all of the results were still far away from the expected behaviours or values (≈ 20 × 10^{-10} m^2s^{-1}).

Once more the diffusion coefficients seem to appear showing a strange pattern. To see if the results were reproducible the experiments were repeated and the values obtained were similar only showing small variations that were expected within the error of the instrument. Therefore, the results were following a reproducible pattern but all the improvements based on different hypothesis that could explain what was happening (bubbles in the sample, volume too large inside the rotor that caused molecules to experience different forces depending on their position in the sample, sedimentation etc…) failed to improve or allow the understanding of what was affecting the diffusive behaviour. These hypothesis will be detailed subsequently. In general all the results showed changes in the value of the diffusion coefficient but the shape of the lines was always the same.

Finally after detailed reviewing of the pulse sequence code, a bug was found by I. J. Day that was producing the incorrect behaviour of any analyte measured. The details about the bug are described below and taken from the published work by Day group [80].

> The Agilent-supplied pulse sequences GCSTE (DgcsteSL.c), BPPSTE [26] (Dbppste.c) and Oneshot [27] (Doneshot.c) each contain two statements performing on-the-fly adjustment of the total area of the diffusion-encoding gradients. For example, the following is from Donehsot.c:
>
> *gt1 = syncGradTime("gt1","gzlvl1",0.5);*
>
> *gzlvl1 = syncGradLvl("gt1","gzlvl1",0.5);*
>
> The first statement adjusts the length of the gradient to be an integral multiple of the rotor period, while the second corrects the power level to preserve the total area. Analysis of these experiments using Agilent's VnmrJ package or DOSY Toolbox [36] makes use of a "*dosytimecubed*" parameter, calculated in the pulse sequence when the experiment is run. This parameter, the product of the gradient duration-squared and the diffusion delay (suitably corrected for the appropriate pulse sequence) is calculated using the new, corrected value of the gradient duration (*gt1*). However, the corrected gradient power levels (*gzlvl1*) are not used, only the requested power levels. Figure 4.8 shows the result of experiments performed with the Agilent-supplied sequences and analysed with DOSY Toolbox [36]. The result of the incorrect "*dosytimecubed*" parameter is the periodic trend in diffusion coefficient. We believe this bug is present in all of the Agilent-supplied diffusion pulse sequences, i.e. those starting D*. The simple fix is to ensure that the *syncGradTime()* and *syncGradLvl()* statements occur after the calculation of "*dosytimecubed*".

4.2.2 The pulse sequence selected for HR-MAS studies

The bug described in the previous section did not affect the raw data that were acquired by the NMR spectrometer but to the analysis of the data after the use of the software of analysis DOSY toolbox [36]. Therefore, to solve the issue it was only needed to reanalyse the raw data after correcting the bug. Thus, the data in figure 4.8 were reanalysed and the corrected results are shown in figure 4.9.

When comparing the three pulse sequences it can be seen that there is wild variation in the observed diffusion coefficients with the variation of the spin rate and the length of the pulses when the GCSTE and the BPPSTE sequences are used without the full rotor synchronization.

However, when the Oneshot is used the results are exactly what it was expected, little variation in the diffusion coefficients and values close to 20 × 10^{-10} m^2s^{-1}.

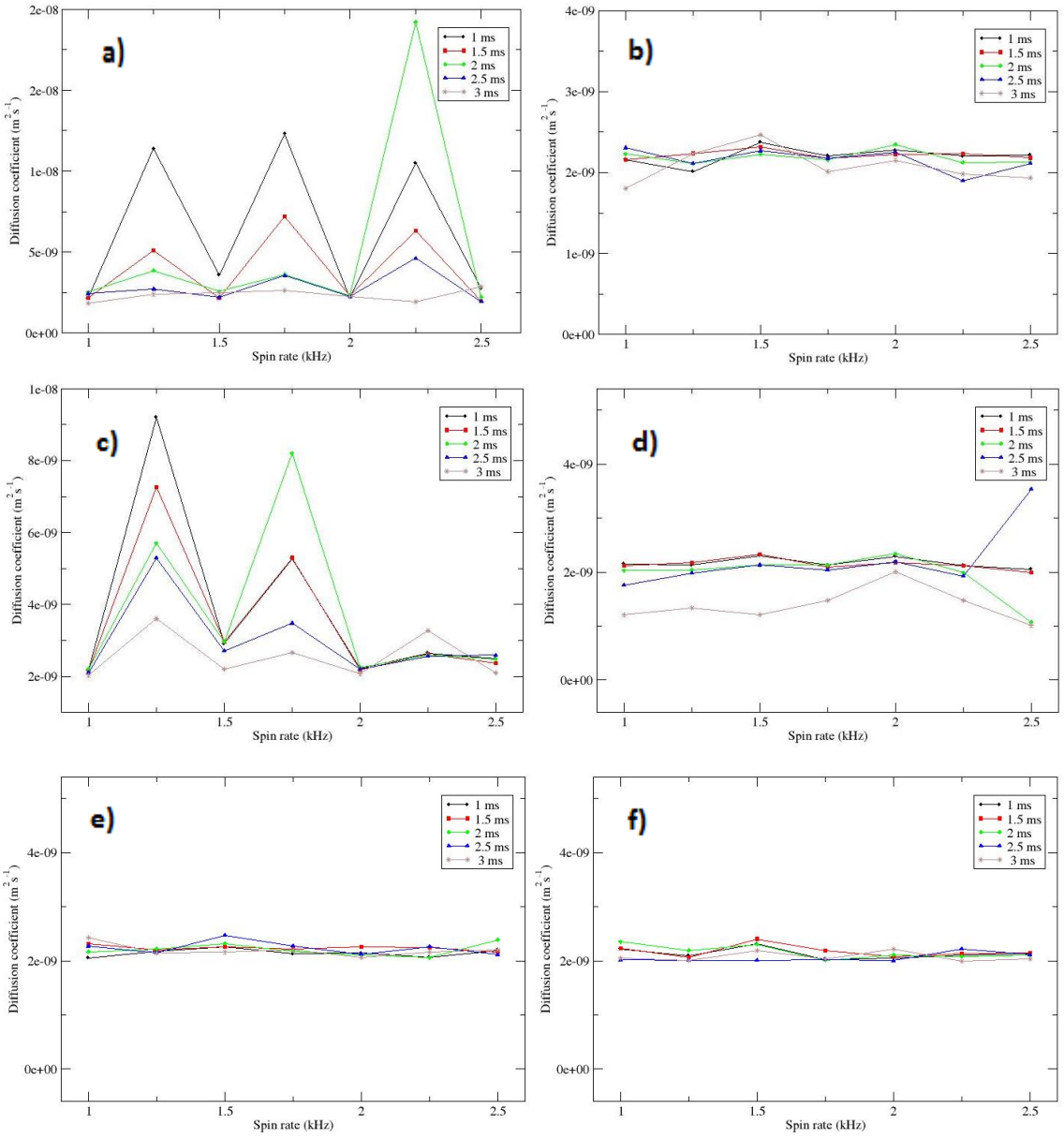

Figure 4.9: Observed variation in the measured diffusion coefficient of HOD with spin rate using the Agilent-supplied pulse sequences. a) and b) are for the GCSTE, c) and d) for the BPPSTE and e) and f) for the Oneshot sequence. a), c) and e) are the pulse sequences as supplied in the Agilent library while b), d) and f) use complete rotor synchronization of the RF-pulses, gradient duration and delays

As it was discussed for the results in the previous section, to obtain accurate diffusion coefficients literature suggested the use of rotor synchronised pulse sequences in both their

duration and interpulse timing [143, 155, 156]. Looking at the results in figure 4.9 the complete rotor synchronization is necessary for both sequences GCSTE and BPPSTE. However, this is not in agreement with what Viel et al. suggested [76]. In their work they mentioned that complete rotor synchronization did not change much the results obtained when measuring diffusion coefficients under HR-MAS [27]. Nonetheless, the results in figure 4.9 clearly showed that there are issues when the BPPSTE sequence is used, especially with long gradient pulses. Although, the performance could be clearly improved by the application of rotor synchronization, the diffusion coefficients still varied more than expected when the gradient length is increased. The BPPSTE sequence incorporated bipolar gradient pulses, which significantly reduce the impact of any gradient induced eddy currents [26]. The Oneshot sequence includes an unbalancing factor to allow unwanted coherences to be destroyed by the diffusion encoding gradients, removing the need for extensive phase cycling [27] and reducing the amount of time needed to perform an experiment. Hence, the Oneshot sequence is an improved version of the BPPSTE sequence and it is not surprising that both sequences produced similar results. The fact that the data collected by the rotor synchronized BPPSTE are similar to the Oneshot sequence with or without synchronization suggest that the improvements in the Oneshot sequence over the BPPSTE remove some of the additional complications that are partially improved by the rotor synchronization.

For all the discussion in the paragraph above, it can be concluded that the results obtained when the Oneshot sequence is used, are both more accurate and reliable. Therefore, to continue optimizing the results obtained when performing DOSY under MAS conditions the pulse sequence that will be used is the rotor synchronized Oneshot sequence.

4.2.3 Improvements in sample preparation for DOSY-NMR under MAS

Previous studies have been made to try to combine chromatographic NMR and HR-MAS. Caldarelli and co-workers showed that there were differences between the diffusion coefficients of static and spinning samples [76]. These differences have been said to be produced by mechanical mixing and vortexing effects. In addition, the shape of the sample was an important factor, when the sample volume was restricted to the regions of high gradient homogeneity the diffusion coefficients for small molecules were in good agreement with literature data [76]. It has also been reported that there were some small intensity fluctuations in the echo attenuation curve in experiments that were performed using samples with similar shapes to the samples prepared for the experiments performed in this thesis [143]. These fluctuations have been said to arise from vortexing due to implication on the spectrum detailed by Bradley et. al. However,

they could be mostly removed by extensive signal averaging [143]. Linear (coherent) motion effects introduced by convection in the sample, can also be reduced using convection-compensated sequences [157]. Nevertheless, due to the increased pulse sequence complexity the systems presented here would show little improvement. One of the advantages restricting the sample diameter is that the sample is less exposed to radial variation in the B_1 RF field, which will be modulated by the MAS due to the lack of cylindrical symmetry in a solenoid coil [158]. It has already been observed that the modulation of the B_1 RF field caused signal loss in TOCSY experiments that were performed under HR-MAS conditions [158, 159]. Convection effects are a common problem when studying diffusion by NMR. Therefore, it has been suggested that slow sample spinning (~20 Hz) can be a method to reduce convection effects in the study of diffusion by NMR [160]. However, Morris and co-workers have seen that convection effects are more important than what was previously thought [161]. In liquid samples, MAS can produce changes in the observed signal behaviour for spin-lattice relaxation measurements. Bakhmutov observed a change from single to biexponential behaviour as a function of the spin rate. This change is said to be caused by the formation of an air bubble that is held concentrically along the rotor axis by centrifugal forces that caused increased paramagnetic relaxation at the interface [162] All the samples prepared for the experiments performed in this thesis, were made by adding an excess of sample that will be removed at the end when the rotor is closed to ensure that there are no bubbles inside the rotor.

Viel et al. reported that full synchronization is not required to perform diffusion studies under HR-MAS [76]. Therefore, to ensure that this is applicable in the conditions used in the experiments performed here, DOSY-NMR experiments performed under MAS were repeated using the fully synchronized Oneshot sequence (figure 4.9 (f)) and restricting the sample active volume to the centre of the sample rotor, this restriction should reduce the dependence on the spin rate of the diffusion coefficients that will be recorded. The restriction was achieved by two methods. The first method is the restriction of the active volume of the sample by introducing a cylindrical Teflon spacer into the sample rotor to reduce the sample to a diameter of 1.5 mm, causing a reduction of 53% in sample volume, see figure 4.10. This method restricted the sample geometry radially making it spin closer to the rotation axis and therefore reducing the effects of radial field inhomogeneities [156], and vortexing of the sample [76, 143]. The diffusion coefficients of the residual HOD signal of a sample of D_2O as a function of the spin rate using this method are shown in figure 4.11 (a). The second method employed was the restriction of the sample axially by the introduction of two 1 mm thick Teflon discs (3.1 mm diameter, matching internal diameter of the rotor, see figure 4.10) at the top and the bottom of the sample rotor.

This method caused a restriction of the sample active volume of 43%. The results of the application of this method are presented in figure 4.11 (b). Finally the combination of both methods, radial and axial sample geometrical restriction, led to sample with an active volume of 4.7 µl restricted to the centre of the sample rotor. The results of this experiments are shown in figure 4.11 (c).

All the measured diffusion coefficients as a function of the spin rate or duration of the diffusion encoding gradient presented in figure 4.11 showed similar trends to the data without restriction of the sample active volume shown in figure 4.9 f). Only slight overestimations are observed in some measurements. These data suggest that restriction of the sample active volume either axially or radially is not necessary in solvents of moderate viscosity such as D_2O, and that minor inconsistencies in the measured diffusion coefficients are probably caused by vortexing of the sample in the manner described by Viel et al. [76]. This is good because a larger volume allows a greater sample, and therefore, a larger signal intensity. Thus, it is easier to perform any DOSY-NMR study.

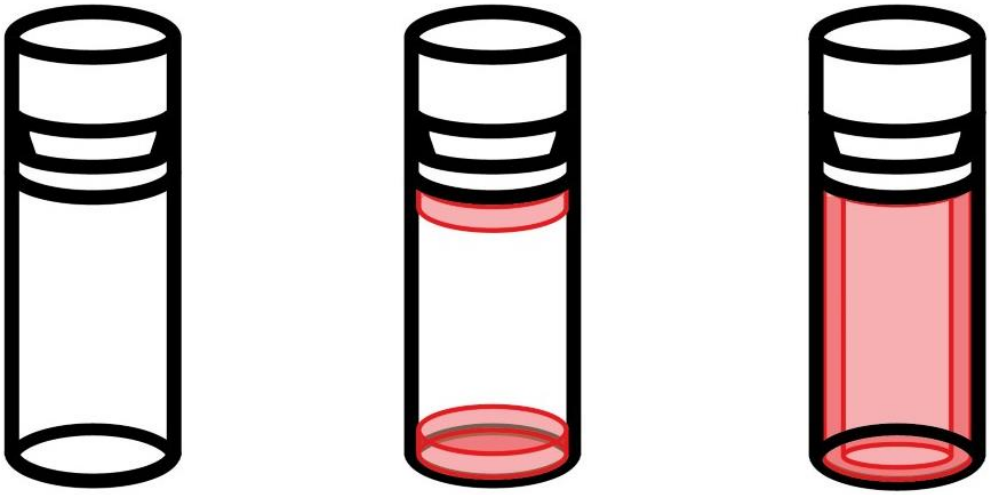

Figure 4.10: Schematic representation of the MAS rotor without sample volume restriction (left), with axial volume restriction restriction (middle) and radial volume restriction (right)

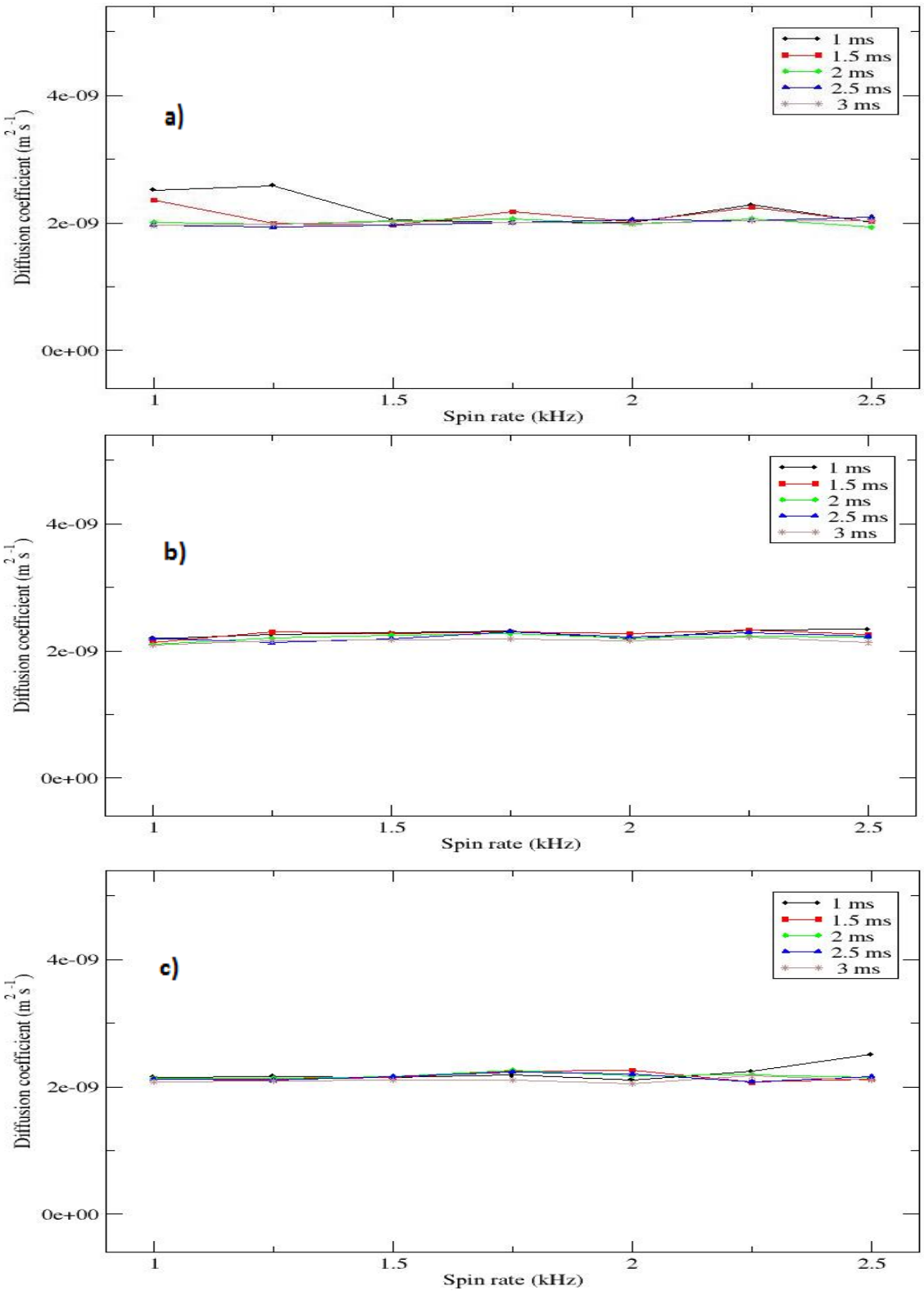

Figure 4.11: Observed variation in the measured diffusion coefficient of HOD with spin rate recorded using the Oneshot sequence and a diffusion encoding time Δ of 100 ms. (a) Shows the sample confined to a diameter of 1.5 mm by the inclusion of a Teflon spacer, (b) shows the sample restricted to a height of 2.6 mm using a pair of 1-mm Teflon discs above and below the sample and (c) is the combination of both sample restriction methods

4.2.4 Sedimentation effects under MAS

It has been proven that spinning the NMR sample at high spinning rate under MAS conditions can provide spectral simplification which is of great importance for DOSY-NMR. However, high spinning rates can also produce other physical effects due to the large mechanical forces that are present in the sample. For example the acceleration produced at the inside wall of the MAS rotor can be significant [163]. Despite the small size of a 4mm rotor, like the ones used in the studies performed in this thesis, with an internal diameter of 3.1 mm, the acceleration at the rotor wall when a moderate speed of 2 kHz is applied is over 20000 × g. These high mechanical forces can cause sedimentation effects. Previous studies done by Bertini and co-workers have demonstrated that large biomolecules can experience sedimentation to the rotor walls like in ultracentrifugation when fast spinning rates are applied [147, 163, 164]. To see the effects of sedimentation, the concentration profile for the poly(styrene sulfonate) (PSS) samples used in the 4 mm HR-MAS rotor at a spinning rate of 2 kHz calculated using the approach of Bertini et al. where, by adapting the sedimentation equilibrium equations to the geometry of the MAS rotor, equation 4.1 (with the integration of constant *A* given by equation 4.2) is obtained to calculate the polymer concentration, *c(r)*, as a function of the distance from the rotation axis, *r*, and the empirically determined maximum achievable concentration, c_{limit} [147, 164, 165] is shown in figure 4.12.

$$c(r) = \frac{c_{limit}}{1 + Ae^{\frac{M\left(1-\frac{\rho_{solvent}}{\rho_{polymer}}\right)\omega_r^2 r^2}{2RT}}} \tag{4.1}$$

$$A = \frac{e^{\left[\frac{M\left(1-\left(1-\frac{\rho_{solvent}}{\rho_{polymer}}\right)\omega_r^2 b^2}{2RT}\left(1-\frac{c_0}{c_{limit}}\right)\right]} - 1}{1 - e^{\left[-\frac{M\left(1-\frac{\rho_{solvent}}{\rho_{polymer}}\right)\omega_r^2 b^2}{2RT}\left(\frac{c_0}{c_{limit}}\right)\right]}} \tag{4.2}$$

where *b* is the rotor radius, $\boldsymbol{c_0}$ the polymer concentration in the static solution, *M* the molecular weight of the polymer, ω_r the angular speed of the rotor, ρ the density, *R* the universal gas constant, and *T* the absolute temperature.

The results did not show complete sedimentation of the polymers to the rotor wall. However, it is clear that the concentration is not uniform across the sample rotor as there is an increase of concentration from the centre of the sample to the edges, reaching the maximum at the rotor

wall. Once the size exclusion stationary phase is present in the sample, it will be exposed to the same physical forces. Hence, as the stationary phase is formed by cross linking dextrans, the effective molecular weight is much larger than the polymers and therefore, the effects of sedimentation will be more significant and the stationary phase will be predominantly found in the outer portions of the rotor. As a result of this sedimentation effect the distribution of polymer solution into the stationary phase will be affected and considerably different compared to the static cases described previously [1, 75]. It has been shown that the loading of the stationary phase, ratio of solution to stationary phase, has a dramatic effect on the modulation of the diffusion coefficient caused by a stationary phase [166]. It has been reported that this effect depends on whether mass transport is happening just to the intraparticle pores or whether there is sufficient solvent to allow escape into the interparticle space [166, 167]. In the case of the studies presented before [1, 75], where static samples were used, the ratio of solution to stationary phase is high. Hence, the polymers were able to explore both spaces, the intraparticle and the interparticle. Under MAS conditions, sedimentation effects will cause a variation of the concentration radially across the rotor of both polymers and stationary phase. In addition, not only the diffusion through the stationary phase will be different due to the loading into the stationary phase but also the diffusion coefficients will be averaged between the diffusion of the polymers in the centre of the sample rotor where likely the amount of stationary phase will be minimum and the polymers into the stationary phase, therefore, this spatial variation in the sample under MAS conditions may lead to a distribution of diffusion modulation effects causing a clear distortion on the measured diffusion coefficients.

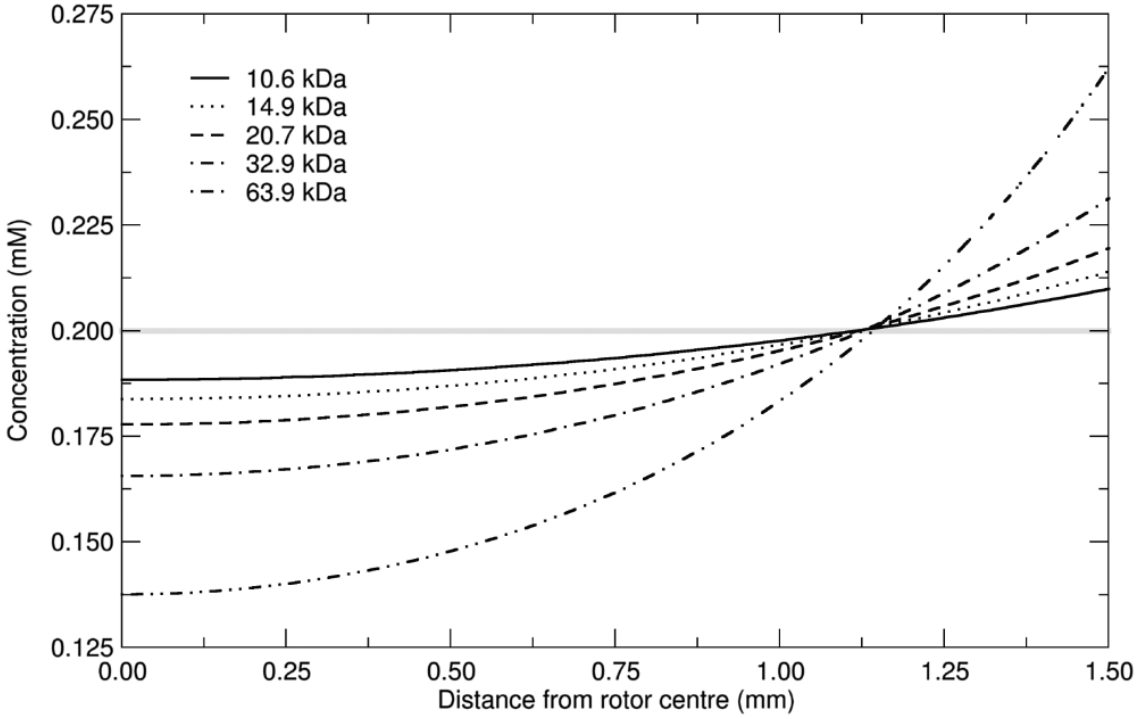

Figure 4.12: Concentration profiles for various poly(styrene sulfonate) PSS samples in a 4-mm (outer diameter) high-resolution MAS rotor spinning at a speed (ν_r) of 2 kHz. The grey horizontal line indicates the static concentration. The curves were calculated using the method of Bertini et al*.* [147], [164] *from sedimentation equilibria* [165]*. Image taken from Day and co-workers publication* [80]

4.3 Conclusions

It has been proven that the use of stationary phases to modulate the diffusion properties of molecules in NMR samples has a great utility in improving the diffusion resolution [70, 72, 96, 141, 168] or providing information on the analyte-stationary phase interaction [166, 169]. Nevertheless, the presence of a stationary phase that it is not soluble in the NMR sample cause broadening of the signals producing low spectral quality [72, 76]. To solve this issue and reduce these effects, in this chapter it has been combined, the use of DOSY-NMR studies with MAS in the context of size exclusion chromatographic stationary phases. Although it has been proven that HR-MAS improves the resolution of the signals when using both stationary phases and high molecular weight analytes such as proteins and polymers (figure 4.1), the diffusion results have been unexpected. The addition of stationary phases to the samples under MAS conditions did not show the expected behaviour as smaller molecules have shown larger diffusion coefficients than larger molecules. In addition, in some cases the diffusion coefficients in the presence of the stationary phases have been larger than without it. Caldarelli and co-workers have postulated

evaporation-condensation for benzene-silica systems [167], that do not seem to be responsible in these cases.

Due to the poor understanding of the issues described above, studies with more simple samples and without the use of stationary phases have been performed. Through these studies, we have confirmed that is possible to obtain reliable estimates of the diffusion coefficients under HR-MAS through the use of rotor synchronized pulses sequences on both gradient pulses and delays [143, 155, 156] applied to different pulse sequences [80].

In this chapter we have found a method that seems to allow us to obtain reliable diffusion coefficients for the residual signal of HOD in a D_2O samples. Therefore, to extend the understanding of HR-MAS in the diffusion of molecules, this method will be applied to record the diffusion coefficients of different molecules in D_2O samples with a wide range of different molecules variying not only their chemical properties but also their molecular weights. These results will be presented along the following chapter.

Chapter 5

Extending the understanding of diffusion NMR studies under magic angle spinning

The application of high spinning rates to NMR samples can seriously affect the diffusion coefficients that are recorded when DOSY-NMR is performed under these conditions for different reasons, such as the appearance of large centrifugal forces that can damage the structure of the sample [78]. In order to enhance the method SEC-DOSY NMR described in chapter three, some experiments using polymers and proteins at high spinning rates under MAS were performed, the results of these experiments were presented in chapter four. These results were completely unexpected both in the value of the diffusion coefficient and the diffusing behaviour when molecules that varied significantly in their molecular weights were compared. Therefore, in chapter four a method was developed to obtain reliable diffusion coefficients under high spinning rates using HR-MAS recording the residual signal of HOD in a D_2O sample [80].

In this chapter, the method that was described in chapter four to obtain accurate diffusion coefficient measurements under MAS will be used to record the diffusion coefficients of a wide range of molecules to extend the understanding of diffusion studies under the complicating effects produced by high spinning rates with the aim of enabling the combination of HR-MAS with chromatographic NMR.

5.1 Experiments with polymers

The aim of combining SEC-DOSY NMR with MAS is to be able to achieve an improvement in the technique through an increase on the resolution of NMR spectrum by removing differences in

magnetic susceptibility and residual dipolar coupling inherent in samples with a stationary phase present [170], to increase the range of application of the technique. Therefore, in order to be able to use the same stationary phases that have been used so far in this thesis, the first experiments performed were with the same polymers that were studied previously in the group [75, 80] and those presented in previous chapters.

5.1.1 Neutral polymers

In order to simplify the first experiments as much as possible to reduce the possible causes of variation of the diffusion coefficients, the first polymers studied were the neutral polymers PVP and PEO (see figure 3.5), these polymers do not need the use of a buffer as they are not electrolytes. Therefore, the samples will only contain the polymer and D_2O. The residual HOD signal can be useful to compare the results with the results presented in chapter 4 and see if the data are reliable. Also these polymers were discarded in our previous studies due to the broadening produced when the stationary phase was added, which caused overlapping signals. Therefore, if the experiments are successful, one of the main objectives, to show an increase of resolution in the spectral domain of SEC-DOSY NMR experiments by averaging differences between the magnetic susceptibility of the stationary phase and the solvent, would be achieved.

5.1.1.1 Diffusion properties without stationary phase under MAS

A set of DOSY NMR experiments using the fully rotor synchronised Oneshot sequence with 50 ms diffusion delay and varying the gradient length at two different spinning rates were performed to record the diffusion coefficient of 10 kDa PVP at different concentrations in D_2O. The results are presented in figure 5.1a. In order to know if the diffusion values recorded are reliable, the diffusion coefficient of the residual signal of HOD was also recorded and shown in figure 5.1b.

The diffusing behaviour shown by the PVP polymer is the expected one. At low polymer concentrations (< 0.5 mM) the molecules are below the overlap concentration. Therefore, the effective size of the polymers does not vary when the concentrations changes and the value of the diffusion coefficient remains the same. Between 0.5 mM and 0.8 mM concentration range, the polymer reaches the overlap concentration. Hence, there is a slight increase of the diffusion coefficient, probably produced due to a minimal reduction in the polymer effective size due to the increasing number of molecules in solution. Finally, while the concentration gradually increases from 0.8 mM the diffusion coefficient gradually decreases due to the more frequent interactions between the molecules in solution. In addition, the diffusing behaviour of the HOD molecules is exactly the same as the behaviour shown in the previous chapter, remaining stable

at the different concentrations of PVP and around 20 × 10^{-10} m^2s^{-1}. Therefore, the following experiments were performed at 0.8 mM concentration because as it was discussed previously, this is the concentration in which the polymers have reached the overlap concentration and their effective size seem to be stable.

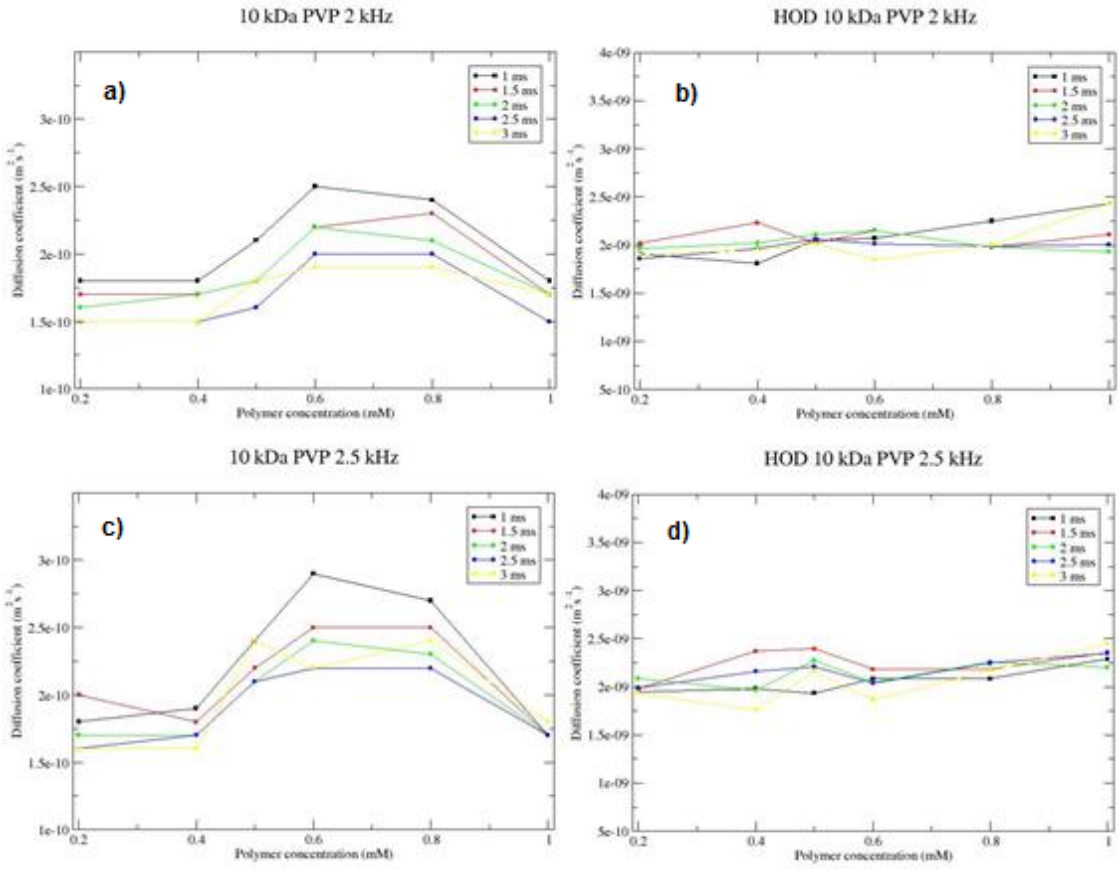

Figure 5.1: Diffusion coefficients of a set of concentrations of 10 kDa PVP and the residual signal of HOD in D_2O at different spinning rates using the fully rotor synchronised Oneshot sequence varying the gradient length

After the behaviour was analysed, it was necessary to check if the values of the diffusion coefficient were reliable (if they were in the range of the diffusion domain that is expected for a molecule of a particular size) and how much they varied from the static experiments. Consequently, a static DOSY-NMR experiment was perform with a sample 0.8 mM of 10 kDa PVP in D_2O and the diffusion coefficient of both the polymer and the HOD were recorded and compared to the values at moderate spinning rates (see table 5.1). The results showed that an increase in the spinning rate caused an increase in the diffusion coefficient of both the polymer and the HOD from the static samples to the spinning samples. However, the variation was not very large which suggest that the values are reliable and close to the expected value, and that the slight increase in the diffusion coefficient is probably caused by the increase of the kinetic energy experienced by the molecules due to the moderate spinning rate. It could also be noticed

that both polymers and the HOD signals increase the value of their diffusion coefficient roughly the same amount. This increase is slightly unexpected as the smaller molecules would be expected to have a larger increase than the larger ones, as they are both under the same speed but larger molecules have a larger weight. It is not very clear why larger molecules show the same increase in the diffusion coefficient than the smaller ones. Meaning that PEO increases its speed ≈ 150 % while HOD only does ≈ 5 %.

0.8 mM polymer	**Diffusion coefficient (× 10^{-10} m^2s^{-1})**		
Spin rate	**Static**	**2 kHz**	**2.5 kHz**
PVP	1.35	2.1	2.4
HOD (PVP)	20.33	20.40	21.89
PEO	0.45	Not recorded	1.6
HOD (PEO)	17.58	Not recorded	20.83

Table 5.1: Comparison of the diffusion coefficients of the 10 kDa PVP polymer and 50 kDa PEO and their corresponding HOD residual signals at different spinning rates in a sample 0.8 mM polymer concentration in D_2O

PVP has shown the expected results for the diffusion coefficient and the diffusion behaviour under high spinning rate. In order to see if it possible to perform SEC-DOSY NMR under MAS in a mixture, the experiments performed with the PVP samples were repeated with a PEO sample. However, as it was discussed in the previous chapter, the spinning sidebands can be shifted by the variation of the spinning rate. Therefore, the experiments were performed at a 2.5 kHz spinning rate because it is high enough to avoid the presence of spinning sidebands in the area of interest of the spectrum (signals of interest shown by PVP and PEO appear in the range between 0.8 – 2 ppm, see figure 3.6). In addition, the experiments were performed varying the polymer concentration range from 0.6 – 1 mM (a narrower range is chosen because that is the range that showed the overlap concentration was reach in the previous polymer and it is not needed to obtain all the measurements of very low concentrations) to see if the diffusing behaviour is the same as the one shown by PVP. The results for these experiments are shown in figure 5.2.

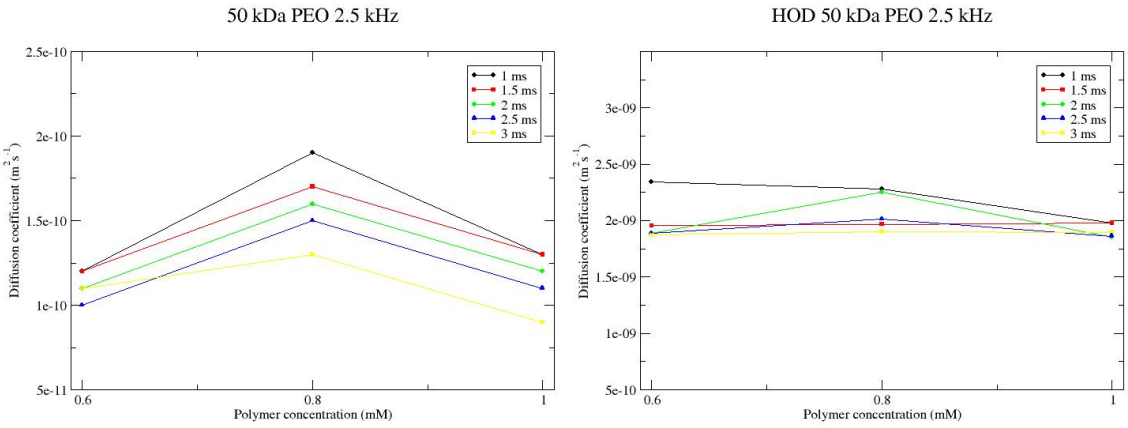

Figure 5.2: Diffusion coefficients of a set of concentrations of 50 kDa PEO and the residual signal of HOD in D_2O at different spinning rates using the fully rotor synchronised Oneshot sequence varying the gradient length

The data presented in figure 5.2 confirms that the diffusing behaviour of PEO is similar to the diffusing behaviour shown by PVP. As it was discussed above for the PVP, PEO also seem to reach the overlap concentration around 0.8 mM as the diffusion coefficient increased until the polymer concentration reached 0.8 and then showed a decrease when the polymer concentration increased. In addition, the behaviour of the HOD residual signal was the same as before showing consistent coefficient diffusion values around 20×10^{-10} m^2s^{-1}.

The value of the diffusion coefficient were lower for the PEO than for the PVP. This fact is in agreement with the size of the molecules as the larger molecule (50 kDa) diffuses slower than the smaller one (10 kDa). In order to know if the values are reliable, the same procedure that was followed with the PVP polymer was repeated, a static DOSY-NMR experiment was perform with a sample 0.8 mM of 50 kDa PEO in D_2O and the diffusion coefficient of both the polymer and the HOD were recorded and compared to the values at moderate spinning rate (see table 5.1). Again, the data are in agreement with the results shown by the PVP polymer, when the spinning rate increased, the diffusion coefficient increased slightly but remained lower than the PVP values. In addition, as it was discussed in chapter 3, when the tube was being filled with the sample of PEO it could be estimated by eye a greater viscosity in the PEO sample than the PVP. This fact is reflected in the diffusion coefficient of the HOD residual signal that is lower in the PEO sample than in the PVP sample.

The results of both polymers so far under the effect of MAS showed the expected behaviour and values. Therefore, the next step was to study their behaviour in presence of a stationary phase.

5.1.1.2 Experiments with stationary phases

Through the experiments performed so far it seem to be possible to obtain accurate diffusion coefficients and diffusing behaviour of molecules under the effect of MAS. Therefore, in order to see if it is possible to extend the use of SEC-DOSY NMR under HR-MAS conditions, PVP and PEO diffusion coefficients were recorded in presence of Sephadex G50. This stationary phase was chosen because of the size of its pores (1.5 – 30 kDa for globular proteins, for full data see table 2.1), which allows 10 kDa PVP to get into the pores. Hence, it is expected a reduction in the diffusion coefficient of this polymer when is in presence of the stationary phase. However, 50 kDa PEO is too big to fit into the pores and no variation or a very slight reduction of the diffusion coefficient is expected in presence of the stationary phase as was shown by Day and co-workers in static conditions [1, 75]. A DOSY NMR experiment was performed on two separate samples of PVP and PEO 0.8 mM polymer concentration in D_2O in presence of Sephadex G50. The results of these experiments compared to the results of the experiments without stationary phases are presented in figure 5.3.

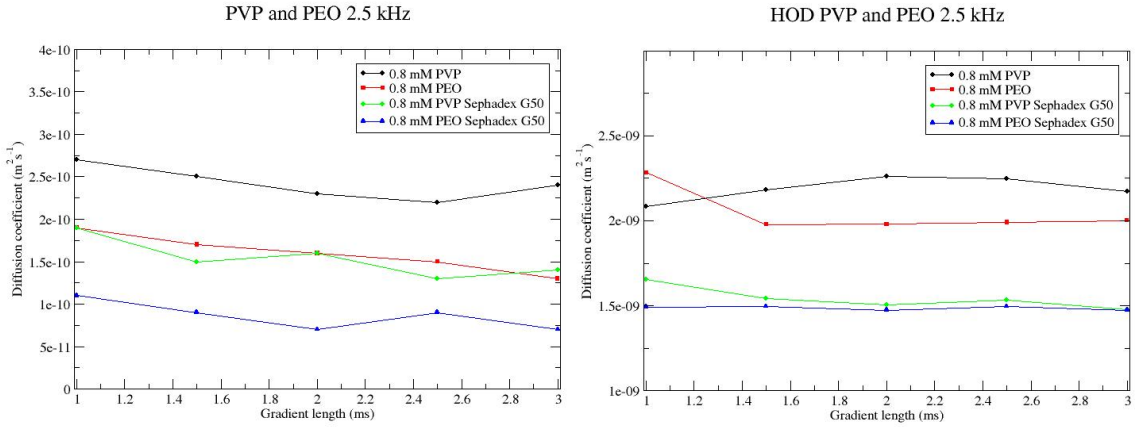

Figure 5.3: Diffusion coefficients of the polymers 10 kDa PVP and 50 kDa PEO and the residual HOD signal in separated samples made of 0.8 mM polymer concentration in D_2O with and without Sephadex G50 at 2.5 kHz spinning rate varying the gradient length

The results that were obtained from the experiments presented in figure 5.3 were very positive. As it was mentioned at the beginning of the section, these polymers were discarded in previous studies (see chapter 3) due to the impossibility to record reliable diffusion coefficients when the stationary phase was present. The combination of the technique with MAS improved the resolution and the diffusion coefficients could be recorded accurately this time. However, The behaviour of the polymers when the stationary phase was added was the expected one for the PVP but not for the PEO polymer. As it was mentioned above, the pores of the Sephadex G50 enable the polymer 10 kDa PVP to explore the stationary phase and experience a major

interaction with the Sephadex G50 that led to a reduction of the diffusion coefficient. This reduction was not expected for the PEO polymer as the size of the molecules are too large to explore the stationary phase. Nevertheless, when the stationary phase was added to the sample containing 50 kDa PEO the same reduction of the diffusion coefficient was experienced (see figure 5.3). The diffusion coefficients of the residual signal of HOD were also recorded to compare with the data of the polymers. In the case of HOD the diffusion behaviour was the expected, both samples showed similar diffusion coefficients for the HOD signals without the stationary phase. After the addition of the stationary phase, the diffusion coefficients of the HOD in both samples were reduced the same amount due to the presence of the stationary phase. Therefore, it was not possible to apply SEC-DOSY under MAS to a mixture of the polymers until it can be explained what is affecting to the diffusion of behaviour of the polymer.

5.1.2 Experiments with PSS

The DOSY NMR experiments performed under MAS with the neutral polymers that were used in previous chapters did not show the expected results when a stationary phase was added. PEO is too large to fit in the pores of the stationary phase. Hence, the addition of a SEC stationary phase should have not affected the diffusion coefficient as much as it is shown in the results presented in figure 5.3. In order to know whether this effect is caused by the stationary phase or the complicating effects that arise when MAS conditions are applied, two new polymers had to be chosen following the same size criteria as before: One had to be too large so it does not fit in the pores of the stationary phase, while the second one should be able to explore the pores of the stationary phase.

As was done in the previous section, the first step was to study the behaviour and values of the diffusion coefficients with a range of different concentrations at high spinning rate in order to discard complicating effects caused by the spinning rate. The first polymer chosen was 70 kDa PSS. This polymer was chosen because its size is large enough to make sure that it does not fit in the pores of Sephadex G50, and it has shown successful results when performing SEC-DOSY NMR in static samples as its diffusion coefficient barely varied after the addition of the stationary phase [1], [75]. Therefore, a DOSY NMR experiment was performed on several samples prepared using different polymer concentrations in presence of a phosphate buffer made with 150 mM NaCl + 50 mM Na_3PO_4 at 2.5 kHz spinning rate varying the gradient strength. The buffer was chosen because as was discussed in chapter 3, it is recommended by SEC literature [115] and is the buffer used in our previous studies. As it was done previously, the diffusion coefficient of

the residual signal HOD was also measured in order to compare the results with the experiments performed previously [80]. The results to this experiments are shown in figure 5.4.

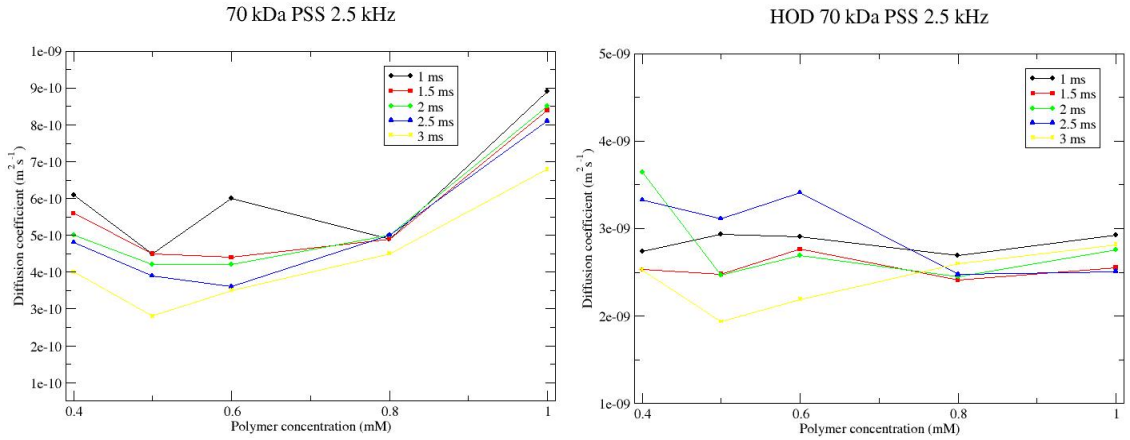

Figure 5.4: Diffusion coefficients of a set of concentrations of 70 kDa PSS and the residual signal of HOD in D_2O with a phosphate buffer at 2.5 kHz spinning rate using the fully rotor synchronised Oneshot sequence varying the gradient length

The behaviour shown by the 70 kDa PSS polymer was completely unexpected. When the concentration varied from 0.4 to 0.6 mM the diffusion coefficient remained stable, which is consistent with an infinite dilution behaviour where the polymer has not reached the overlap concentration. However, for concentrations higher than 0.6 mM the diffusion coefficient increased significantly while the concentration of the polymer increased. In addition, the values of the diffusion coefficient were also perplexing (see table 5.2). The neutral polymers showed an increase in the diffusion coefficient around 2x or 3x times the static value, which could be related to the high spinning of the sample. However, the PSS polymer experienced an increase in the diffusion coefficient of 16x times the static value when the concentration was 0.8 mM but even larger (30x times approximately see figure 5.4) when the polymer concentration was 1 mM.

In order to see if this abnormal behaviour was shown only by the polymer or if it was also affecting the residual HOD, the diffusing behaviour and the diffusion coefficients recorded from the residual signal of the HOD were compared with both the static and high spinning value (approx. 20×10^{-10} m^2s^{-1} [80]) and the values obtained with the neutral polymers.

The diffusing behaviour shown in figure 5.4 of the residual HOD was the expected one, while the polymer concentration increased the diffusing behaviour value remained constant, which suggests that the diffusion coefficient of HOD is not depending on the polymer concentration. However the value was extremely large. Both PVP and PEO samples showed a slight increase of the diffusion coefficient of the water signal (approx. 21×10^{-10} m^2s^{-1}). However, the HOD signal

of the PSS samples gave diffusion coefficients notably higher (approx. 25 × 10^{-10} m^2s^{-1}), but still far away of the significant increase experienced by the PSS polymer.

0.8 mM polymer	**Diffusion coefficient (× 10^{-10} m^2s^{-1})**		
Spin rate	**Static**	**2 kHz**	**2.5 kHz**
PVP	1.35	2.1	2.4
HOD (PVP)	20.33	20.40	21.89
PEO	0.45	Not recorded	1.6
HOD (PEO)	17.58	Not recorded	20.83
PSS	0.3	Not recorded	5
HOD (PSS)	18.65	Not recorded	25.25

Table 5.2: Comparison of the diffusion coefficients of different polymers and their corresponding HOD residual signals at different spinning rates in a sample 0.8 mM polymer concentration in D_2O and buffer for the charged polymer

The results presented so far have shown that there is a strange effect on the diffusion behaviour and the value of the diffusion coefficients at high spinning rates. Therefore, it was not possible to continue trying to perform size exclusion chromatography under this condition until this effect had been understood.

5.1.2.1 The Lorentz force hypothesis

The PSS polymer is the largest of the polymers studied in this chapter. Therefore, the expected diffusion coefficient for this polymer should be the lower in value. Nevertheless, it is exactly the opposite. The main difference between the samples studied is the presence of charges on the molecule, somehow, the presence of charges seem to produce an increase in the diffusion coefficient values. In addition, the higher the polymer concentration is, the larger is this increase. Therefore, the cause could be the Lorentz force [171, 172]. The Lorentz force, is a force experienced by any charged particle moving with a particular velocity in presence of an electric or magnetic field and it is described by the equation 5.1.

$$\boldsymbol{F} = q\boldsymbol{E} + q\boldsymbol{v} \times \boldsymbol{B} \tag{5.1}$$

Where ***F*** is the Lorentz force, *q* is the charge of the particle, ***E*** is the electric field, $\boldsymbol{v}$ is the velocity of the charged particle and ***B*** is the magnetic field. In order to see if this force could actually be the cause of large the variation in the diffusion coefficient, it is required to know the value of the force generated and the acceleration experienced by a molecule of 70 kDa PSS. Therefore,

the force was calculated fitting into equation 5.1 the following values: 2.5 kHz spinning rate into a 3.1 mm diameter rotor in presence of a 14.1 T (600 MHz spectrometer) magnetic field for a molecule with a net charge of 1137 (as the weight of a monomer is 185 and the maximum possible net charge is 3). The value was: 6.06×10^{-14} N (These calculations are shown in appendix A). That force will produce an acceleration on a molecule of 70000 Da, that can be calculated using the Newton second law $F = ma$ which gives an acceleration value of 5.17×10^{8} ms^{-2}. The value calculated seem high enough to consider the Lorentz force as a valid hypothesis of a possible effect that arise under MAS conditions. Even more, if it is compared with the value of acceleration produced at the rotor wall at 2.5 kHz which is 3.82×10^{5} ms^{-2} (These calculations are shown in appendix A). Therefore, the following studies will try to determine if the main cause of disruption of the diffusion coefficient is the Lorentz force. These forces do not act in the same direction, they are perpendicular to each other. For this reason the effect of the Lorentz force is supposed to affect more DOSY experiments as it affects along the rotor axis.

It is worth mentioning here, that although many more experiments need to be performed in order to fully understand the diffusion under MAS, the possibility of varying the diffusion coefficient through the appearance of the Lorentz force opens the door to a pseudo-chromatographic study where the use of a stationary phase is not needed. Meaning that two molecules with same diffusion coefficient in static conditions could potentially show a separation in the diffusion domain if high spinning rates are applied, as long as the net charge of one of the molecules is different enough to experience a significantly different Lorentz force. However, this hypothesis is something that will be studied in the future if it is possible to determine all the causes of diffusion disruption at high spinning rates.

5.1.3 Understanding of diffusion under the Lorentz force hypothesis

In chapter 3, some factors that were affecting the diffusion coefficient of molecules have been studied. The most relevant ones were the effective size of the molecule, the concentration and the viscosity of the sample. However, in chapters 4 and 5 it has been noticed that under MAS spinning conditions, there are other causes of variation of the diffusion coefficients that have made impossible to understand the diffusing behaviour, such as the high spinning rate and the acceleration experienced by the charged molecules due to the Lorentz force, as well as other effects described in the literature such as sedimentation due to the high spinning rate [147]. In the experiments performed in this chapter it has been seen that depending on the conditions in which the diffusion coefficient had been recorded, some factors became more relevant than others. Therefore, it is of vital importance to study the influence that all these factors have on

the diffusion coefficient in order to extend the understanding of diffusion behaviour under MAS conditions. Consequently, DOSY NMR experiments were performed varying some of their conditions, such as a different spinning rate or the use of buffer to a set of polymers, including neutral and charged polymers with a wide range of molecular weights (2.1 – 70 kDa). The results of these experiments will be presented along the following subsections to focus in each individual factor separately. Due to the different sizes of the polymers, the concentration used to perform the experiments were different, as some of them (the polymers with smaller sizes e.g. 2.1 and 5.1 kDa) would not show signals intense enough to record accurately the diffusion coefficient at low concentrations and some other polymer (the polymers with larger sizes e.g. 70 kDa) diffusion coefficients will be affected by a high polymer concentration. The polymers and concentrations used for these experiments are presented in table 5.3.

Polymer	M_w (kDa)	Concentration (mM)
Poly (Styrene Sulfonate) (PSS)	70	0.5
Poly (allylamine) (Paa)	56	0.5
Poly (2-Ethyl-2-Oxazoline) (PEO)	50	0.5
Poly (allylamine) (Paa)	15	0.5
Poly (Vinyl Pirrolidone) (PVP)	10	0.5
Poly (acrylic acid sodium salt) (PAA)	5.1	2.5
Poly (acrylic acid sodium salt) (PAA)	2.1	2.5

Table 5.3: Summary of polymers and concentrations used to perform DOSY NMR studies under MAS conditions

5.1.3.1 Effect of size and viscosity

The effect that size and viscosity have in the diffusion coefficient is the most intuitive one as it is related to the diffusion coefficient through the Stokes-Einstein equation, which is described in equation 5.2 and have been largely discussed along chapter 3.

$$D = \frac{k_b \times T}{6\pi\eta r_s} \tag{5.2}$$

Where D is the diffusion coefficient, k_b is the Boltzmann constant, T is the absolute temperature, η is the viscosity and r_s is the radius of the molecule supposing that it is spherical. As a summary, the molecules that have larger effective sizes, also have lower diffusion coefficients. Besides, the samples that have higher viscosity, also have lower diffusion coefficients. The diffusion coefficient recorded in a static sample of the polymers shown in table 5.4 are presented with the diffusion coefficient of their corresponding residual HOD signal in figure 5.5.

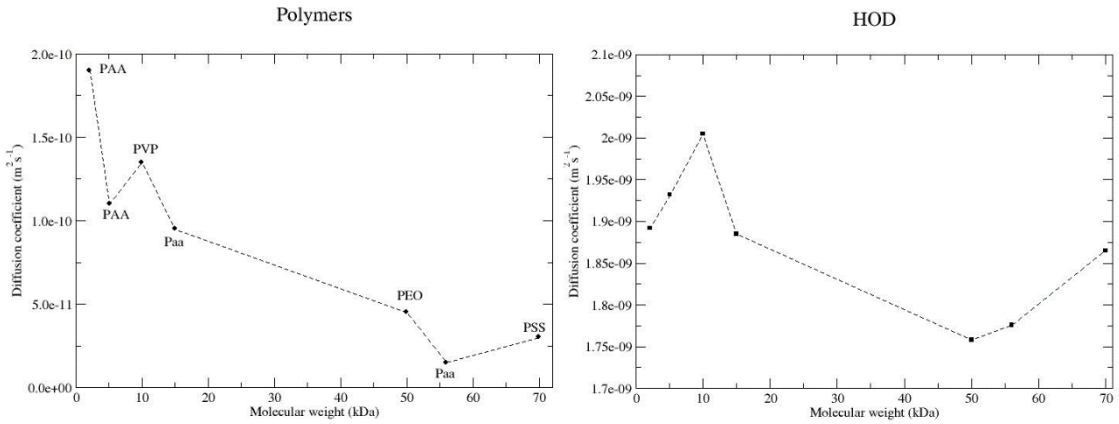

Figure 5.5: Diffusion coefficients of the polymers shown in table 5.4 and their corresponding HOD residual signal in a static sample in D_2O and phosphate buffer for the charged polymers

The results presented in the figure above clearly show that the smaller molecules have higher diffusion coefficients than the larger molecules. Only in a couple of cases (10 kDa PVP and 56 kDa Paa) the polymers did not follow the pattern. Nevertheless, the diffusion coefficient of these two polymers could be explained through the viscosity of the sample. During the process of the sample preparation it could be estimated by eye that the samples of 50 kDa PEO and 56 kDa Paa had the highest viscosity and the 10 PVP had the lowest one. In addition, the differences in the diffusion coefficients of the residual signal of HOD could also be explained through the viscosity of the samples, as the fastest and slowest HOD diffusion coefficients matched with the highest and the lowest viscosities estimated by eye when filling the tube. Therefore, the results in figure 5.5 confirm the previous statements about the effect of both size and viscosity on the diffusion coefficient and it can also be concluded that in static samples the effect of viscosity has shown to be more relevant than the effect of the size.

The same experiments were repeated at the lowest spin rate (0.7 kHz) allowed by the nanoprobe (see figure 5.6) to keep to a minimum the causes of diffusion disruption that arise with the addition of moderate spinning rates. However, even though the spin rate was kept to its minimum value the results were completely different to the results shown by the static samples, and also clearly matched the effects discussed in the section 5.1.2.1. The residual signal of the HOD showed similar variations in their diffusion coefficient to the ones shown by their corresponding polymer, which suggest that there are some effects arising when moderate spinning rates are applied that need to be understood in order to combine MAS with diffusion studies.

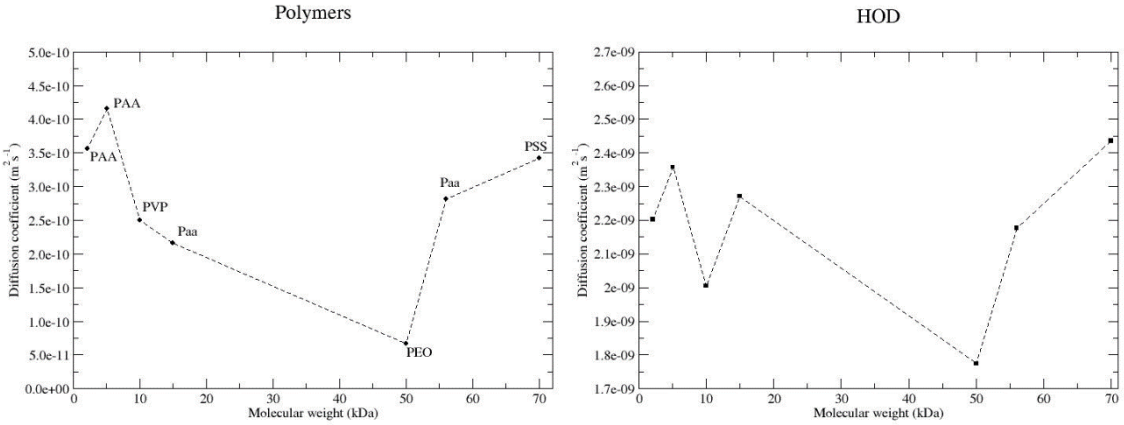

Figure 5.6: Diffusion coefficients of the polymers shown in table 5.4 and their corresponding HOD residual signal at 0.7 kHz in D_2O and phosphate buffer for the charged polymers

5.1.3.2 Effect of the spin rate

The effect of the spin rate has also been discussed previously both in chapter 4 and in the first section of this chapter. Unfortunately, to see the effect of the spin rate the experiments have to be performed with neutral polymers as charged polymers show a stronger dependence on spin rate observed likely due to the influence of the Lorentz force which is directly related to the velocity of the molecules (see equation 5.1). Therefore, to see the effect of the spin rate, the diffusion coefficients of 10 kDa PVP and 50 kDa PEO were measured at three different spinning rates, the lowest one that the probe allows to minimize the effect of the spin rate, a high spin rate to maximize the effect and one in between to compare the change from static to spinning and to see the effects of increasing the spinning rate when the sample is already at moderate spin rates (0.7, 2.5 and 3 kHz) in D_2O. The results are presented in figure 5.7.

The effect of the spin rate can clearly be observed when comparing the values of the diffusion coefficients in static samples (figure 5.5) and the values at different spin rates (figure 5.7). Under the effect of MAS the values of the diffusion coefficients grow significantly (2 - 3x times the static value for the PVP and 3 - 4x times for the PEO) compared to the static value. However, once the spin rate is already high the differences in the diffusion coefficients with a gradual increase of the spin rate are not so visible. The effects that can be observed in the diffusion coefficient recorded from the residual signal of the HOD are slightly different. First, the increase in the diffusion coefficient value is not as large as in the polymers. Second, the increase in the diffusion value seem to be larger for the more viscous sample. Finally, two conclusions can be taken. First, it seems that the spin rate affects more the larger molecules than small ones, as the diffusion coefficients varied more for PEO than PVP and finally HOD. Second, there is a big change in the

diffusion coefficient from static to high spinning (0 Hz to 0.7 kHz), but after that step the diffusion coefficients increases slowly with the spin rate (0.7 kHz to 2.5 kHz).

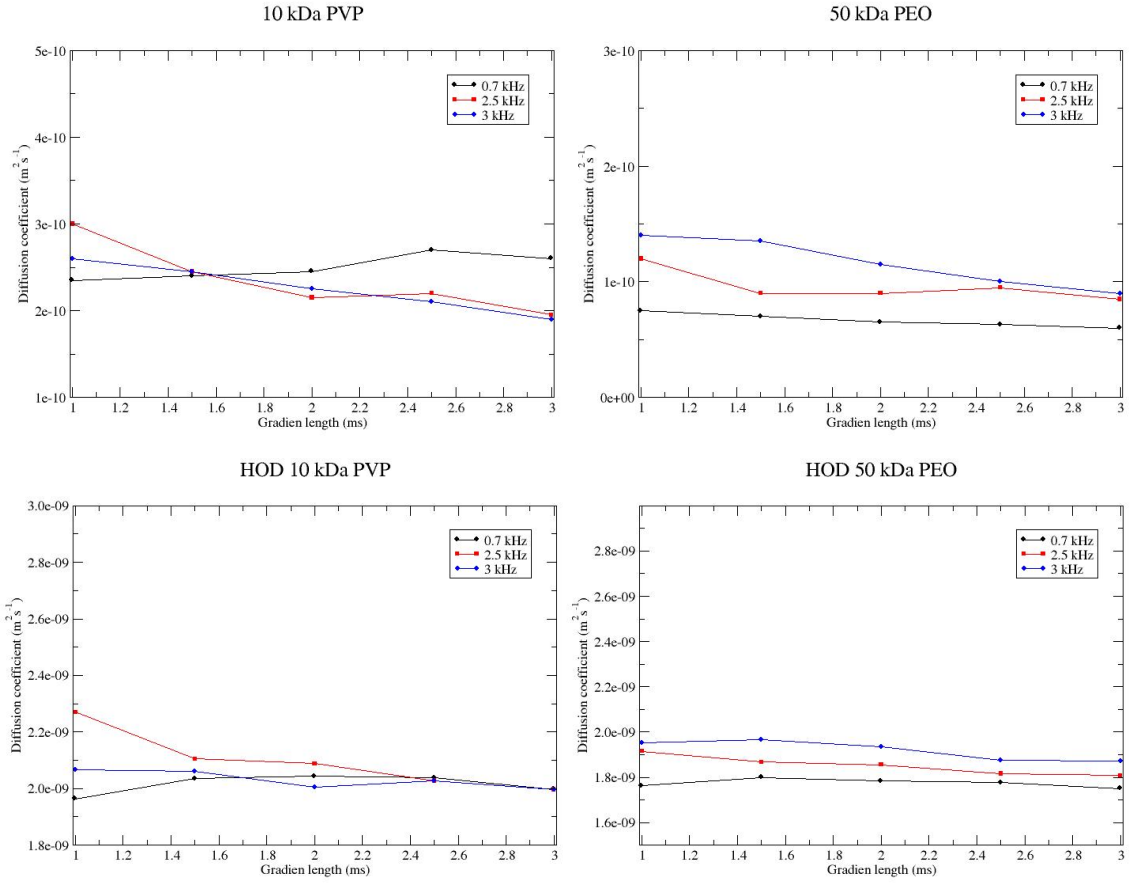

Figure 5.7: Diffusion coefficients of 10 kDa PVP and 50 kDa PEO and their corresponding HOD residual signal in D_2O at three different spin rates varying the gradient length

5.1.3.3 Effect of the charge

A charged particle that is moving in presence of a magnetic field experience a force known as Lorentz force [172]. The strength of this force is directly proportional to the strength of the magnetic field, the net charge of the particle and the speed of the particle as it is shown in equation 5.1. In this section, the diffusion coefficient of some polymers will be studied after a variation of both the net charge of the molecules in solution and the speed at which the molecules are moving. The results will be compared with neutral molecules in order to see if the Lorentz force is strong enough to produce acceleration in the molecules in a 600 MHz spectrometer (14.1 T magnetic field strength). Therefore, a DOSY NMR spectrum under MAS conditions was performed at different spinning rates to the polymers shown in table 5.3, in order to see the effect that the Lorentz force has in the value of the diffusion coefficient and in the

diffusing behaviour of the polymers. The diffusion coefficient recorded from the residual signal of the HOD was also recorded to compare it with previous static and MAS results. A buffer made with 150 mM NaCl and 50 mM Na_3PO_4 was added to the samples of charged polymers. The results of these experiments are presented in figure 5.8

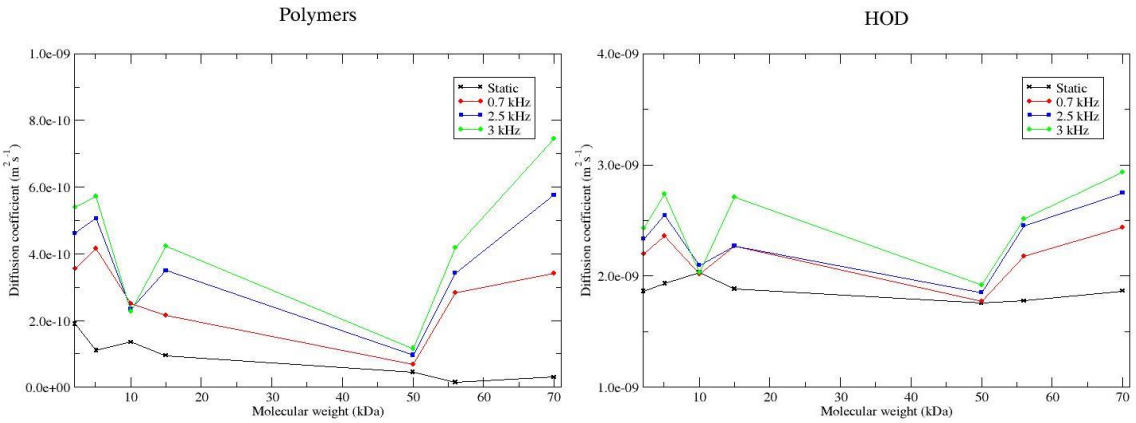

Figure 5.8: Diffusion coefficient of the polymers in table 5.3 and their corresponding residual HOD at different spin rates in D_2O for neutral polymers and phosphate buffer for the charged ones. The dips in the diffusion coefficients shown in the figure at 10 and 50 kDa correspond to the neutral polymers PVP and PEO which is in agreement with both the Lorentz force and the effect of charged particles in diffusion

As it was mentioned before there are two factors that were varied in order to study the effect of the Lorentz force in the diffusion coefficient, the net charge of the molecules and the speed of the molecules. Therefore, these factors will be discussed separately using the data presented in figure 5.8.

In general large molecules are expected to diffuse slower than small molecules. However, since in these experiments the charged molecules used are polymers formed by charged repeating units, if a polymer is larger it also possess more repeating units, and each unit has a net charge of one, then larger polymers have a higher net charge. Hence, they experience a larger Lorentz force, but they should be less affected as they are heavier molecules. When the diffusion coefficient of charged polymers in static samples is compared to any of the values obtained at high spinning rates, it can be seen that diffusion coefficient of large molecules increase far more than small molecules (eg. 2.1 kDa PAA varies from 2 to 3.8 × 10^{-10} m^2s^{-1}, while 70 kDa PSS varies from 0.3 to 3.8 at 0.7 kHz). In addition this variation is significantly higher when neutral polymers are compared with charged polymers (eg. 50 kDa PEO varies from 0.45 to 0.67 × 10^{-10} m^2s^{-1}, while 70 kDa PSS varies from 0.3 to 3.8 at 0.7 kHz). Although HOD is not a charged molecule, the

presence of charges in the solution make the HOD molecules that are under the effect of intermolecular forces to also experience an increase in the diffusion coefficient. Therefore, the results of HOD are in agreement with the polymer results, without the buffer the diffusion coefficient of HOD barely varies, but when there is buffer in the sample the variation is significant see figure 5.8. Hence, it seem to be a direct relationship between the net charge and the diffusion coefficient of moving charged molecules.

The second factor to be studied is how a higher velocity of the molecule affect to the diffusion coefficient. In the previous section, we have seen that after the initial step when the sample passes from static to high spinning rate (where the variation of the diffusion coefficient is significant, 0 to 0.7 kHz), the diffusion coefficient grows slowly while the spinning rate increases. The results presented in figure 5.8 show a completely different variation when there are charges in the sample. All the charged polymers experience a significant growth in their diffusion coefficient every time the spinning rate is increased, while the neutral polymers barely change (eg. 50 kDa PEO varies from 0.67×10^{-10} m^2s^{-1} at 0.7 kHz to 1.16×10^{-10} m^2s^{-1} at 3 kHz, while 70 kDa PSS varies from 0.3×10^{-10} m^2s^{-1} at 0.7 kHz to 7.46×10^{-10} m^2s^{-1} at 3 kHz). The variation of the HOD diffusion coefficient is also in agreement with this results. However, as it happened with the spin rate the variation in small molecules seem to be mild compare to large molecules.

One last experiment was performed to understand the effect of charges in the solution when diffusion coefficients are measured. It has been seen that not only the molecules directly charged like the polymers increased their diffusion coefficient, but also neutral molecules like HOD that are affected through the intermolecular interactions with molecules that are now moving faster. Therefore, the diffusion coefficient of a neutral polymer (50 kDa PEO), was measured in a sample containing the same phosphate buffer as the charged polymers (150 mM NaCl + 50 mM Na_3PO_4) and compared to the diffusion coefficient without buffer. The results are shown in figure 5.9.

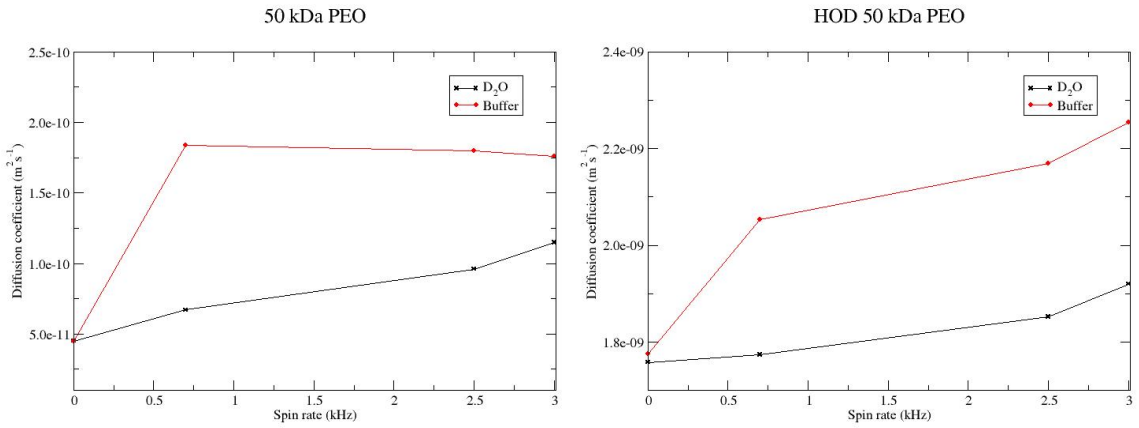

Figure 5.9: Diffusion coefficient of 50 kDa PEO and the residual HOD with and without buffer at different spinning rates

The presence of a buffer in the sample affected the diffusion coefficient of the polymer in solution. Without the buffer the polymer experienced a slow gradual increase of the diffusion coefficient while the spinning rate increased. However, when there was a buffer in the solution the polymer increased significantly more the diffusion coefficient as soon as the sample started a high spinning rate (0 to 0.7 kHz) and then remained stable while the spinning rate increased (0.7 to 3 kHz). Meanwhile, the HOD was in agreement with the charge effect seen before, the presence of charges in the solution made the water molecules move notably faster, possibly due increased motion added as a result of being the solvent of multiple ions. This fact suggested that the water molecules around the polymer also made the polymer move faster because the polymer shown in figure 5.9 is neutral and the diffusion coefficient is notably higher in presence of the buffer than in the absence of it.

Following an idea presented at the end of section 5.1.2.1, it is worth mentioning that these results also open the door for a possible pseudo-chromatographic effect without the use of stationary phase. Under static conditions the buffer did not produce any change in the diffusion domain. However, it seems to be possible to add a buffer and increase the spinning rate to produce separation in the diffusion domain between two molecules that have similar diffusion coefficients at static conditions. Therefore, this is something that will also be studied in the future if it is possible to clarify the causes of diffusion disruption under MAS.

Both charge and velocity of the molecules have shown to be directly related to the value of the diffusion coefficient. However, both factors increase the value of the diffusion coefficient so it is difficult to study them separately and see which one is more relevant. In addition, the molecules that have been studied in this section have very different scaffolds. Therefore, to

continue the study of the Lorentz force it is needed a set of polymer with the same scaffold but different molecular weights.

5.1.4 Study of the Lorentz force with a set of PSS polymers

Study diffusion by NMR under MAS conditions have shown to be a challenging task due to the number of unpredicted effects that the high spinning rate has in the diffusion coefficient of the molecules studied. Several experiments with a wide range of polymers, both in structure and weight, have been useful to determine that some of those effects are caused directly by the spinning rate, because of the charge of the molecules or even by the use of a buffer in the solution. However, in addition to the new effects discovered, is important to realise that the effects that vary diffusion in static samples such as concentration, polymer structure or viscosity of the sample also have an effect under MAS. Therefore, to be able to focus in particular effects, in this section, a set of PSS polymers of low polydispersity with a wide range of molecular weights (see table 5.4) are used to continue extending the understanding of diffusion under MAS conditions with the simplification of a common scaffold of the polymers, this way is easier to simplify the effects that affect in static conditions and to focus the effects that arise under MAS.

M_w (kDa)	**Polydispersity (PDI)**	**Concentration (mM)**
10	< 1.20	3.9
15	< 1.20	2.6
20	< 1.20	1.95
30	< 1.20	1.34
65	< 1.20	0.6
79	< 1.20	0.5

Table 5.4: Summary of the molecular weight, polydispersity and concentrations of the set of PSS polymers used to perform DOSY NMR studies under MAS conditions

All the experiments performed so far with different polymers in the previous section contained the same polymer concentration, except for the PAA polymers that were too small and the technique is not sensitive enough to produce spectra and record the diffusion coefficient with a concentration as low as 0.5 mM. However, due to the huge weight difference between some of the polymers the charge content in the solution can vary notably from the smaller polymers to the larger ones if the concentration is kept the same for both samples. After proving that not only the charge on molecules has an effect on the diffusion coefficient, but also the amount of

charges in solution, if the effect of the Lorentz force wants to be studied, it is needed to repeat the studies of different net charge of the molecules (different sizes as the molecules are formed by charged repeating units), with the same amount of charges in the solution. Therefore, a DOSY NMR experiment was performed with the polymers shown in table 5.4, using different polymer concentrations that will ensure that the total amount of monomer in solution is the same in all the samples. Hence, there will be the same amount of charges and in terms of space (repeating units per volume) the same amount of monomers. This experiments were performed in presence of the previously used phosphate buffer (150 mM NaCl + 50 mM Na_3PO_4) in D_2O at two different spin rates, the minimum allowed by the nanoprobe (0.7 kHz) to minimize the spin rate effect, and one of the higher spinning rates allowed by this probe (3 kHz) to see the effects of charge and spin rate. The results are presented in figure 5.10 with the results of the diffusion coefficient recorded from the residual signal of the HOD, which allows to compare the reliability of the results obtained.

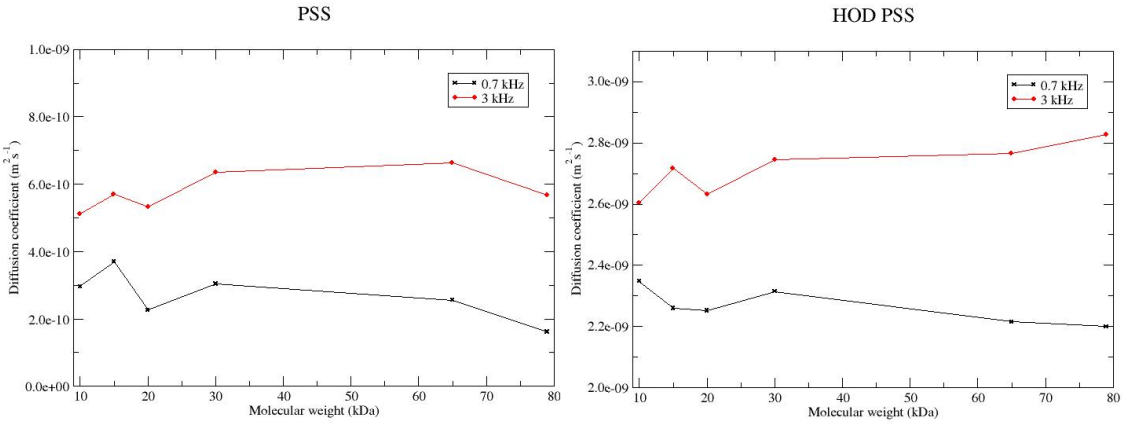

Figure 5.10: Diffusion coefficient of a set of PSS polymers with different molecular weights and their corresponding residual HOD signal at different concentrations (presented in table 5.4) that ensure the same amount of monomer in solution in presence of 150 mM NaCl and 50 mM Na_3PO_4 buffer in D_2O at two different spin rates

The results presented in figure 5.10 show that the diffusion coefficient barely change with the increase of the molecular weight when the amount of monomer in solution is kept the same. In contrast, the results presented in figure 5.8 with same concentration for all polymers the diffusion coefficient grew with the increase of the molecular weight. However, all the results recorded so far for charged polymers show a larger increase of the diffusion coefficient for the larger polymers when the spin rate is increased. Therefore, it seem that is not only important when studying the diffusion of molecules under MAS the charge of this molecules but also the total net amount of charges that is present in the sample.

5.1.4.1 Charged ion concentration in solution

In the previous section it has been seen that the amount of charged particles in solution has an effect in the diffusion coefficient of the molecules when it is studied under MAS conditions. Some of the polymers presented in figure 5.10 show a slightly irregular behaviour that could be the result of using many different polymer weights that produced solutions with slightly different viscosities. In order to study the effect of the amount of charges in the solution, a DOSY NMR experiment was performed to only two of the polymers of the PSS set varying the polymer concentration with and without buffer at two different spin rates, the minimum allowed by the nanoprobe (0.7 kHz) and one of the higher spinning rates allowed by this probe (3 kHz) to see the effects of charge and spin rate. The polymers chosen were 65 kDa and 20 kDa PSS, because keeping low concentrations allow to obtain spectra with good enough sensitivity to obtain accurate diffusion measurements. In addition, it allows to compare how polymers of two different sizes are affected by these effects. So far larger polymers have been shown to be more affected by the effects that arise after the increase of the spinning rates. The results of these experiments are shown in figure 5.11 with the results of the diffusion coefficient recorded from their corresponding residual signals of the HOD.

As it has been discussed several times in this thesis the increase of polymer concentration when diffusion is measured, should either produce a decrease in the diffusion coefficient, due to more frequent interactions between the molecules in solution after the overlap concentration is reached, or remain stable while the molecules are below the overlap concentration. The results in figure 5.11, show the expected behaviour for the 65 kDa PSS no matter with or without buffer when the spin rate was low (0.7 kHz) for both the polymer and the residual HOD. However, it shows a slight increase with the concentration for the 20 kDa PSS polymer that can only be associated to an increase in the diffusion coefficient due to the bigger amount of charges and the low weight of the polymer, in the case of the 65 kDa PSS the effect of the charges does not seem to be strong enough to accelerate the molecules at a low spinning rate while the 20 kDa PSS seem to be small enough to show the acceleration produced by the charges.

The results were unexpected when the spinning rate was high (3 kHz). The diffusion coefficient increased as the concentration was increasing for both of the polymers and their corresponding residual HOD more significantly than the increase observed on 20 kDa PSS at a slow spinning rate. In terms of being affected only by the Lorentz force, this result does not make sense as the molecules used have all the same charge and size. Therefore, the diffusion coefficient should

either remain stable or decrease due to the bigger amount of intermolecular interactions but not grow.

For both polymers there is a rise of the diffusion coefficient of the polymers when the spinning rate is increased. When the results without the buffer are compared to the results with buffer, it can be seen that while the spin rate grow, the polymer in presence of buffer increase their diffusion coefficient approximately the same amount in every concentration for both polymers. However, the results without buffer show that the diffusion coefficient increases notably more at high polymer concentrations (3×10^{-10} m^2s^{-1} at 1 mM for 65 kDa PSS and 4×10^{-10} m^2s^{-1} at 3 mM for 20 kDa PSS) than at low polymer concentrations (0.5×10^{-10} m^2s^{-1} at 0.1 mM for 65 kDa PSS and 1.1×10^{-10} m^2s^{-1} at 0.5 mM for 20 kDa PSS). Therefore, the absence of buffer seem to make more noticeable the effect of the Lorentz force, but when the buffer is present it seem to have a balancing effect on the acceleration that the molecules experience under MAS conditions.

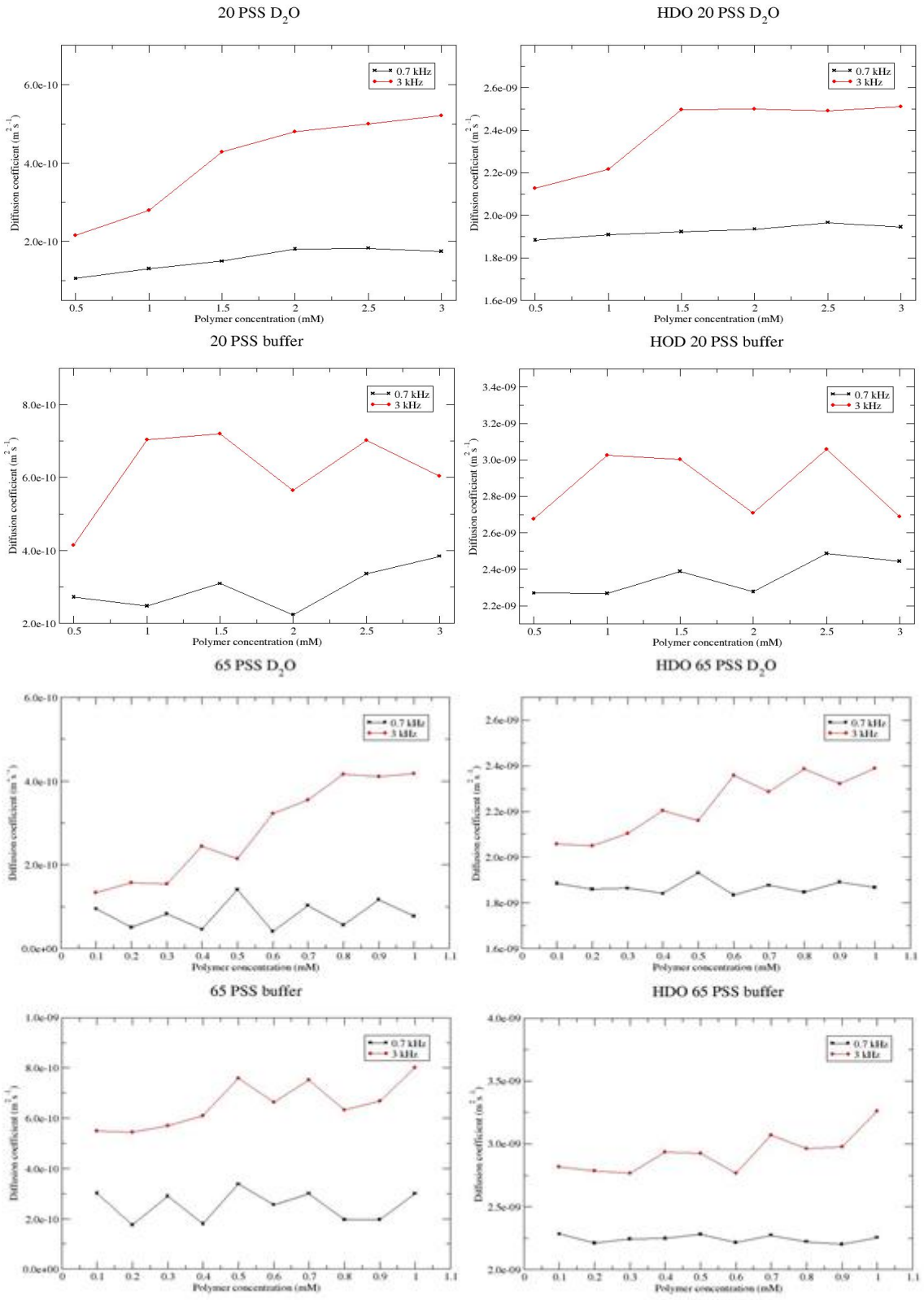

Figure 5.11: Diffusion coefficient of 65 kDa PSS, 20 kDa PSS and their corresponding residual signal of HOD at different concentrations and spin rates with and without phosphate buffer (150 mM NaCl + 50 mM Na_3PO_4) in D_2O

In addition to the effect on the diffusion coefficient when varying from low spinning rates to high spinning rates, there is also a significant difference in the effect on the value of the diffusion coefficient when the results with and without buffer are compared to the static value of the diffusion coefficients for both polymers. The variation of the diffusion coefficient from static to spinning is much larger when the buffer is present, as it is shown in table 5.5. Also these numbers reflect that the diffusion coefficient of the larger polymer varies more than the smaller one. Therefore, it can be concluded that a larger amount of charges in the solution is translated in higher diffusion coefficient of the molecules in the sample, but also that the differences in the behaviour are more subtle when the buffer is present.

Polymer	D ($\times 10^{-10}$ m^2/s) Static	D ($\times 10^{-10}$ m^2/s) 0.7 kHz	D ($\times 10^{-10}$ m^2/s) 3kHz
65PSS + Buffer	0.3	2.5	6.5
20PSS + buffer	0.7	1	6
65PSS	0.3	0.8	3
20PSS	0.7	0.8	4.5

Table 5.5: Summary of the diffusion coefficient of PSS polymers in the presence and the absence of a buffer at different spin rates

5.1.4.2 Effect of the spin rate at different concentrations

In the previous section it has been shown the effect that the amount of charges in the solution has on the diffusion coefficients of the polymers at two different spin rates. In this section, a closer look will be given to the effect of the spin rate and see if it is possible to know which effect is more relevant (charges or spin rate) and in which conditions (concentration and spin rate). Therefore, a DOSY NMR experiment was performed to three samples of 65 kDa PSS at three different concentrations (0.5, 0.8 and 0.9 mM) varying the spin rate from 0.7 to 3 kHz in intervals of 0.1 kHz in D_2O. The results of these experiments are shown in figure 5.12.

In general terms the results were the expected ones. The increase of the spinning rate involves an increase in the diffusion coefficient of the polymer. Also as it was discussed in the previous section, at high polymer concentrations there are more amount of charges in the solution and that involves a larger increase in the diffusion coefficient. However, although the general behaviour is expected, if we look at the results presented in figure 5.12 it can be seen that the increase is not consistent, some spin rates produce a massive increase (e. g. 0.9 kHz to 1 kHz at 0.5 mM) and some other produce a significant decrease (e. g. 1 kHz to 1.2 kHz at 0.5 mM). In addition this sudden variations of the diffusion coefficient of the polymers do not occur always at the same spin rate, they also seem to depend on either the concentration, the amount of

charges or both. Therefore, in order to see if they are related to the concentration and if the buffer will change the behaviour of the polymer, a DOSY NMR experiment was performed to a sample containing 0.8 mM but in presence of the phosphate buffer used in previous experiments and compare to the 0.8 mM in D_2O. The results are presented in figure 5.13.

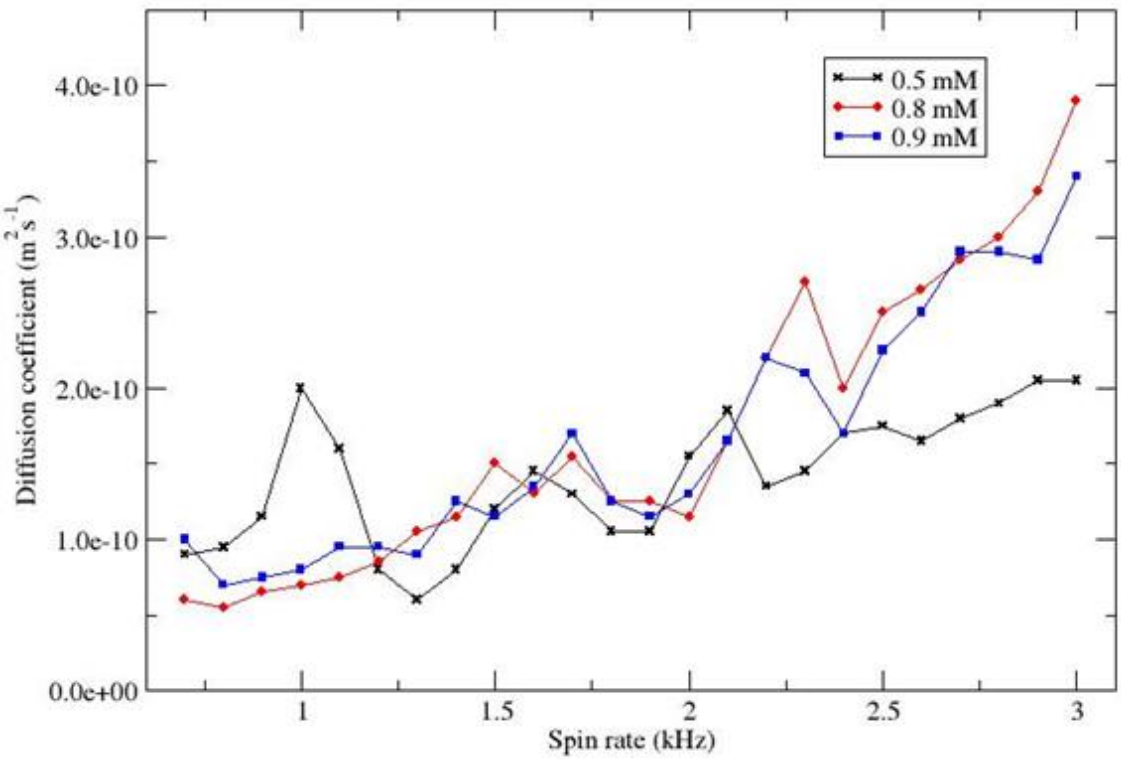

Figure 5.12: Diffusion coefficient of 65 kDa PSS at different concentrations varying the spinning rate in D_2O. HOD residual signal it is not presented as it showed the same pattern

The addition of the buffer meant a massive increase on the amount of charged particles that are present in solution. Therefore, an increase in the value of the diffusion coefficient of the polymer is expected. However, if the variation is caused by the spin rate and it is happening to the same polymer, then it is expected that the same spinning rates that caused sudden variations on the diffusion coefficient of the polymer will be the same spinning rates that will cause them again.

The results presented in figure 5.13 are in agreement with the effect produced by the amount of charges discussed in the section before. The diffusion coefficient at the same spinning rates of the polymer in presence of the buffer were larger than the diffusion coefficients of the polymer without the buffer. However, the sudden changes produced to the diffusion coefficients of the polymer at particular spin rates, occurred at different spin rates. Therefore, there seem to be some other effect that is not the amount of charges or the spin rate.

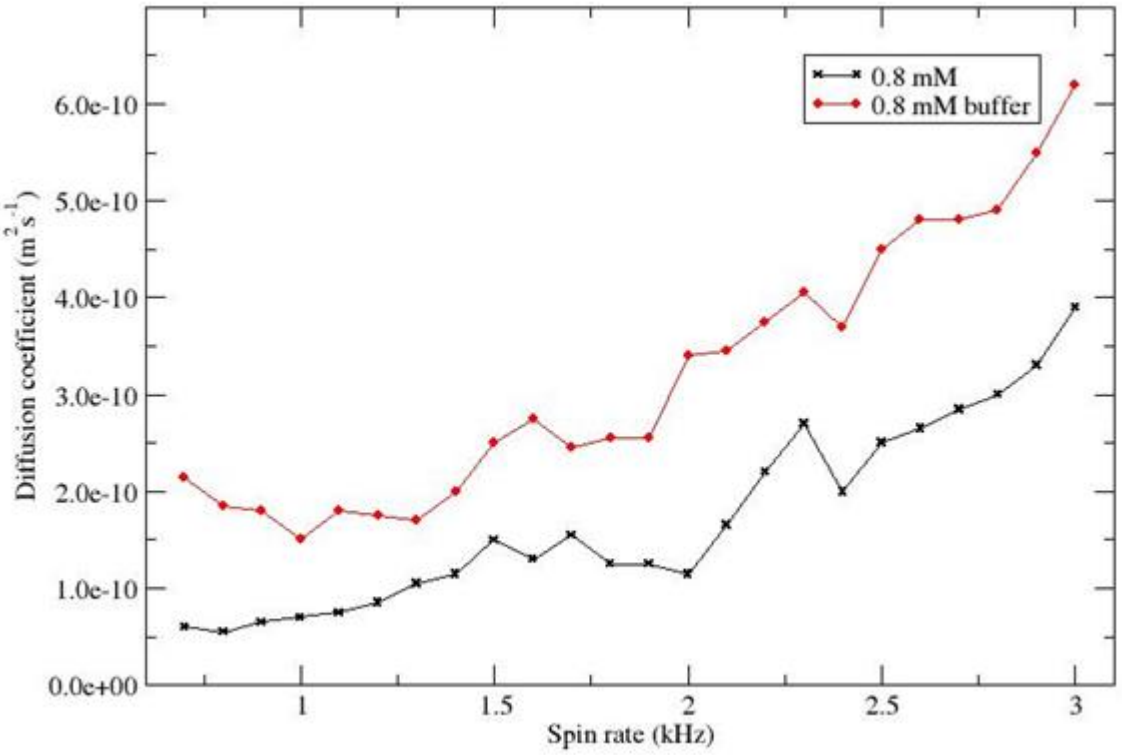

Figure 5.13: Diffusion coefficient of 65 kDa PSS at 0.8 mM concentration varying the spinning rate with and without buffer in D_2O. HOD residual signal it is not presented as it showed the same pattern

5.1.4.3 Variation of the diffusion delay

In the previous section, it has been seen that there is something that is causing variation in the diffusion coefficient of the polymer, but it is not clear what it is. All the experiments performed so far had been performed setting a diffusion delay of 50 ms. Therefore, it is possible that the cause could not be found because the molecules were diffusing either for too long or for a very short time. In order to see how the diffusing delay time affects the diffusion coefficient of the polymer, a DOSY NMR experiment was performed to two samples one of 65 kDa PSS and another one of 20 kDa PSS setting different diffusion delay times. The results of these experiments are presented in figure 5.14.

The diffusion delay is the period of time in the pulse sequence between the two field gradients that encode spatial information. During this time the molecules travel through the sample and depending on the mean square displacement, there is a reduction of the intensity of the signal, the longer it travels the larger is the decrease in the intensity and therefore the higher is the diffusion coefficient. This reduction is used later to calculate the diffusion coefficient. Therefore, in general in static samples the diffusion coefficient should not vary too much when the diffusion

delay is changed unless it is either too short or too long. This behaviour is reflected in figure 5.14. Three different diffusion delay times have been tried (30, 50 and 80 ms), and for both polymers the diffusion coefficient remains constant in static conditions. However, the results are notably different when the experiments were repeated at high spinning rates. Not only the diffusion coefficient`s value change from one diffusion delay to the other, but the trend also varied depending on the spin rate, at low spinning rates the diffusion coefficient decreases while the diffusion delay increases, but at high spinning rate the diffusion coefficient increases with the increase of the diffusion delay. It is not clear why this happens as it is shown in figure 5.14.

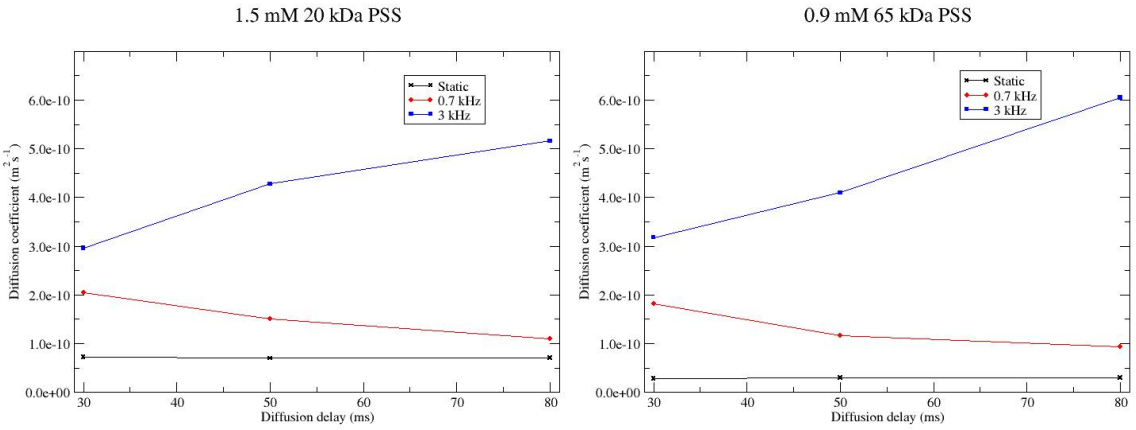

Figure 5.14: Diffusion coefficients of 20 kDa and 65 kDa PSS at different spin rates varying the diffusion delay in D_2O

5.2 Experiments with small molecules

The experiments performed to record the diffusion coefficient through the use of DOSY NMR under MAS conditions with several polymers, gave a first insight on which effects that can vary diffusion coefficients appear under MAS conditions. One of the most interesting effects that seem to be happening is the appearance of the Lorentz force that increases notably the diffusion coefficient of the polymers studied. However, many more factors have been found to have an effect on the diffusion coefficient such as the spin rate or the amount of charges in the sample, as well as the diffusion delay. All of them, have to be considered in combination with the usual non spinning causes of variation of the diffusion coefficient such as viscosity and molecular size. Therefore, in order to simplify slightly the studies, the diffusion coefficients of small molecules were studied. The difference in molecular weight from one molecule to another is notably smaller than between some of the polymers used. This fact will reduce the importance of the size of the molecule, which is one of the main causes of diffusion variation in non-spinning samples, and will let us focus in the rest of the effects that arise under MAS and that affect the diffusion coefficient.

5.2.1 Experiments in static conditions

The experiments with polymers have shown that a lot of new effects that produce variation in the diffusion coefficient arise when MAS conditions are applied. Therefore, is necessary to understand diffusion in non-spinning conditions, in order to know which possible new effects arise in the diffusion coefficient when the experiments are performed under MAS conditions. Hence, a wide range of small molecules were chosen to perform the DOSY NMR studies (see table 5.6). In order continue with the same solvent and buffer, all of the molecules studied were soluble in D_2O and the buffer used was the same as in the previous section (150 mM NaCl + 50 mM Na_3PO_4) the molecules concentration was 100 mM except on those cases that were hard to dissolve at that concentration. All the molecules are either salts or present charges in solution, which will enable the study of the effect of the Lorentz force when MAS conditions are applied.

Molecule	**Molecular weight**	**Concentration (mM)**	**Net charge in solution**
Me_4NCl	109.6	100	+1
4-Fluorophenol	112.1	100	0
Nicotinamide	122.1	100	+1
Tartaric acid	150	100	-2
Pyridoxine hydrochloride	169.2	100	+1
Tyrosine	181.2	20	+1 ; -1
p-Styrene sulfonate	206.2	100	-1
Lidocaine	234.3	25	0
EDTA	292.24	25	-4
Thiamine hydrochloride	337.26	100	+1
$[Co(en)_3]Cl_3$	345.59	50	+3

Table 5.6: Summary of the small molecules, molecular weights, concentrations and charges used to record their diffusion coefficient in static conditions with and without phosphate buffer in D_2O

The diffusion coefficients of all the molecules presented in table 5.6 were recorded using the Oneshot sequence [27], with a 50 ms diffusion delay and 2 ms gradient length with and without phosphate buffer in static conditions as well as their corresponding diffusion coefficients for the residual signal of HOD. The results to these experiments are presented in figure 5.15.

In static conditions the expected results depend mostly on the size of the molecule, the larger the molecule the higher the diffusion coefficient will be. This is the general behaviour shown by the molecules that are presented in figure 5.15 both in presence of the buffer or in absence of it. However, there could be seen some anomalies in some of the molecules such as the tartaric acid in D_2O. Some of the tartaric acid measurable signals come from exchangeable protons. Therefore, the relaxation of the nucleus that produced these signals occurs faster than it should be due to the fast exchange between the acid and the protons in water. This fast exchange is reflected in a significant increase in the apparent diffusion coefficient of the tartaric acid. Nevertheless, there must be some other kind of relaxation mechanism that is affecting also to the signals of the protons attached to the carbons in the backbone of the molecule as these show also extremely high diffusion coefficients. However, the presence of the buffer minimize or slows the exchange rate. Thus, this effect is not visible when the buffer is present.

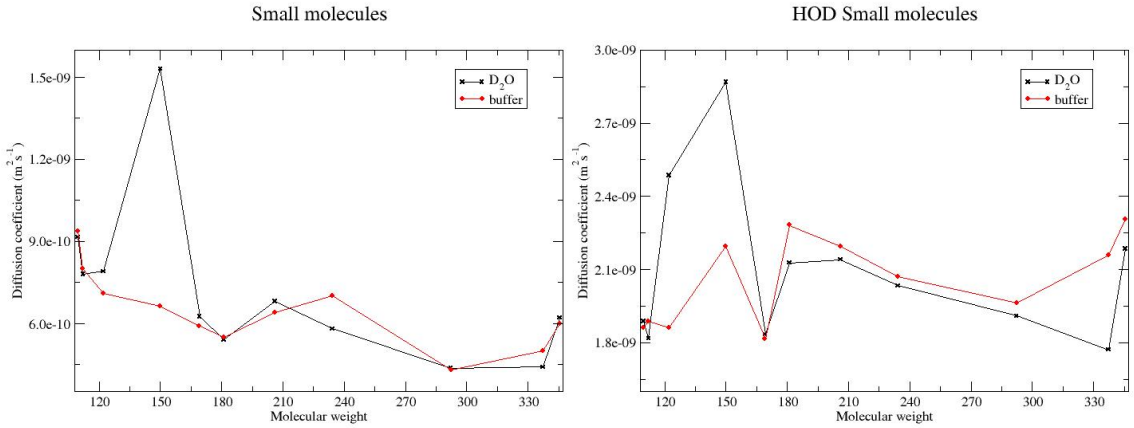

Figure 5.15: Diffusion coefficients of the molecules summarised in table 5.6 and their corresponding HOD residual signal with and without buffer in D_2O in static conditions

The diffusion coefficients of the residual signal of HOD are not as consistent as they were in previous experiments with polymers, meaning that the diffusion coefficients suffered several strong variations. These variations are probably produced for the same reasons as the variation produced in the tartaric acid sample, most of the molecules have exchangeable protons. Therefore, the decrease on the intensity of the HOD signal occurs faster than it would do if these molecules were not present in the solution.

5.2.2 Experiments under MAS conditions

The causes of diffusion coefficient variation for small molecules are similar to polymer ones for static samples, except for those that have some kind of strong exchange with the water molecules. However, in general it has been observed that the larger molecules are the slower they diffuse. In this section it will be explore if the diffusion coefficient varies the same as in

static conditions for small molecules, or if as it happened with the polymers, some other effects appear that can affect to the diffusion coefficient.

One of the main causes of variation of the diffusion coefficient of the polymers under MAS seemed to be the appearance of the Lorentz force. However, this force is directly dependent on the charge of the molecules which for the smallest polymer studied was 2100 net charge (2.1 kDa PAA see table 5.3). The largest small molecule studied here has a net charge of 3 (Cobalt complex see table 5.6). Therefore, although this molecules are significantly smaller and would be more affected by the force, the magnitude of the force experience by them is at least a thousand times smaller.

A DOSY NMR spectrum of each of the molecules in table 5.6 was performed with and without the buffer varying the spinning rate from 0.7 to 3 kHz in intervals of 0.1 kHz using the fully rotor synchronized Oneshot sequence with a 50 ms diffusion delay and a 2 ms gradient length. The results obtained revealed different behaviours for different molecules. Therefore, in this section the data are presented in groups of molecules that show a similar diffusing behaviour after they have been measured under MAS conditions.

Most of the molecules studied under MAS presented exactly the expected behaviour, which was, a noticeable increase in the diffusion coefficient value compared to the static value due to the effect of the high spinning rate and a faster diffusion for the molecules that are in presence of the phosphate buffer. In addition, it could also be observed that the Lorentz force does not seem to be the cause of any significant variation in the diffusion coefficient, as opposed as what happened with the polymer samples, the diffusion coefficient remain quite stable with the increase of the spinning rate, a slight increase was shown but not as significant as it was seen on the polymer samples. Also the diffusion coefficient shown by the HOD residual signal of each molecule is consistent with their corresponding molecule, as they presented a very similar behaviour. The results of the molecules that presented this variations on their diffusion coefficient when MAS conditions were applied, can be seen in figure 5.16 with their corresponding diffusion coefficient recorded from the residual HOD signal.

25 mM EDTA

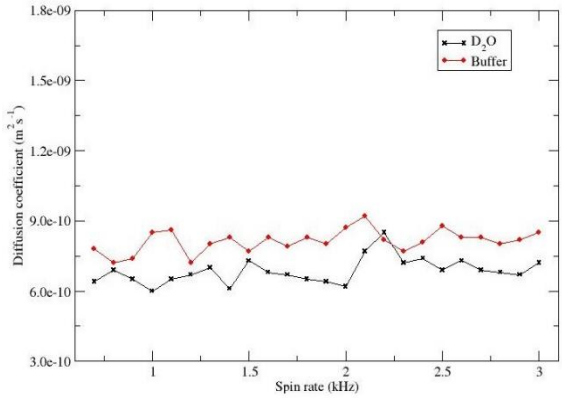

HOD 25 mM EDTA

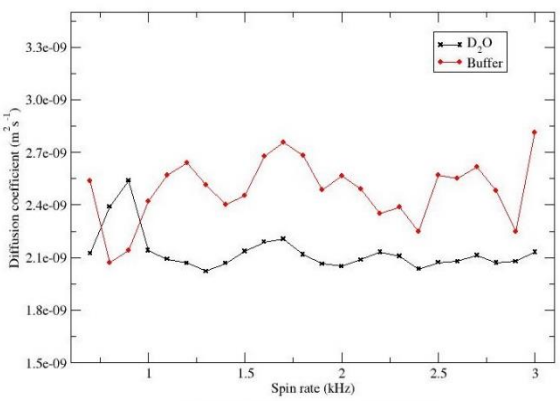

100 mM 4-Fluorophenol

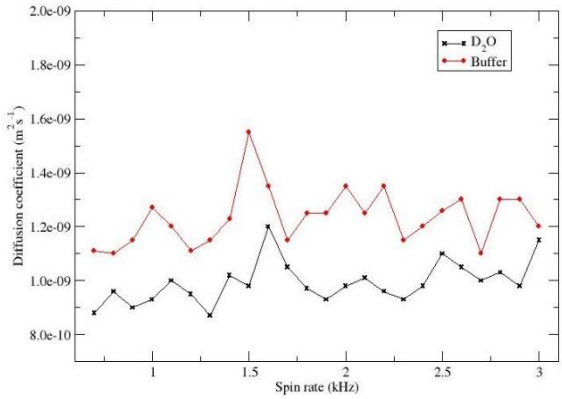

HOD 100 mM 4-Fluorophenol

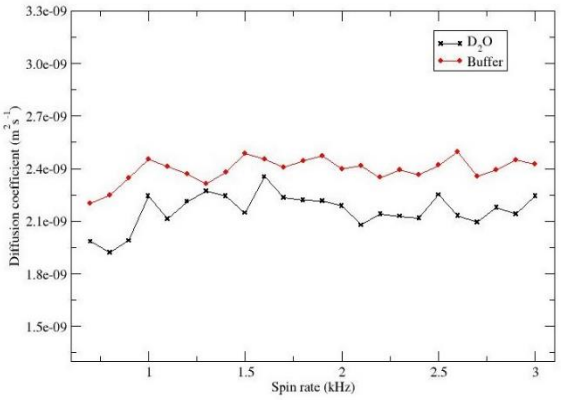

100 mM Pyridoxine

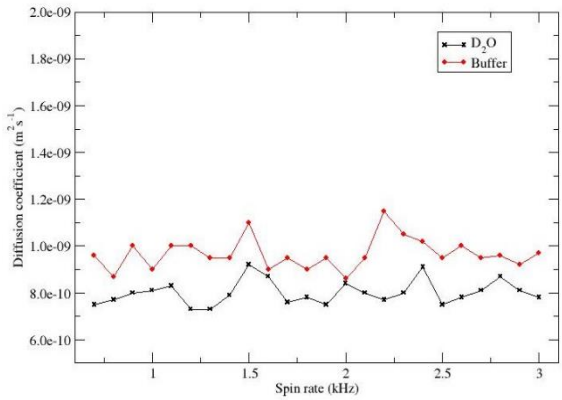

HOD 100 mM Pyridoxine

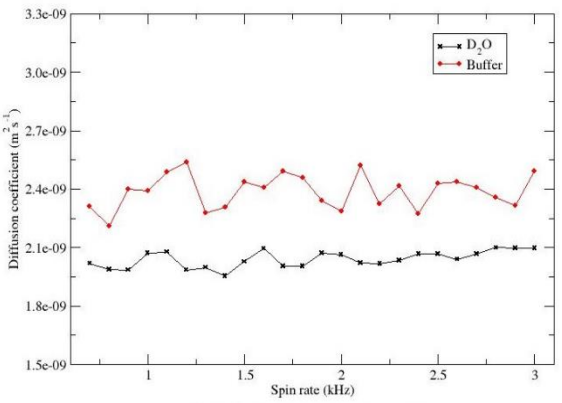

100 mM Nicotinamide

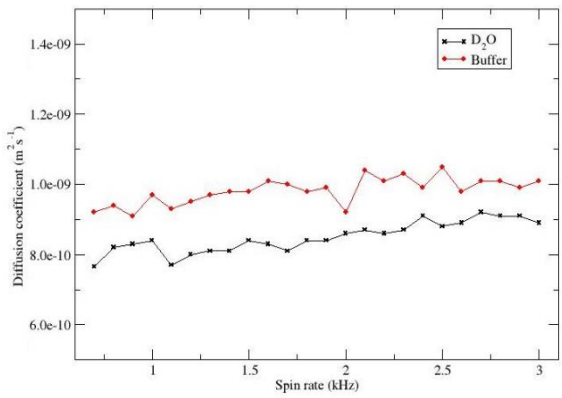

HOD 100 mM Nicotinamide

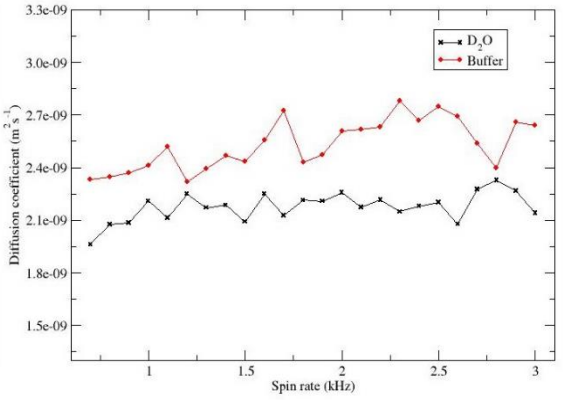

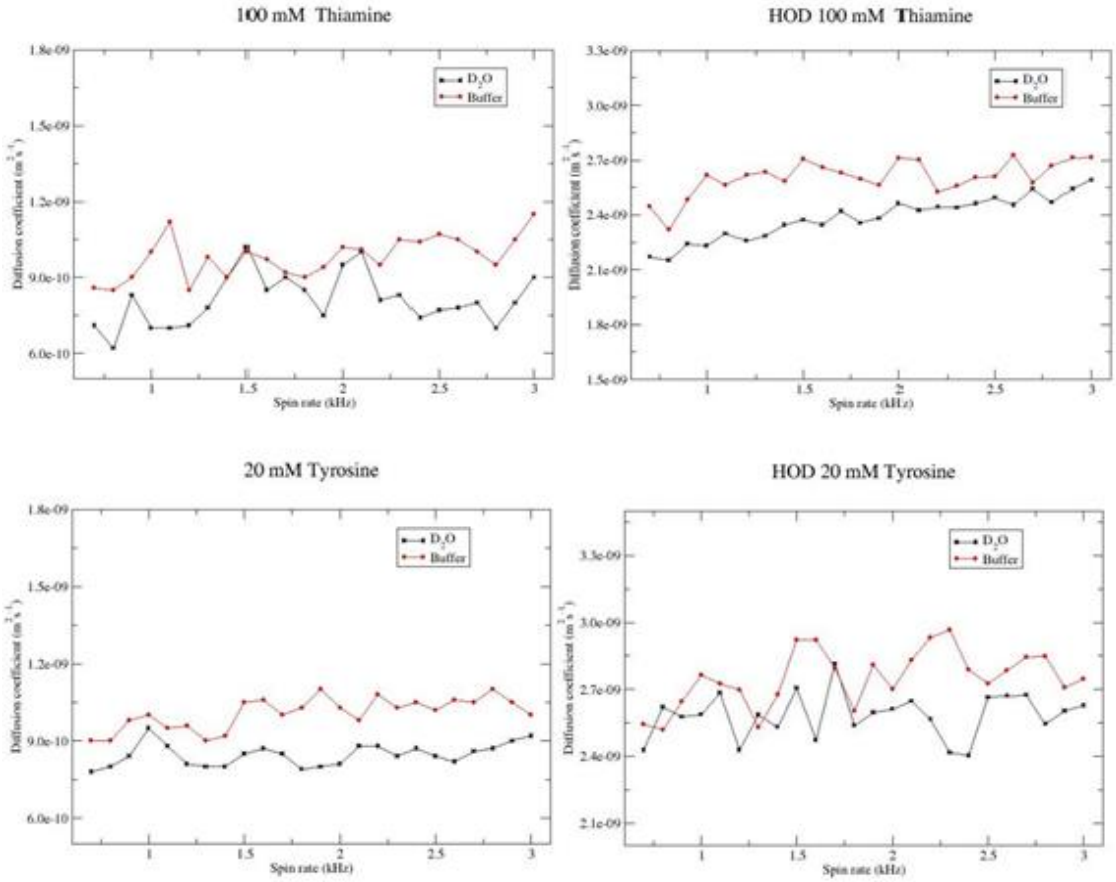

Figure 5.16: Diffusion coefficients of the molecules presented on table 5.6 that show the expected diffusion behaviour at different spin rates with and without buffer

The diffusing behaviour observed on the following set of molecules (tartaric acid, p-styrene sulfonate and Me_4NCl), was not expected (see figure 5.17). These molecules show diffusion coefficient that had sudden variations at particular spinning rates. In the case of the tartaric acid and the Me_4NCl both in with and without the buffer. However, p-styrene sulfonate only show this sudden variation (although they were the ones that revealed the most significant changes) when the buffer was not present. In presence of the buffer the behaviour was similar to the results presented in figure 5.16. The same behaviour as the molecules was presented by their corresponding HOD residual signal. However the sudden changes did not appear at the same particular spinning rates.

Although it is not clear why this sudden variation to the diffusion coefficient occurred, the main hypothesis is that there is some kind of resonance effect at those particular spinning rates between the spinning rate and possibly some sort of movement affecting the oscillating local magnetic fields, such as maybe some particular stretch of the bonds that produces a relaxation mechanism that it is not fully understood at this stage. Therefore, it is something that requires

a further experiment to fully determine which this mechanism is. It has not been found any source in the literature that clarifies the possible mechanism that occurs here.

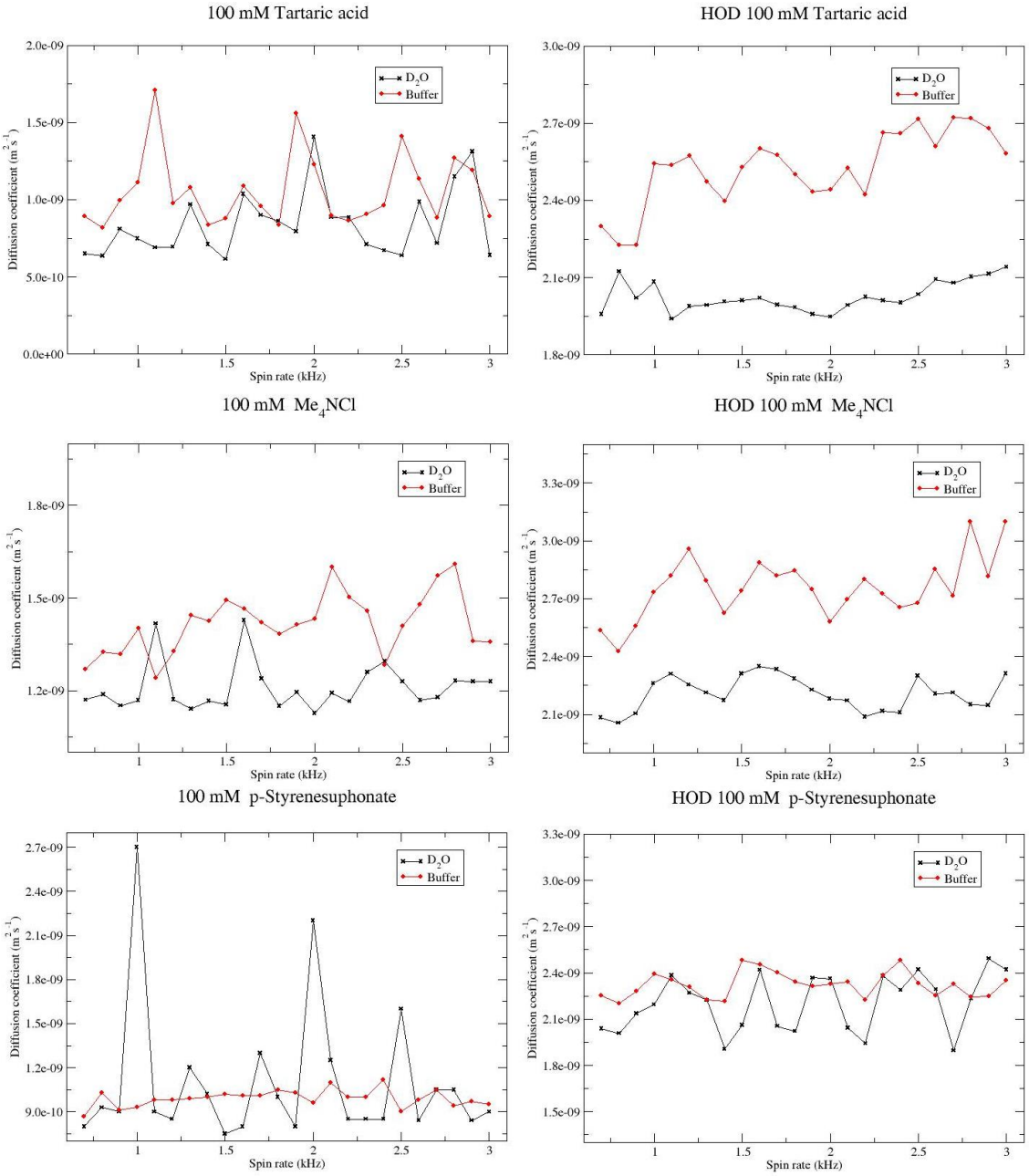

Figure 5.17: Diffusion coefficients of tartaric acid, Me_4NCl, p-styrene sulfonate and their corresponding HOD residual signal varying the spinning rate with and without buffer

Finally the last two molecules studied were lidocaine and $[Co(en)_3]Cl$. The results shown by this molecules were completely different (see figure 5.18) between them and to the molecules presented so far. In the case of lidocaine the results were perplexing. Not only is the only molecule that show faster diffusion coefficients when the buffer is not present that when it is, but also the diffusing values of both the lidocaine and the residual HOD signal were extremely

high compared to the static value (the diffusion coefficient varied from 5.8×10^{-10} m^2s^{-1} and 7×10^{-10} m^2s^{-1} in static conditions with and without buffer to 21.67×10^{-10} m^2s^{-1} and 16.08×10^{-10} m^2s^{-1} as an average of the different diffusion coefficients at the different spinning rates measured with and without buffer).

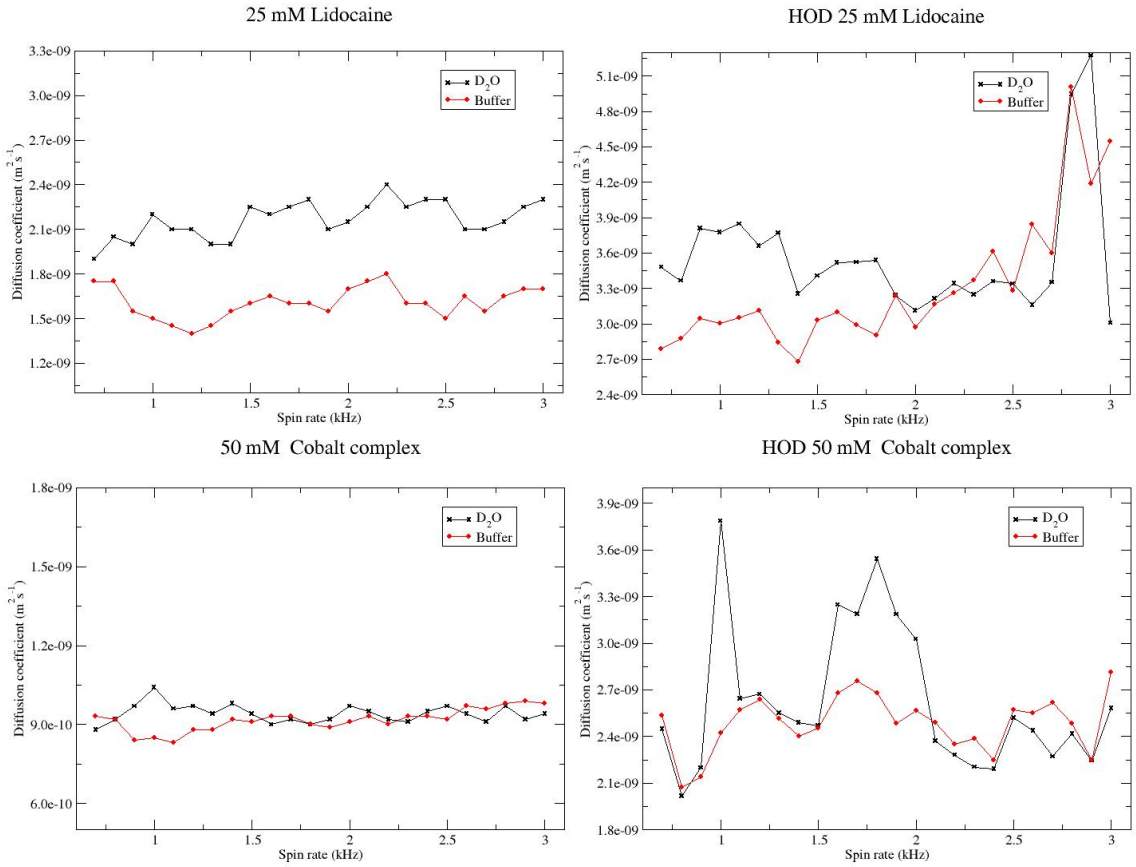

Figure 5.18: Diffusion coefficients of lidocaine and $[Co(en)_3]Cl_3$ their corresponding HOD residual signal varying the spinning rate with and without buffer

The case of the cobalt complex is different to the rest because is the only one that shows a very similar diffusion coefficient with and without the buffer. In terms of diffusing behaviour it is similar to the molecules of the first group that show an expected behaviour. However, the diffusion of the residual signal of the HOD is pretty inconsistent and suffers sudden variations when the spinning rate is varied. Finally the cobalt complex is the heaviest molecule (345.59 Da) but it also one of the molecules that increases its diffusion coefficient value the most when is under MAS. As it was mentioned at the beginning of this section is the molecule with the highest net charge (3). Therefore, it is the molecule that is more likely to be affected by the appearance of the Lorentz force.

5.2.3 Separation in the diffusion domain without stationary phases

All the experiments performed so far have shown that it is possible modulate the diffusion properties of molecules without the use of sample modifiers. In this chapter the possibility of both the use of the spinning rate and the addition of the buffer had been suggested to try to perform chromatographic NMR studies without the use of stationary phase, both of these effects can be observed in figure 5.19.

The results presented in figure 5.19 show the diffusion coefficients of the small molecules that exhibited an expected behaviour (figure 5.16) as function of their molecular weight, in static and high spinning conditions, as well as with the buffer and in absence of it.

Regarding the use of the buffer, this technique would not even need the use of high spinning rates. Without the buffer the two smallest molecules presented in figure 5.19 have a very similar diffusion coefficient. However, when the buffer is present there is a huge variation on one of the diffusion coefficients while the diffusion coefficient of the other molecule remained very similar to the diffusion coefficient without buffer. The same behaviour could be observed between the two largest molecules in that figure, although they show a significantly smaller difference between the diffusion coefficients, the separation is large enough to be appreciated by DOSY-NMR studies.

Regarding the use of the spin rate, this technique could be even more useful because it is possible to combine both spinning rates and use of buffer in case it is needed. As it happened before, in static conditions the two smallest molecules in the figure 5.19 presented the same diffusion coefficient, as well as the two largest molecules did. After the application of MAS conditions the diffusion coefficients were clearly different. However, all the samples presented in figure 5.19 had been measured separated in presence and absence of the buffer in D_2O. Therefore, future studies will include the repletion of these analysis with a mixture of molecules. Also the results presented show an average of the diffusion coefficients recorded at different spinning rates between 0.7 and 3 kHz. Hence, it should be possible to obtain different grades of separation while the spinning rate is varied.

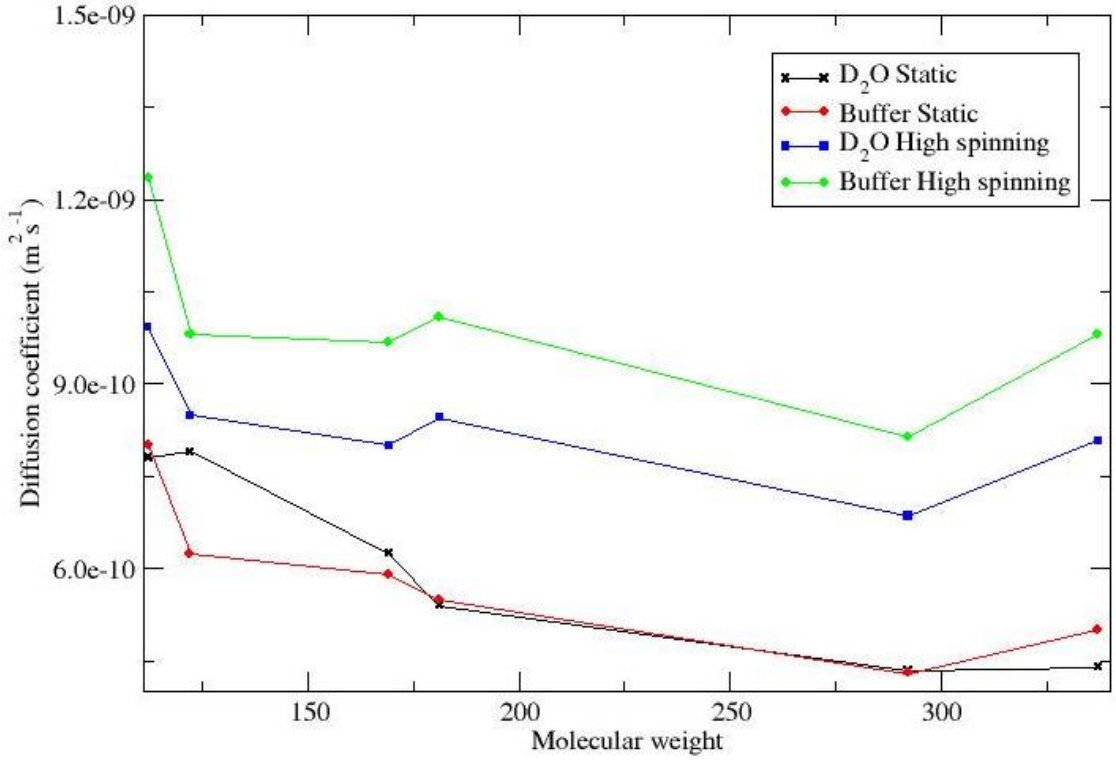

Figure 5.19: Static diffusion coefficients of the molecules presented in figure 5.16 compared to the average diffusion coefficient at different spinning rates with and without buffer

5.3 Conclusions and future work

In this chapter it has been proven that there are a whole new set of causes of variation to the diffusion coefficient when the experiments are performed under high spinning conditions. Unfortunately, during the timeline of these thesis there was no time to perform more experiments and clarify all of the effects that have been noticed. Hence, it was also not possible to combine the results of these studies with the use of any stationary phase in order to extend the use of chromatographic NMR. However, there have been two interesting suggestions presented in section 5.2.3, that should be the future of these studies, and that could mean an incredible twist in the field of NMR chromatography, this suggestions could enable separation of molecules in the diffusion domain without the use of any stationary phase, or sample modifier that will reduce the resolution of the spectra or increase the amount of overlapping signals.

Chapter 6

Size exclusion chromatographic NMR applied to the separation of enantiomers

All the studies presented and discussed in the previous chapters had been trying to perform successful SEC-DOSY NMR. However, there are other types of chromatography such as silica based chromatography [173], where the interaction between the analyte and the stationary phase is due to electrostatic, polar or hydrophobic forces, as well as, chiral chromatography where the chirality of both stationary phase and analyte make the interaction between one of the enantiomers and the stationary phase stronger than with the other one [52].

Enantiomers, are molecules that have the exact same formula and their only difference is that are mirror images of each other, and are impossible to superimpose and therefore, different molecules [174]. Nevertheless, they have always been difficult to study by NMR because both enantiomers show the exact same chemical environments, formula (molecular weight) and as mirror images the shape is very similar (slightly different three dimensional spatial distribution). Therefore, there is no difference in chemical shift, size of molecule or diffusion coefficient. However, there are some methods that could allow the study of these molecules using NMR. Such as the use of chiral alignment media and their induction of enantiomerically dependent anisotropic NMR parameters like residual dipolar couplings, residual quadrupolar couplings and residual chemical shift anisotropy [175]–[177] or the use of chiral lanthanide shift reagents [178]. In this chapter a new way to study enantiomers through NMR was explore. This way was with the addition of a stationary phase with chiral properties to the NMR sample [179, 168]. This fact will make possible to produce a small change in either the chemical shift or the diffusion coefficient, and it could be a great alternative to the use of lanthanide shift reagents (LSR) which due to their paramagnetism, shorten the spin-spin relaxation times of the nuclei, which causes uncertainty broadening and loss of resolution [180].

Sephadex G-50 has been described before in chapter 2, as a crosslinking dextran with epichlorohydrin which is usually used for SEC [84]. However, the dextrans in the structure possess a large number of rich chiral centers that can potentially be used to perform chiral chromatography as it has been used in electrophoresis or multiwavelength surface plasmon resonance [181, 182].

As it has been discussed before the use of stationary phases produces broadening of the NMR signals. Hence, it is not probable that a small change in the chemical shift will be noticed when studying enantiomers by NMR without the use of MAS, but it is possible to observe a change in the diffusion coefficient. If the diffusion coefficient of a racemic mixture of enantiomers is measured in presence of the stationary phase, it would be expected to obtain an average diffusion coefficient between the diffusion coefficients of the pure enantiomers in presence of the stationary phase.

In this chapter chiral chromatography NMR results will be presented using Sephadex as the stationary phase and a wide range of enantiomers including cobalt complexes synthesized in our labs and some purchased small organic molecules. The use of cobalt complexes is extremely convenient, particularly $[Co(en)_3]Cl_3$, because it has been suggested by Werner first and Gladysz and co-worker later, that it is possible to separate the enantiomers Δ and Λ by crystallization of the diastereomeric tartrate salts [183, 184, 185]. Moreover, Gladysz and co-workers have also suggested that it is possible to achieve the separation of some other octahedral cobalt complex enantiomers Δ and Λ with Sephadex stationary phases [186].

First, DOSY-NMR experiments will be performed without the presence of stationary phase to both the racemic mixture and the pure enantiomers. These experiments are expected to show no difference in the diffusion coefficient between the mixture and the pure enantiomers, as there is no stationary phase. To continue, SEC-DOSY experiments will be performed in presence of the stationary phase. Hence, due to the major interaction that should be experienced between one of the enantiomers and the stationary phase, it is expected to obtain different diffusion coefficients for the pure enantiomers, and a diffusion coefficient with a value in between of the values of the pure enantiomers for the racemic mixture.

6.1 Cobalt complexes

Modern coordination chemistry history started in 1893 with the theories about the octahedral configuration of transition metal ion complexes of Alfred Werner [187]. Depending on the ligands it is possible to obtain an octahedral configuration that can lead to the possibility of optical isomers represented with the symbols Δ and Λ (See figure 6.1). This fact, made the cobalt

complexes synthetized great for chiral chromatography studies. As these isomers could be formed by the reaction of a cobalt ion (Co^{3+}) with three identical ligands of ethylenediamine with two amino bonding groups to the metal center. The isomers are shown in figure 6.1.

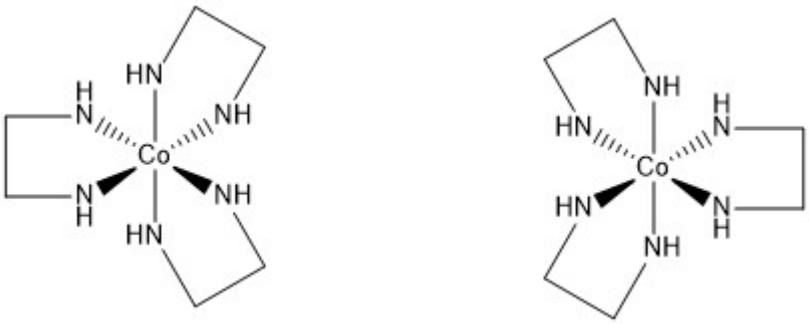

Figure 6.1: Enantiomers Δ (left) and Λ (right) of the complex tris(ethylenediamine)cobalt (III)

The synthesis of these complexes is relatively straightforward [188]. Therefore, to avoid the problem of overlapping signals when the stationary phase is added, three alternative cobalt complexes with a different diamine ligand were synthetized to ensure the appearance of signals in different regions of the spectrum. The ligands chosen were: ethylenediamine (2.5ppm – 3ppm), 1,2-Diphenylethylenediamine (aromatic region) and 1,2-diaminopropane (2.5ppm – 3ppm and 0.5ppm – 1.5 ppm).

6.1.1 Tris(ethylenediamine)Cobalt (III) chloride: $[Co(en)_3]Cl_3$

The method followed to synthesized $[Co(en)_3]Cl_3$ was described using inexpensive chemicals. Therefore, the amounts of reagents that are described in the method are very large compared to the amounts that would be used if the reaction was done with an expensive enantiopure ligand [188]. Hence, since some of the ligands that will be used in future experiments are expensive (as they are enantiopure) and possess quite bulky organic groups, which means that a huge amount of solvent is needed to dissolve the ligand in D_2O. Then, the first synthesis was performed with ethylendiamine (inexpensive and the ligand used in the method described in the literature [89]) and with much smaller amounts of reagents to see if the yield that is obtained is high enough to obtain an amount that will allow to check the purity of the reaction before using the more expensive ligands. This fact is important because it is needed to obtain a sufficient amount to both purify the compound by recrystallization and to have enough product to perform some optical rotation measurements that will determine the purity of the enantiomer that has been synthesized. The results of the reaction are shown in figure 6.2 and compared with a commercially available sample of the $[Co(en)]_3Cl_3$ purchased from Sigma-Aldrich.

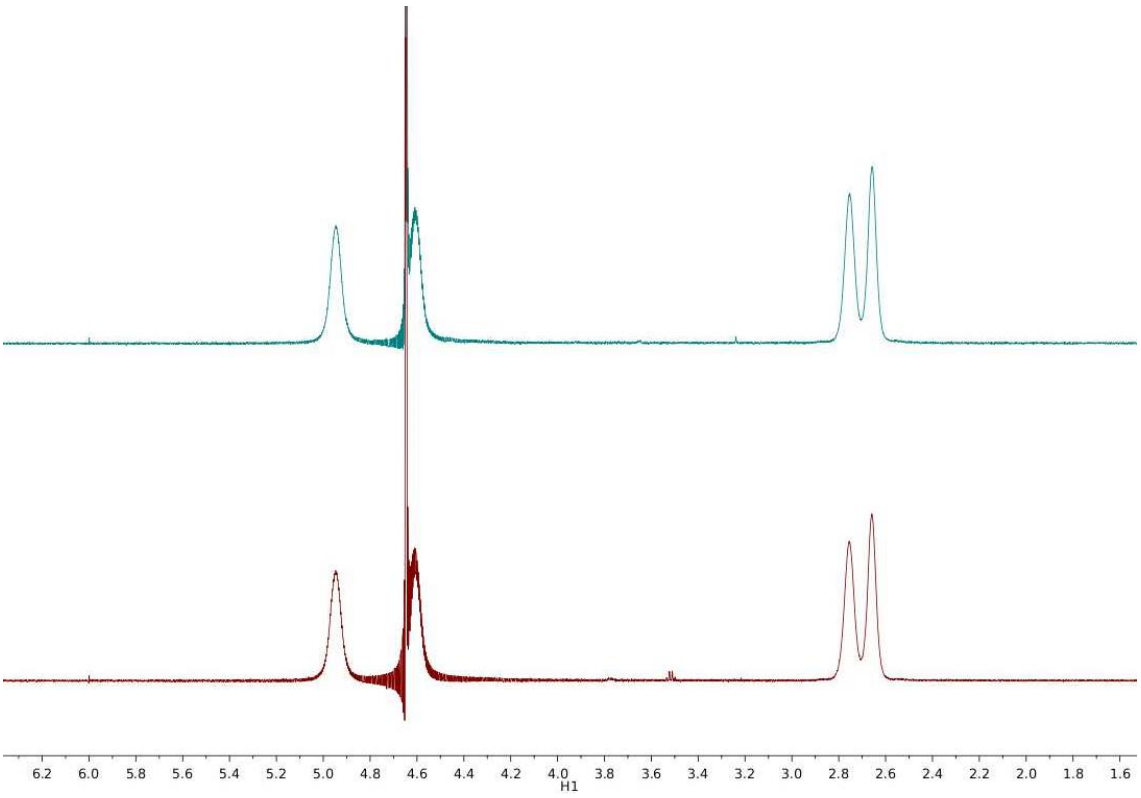

Figure 6.2: Stacked spectrum of 10mM $[Co(en)_3]Cl_3*2H_2O$ for comparison between purchased (top) and 10mM synthetized (bottom)

The yield of the reaction was 63% when the described method corrected with smaller amounts of reagents was followed as described in chapter 2 section 2.2.2. However, it was improved by sealing the joints in the reaction vessel with parafilm to avoid any loss of solvent, heating to a temperature just below the boiling point and performing a slower crystallization process, which was finished letting it cool with ice instead of room temperature. After all this slight variations in the method, the yield achieved went up to a range of 82 - 88%, a range is given because this reaction was repeated several times and the yields achieved were always different but within that range. Finally, the resulting product produced the same spectrum as the purchased complex and with a similar purity (see figure 6.2). In addition to the ^{1}H-NMR spectrum, to make sure that the diffusion behaviour was the same for the synthetized and the purchase complex, DOSY-NMR experiments were performed with 10mM concentration in D_2O with and without Sephadex G50 to both the purchased and the synthetized complex. The diffusion coefficients that were recorded are shown in table 6.1.

Complex $[Co(en)_3]Cl_3*2H_2O$	**Diffusion coefficient (D)*10^{-10} m^2/s**	
	Free	**Sephadex G50**
Sigma-Aldrich	3.50	2.49
This work	3.51	2.40

Table 6.1: Summary of $[Co(en)_3]Cl_3*2H_2O$ diffusion data – D_2O

The results were the expected ones when the ligand ethylendiamine was used. Both purchased and synthetized complexes showed exactly the same ^{1}H-NMR spectrum and similar diffusion coefficients compared to each other with and without stationary phase. The only potential problem was that the signals shown are very close to the signals of the stationary phase.

Also as it was expected, when the racemic mixture was measured, there was not any difference in chemical shift between the two optical isomers of the complex, which only showed a single set of signals when the stationary phase was added. This could be either due to the broadening experienced by the signals when the stationary phase is added, due to a not sufficiently strong interaction between the complex and the stationary phase or to a combination of both factors.

To be able to see if the diffusion of the enantiomers is different when Sephadex G-50 is present in the sample, the pure enantiomers of the complex are needed in order to perform NMR experiments on each isolated isomer. Due to a slight difference in their solubility when a diasterotopic complex is formed, it is possible to separate them following a straightforward procedure of recrystallization using L-(+)-tartaric acid [188], adapted with smaller amounts of reagents in chapter 2 section 2.2.2. The optical isomers can rotate the angle of polarized light. Hence, optical purity can be determined by measuring the optical rotation of the sample with a polarimeter.

Both of the enantiomers were separated. After several recrystallizations, the isomer showing a positive rotation of the light plane was separated without a problem. However, the other isomer required at least two more recrystallizations to obtain similar purity values. These values were $[\alpha]_{589}$ = + 95° and $[\alpha]_{589}$ = -92° which are very close to the literature values [188] which is $[\alpha]_{589}$ = + 102 and suggest an optical purity of 93% for the isomer that showed positive rotation and 90% for the isomer that showed negative rotation. The enantiopure complexes purity and structure were also checked by recording the ^{1}H-NMR spectrum of the pure enantiomers and compare them to the racemic mixture.

6.1.2 Tris(1,2-Diphenylethylenediamine)Cobalt (III) chloride: $[Co(diphenen)_3]Cl_3$

$[Co(diphenen)_3]Cl_3$ is a complex with the same octahedral structure described by Werner and the ligands have aromatic rings that show signals in a different region of the spectrum to the signals shown by the complex form with ethylendiamine. Therefore, it is a good candidate for DOSY-NMR studies as the signals shown are far away in chemical shift from the signals shown by the stationary phase. In addition, it has bulky ligands that will notably increase the size of the complex, and since the pores of Sephadex G-50 are mean to fit much bigger molecules (see table 2.1), an increase of the size of the complex will also increase the possibility of a strong interaction between complex and stationary phase.

Nonetheless, the presence of these aromatic rings is as well one of the main drawbacks of this ligands. Each of them possess two phenyl groups that will contribute to reduce the solubility of the complex in water. Also the enantiopure ligands are very expensive reagents due to how difficult is the process of separation of the isomers. For these reasons, although the reaction that takes place to synthesize the complex is the same as in the previous section, the synthesis of the complex was tried before following the method of $[Co(en)_3]Cl_3*2H_2O$ [188]. But using the ligand *meso*-1,2-diphenylethylenediamine. The reason is that the *meso* ligand is not as expensive as the enantiopure ligands and is a good route to check both if the reaction has high yield and if it is possible in water.

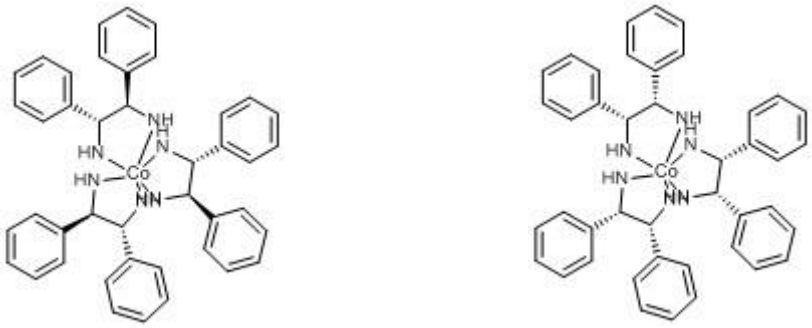

Figure 6.3: Structures of $[Co(Meso\text{-}1,2\text{-}diphenen)_3]^{3+}$ (Left) and $[Co((1R,2R)\text{-}(+)\text{-}diphenen)_3]^{3+}$ (Right)

As it was expected the reaction required a large amount of solvent due to the low solubility of the ligand compare to the amounts used in the previous synthesis (see chapter 2 section 2.2.2). However, it was performed successfully as an 89% yield was achieved. With this results the reaction was repeated with the enantiopure ligand (1R,2R)-(+)-diphenylethylenediamine. However, in this case the reaction did not happen. It was concluded that the reaction was not possible because all the carbons that hold the phenyl groups when the ligand (1R,2R)-(+)-

diphenylethylenediamine is used possess the same stereochemistry and therefore are in the same side of the molecule (see figure 6.3). Hence, the final molecule is formed by very bulky ligands with a physical arrangement that prevent the formation of a bond between the N and the Co due to a high steric interference between the phenyl groups of the ligands. Therefore, the formation is not possible. However, when *meso*-1,2-diphenylethylenediamine was used the phenyl groups are in alternated positions so there is less steric interference and the complex can be formed.

Finally the complex that was formed using the *meso* ligand was also discarded for NMR studies as it was impossible to obtain the Δ and Λ optical isomers with a simple recrystallization method due to their very low solubility in water. The separation of the isomers would have probably been achieved by chiral chromatography. However, this method is very expensive and time consuming.

6.1.3 Tris(1,2-diaminopropane)cobalt (III) chloride: $[Co(meten)_3]Cl_3$

The phenyl groups in the previous ligand were too big to allow the reaction to be completed and form the complex or obtain pure separated isomers. Therefore, to reduce the volume of the ligand and increase the solubility but still have signals in different regions of the spectrum, the reaction was repeated with 1,2-diaminopropane (see figure 6.4). This ligand will form a smaller and more soluble complex in water than the formed with 1,2-diphenylethylenediamine.

Following the process carried before with the *meso*-1,2-diphenylethylenediamine of using the cheapest form of the ligand to see if it is possible to obtain the complex, the reaction was successfully done with the racemic mixture of the ligands but with a low yield of 62%, which was impossible to increase as it was done with the ethylendiamine ligand at the beginning of this section. However, the NMR spectrum showed that not only the expected pair of isomers of the complex were formed, but also some of the other 30 possible isomers which are listed in table 6.2. It was not possible to describe how many of them were formed only with a ^{1}H-NMR spectrum. Although the use of enantiopure ligands would notably reduce the number of isomers formed from 32 to 16, there would still be 8 NMR observable species that are impossible to separate by simple recrystallization chemical methods as the amount of compound obtained were quite low due to both low yield and the use of limited quantities due to the high price of enantiopure ligands. Therefore, this complex had to be discarded as a candidate for NMR diffusion studies.

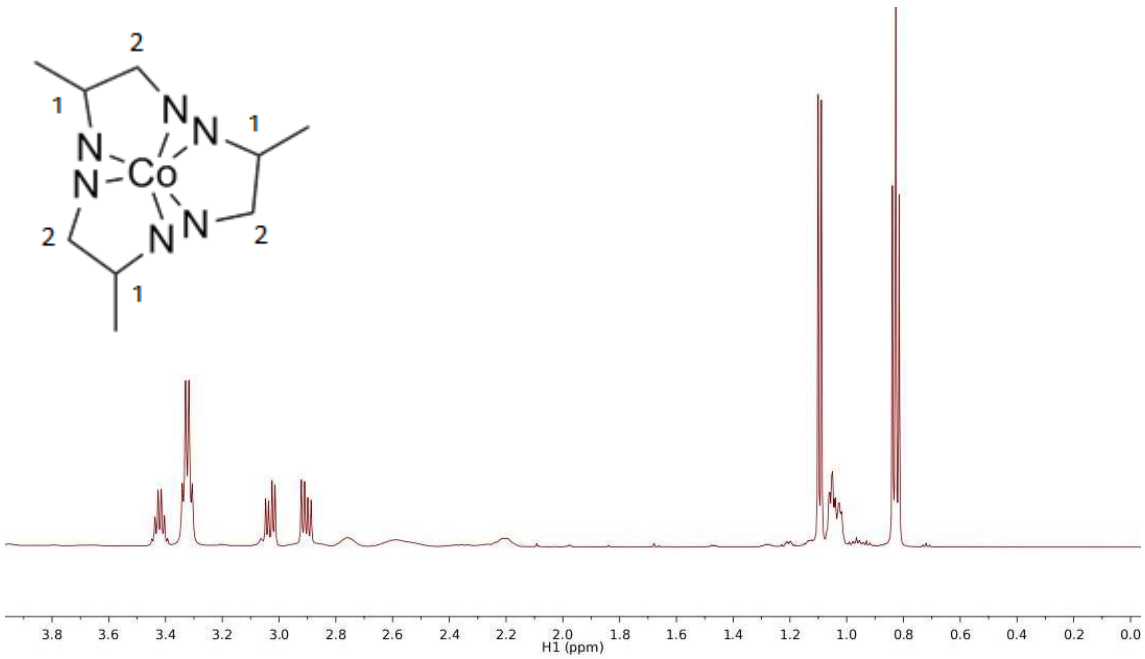

Figure 6.4: Spectrum of the 32 possible isomers of the complex $[Co(meten)_3]Cl_3$ and structure of the expected racemic mixture of the complex. Numbers 1 and 2 show the position that the methyl group could take and are used to name the possible enantiomers in table 6.2

111		**112**		**122**		**222**	
Δ	**Λ**	**Δ**	**Λ**	**Δ**	**Λ**	**Δ**	**Λ**
RRR	**RSS**	**RRR**	**RSS**	**RRR**	**RSS**	**RRR**	**RSS**
SSS	**RRS**	**SSS**	**RRS**	**SSS**	**RRS**	**SSS**	**RRS**

Table 6.2: Different isomers from the complex $[Co(meten)_3]Cl_3$. First row refers to the position of the methyl group on the ligand, second row refers to the two possible enantiomers of the octahedral complexes and third and fourth rows refers to the chiral center configuration

6.2 Chiral Chromatography combined with NMR

The only enantiomers of the cobalt complex that were possible to be synthesized and separated pure were $[(+)\text{-}Co(en)_3]Cl_3$ and $[(-)\text{-}Co(en)_3]Cl_3$. Therefore, a small range of small organic molecules with different functional groups and pairs of optical isomers were purchased (see table 6.3) to perform chromatographic NMR studies along with the cobalt complex isomers.

As it was done in previous studies the solvent was D_2O which does not dissolve the stationary phase. However, organic molecules are not very soluble in water. In addition, some pure enantiomers can be really expensive. For this reasons, to slightly increase the range of molecules

that could be chosen for the studies some of the experiments were performed either in a mixture of D_2O and MeOD-d_4 or in D_2O with a few drops of DCl. Neither of this solvents dissolved the stationary phase.

Compound	**Mw**
1-ph-1-propanol	136.19
Menthol	156.27
Tyrosine	181.19
$[Co(en)_3]Cl_3*2H_2O$	381.62

Table 6.3: Summary of compounds with their corresponding molecular weights used to perform chiral DOSY NMR

6.2.1 DOSY-NMR studies with Sephadex G50

In order to study the effect of the stationary phase in the different enantiomers the first step was to make sure that the racemic mixture in solution behaved very similarly to the pure enantiomers when there is no stationary phase. Therefore, DOSY-NMR experiments of every racemic mixture and each of the pure enantiomers were performed to compare their diffusion coefficients in absence of the stationary phase. An example of DOSY plot of a menthol sample is shown in figure 6.6. In order to prevent overlapping problems that, as it was mentioned before, can arise due to the proximity of the signals of the cobalt complexes and the stationary phase, all the experiments were performed with a concentration of 50mM instead of the previous 10mM. The diffusion coefficient that were recorded for the different compounds are shown in figure 6.5.

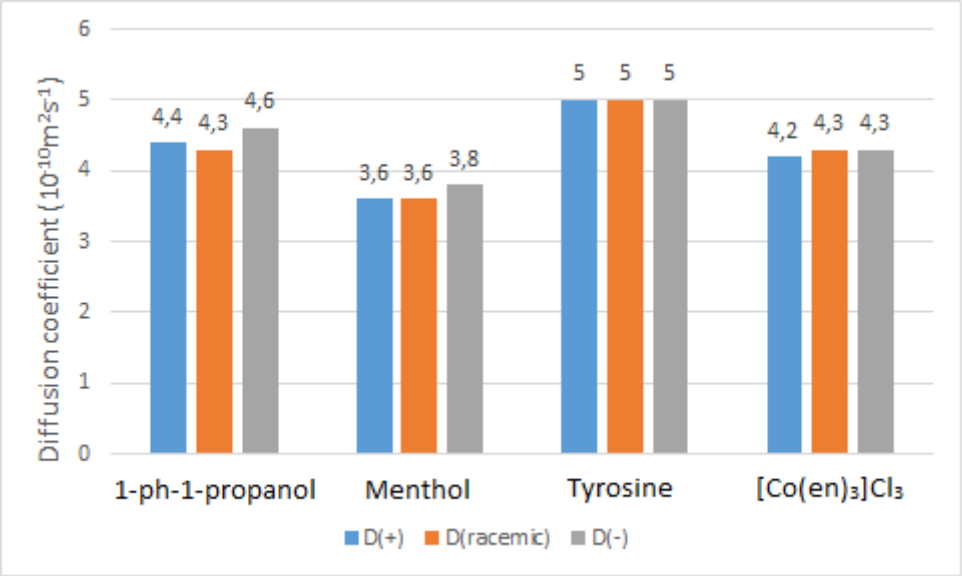

Figure 6.5: Diffusion coefficient of racemic mixture and enantiomers at 50mM in absence of stationary phase. 1-ph1-propanol and menthol are dissolved in D_2O:MeOD, tyrosine is dissolved in D_2O:HCl and $[Co(en)_3]Cl_3$ in D_2O

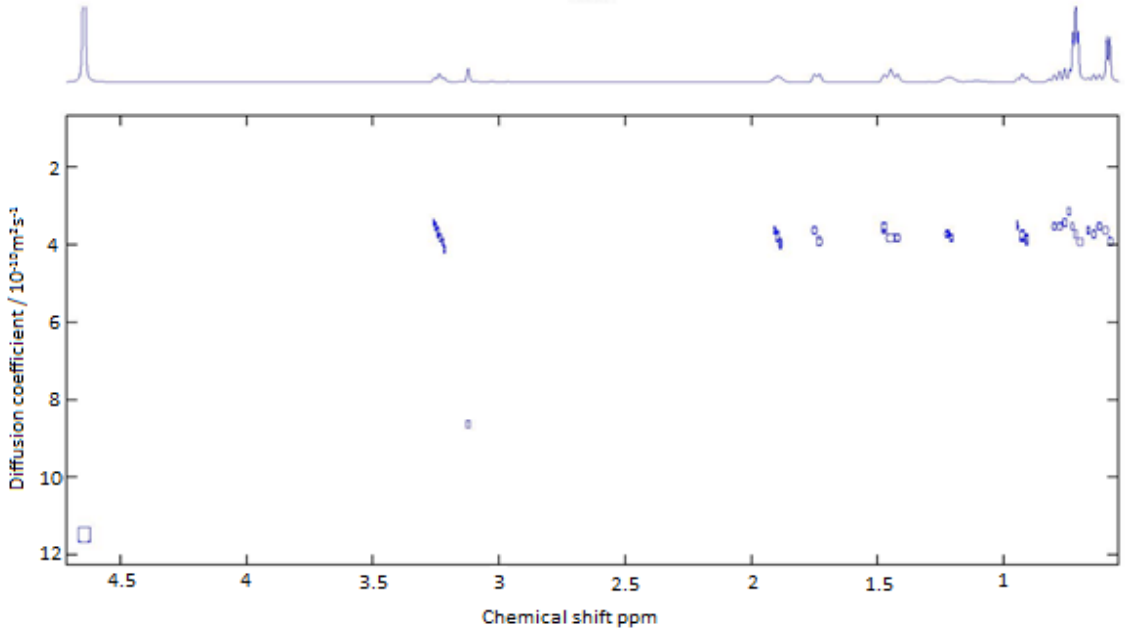

Figure 6.6: DOSY-NMR spectrum of 50mM Menthol in a mix 2:1 D_2O:MeOD

Looking at the results of the figure 6.5, it can be noticed that the biggest molecules are not the molecules that diffuse slower. This is due to the use of different solvents with diverse viscosities. The different densities and amount of charges in the solution affect to diffusion coefficients. However, it can be seen that the two molecules that use the same solvent follow the expected behavior where the largest molecule (menthol) diffuses slower than the smallest (1-ph-1-propanol). Although this is not relevant for the separation of the enantiomers it is a good indication of a correct diffusion behavior and the absence of unexpected effects. Regarding the

diffusing behavior between the racemate and their corresponding pure enantiomers, the results were completely expected, without the stationary phase, both the racemate and the pure enantiomers diffused very similarly (See figure 6.5).

At this point, in order to see if it is possible to perform chiral chromatography into the NMR spectrometer, it is needed to repeat the previous studies in presence of a stationary phase. Therefore, Sephadex G-50 was added to the samples shown in figure 6.5 to see if there is any difference in the diffusion behavior of the two different optical isomers. The results of the addition of Sepahdex G-50 are shown in figure 6.7. An example of DOSY plot of $[Co(en)_3]Cl_3$ in presence of Sephadex G-50 is shown in figure 6.8.

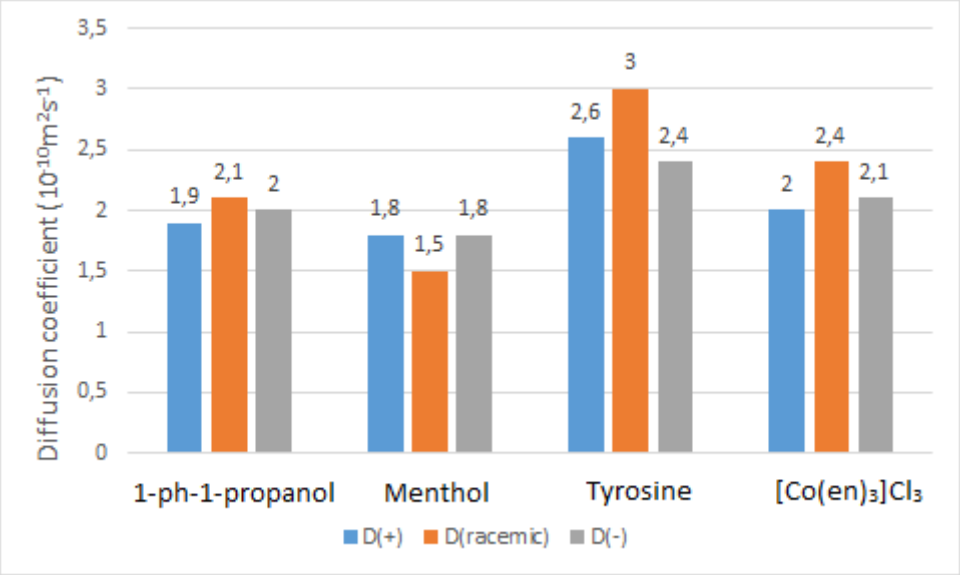

Figure 6.7: Diffusion coefficient of racemic mixture and enantiomers in presence of Sephadex G50 at 50mM. 1-ph1-propanol and menthol are dissolved in D_2O:MeOD, tyrosine is dissolved in D_2O:HCl and $[Co(en)_3]Cl_3$ in D_2O

After the addition of the stationary phase it is expected a reduction of the diffusion coefficient for every molecule due to both the interaction analyte-stationary phase and possible interferences produced by the presence of the stationary phase. Also, due to the chirality of the stationary phase one of the enantiomers should have a stronger interaction with the stationary phase and therefore, experience a larger reduction in the diffusion coefficient. Meanwhile, the racemate should show a diffusion coefficient in between of the two enantiomers, as a result of averaging the diffusion coefficients of the two enantiomers assuming that the peaks overlap and a suitable exchange regime.

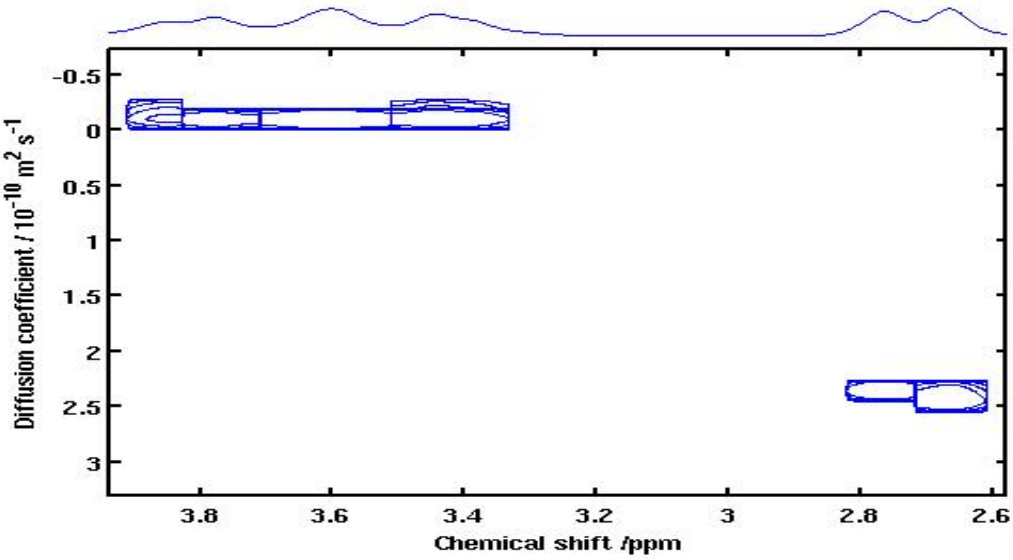

Figure 6.8: DOSY-NMR spectrum of 50mM $[Co(en)_3]Cl_3*2H_2O$ in presence of Sephadex G-50 in D_2O

The results shown in figure 6.7 do not show completely the expected pattern. On the one side, the diffusion coefficient of all the molecules have been reduced. On the other side, the racemate and the isomers keep showing very similar diffusion coefficients and there is no sign of larger interaction between the stationary phase and any of the isomers. Also, due to the broadening of the signals and the proximity of the stationary phase the resolution was reduced and it was harder to obtain accurate diffusion coefficients.

Sephadex G-50 is a stationary phase that is normally used for size exclusion chromatography and looking at the pore sizes shown in table 2.1, the pores of this stationary phases are too large (1.5 – 30 kDa for globular proteins) for the size of the molecules that were used in this studies (136 – 382 Da) and that could be the reason why there is no stronger interaction between the stationary phase and one of the isomers than with the other. This is not in agreement with the results found on the literature where it was suggested that it is possible to separate the enantiomers of the cobalt complex [186, 189]. Therefore, a Sephadex stationary phase with a smaller pore size (Sephadex G10) was chosen to repeat the previous experiments.

6.2.2 DOSY-NMR studies with Sephadex G10

Sephadex G-50 did not work well to perform chiral chromatography into the NMR under these conditions due to the mismatch between the size of the analytes used and the pores of the stationary phase. To solve this issue, Sephadex G10 which is a stationary phase with the same chemical structure but smaller pores (0 - 0.7 kDa for globular proteins, see table table 2.1) was used instead. The pores are still large for the molecules used. However, the same experiment

that was perform before with the samples of the table 6.4 was repeated in presence of Sephadex G10 to see if the pore size affect to the studies or if Sephadex is not the right stationary phase to continue with these studies.

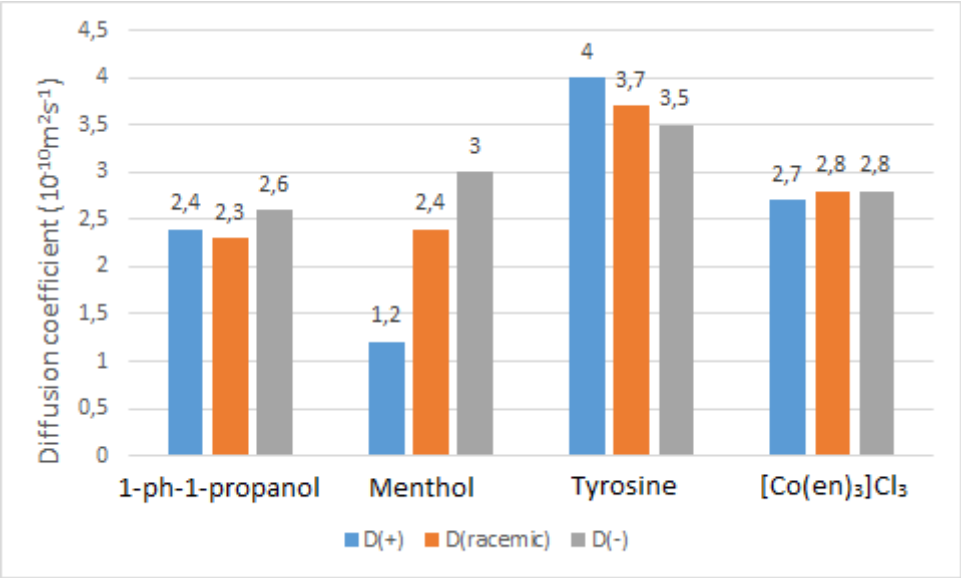

Figure 6.9: Diffusion coefficient of racemic mixture and enantiomers in presence of Sephadex G10 at 50mM. 1-ph1-propanol and menthol are dissolved in D_2O:MeOD, tyrosine is dissolved in D_2O:HCl and $[Co(en)_3]Cl_3$ in D_2O

With the use of Sephadex G-10 it seemed that chiral chromatography can be achieved in combination with NMR. Although the separation for some of the molecules was not big enough to conclude that chiral chromatography phenomena is happening they were still into the range of results expected. In addition, menthol and tyrosine both showed clearly different diffusion coefficients for its enantiomers and an intermediate diffusion coefficient for the racemic mixture. The results are shown in figure 6.9.

Another unexpected advantage that was found with the use of Sephadex G-10 was that the stationary phase did not appear in the spectrum, this was probably due to a very slow tumbling of the stationary phase molecules which affected to the relaxation of the nuclear magnetic moments of the hydrogens that are part of the structure of Sephadex G10 as the stationary phase is a solid. The broadening of the rest of the signals was still produced but there was no overlapping with the stationary phase see figure 6.10, which shows a signal of the tyrosine that could not be measured in presence of Sephadex G50 but it was possible with the use of Sephadex G10 between 3 and 3.5 ppm chemical shift.

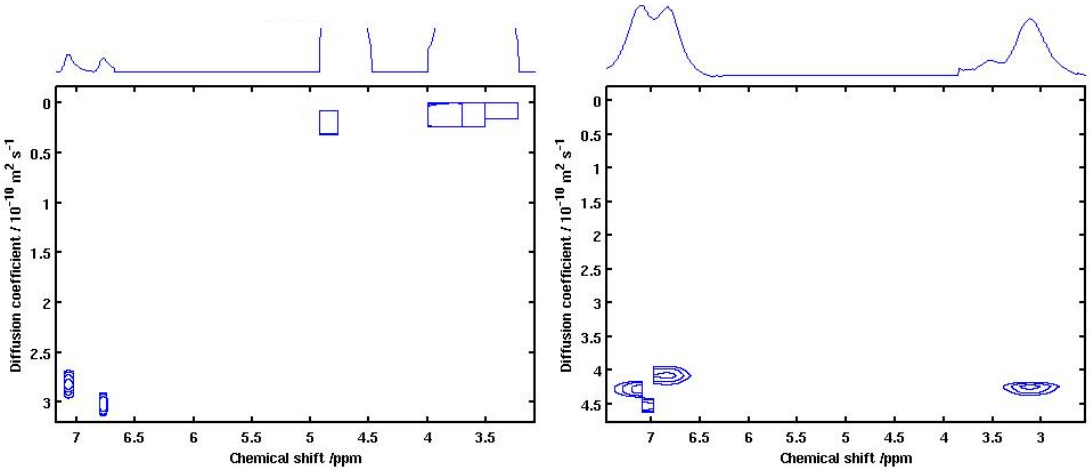

Figure 6.10: DOSY-NMR spectra of 50mM tyrosine in presence of Sephadex G-50 (left) and 50mM tyrosine in presence of Sephadex G-10 (right) both in D_2O with 3 drops of DCl

As it was mentioned above the pore size of this stationary phase is still too big for the size of these molecules. Hence, although some of the molecules have shown that chiral separation in the diffusion domain seem possible, it is not strange that the behavior of the molecules that did not show any separation as they still remain diffusing very similarly between them. Nevertheless, the positive results of menthol and tyrosine give a proof of concept for the combination of chiral chromatography and NMR, because even with a big pore size it is possible to see some differences in the diffusion coefficient between optical isomers when they are into the stationary phase, while their diffusion coefficient without the stationary phase is the same or very similar.

Chapter 7

Final thoughts

The area of chromatographic NMR is considered to have its place among the diffusion NMR techniques where an additive is added to the samples to modulate the diffusion properties of the analytes. Chromatographic NMR using as an additive a chromatographic stationary phase have been studied during the past 15 years [70, 137, 72, 3, 75]. The use of these stationary phase have extended the possibility of performing diffusion studies by NMR and increased the understanding the interactions that take place between the analytes and the stationary phases. However, there is still a lot of room for study and enhancement of the technique. Herein we have extended the studies in the area in diffusion liquids NMR with the addition of a size exclusion stationary phase in static samples and under MAS.

The studies presented in this thesis, have been divided in two main categories. The first one to be experiments that have been performed into a 5mm tube in static conditions. The second one to be experiments performed into a 40 µl volume rotor at a 54.74° angle respect to the main magnetic field at moderate spinning rates (0.7 kHz – 2.5 kHz), technique known as magic angle spinning (MAS).

7.1 Experiments into a 5 mm tube in static conditions

All the chromatographic NMR experiments that were performed, used as a stationary phase Sephadex, which is a common size exclusion stationary phase. However, it is comprised of a crosslinked polydextrans matrix that provide the possibility of performing chiral chromatographic NMR through the formation of a diastereomeric complex with one of the enantiomers of a racemic mixture and therefore to produce separation in the diffusion domain. For these reasons, the discourse in the experiments performed in static conditions is broken into two sections. First, experiments showing size exclusion phenomena. Second, experiments showing chiral separation phenomena.

7.1.1 Size exclusion chromatography phenomena

The measurement of diffusion coefficients when a size exclusion stationary phase is used, do not cause separation in the diffusion domain, but the opposite, the diffusion coefficient of each molecule is closer to each other in the diffusion domain. Therefore, it is not an advisable technique to produce improved separation. However, it allows to increase the understanding of the interactions that take place between the analytes and the stationary phase, and to extend the knowledge in the area of NMR chromatography.

Herein we tried to extend the studies that showed size exclusion phenomena performed previously by Day and co-workers [3], and to see if the results are reproducible when they are performed in a mixture instead of free in solution. The experiments that were performed free in solution (not in a mixture) with polymers of a wide range of molecular weights have shown that it is possible to see the size exclusion phenomena performing a DOSY NMR experiment in presence of the Sephadex G50 stationary phase, as the smallest molecules reduced the value of their diffusion coefficient much more than the largest polymers. This effect was harder to see when the experiments were repeated to a mixture of polymers. The addition of a stationary phase not only added signals to the NMR spectrum, but also produced broadening on the signals shown by the polymers. These two facts caused overlapping between the signals that appeared in the spectrum and hindered analysis of diffusion studies. Nevertheless, some of the polymers used to perform these experiments showed signals that did not overlap with other signals of the spectrum and in these cases, size exclusion phenomena was possible [75]. The main drawback was that the range of molecules that were actually suitable for the studies is quite narrow. Therefore, a technique that enable the extension of these range, such as magic angle spinning (MAS), which reduced the broadening cause by the stationary phases, is needed to continue with these studies.

7.1.2 Chiral chromatography phenomena

The study of racemic mixtures of enantiomers by NMR has always been complicated due to the identical electronical environments of the nucleus that form the molecules. Therefore, herein we tried to extend the study of racemic mixtures by NMR through the use of a stationary phase with chiral properties that could show separation in the diffusion domain or in the chemical shift between the two enantiomers of a racemic mixture.

The enantiomers that were used in these studies are small molecules, and the stationary phase that were used are size exclusion stationary phases. Therefore, the main issue when these experiments were performed was clearly seen in presence of Sephadex G50. The pore size of

this stationary phase was too large for the molecules that were studied and it was not possible to see any separation in the diffusion domain or in the chemical shift of the two different enantiomers. The experiments were repeated in presence of the same stationary phase but with a smaller pore size (Sephadex G10). The pore size of this stationary phase is still large compared to the size of the molecules that were used in these studies. However, it was possible to see the expected separation in the diffusion domain for some of the molecules, which is different diffusion coefficients for the different enantiomers and a diffusion coefficient with a value in between of the shown by the different enantiomers. The molecules that did not show this behaviour, showed a similar behaviour that the experiments performed in presence of Sephadex G50 which is the behaviour expected if the pore size is too large and the molecules do not experience any separation in the diffusion domain. As happened in the experiments where size exclusion phenomena was the aim, the addition of a stationary phase produced broadening in the signals shown by the enantiomers and this could be the reason why there was no separation in the chemical shift. Therefore, it is necessary to repeat these experiments with a technique that can correct this issue such as MAS. However, during the timeline of this work it was not possible to perform those studies. In the future, the next step will be to repeat the experiments performed under MAS conditions to see if it is possible to obtain better resolution, which can cause separation not only in the diffusion domain but also in the chemical shift. Although, in order to be able to carry on with these experiments it is needed to extend the understanding of diffusion under MAS.

7.2 Experiments under magic angle spinning

The main issue when chromatographic NMR is performed is overlapping signals due to the broadening produced in the signals by the addition of a solid stationary phase. In diffusion NMR if two signals are not well resolve the diffusion coefficient shown is an average diffusion coefficient of the two molecules producing that signal. Thus, usually when a stationary phase is added to the sample, there is a loss of resolution. Therefore, it is vital to find a technique that increases the resolution of the spectrum and recover the liquid like shape of the signals. Herein it has been shown that HR-MAS is a technique that can recover the liquid like shape of the signals in the spectrum and increase the resolution by matching the magnetic susceptibility between the solvent and the stationary phase. However, the addition of moderate spinning rates to the sample has not only shown to have complicating effects in the diffusion of the polymers studied in presence of the stationary phase but also made impossible to see any size exclusion phenomena when the experiments performed in static conditions were repeated under MAS conditions.

7.2.1 Optimization of diffusion measurements under MAS

Herein a method has been described to obtain accurate diffusion coefficient measurements by NMR under MAS for a sample of D_2O through the measurement of the diffusion coefficient of the residual signal HOD. This method have had into account most of the issues that have been reported by the literature such as selection of the appropriate pulse sequence and synchronization of it to the rotor period [76], reduction of the volume of the sample [76], location of the sample into the RF coil to prevent radial-field sidebands [79] or appropriate procedure of sample preparation to minimize the possibility of bubbles into the rotor sample. The method described have proven to give accurate diffusion coefficients for HOD and similar values to the values reported in the literature. This method have also been used to increase the understanding of diffusion under MAS.

7.2.2 Understanding diffusion under MAS

The method described in chapter four allowed the recording of reliable and accurate diffusion coefficients under MAS. Therefore, several experiments were performed applying this method. The aim of these experiments was to explain the additional effects that arise under MAS conditions, which affect to the diffusion behaviour of molecules. Some of those effect have been identified and studied the most important ones were the spin rate and the Lorentz force.

The spin rate produces acceleration in the molecules of the sample and increases the value of the diffusion coefficients of the molecules compared to the diffusion coefficients recorded under static conditions. However, the Lorentz force seemed to be the effect that had the largest influence in the diffusion coefficients. In every experiment performed with polymers, the molecules that possessed a high net charge in solution experienced a significant increase in the diffusion coefficient if it was measured under MAS due to the effect of the Lorentz force. This fact is of vital importance because it opens the door to the possibility of modulating the diffusion properties of molecules without the use of any sample modifier such as stationary phases, surfactants or others. It is important to mention that under the spin rates that were used in these experiments, the Lorentz force was only relevant if the molecules possessed a large net charge. Hence, the significant variations were seen if the analytes were polymers, but not when the analytes were small molecules.

Apart of the spin rate and the Lorentz force, some other effects were identified. However, there was not enough time to fully understand their effect. The first one is the concentration of charges in solution. This effect was studied by the application of a buffer that increased the concentration of charges in solution. In general, the experiments performed showed that the

increase of concentration of charges led to an increase in the diffusion coefficient of molecules if the experiments are performed under MAS. However, as happened with the Lorentz force the variation produced in the diffusion coefficients of different molecules was not identical. Therefore, it could also open the door to the possibility of modulating the diffusion properties of molecules without the use of any sample modifier and cause a separation in the diffusion domain. The last effect that was identified was a combination of the length of diffusion delay in the pulse sequence and the spin rate. We have seen that the variation of the length of the diffusion delay cause a variation in the diffusion behaviour. However, the pattern of the variation was different depending on the spin rate. This means that at low spin rates the increase of the length of the diffusion delay caused a reduction in the diffusion coefficients, meanwhile at moderate spin rates the variation was the opposite. Unfortunately, we did not have enough time to perform more experiments that could clarify this variations.

In future experiments in this area, it is needed to continue identifying the effect that arise under MAS that affect to the diffusion behaviour to fully understand them. The completion of this task would probably lead to the possibility of modulating the diffusion properties of molecules and cause separation in the diffusion domain without the use of sample modifiers. These is important because it will remove all the drawbacks that arise when sample modifiers are used to achieve this separation.

Bibliography

[1] R. E. Joyce and I. J. Day, “Chromatographic NMR with size exclusion chromatography stationary phases,” *J. Magn. Reson.*, vol. 220, pp. 1–7, 2012.

[2] T. C. Chan, H. T. Li, and K. Y. Li, “Effects of Shapes of Solute Molecules on Diffusion: A Study of Dependences on Solute Size, Solvent, and Temperature,” *J. Phys. Chem. B*, vol. 119, no. 51, pp. 15718–15728, 2015.

[3] R. E. Joyce and I. J. Day, “In situ size exclusion chromatographic NMR of sunset yellow FCF in solution,” *J. Phys. Chem. C*, vol. 117, no. 34, p. 17503, 2013.

[4] J. R. Katz, L. J. Day, and I. J. Day, “NMR investigations of the interaction between the azo-dye sunset yellow and fluorophenol,” *J. Phys. Chem. B*, vol. 117, no. 39, pp. 11793–11800, 2013.

[5] M. Jansson, T. E. Eriksen, and S. Wold, “LOT - in situ diffusion experiments using radioactive tracers,” *Appl. Clay Sci.*, vol. 23, no. 1–4, pp. 77–85, 2003.

[6] B. J. Berne and R. Pecora, “Dynamic light scattering: with applications to chemistry, biology, and physics.,” *Dover Publications*. 2000.

[7] E. L. Elson and D. Magde, “Fluorescence correlation spectroscopy. I. Conceptual basis and theory,” *Biopolymers*, vol. 13, no. 1, pp. 1–27, 1974.

[8] M. J. Hollas, “Modern Spectroscopy,” *Angew. Chemie Int. Ed. English*, vol. 5, no. 7, 2004.

[9] W. F. Murphy, *Modern spectroscopy*, vol. 4. 1993.

[10] P. J. Hore, *Nuclear Magnetic Resonance*, 2nd edition, Oxford university press, 2014.

[11] J. Keeler, *Understanding NMR*, 2nd edition, Wiley & Sons, 2010.

[12] T. D. W. Claridge, *High-Resolution NMR Techniques in Organic Chemistry*, vol. 27. 2009.

[13] M. H. Levitt, *Spin Dynamics: Basics of Nuclear Magnetic Resonance*. 2001.

[14] P. T. Callaghan, *Translational dynamics & magnetic resonance: principles of pulsed gradient spin echo NMR*. Oxford university press, 2011.

[15] E. L. Hahn, “Spin Echoes,” *Phys. Rev.*, vol. 80, no. 4, pp. 580–594, 1950.

[16] H. Carr and E. Purcell, “Effects of Diffusion on Free Precession in Nuclear Magnetic Resonance Experiments,” *Phys. Rev.*, vol. 94, no. 3, pp. 630–638, 1954.

[17] W. S. Price, *NMR studies of translational motion*. 2009.

[18] E. O. Stejskal and J. E. Tanner, “Spin Diffusion Measurements: Spin Echoes in the Presence of a Time-Dependent Field Gradient,” *J. Chem. Phys.*, vol. 42, no. 1, pp. 288–292, 1965.

[19] W. S. Price, “Pulsed-Field Gradient Nuclear Magnetic Resonance as a Tool for Studying

Translational Diffusion: Part 1. Basic Theory," *Concepts Magn. Reson.*, vol. 9, no. 5, pp. 299–336, 1997.

[20] P. Stilbs, "Fourier transform pulsed-gradient spin-echo studies of molecular diffusion," *Progress in Nuclear Magnetic Resonance Spectroscopy*, vol. 19, no. 1. pp. 1–45, 1987.

[21] C. Johnson Jr, "Diffusion ordered nuclear magnetic resonance spectroscopy: principles and applications," *Prog. Nucl. Magn. Reson. Spectrosc.*, vol. 34, pp. 203–256, 1999.

[22] "magnetic field gradients." [Online]. Available: https://www.chemie.uni-hamburg.de/nmr/insensitive/tutorial/en.lproj/gradients.html. [Accessed: 30-May-2017].

[23] D. Grosso, F. Ribot, C. Boissiere, and C. Sanchez, "Molecular and supramolecular dynamics of hybrid organic–inorganic interfaces for the rational construction of advanced hybrid nanomaterials," *Chem. Soc. Rev.*, vol. 40, no. 2, pp. 829–848, 2011.

[24] "spin echo vector representation." [Online]. Available: http://pages.physics.cornell.edu/p510/w/images/p510/a/a3/G7A_SpinEcho.jpg. [Accessed: 31-May-2017].

[25] R. P. Feynman, R. B. Leighton, M. Sands, and E. M. Hafner, "The Feynman Lectures on Physics; Vol. I," *Am. J. Phys.*, vol. 33, no. 9, pp. 750–752, 1965.

[26] D. H. Wu, A. D. Chen, and C. S. Johnson, "An Improved Diffusion-Ordered Spectroscopy Experiment Incorporating Bipolar-Gradient Pulses," *J. Magn. Reson. Ser. A*, vol. 115, no. 2, pp. 260–264, 1995.

[27] M. D. Pelta, G. A. Morris, M. J. Stchedroff, and S. J. Hammond, "A one-shot sequence for high-resolution diffusion-ordered spectroscopy," *Magn. Reson. Chem.*, vol. 40, no. SPEC. ISS. 13, p. S2, 2002.

[28] M. D. Pelta, H. Barjat, G. A. Morris, A. L. Davis, and S. J. Hammond, "Pulse sequences for high-resolution diffusion-ordered spectroscopy (HR-DOSY)," *Magn. Reson. Chem.*, vol. 36, no. 10, pp. 706–714, 1998.

[29] L. Mahi, J. C. Duplan, and B. Fenet, "Suppression of J-modulation effects for resonance editing by NMR spin-echo experiments," *Chem. Phys. Lett.*, vol. 211, no. 1, pp. 27–30, 1993.

[30] A. Botana, J. A. Aguilar, M. Nilsson, and G. A. Morris, "J-modulation effects in DOSY experiments and their suppression: The Oneshot45 experiment," *J. Magn. Reson.*, vol. 208, no. 2, pp. 270–278, 2011.

[31] K. I. Momot and P. W. Kuchel, "Convection-compensating PGSE experiment incorporating excitation-sculpting water suppression (CONVEX)," *J. Magn. Reson.*, vol. 169, no. 1, pp. 92–101, 2004.

[32] W. S. Price, “Pulsed-field gradient nuclear magnetic resonance as a tool for studying translational diffusion: part II. experimental aspects,” *Concepts Magn. Reson.*, vol. 10, pp. 197–237, 1998.

[33] G. Wider, V. Dotsch, and K. Wuthrich, “Self-Compensating Pulsed Magnetic-Field Gradients for Short Recovery Times,” *J. Magn. Reson. Ser. A*, vol. 108, no. 2, pp. 255–258, 1994.

[34] K. F. Morris and C. S. Johnson Jr., “Diffusion-ordered two-dimensional nuclear magnetic resonance spectroscopy.,” *J. Am. Chem. Soc.*, vol. 114, no. 8, pp. 3139–3141, 1992.

[35] H. Barjat, G. A. Morris, A. G. Swanson, S. Smart, and S. C. R. Williams, “Reference Deconvolution Using Multiplet Reference Signals,” *J. Magn. Reson. Ser. A*, vol. 116, pp. 206–214, 1995.

[36] M. Nilsson, “The DOSY Toolbox: A new tool for processing PFG NMR diffusion data,” *J. Magn. Reson.*, vol. 200, no. 2, pp. 296–302, 2009.

[37] W. Windig and B. Antalek, “Direct exponential curve resolution algorithm (DECRA): A novel application of the generalized rank annihilation method for a single spectral mixture data set with exponentially decaying contribution profiles,” *Chemom. Intell. Lab. Syst.*, vol. 37, no. 2, pp. 241–254, 1997.

[38] E. O. Stejskal and J. D. Memory, *High resolution NMR in the solid stateNo Title*. Oxford university press, 1994.

[39] M. J. Duer, *Solid-State NMR Spectroscopy Principles and Applications*. 2002.

[40] M. J. Duer, *Introduction to Solid-State NMR Spectroscopy*. Wiley-Blackwell, 2004.

[41] M. J. Duer, *Solid-State NMR Spectroscopy principles and applications*. Blackwell Science Ltd, 2002.

[42] F. Castellani, B. van Rossum, A. Diehl, M. Schubert, K. Rehbein, and H. Oschkinat, “Structure of a protein determined by solid-state magic-angle-spinning NMR spectroscopy,” *Nature*, vol. 420, no. 6911, pp. 98–102, 2002.

[43] A. Mcdermott, “Structure and dynamics of membrane proteins by magic angle spinning solid-state NMR,” *Annu. Rev. Biophys.*, vol. 38, p. 385, 2009.

[44] G. Scholtyssek, J. Sohma, and H. G. Zachmann, “Magic angle nuclear magnetic resonance studies of molecular motions in cross-linked polyethylene,” *Polymer (Guildf).*, vol. 32, no. 6, p. 1031, 1991.

[45] D. Freude, H. Ernst, M. Hunger, H. Pfeifer, and E. Jahn, “Magic-angle-spinning NMR studies of zeolite SAPO-5,” *Chem. Phys. Lett.*, vol. 143, no. 5, pp. 477–481, 1988.

[46] E. Lundanes, L. Reubsaet, and T. Greibrokk, *Chromatography: Basic principles, sample preparations and related methods*. Wiley, 2013.

[47] S. Fanali, P. R. Haddad, C. Poole, P. Schoenmakers, and D. Lloyd, *Liquid Chromatography: Applications*. Elsevier Inc., 2013.

[48] K. Mihlbachler and O. Dapremont, “Preparative Chromatography,” in *Green Techniques for Organic Synthesis and Medicinal Chemistry*, 2012, pp. 589–611.

[49] G. Guiochon, “Preparative liquid chromatography: Review,” *J. Chromatogr. A*, vol. 965, no. 12, pp. 129–161, 2002.

[50] J. S. Fritz, “Principles and applications of ion-exclusion chromatography,” *Journal of Chromatography A*, vol. 546, no. C. pp. 111–118, 1991.

[51] H. G. Barth, B. E. Boyes, and C. Jackson, “Size Exclusion Chromatography,” *Anal. Chem.*, vol. 68, no. 12, pp. 445–466, 1996.

[52] T. E. Beesley and R. P. W. Scott, “Chiral Chromatography,” *Techniques*, p. 552, 1998.

[53] B. Paull and P. N. Nesterenko, “Ion Chromatography,” in *Liquid Chromatography: Fundamentals and Instrumentation*, 2013, pp. 157–191.

[54] B. K. Glód, “Principles and Applications of Ion Chromatography,” *acta Chromatogr.*, no. 7, pp. 72–87, 1997.

[55] “SEC stationary phases.” [Online]. Available: http://chemphys.armstrong.edu/nivens/chem3801/SizeExclusionChromatography.htm. [Accessed: 22-May-2017].

[56] P. Hong, S. Koza, E. S. P. Bouvier, and W. Corporation, “Size-Exclusion Chromatography for the Analysis of Protein Biotherapeutics and their Aggregates,” *J. Liq. Chromatogr. Relat. Technol.*, vol. 35, no. 20, pp. 2923–2950, 2012.

[57] T. Ruysschaert, A. Marque, J.-L. Duteyrat, S. Lesieur, M. Winterhalter, and D. Fournier, “Liposome retention in size exclusion chromatography,” *BMC Biotechnol.*, vol. 5, p. 11, 2005.

[58] B. Trathnigg, “Size-Exclusion Chromatography of Polymers,” *Encycl. Anal. Chem.*, pp. 8034–8088, 2000.

[59] G. S. Duesberg, M. Burghard, J. Muster, and G. Philipp, “Separation of carbon nanotubes by size exclusion chromatography,” *Chem. Commun.*, vol. 3, no. 3, pp. 435–436, 1998.

[60] S. Nguyen, F. M. Winnik, and M. D. Buschmann, “Improved reproducibility in the determination of the molecular weight of chitosan by analytical size exclusion chromatography,” *Carbohydr. Polym.*, vol. 75, no. 3, pp. 528–533, 2009.

[61] A. Sepsey, I. Bacskay, and A. Felinger, “Molecular theory of size exclusion chromatography for wide pore size distributions,” *J. Chromatogr. A*, vol. 1331, pp. 52–60, 2014.

[62] P. Andrews, *Modern Size-Exclusion Liquid Chromatography*, vol. 8, no. 3. 1980.

[63] D. A. Skoog, F. J. Holler, and S. R. Crouch, *Principles of Instrumental Analysis Sixth Edition*. Thomson Brooks/Cole 2007, 1998.

[64] M. Khajeh, A. Botana, M. A. Bernstein, M. Nilsson, and G. A. Morris, "Reaction kinetics studied using diffusion-ordered spectroscopy and multiway chemometrics," *Anal. Chem.*, vol. 82, no. 5, pp. 2102–2108, 2010.

[65] J. R. Katz and I. J. Day, "Investigating the interaction of sunset yellow aggregates and 6-fluoro-2-naphthoic acid: Increasing probe molecule complexity," *Magn. Reson. Chem.*, vol. 52, no. 8, pp. 435–439, 2014.

[66] R. E. Joyce, *Development of NMR tools to investigate aggregation phenomena*. Ph. D. Thesis University of Sussex, 2013.

[67] A. Métais and F. Mariette, "Determination of water self-diffusion coefficient in complex food products by low field 1H PFG-NMR: Comparison between the standard spin-echo sequence and the T1-weighted spin-echo sequence," *J. Magn. Reson.*, vol. 165, no. 2, pp. 265–275, 2003.

[68] P. Occhipinti and P. C. Griffiths, "Quantifying diffusion in mucosal systems by pulsed-gradient spin-echo NMR," *Advanced Drug Delivery Reviews*, vol. 60, no. 15. pp. 1570–1582, 2008.

[69] S. Caldarelli, "Chapter 5: Chromatographic NMR," in *Annual Reports on NMR Spectroscopy*, vol. 73, Elsevier Ltd., 2011, pp. 159–173.

[70] S. Viel, F. Ziarelli, and S. Caldarelli, "Enhanced diffusion-edited NMR spectroscopy of mixtures using chromatographic stationary phases.," *Proc. Natl. Acad. Sci. U. S. A.*, vol. 100, no. 17, pp. 9696–8, 2003.

[71] C. Carrara, S. Viel, C. Delaurent, F. Ziarelli, G. Excoffier, and S. Caldarelli, "Chromatographic NMR in NMR solvents," *J. Magn. Reson.*, vol. 194, no. 2, pp. 303–306, 2008.

[72] R. E. Hoffman, H. Arzuan, C. Pemberton, A. Aserin, and N. Garti, "High-resolution NMR 'chromatography' using a liquids spectrometer," *J. Magn. Reson.*, vol. 194, no. 2, pp. 295–299, 2008.

[73] C. Pemberton, R. Hoffman, A. Aserin, and N. Garti, "New insights into silica-based NMR 'chromatography,'" *J. Magn. Reson.*, vol. 208, no. 2, pp. 262–269, 2011.

[74] K. A. Heisel, J. J. Goto, and V. V Krishnan, "NMR Chromatography: Molecular Diffusion in the Presence of Pulsed Field Gradients in Analytical Chemistry Applications," *Am. J. Anal. Chem.*, vol. 3, pp. 401–409, 2012.

[75] G. Lucena Alcalde, R. E. Joyce, and I. J. Day, "Size-exclusion chromatographic NMR of

polymer mixtures," *Magn. Reson. Chem.*, vol. 52, no. 12, pp. 760–763, 2014.

[76] S. Viel, F. Ziarelli, G. Pages, C. Carrara, and S. Caldarelli, "Pulsed field gradient magic angle spinning NMR self-diffusion measurements in liquids," *J Magn Reson*, vol. 190, no. 1, pp. 113–123, 2008.

[77] N. Esturau, F. Sánchez-Ferrando, J. A. Gavin, C. Roumestand, M.-A. Delsuc, and T. Parella, "The Use of Sample Rotation for Minimizing Convection Effects in Self-Diffusion NMR Measurements," *J. Magn. Reson.*, vol. 153, no. 1, pp. 48–55, 2001.

[78] M. Renault, L. Shintu, M. Piotto, and S. Caldarelli, "Slow-spinning low-sideband HR-MAS NMR spectroscopy: delicate analysis of biological samples.," *Sci. Rep.*, vol. 3, p. 3349, 2013.

[79] P. Tekely and M. Goldman, "Radial-Field Sidebands in MAS," *J. Magn. Reson.*, vol. 148, no. 1, pp. 135–141, 2001.

[80] G. Lucena Alcalde, N. Anderson, and I. J. Day, "Size-exclusion chromatographic NMR under HR-MAS," *Magn. Reson. Chem.*, no. May, 2016.

[81] Q. Ying and B. Chu, "Overlap Concentration of Macromolecules in Solution," *Macromolecules*, vol. 20, no. 2, pp. 362–366, 1987.

[82] P. F. Onyon, "Textbook of polymer science," *Polymer (Guildf).*, vol. 13, no. 12, p. 597, 1972.

[83] M. Moeller and K. Matyjaszewski, *Polymer Science: A Comprehensive Reference*, vol. 8. 2012.

[84] "Sephadex stationary phases and gels," *January 2014*. [Online]. Available: http://www.gelifesciences.com/webapp/wcs/stores/servlet/CategoryDisplay?categoryId=3297534&catalogId=123607&productId=&top=Y&storeId=12751&langId=-1.

[85] "Superdex Size Exclusion Media," *January 2014*. [Online]. Available: http://www.gelifesciences.com/webapp/wcs/stores/servlet/catalog/en/GELifeSciences-uk/brands/superdex/.

[86] "Sigma Aldrich, Sephadex G10," *May 2017*. [Online]. Available: http://www.sigmaaldrich.com/catalog/product/sigma/g10120?lang=en&region=GB. [Accessed: 16-May-2017].

[87] "Sigma Aldrich Sephadex G50," *May 2017*. [Online]. Available: http://www.sigmaaldrich.com/catalog/product/sigma/g5050?lang=en&region=GB. [Accessed: 20-Jul-2005].

[88] Girolami, Rauchfuss, and Angelici, "Synthesis and Technique in Inorganic Chemistry," in *Synthesis and Technique in Inorganic Chemistry*, 1999, pp. 85–91.

[89] R. A. Krause and E. A. Megargle, "Student synthesis of tris(ethylenediamine)cobalt(III)

chloride," *J. Chem. Educ.*, vol. 53, no. 10, p. 667, 1976.

[90] F. Rouessac and A. Rouessac, *Chemical Analysis: Modern Instrumentation Methods and Techniques*. John Wiley and Sons Ltd, 2007.

[91] R. O. Okotore, *Basic separation techniques in biochemistry*. New age international Ltd., 1998.

[92] J. M. Hollas, "Modern Spectroscopy, 4th Edition," *J. Chem. Educ.*, vol. 82, p. 43, 2005.

[93] W. L. F. Armarego and C. L. L. Chai, *Purification of Laboratory Chemicals: Fifth Edition*. Butterworth-Heinemann, 2003.

[94] L. H. Lucas and C. K. Larive, "Measuring ligand-protein binding using NMR diffusion experiments," *Concepts Magn. Reson. Part A Bridg. Educ. Res.*, vol. 20, no. 1, pp. 24–41, 2004.

[95] R. Evans and I. J. Day, "Matrix-assisted diffusion-ordered spectroscopy," *RSC Adv.*, vol. 6, no. 52, pp. 47010–47022, 2016.

[96] R. Evans, S. Haiber, M. Nilsson, and G. A. Morris, "Isomer resolution by micelle-assisted diffusion-ordered spectroscopy," *Anal. Chem.*, vol. 81, no. 11, pp. 4548–4550, 2009.

[97] C. F. Tormena, R. Evans, S. Haiber, M. Nilsson, and G. A. Morris, "Matrix-assisted diffusion-ordered spectroscopy: Mixture resolution by NMR using SDS micelles," *Magn. Reson. Chem.*, vol. 48, no. 7, pp. 550–553, 2010.

[98] C. F. Tormena, R. Evans, S. Haiber, M. Nilsson, and G. A. Morris, "Matrix-assisted diffusion-ordered spectroscopy: Application of surfactant solutions to the resolution of isomer spectra," *Magn. Reson. Chem.*, vol. 50, no. 6, pp. 458–465, 2012.

[99] J. S. Kavakka, V. Parviainen, K. Wähälä, I. Kilpeläinen, and S. Heikkinen, "Enhanced chromatographic NMR with polyethyleneglycol. A novel resolving agent for diffusion ordered spectroscopy," *Magn. Reson. Chem.*, vol. 48, no. 10, pp. 777–781, 2010.

[100] J. Cassani, M. Nilsson, and G. A. Morris, "Flavonoid mixture analysis by matrix-assisted diffusion-ordered spectroscopy," *J. Nat. Prod.*, vol. 75, no. 2, pp. 131–134, 2012.

[101] K. Zangger, "Pure shift NMR," *Prog. Nucl. Magn. Reson. Spectrosc.*, vol. 86–87, pp. 1–20, 2015.

[102] L. Castañar, "Pure shift ^{1}H NMR: what's next?," *Magn. Reson. Chem.*, no. July 2016, pp. 47–53, 2016.

[103] G. Hamdoun, M. Sebban, E. Cossoul, A. Harrison-Marchand, J. Maddaluno, and H. Oulyadi, "(1)H Pure Shift DOSY: a handy tool to evaluate the aggregation and solvation of organolithium derivatives," *Chem. Commun.*, vol. 50, no. c, pp. 4073–4075, 2014.

[104] J. A. Aguilar, S. Faulkner, M. Nilsson, and G. A. Morris, "Pure Shift 1H NMR: A resolution of the resolution problem?," *Angew. Chemie - Int. Ed.*, vol. 49, no. 23, pp. 3901–3903,

2010.

[105] M. Nilsson and G. A. Morris, “Pure shift proton DOSY: diffusion-ordered 1H spectra without multiplet structure.,” *Chem. Commun. (Camb).*, pp. 933–935, 2007.

[106] R. Huo, R. Wehrens, and L. M. C. Buydens, “Improved DOSY NMR data processing by data enhancement and combination of multivariate curve resolution with non-linear least square fitting,” *J. Magn. Reson.*, vol. 169, no. 2, pp. 257–269, 2004.

[107] A. A. Colbourne, S. Meier, G. A. Morris, and M. Nilsson, “Unmixing the NMR spectra of similar species - vive la différence.,” *Chem. Commun. (Camb).*, vol. 49, no. 89, pp. 10510–2, 2013.

[108] K. Sanderson, “Chemistry: It’s not easy being green,” *Nature*, vol. 469, pp. 18–20, 2011.

[109] J. L. Duda, “Molecular diffusion in polymeric systems,” *Pure Appl. Chem.*, vol. 57, no. 11, pp. 1681–1690, 1985.

[110] A. M. Striegel, W. W. Yau, J. J. Kirkland, and D. D. Bly, *Modern Size-Exclusion Liquid Chromatography: Practice of Gel Permeation and Gel Filtration Chromatography: Second Edition*. 2009.

[111] A. V. Dobrynin and M. Rubinstein, “Theory of polyelectrolytes in solutions and at surfaces,” *Prog. Polym. Sci.*, vol. 30, no. 11, pp. 1049–1118, 2005.

[112] R. Everaers, A. Johner, and J.-F. Joanny, “Complexation and precipitation in polyampholyte solutions,” *Europhys. Lett.*, vol. 37, no. 4, pp. 275–280, 2007.

[113] A. V. Dobrynin, R. H. Colby, and M. Rubinstein, “Polyampholytes,” *J. Polym. Sci. Part B Polym. Phys.*, vol. 42, no. 19, pp. 3513–3538, 2004.

[114] N. C. Billingham, “Degradable polymers: Principles and applications,” *Polym. Degrad. Stab.*, vol. 53, pp. 269–270, 1996.

[115] GE Healthcare, “Size exclusion chromatography: Principles and Methods,” *GE Heal. Handbooks*, p. 139, 2012.

[116] W.-S. Sheu, “Molecular Weight Averages and Polydispersity of Polymers,” *J. Chem. Educ.*, vol. 78, no. 4, p. 554, 2001.

[117] D. M. W. Anderson and J. F. Stoddart, “Studies on uronic acid materials : Part XV. The use of molecular-sieve chromatography in studies on acacia senegal gum (gum arabic),” *Carbohydr. Res.*, vol. 2, pp. 104–114, 1966.

[118] D. M. W. Anderson and J. F. Stoddart, “Some observations on molecular weight estimations by molecular-sieve chromatography,” *Anal. Chim. Acta*, vol. 34, p. 401, 1966.

[119] I. W. H. Determann, “Source of Aromatic Affinity to ‘Sephadex’ Dextran Gels,” *Nature*, vol. 219, pp. 604–605, 1968.

[120] A. J. W. Brook and S. Housley, “The interaction of phenols with sephadex gels,” *J. Chromatogr. A*, vol. 41, pp. 200–204, 1969.

[121] B. Gelotte, “Studies on gel filtration sorption properties of the bed material Sephadex,” *J. Chromatogr. A*, vol. 3, pp. 330–342, 1960.

[122] A. J. W. Brook and K. C. Munday, “The interaction of phenols, anilines, and benzoic acids with sephadex gels,” *J. Chromatogr. A*, vol. 47, pp. 1–8, 1970.

[123] I. Teraoka, *Polymer Solutions: An Introduction to Physical Properties*. John Wiley and Sons Ltd, 2002.

[124] M. Rubinstein and R. H. Colby, “Polymer physics,” *Polymer International*. p. 440, 2003.

[125] L. B. T Kremmer, *Gel chromatography: theory, methodology and applications*. John Wiley and Sons Ltd, 1979.

[126] S. Glanzer and K. Zangger, “Directly decoupled diffusion-ordered NMR spectroscopy for the analysis of compound mixtures,” *Chem. - A Eur. J.*, vol. 20, no. 35, pp. 11171–11175, 2014.

[127] J. E. Tanner, “Use of the Stimulated Echo in NMR Diffusion Studies,” *J. Chem. Phys.*, vol. 52, no. 5, pp. 2523–2526, 1970.

[128] W. F. Reynolds, “NMR Pulse Sequences,” in *Encyclopedia of Spectroscopy and Spectrometry*, 2010, pp. 1841–1854.

[129] J. C. Lindon, J. K. Nicholson, and I. D. Wilson, “Direct coupling of chromatographic to NMR spectroscopy separations,” *Prog. Nucl. Magn. Reson. Spectrosc.*, vol. 29, no. 95, pp. 1–49, 1996.

[130] M. Cudaj, G. Guthausen, T. Hofe, and M. Wilhelm, “SEC-MR-NMR: Online coupling of size exclusion chromatography and medium resolution NMR spectroscopy,” *Macromol. Rapid Commun.*, vol. 32, no. 8, pp. 665–670, 2011.

[131] G. N. M. Reddy and S. Caldarelli, “Maximum-quantum (MaxQ) NMR for the speciation of mixtures of phenolic molecules.,” *Chem. Commun. (Camb).*, vol. 47, no. 14, pp. 4297–9, 2011.

[132] G. N. Manjunatha Reddy and S. Caldarelli, “Demixing of severely overlapping NMR spectra through multiple-quantum NMR,” *Anal. Chem.*, vol. 82, no. 8, pp. 3266–3269, 2010.

[133] B. Antalek, “Using pulsed gradient spin echo NMR for chemical mixture analysis: How to obtain optimum results,” *Concepts Magn. Reson. Part A Bridg. Educ. Res.*, vol. 14, no. 4, pp. 225–258, 2002.

[134] M. V. Salvia *et al.*, “Nanoparticle-assisted NMR detection of organic anions: From chemosensing to chromatography,” *J. Am. Chem. Soc.*, vol. 137, no. 2, pp. 886–892,

2015.

[135] T. González-García, T. Margola, A. Silvagni, F. Mancin, and F. Rastrelli, "Chromatographic NMR Spectroscopy with Hollow Silica Spheres," *Angew. Chemie - Int. Ed.*, vol. 55, no. 8, pp. 2733–2737, 2016.

[136] J. S. Kavakka, I. Kilpeläinen, and S. Heikkinen, "General chromatographic NMR method in liquid state for synthetic chemistry: polyvinylpyrrolidone assisted DOSY experiments," *Org. Lett.*, vol. 11, no. 6, pp. 1349–1352, 2009.

[137] S. Caldarelli, "Chromatographic NMR: A tool for the analysis of mixtures of small molecules," *Magnetic Resonance in Chemistry*, vol. 45, no. SUPPL. 2007.

[138] R. Evans *et al.*, "Matrix-assisted diffusion-ordered NMR spectroscopy with an invisible matrix: a vanishing surfactant," *RSC Adv.*, vol. 7, no. 1, pp. 449–452, 2017.

[139] M. E. Zielinski and K. F. Morris, "Using perdeuterated surfactant micelles to resolve mixture components in diffusion-ordered NMR spectroscopy," *Magn. Reson. Chem.*, vol. 47, no. 1, pp. 53–56, 2009.

[140] C. Pemberton, R. E. Hoffman, A. Aserin, and N. Garti, "NMR chromatography using microemulsion systems," *Langmuir*, vol. 27, no. 8, pp. 4497–4504, 2011.

[141] G. Pages, C. Delaurent, and S. Caldarelli, "Simplified analysis of mixtures of small molecules by chromatographic NMR spectroscopy," *Angew. Chemie - Int. Ed.*, vol. 45, no. 36, pp. 5950–5953, 2006.

[142] J. Z. Hu and R. A. Wind, "The evaluation of different MAS techniques at low spinning rates in aqueous samples and in the presence of magnetic susceptibility gradients," *J. Magn. Reson.*, vol. 159, no. 1, pp. 92–100, 2002.

[143] S. A. Bradley, J. Paschal, and P. Kulanthaivel, "DOSY of sample-limited mixtures: Comparison of cold, nano and conventional probes," *Magn. Reson. Chem.*, vol. 43, no. 1, pp. 31–35, 2005.

[144] J. J. Pesek, M. T. Matyska, and K. V Prajapati, "Synthesis and evaluation of silica hydride-based fluorinated stationary phases.," *J. Sep. Sci.*, vol. 33, no. 19, pp. 2908–16, 2010.

[145] M.-P. Krafft, F. Jeannaux, M. Le Blanc, J. G. Riess, and A. Berthod, "Highly fluorinated stationary phases for analysis of polyfluorinated solutes by reversed-phase high-performance liquid chromatography," *Anal. Chem.*, vol. 60, no. 18, pp. 1969–1972, 1988.

[146] J. Klinowski, "New Techniques in Solid-State NMR," *Springer Berlin Heidelb.*, vol. 246, p. 364, 2005.

[147] I. Bertini, C. Luchinat, G. Parigi, and E. Ravera, "SedNMR: On the edge between solution and solid-state NMR," *Acc. Chem. Res.*, vol. 46, no. 9, pp. 2059–2069, 2013.

[148] J. L. Taylor, C.-L. Wu, D. Cory, R. G. Gonzalez, A. Bielecki, and L. L. Cheng, “High-resolution magic angle spinning proton NMR analysis of human prostate tissue with slow spinning rates.,” *Magn. Reson. Med.*, vol. 50, no. 3, pp. 627–632, 2003.

[149] C. Ammann, P. Meier, and A. Merbach, “A simple multinuclear NMR thermometer,” *J. Magn. Reson.*, vol. 46, no. 2, pp. 319–321, 1982.

[150] N. Anderson, “New insight into the Combination of DOSY and HR-MAS and New developments in NMR Chromatography,” 2012.

[151] F. Vella, “Introduction to Protein Structure,” *Biochemical Education*, vol. 20. p. 122, 1992.

[152] B. J. Bennion and V. Daggett, “The molecular basis for the chemical denaturation of proteins by urea.,” *Proc. Natl. Acad. Sci. U. S. A.*, vol. 100, no. 9, pp. 5142–7, 2003.

[153] J. R. Jones, D. L. G. Rowlands, and C. B. Monk, “Diffusion coefficient of water in water and in some alkaline earth chloride solutions at 25°C,” *Trans. Faraday Soc.*, vol. 61, pp. 1384–1388, 1965.

[154] M. Holz, S. R. Heil, and A. Sacco, “Temperature-dependent self-diffusion coefficients of water and six selected molecular liquids for calibration in accurate 1H NMR PFG measurements,” *Phys. Chem. Chem. Phys.*, vol. 2, no. 20, pp. 4740–4742, 2000.

[155] J. M. Wieruszeski, G. Montagne, G. Chessari, P. Rousselot-Pailley, and G. Lippens, “Rotor synchronization of radiofrequency and gradient pulses in high-resolution magic angle spinning NMR.,” *J. Magn. Reson.*, vol. 152, no. 1, pp. 95–102, 2001.

[156] K. Elbayed, B. Dillmann, J. Raya, M. Piotto, and F. Engelke, “Field modulation effects induced by sample spinning: Application to high-resolution magic angle spinning NMR,” *J. Magn. Reson.*, vol. 174, no. 1, pp. 2–26, 2005.

[157] N. M. Alexej Jerschow, “Suppression of Convection Artifacts in Stimulated-Echo Diffusion Experiemnts. Double-Stimulated-Echo Experiments,” *J. Magn. Reson.*, vol. 375, no. 125, pp. 372–375, 1997.

[158] M. Piotto, M. Bourdonneau, J. Furrer, A. Bianco, J. Raya, and K. Elbayed, “Destruction of magnetization during TOCSY experiments performed under magic angle spinning: Effect of radial B-1 inhomogeneities,” *J. Magn. Reson.*, vol. 149, no. 1, pp. 114–118, 2001.

[159] E. Kupce, P. a Keifer, and M. Delepierre, “Adiabatic TOCSY MAS in liquids.,” *J. Magn. Reson.*, vol. 148, no. 1, pp. 115–20, 2001.

[160] N. Esturau, F. Sánchez-Ferrando, J. a Gavin, C. Roumestand, M. a Delsuc, and T. Parella, “The use of sample rotation for minimizing convection effects in self-diffusion NMR measurements.,” *J. Magn. Reson.*, vol. 153, no. 1, pp. 48–55, 2001.

[161] I. Swan *et al.*, “Sample convection in liquid-state NMR: Why it is always with us, and

what we can do about it," *J. Magn. Reson.*, vol. 252, pp. 120–129, 2015.

[162] V. I. BAKHMUTOV, "On the Artifact Behavior of Simple Liquids in the Inversion-Recovery Experiments Under MAS Conditions at High Spinning Rates," *Concepts Magn. Reson.*, vol. 40, no. 4, pp. 186–191, 2012.

[163] I. Bertini, C. Luchinat, G. Parigi, E. Ravera, B. Reif, and P. Turano, "Solid-state NMR of proteins sedimented by ultracentrifugation.," *Proc. Natl. Acad. Sci. U. S. A.*, vol. 108, no. 26, pp. 10396–10399, 2011.

[164] I. Bertini *et al.*, "NMR properties of sedimented solutes.," *Phys. Chem. Chem. Phys.*, vol. 14, no. 2, pp. 439–47, 2012.

[165] K. E. Van Holde and R. L. Baldwin, "Rapid Attainment of Sedimentation Equilibrium," *J. Phys. Chem.*, vol. 62, no. 7, pp. 734–743, 1958.

[166] C. Carrara and S. Caldarelli, "Relative average mass transport properties of mixture components in the presence of a porous silica gel depend on the solution/solid phase ratio," *J. Phys. Chem. C*, vol. 116, no. 37, pp. 20080–20084, 2012.

[167] C. Carrara, G. Pages, C. Delaurent, S. Viel, and S. Caldarelli, "Mass transport of volatile molecules in porous materials: Evaporation-condensation phenomena described by NMR diffusometry," *J. Phys. Chem. C*, vol. 115, no. 38, pp. 18776–18781, 2011.

[168] R. W. Adams, J. a Aguilar, J. Cassani, G. a Morris, and M. Nilsson, "Resolving natural product epimer spectra by matrix-assisted DOSY.," *Org. Biomol. Chem.*, vol. 9, no. 20, pp. 7062–4, 2011.

[169] C. Carrara, C. Lopez, and S. Caldarelli, "Chromatographic-nuclear magnetic resonance can provide a prediction of high-pressure liquid chromatography shape selectivity tests," *J. Chromatogr. A*, vol. 1257, pp. 204–207, 2012.

[170] M. Todd and E. Janelle, "HR-MAS NMR Spectroscopy in Material Science," in *Advanced Aspects of Spectroscopy*, 2012, pp. 279–306.

[171] S. Hughes, "Lorentz Force Law," *MIT Dep. Phys.*, vol. Lecture 10, p. 90, 2005.

[172] "http://hyperphysics.phy-astr.gsu.edu/hbase/magnetic/magfor.html#c2," *May 2017*. .

[173] H. Qiu, X. Liang, M. Sun, and S. Jiang, "Development of silica-based stationary phases for high-performance liquid chromatography," *Analytical and Bioanalytical Chemistry*, vol. 399, no. 10. pp. 3307–3322, 2011.

[174] J. Jacques, A. Collet, and S. H. Wilen, *Enantiomers, Racemates and Resolutions*. 1981.

[175] C. M. Thiele, "Residual dipolar couplings (RDCs) in organic structure determination," *European Journal of Organic Chemistry*, no. 34. pp. 5673–5685, 2008.

[176] G. Kummerlöwe and B. Luy, "Residual dipolar couplings as a tool in determining the structure of organic molecules," *Trends Anal. Chem.*, vol. 28, no. 4, pp. 483–493, 2009.

[177] G. Kummerlöwe and B. Luy, “Residual Dipolar Couplings for the Configurational and Conformational Analysis of Organic Molecules,” *Annu. Reports NMR Spectrosc. Vol. 68*, vol. 68, no. 9, pp. 193–232, 2009.

[178] B. Luy, “Disinction of enantiomers by NMR media,” *J. Indian Inst. Sci.*, vol. 90, pp. 119–132, 2010.

[179] A. Laverde, G. J. A. Da Conceiçao, S. C. N. Queiroz, F. Y. Fujiwara, and A. J. Marsaioli, “An NMR tool for cyclodextrin selection in enantiomeric resolution by high-performance liquid chromatography,” *Magn. Reson. Chem.*, vol. 40, no. 7, pp. 433–442, 2002.

[180] S. K. Mishra, S. R. Chaudhari, A. Lakshmipriya, I. Pal, N. Lokesh, and N. Suryaprakash, “Novel Synthetic As Well As Natural Auxiliaries With a Blend of NMR Methodological Developments for Chiral Analysis in Isotropic Media,” *Annual Reports on NMR Spectroscopy*, 2017.

[181] P. Sun, G. E. Barker, G. J. Mariano, and R. A. Hartwick, “Enhanced chiral separation of dansylated amino acids with cyclodextrin-dextran polymer network by capillary electrophoresis,” *Electrophoresis*, vol. 15, no. 1, pp. 793–798, 1994.

[182] Y. Chen, H. Huang, X. Yu, and L. Qi, “Chiral recognition of dextran sulfate with d- and l-cystine studied by multiwavelength surface plasmon resonance,” *Carbohydr. Res.*, vol. 340, no. 12, pp. 2024–2029, 2005.

[183] W. G. Jackson, J. A. McKeon, and S. Cortez, “Alfred Werner’s inorganic counterparts of racemic and mesomeric tartaric acid: A milestone revisited,” *Inorg. Chem.*, vol. 43, no. 20, pp. 6249–6254, 2004.

[184] C. Ganzmann and J. A. Gladysz, “Phase transfer of enantiopure werner cations into organic solvents: An overlooked family of chiral hydrogen bond donors for enantioselective catalysis,” *Chem. - A Eur. J.*, vol. 14, no. 18, pp. 5397–5400, 2008.

[185] S. K. Ghosh, A. S. Ojeda, J. Guerrero-Leal, N. Bhuvanesh, and J. A. Gladysz, “New media for classical coordination chemistry: Phase transfer of Werner and related polycations into highly nonpolar fluorous solvents,” *Inorg. Chem.*, vol. 52, no. 16, pp. 9369–9378, 2013.

[186] S. K. Ghosh, C. Ganzmann, N. Bhuvanesh, and J. A. Gladysz, “Werner complexes with ??-dimethylaminoalkyl substituted ethylenediamine ligands: Bifunctional hydrogen-bond-donor catalysts for highly enantioselective Michael additions,” *Angew. Chemie - Int. Ed.*, vol. 55, no. 13, pp. 4356–4360, 2016.

[187] A. M. Greenaway and R. J. Lancashire, “Cobalt(III) ammines-‘Werner’ complexes: An undergraduate experiment,” *J. Chem. Educ.*, vol. 59, no. 5, p. 419, 1982.

[188] “http://chemistry.bd.psu.edu/jircitano/Optical3.pdf,” *September 2014*. .

[189] Y. Yoshikawa and K. Yamasaki, “Chromatographic resolution of metal complexes on sephadex ion exchangers,” *Rev. Coord. Chem.*, vol. 28, pp. 205–229, 1979.

Appendix A

Calculations of the acceleration produced by the Lorentz force

To calculate the Lorenz force we have to fit the values in the equation:

$$F = qv \times B$$

- The calculations are going to be shown for a molecule of 70 PSS. Therefore, to calculate the *q* first it is needed the net charge of a molecule.

The molecular weight of a monomer of PSS, which is formed by 8C + 9H + 3O + 1S, is:

M_w(PSS) = (8×12)+(9×1)+(3×16)+(1×32) = 185

If each molecule of the polymer has a molecular 70 kDa the number of monomers will be:

70000/185 ≈ 379 if we assume that the maximum net charge is 3 per monomer, then the maximum possible charge will be 1137 = $1137 \times 1.6 \times 10^{-19} = 1.82 \times 10^{-16}$ C

- To calculate the velocity, we are going to show the calculations of the molecules that are next to the wall, which are the ones that will have the largest velocity. Hence, the largest force.

If the inner diameter of the rotor is 3.1mm and the spin rate is 2.5kHz, then the *v* will be:

v = 2π×1.55×2500 = 24347 $mms^{-1} \approx 24.35 ms^{-1}$

- The value of B comes from the magnetic field produced by the spectrometer which is 14.1 T

Then the value of the Lorentz force is:

$$F = 1.82 \times 10^{-16} \times 24.35 \times 14.1 = 6.25 \times 10^{-14} \text{N}$$

Now to know the acceleration produce in a 70kDa molecule we need to use the Newton second law:

$$F = m \times a$$

The mass of one molecule of PSS is $70/N_a = 1.16 \times 10^{-22}$ kg. Therefore the acceleration is:

$$a = \frac{6.25 \times 10^{-14} \times 6.023 \times 10^{23}}{70} = 5.38 \times 10^{8} \text{ ms}^{-2}$$

Calculations of the acceleration produced at the rotor wall

To calculate the acceleration produced at the rotor wall at 2500 kHz We need to calculate first the velocity of the molecules that are in contact with the rotor wall.

If the diameter of the rotor wall is 3.1mm then the radius is r = 1.55 mm = 1.55×10^{-3}

$$v = \omega r = 2500 \times 2\pi r = 24.35 \text{ ms}^{-1}$$

The acceleration is then:

$$a_n = \frac{v^2}{r} = \frac{24.35^2}{0.00155} = 3.82 \times 10^5 \text{ms}^{-2}$$

Appendix B

Publications

B.1 Size-exclusion chromatographic NMR of polymer mixtures…….. 162

B.2 Size-exclusion chromatographic NMR under HR-MAS…….. 166

Research article

MRC

Received: 17 June 2014 Revised: 17 July 2014 Accepted: 27 July 2014 Published online in Wiley Online Library: 22 August 2014

(wileyonlinelibrary.com) DOI 10.1002/mrc.4127

Size-exclusion chromatographic NMR of polymer mixtures

Guillermo Lucena Alcalde, Rebecca E. Joyce and Iain J. Day*

The use of chromatographic stationary phases or solvent modifiers to modulate diffusion properties in NMR experiments is now well established. Their use can be to improve resolution in the diffusion domain or to provide an insight into analyte–modifier interactions and, hence, the chromatography process. Here, we extend previous work using size-exclusion chromatographic stationary phases to the investigation of polymer mixtures. We demonstrate that similar diffusion modulation behaviour is observed with a size-exclusion chromatographic stationary phase that can be understood in terms of size-exclusion behaviour. Copyright © 2014 John Wiley & Sons, Ltd.

Keywords: NMR; ^{1}H; diffusion NMR; chromatographic NMR; polymer

Introduction

Diffusion ordered spectroscopy is often described as 'NMR chromatography' in that it enables the pseudo-separation of mixtures based on the relative diffusion coefficients of the various constituent components.[1,2] Over the past ten years or so, this concept has been extended and enhanced by the addition of chromatographic stationary phases[3–6] or other sample modifiers.[7–10] These additives modulate the observed diffusion coefficients as a result of some favourable interaction between the additive and the analyte of interest. In some cases, this can significantly improve the attainable resolution in the diffusion dimension.[4,7,8] The exact nature of the interactions responsible for the diffusion modification is not fully understood. However, recent studies have shown that in the case of chromatographic NMR, the loading of the stationary phase, that is, the relative amount of stationary phase to 'mobile phase', plays an important role.[11,12] Indeed, high mobile phase to stationary phase ratios are required to reproduce results that are consistent with on-flow liquid chromatography.[12,13] One minor drawback of adding a stationary phase to the NMR sample is the increased line width observed as a result of susceptibility broadening due to the mismatch in magnetic susceptibilities of the solvent and the stationary phase.[3–6,14] Previous studies with small molecules have either utilised magic angle spinning[5] or matching of the solvent magnetic susceptibility to that of the stationary phase[6] to reduce the line broadening to acceptable levels.

Recently, we have adapted this chromatographic NMR approach to the use of size-exclusion chromatographic stationary phases.[15] We have demonstrated that the observed changes in diffusion properties of a series of polymer molecular weight reference standards is consistent with size-exclusion behaviour, in which smaller polymers show greater retardation in their diffusion than larger polymers.[15] These systems have also been used to investigate aggregating systems, with assemblies of the azo-dye sunset yellow partitioning between the pores in the stationary phase and the free solution surrounding the particles, depending on the overall aggregate size.[16] In both cases, the large size of the analyte molecules or assemblies means that the addition of the stationary phase causes only minor additional line broadening.[15,16]

In this paper, we demonstrate extending of the range of applicability of *in situ* size-exclusion chromatographic NMR to polymer mixtures. We show that under dilute or near-dilute conditions, the size-exclusion behaviour is similar for polymer mixtures as for the individual components using pairs of polymers that are closely matched in molecular weight and a 'mismatched' pairing. We interpret the results using the same framework as previously.[15]

Materials and methods

Materials

Poly(styrene sulfonate) (PSS) and polymethacrylate (PMA) molecular weight reference standards with low polydispersity (typically $<$1.20) were purchased as their sodium salts from Kromatek (Essex, UK) and used as obtained. Sephadex G-50 size-exclusion chromatographic stationary phase (dry bead size 20–50 μm, fractionation range: 1.5–30 kDa for globular proteins, 05–10 kDa for dextrans, pore size ~3 nm)[17,18] was obtained from Sigma-Aldrich (Dorset, UK). Deuterium oxide was purchased from Goss Scientific (Cheshire, UK).

The samples were prepared following the previously published procedure.[15] Briefly, 1 mL of a stationary phase suspension (at 60 mg mL^{-1}) in 50 mM sodium phosphate (pH 9) and 150 mM sodium chloride was allowed to settle under gravity. Of the supernatant, 200 μL was then removed and replaced with 200 μL of a 1 mM solution of the required polymer or polymer mixture, resulting in a final total polymer concentration of 0.2 mM. The suspension was then thoroughly mixed and transferred to a 5-mm NMR tube where it was allowed to settle under gravity for at least 30 min prior to use. The sample position was adjusted such that the stationary phase filled the RF coil region.[15] The sample therefore has a high solution to solid volume ratio.[12]

* *Correspondence to: Iain J. Day, School of Life Sciences, University of Sussex, Falmer, Brighton, BN1 9QJ, UK. E-mail: i.j.day@sussex.ac.uk*

School of Life Sciences, University of Sussex, Falmer, Brighton, BN1 9QJ, UK

NMR spectroscopy

All NMR data were acquired using a Varian VNMRS 600 spectrometer (Agilent Technologies, Yarnton, UK) equipped with an X{^{1}H} broadband probe and *z*-gradient coil capable of up to 0.7 T m^{-1}. All ^{1}H data were obtained at 599.7 MHz and a temperature of 298 K.

Diffusion NMR data were obtained using the Oneshot sequence of Pelta *et al.*,[19] with 16 gradient points spanning 0.0020–0.6066 T m^{-1}, equally spaced in g^2. The diffusion encoding time was 100 ms, with 2 ms gradient pulses. The spectral window was 9.6 kHz over 16 k complex data points. The resulting data were processed with either 4 or 8 Hz exponential line broadening prior to Fourier transformation, and the resulting peak intensities were fitted to the appropriately modified Stejskal–Tanner equation[19] using the Levenburg–Marquardt algorithm within DOSY Toolbox.[20]

Results and discussion

Previous proof of concept studies using two different size-exclusion stationary phases to modulate the diffusion properties of a single polymer, PSS, showed a sized-dependent effect, with smaller polymers showing larger changes in the observed diffusion coefficient.[15] This behaviour was interpreted in terms of the polymers accessing the pores of the stationary phase resulting in size-exclusion behaviour.[15] Because the overlap of spectral signals presents a challenge for diffusion experiments,[21,22] for this work, two polymers with different functional groups were chosen, PMA and PSS as used previously.[15] These have signals from the side chains in very different regions of the spectrum. There should also be little overlap between the methyl group of the PMA and the CH_2 fragments of the dextran supports of the stationary phase.

Figure 1 shows the results of diffusion measurements of a series of PMA molecular weight reference standards in the presence and absence of Sephadex G-50 size-exclusion stationary phase. The data clearly show similar trends to those reported previously with PSS.[15] In the absence of the stationary phase, the diffusion coefficient decreases with increasing molecular weight as is expected.[2] Upon the addition of the stationary phase, changes in the diffusion coefficient are clearly observed, with those changes being more dramatic for the smaller polymers. This behaviour is consistent with size-exclusion behaviour occurring in the presence of the Sephadex G-50 stationary phase, in that the smaller polymers spend longer inside the pores of the stationary phase and hence show greater retardation in their diffusion coefficients.[15,23] As previously, the data are interpreted in terms of an empirical equation,[15] similar to that used by Anderson and Stoddart[24,25] and Determann and Michel.[26] The equation is of the form:

$$\log\ M_w = a_0 - a_1 D \qquad (1)$$

where M_w is the weight-average molecular weight and D the measured diffusion coefficient. This is a phenomenological expression, and more precise models exist for describing the diffusion properties of homologous polymer series.[27] The results of fitting this expression to the data in Fig. 1 are given in Table 1. For comparison, the previous results obtained using PSS[15] are also included. The PMA samples chosen span a similar range of molecular weights to the PSS samples used previously, and as such, reveal similar a_0 and a_1 parameters. As seen before, the addition of the chromatographic stationary phase causes changes principally in the a_1 parameter, which is consistent with size-exclusion effects.[23] The small difference in the changes between the two polymers is likely related to differences in the interaction of polymer with the stationary phase, that is, differences between aromatic PSS and alkyl PMA side-chains.[28–31]

In order to investigate whether the presence of multiple species influences the ability of the size-exclusion stationary phase to modulate diffusion properties, an equimolar mixture of two polymers was used. The binary mixture was prepared using pairs of polymers with similar molecular weights, for example, 32.9 kDa PSS was paired with 36.3 kDa PMA. Diffusion NMR experiments were then performed on mixtures in the presence and absence of Sephadex G-50. The results are presented in Fig. 2. In the absence of the stationary phase, a similar trend to that shown in Fig. 1 for PMA, and

Table 1. Parameters returned from fitting Eqn (1) to the data in Fig. 1. The data for poly(styrene sulfonate) is from Joyce and Day[15]

Sample	a_0	$a_1/10^{10}$ s m^{-2}	R^2
PMA only	5.05	1.68	0.99
PMA + Sephadex G-50	5.36	3.19	0.98
PSS only[15]	5.11	1.50	0.96
PSS + Sephadex G-50[15]	5.30	2.52	0.94

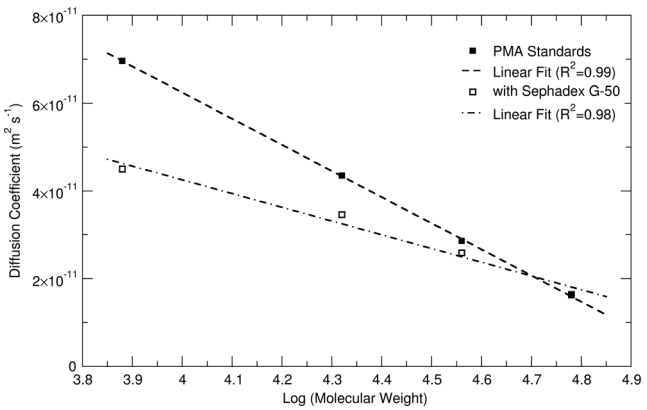

Figure 1. Diffusion coefficients for some polymethacrylate molecular weight reference standards in the presence and absence of Sephadex G-50. The straight lines are the result of fitting Eqn (1) to the experimental data, with parameters given in Table 1.

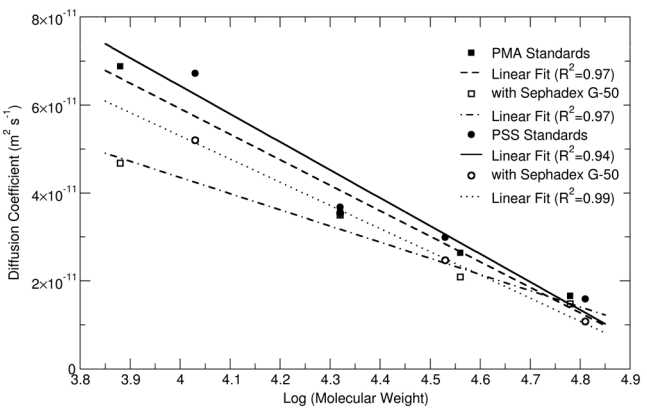

Figure 2. Diffusion coefficients for paired mixtures of polymethacrylate and poly(styrene sulfonate) in the presence and absence of Sephadex G-50. The straight lines are the result of fitting Eqn (1) to the experimental data, with parameters given in Table 2.

reported previously for PSS,[15] is observed. The measured diffusion coefficients are in broad agreement with those obtained for the individual polymers at the same concentrations. The parameters obtained from fitting Eqn (1) are given in Table 2. The values are altered slightly in the case of the polymer mixture as opposed to solutions of the individual polymers, which suggests that there may be some interaction between the polymers.[32,33] On addition of the Sephadex G-50, there is a noticeable change in the observed diffusion coefficients, which as expected is more pronounced for the smaller polymers. This is consistent with size-exclusion behaviour and indicates that the presence of the polymer mixture does not alter the gross diffusion modulating effect. Fitting the observed data to Eqn (1) results in the straight lines shown in Fig. 2 and the parameters reported in Table 2. While there is a clear change in the parameters on addition of the stationary phase, the magnitude of the change is not as large as in the case of the individual polymers only. Differences in the interactions between polymers and stationary phase,[28–31] in addition to small changes in the viscosity of the solution, may be a contributing factor here.[23] In traditional on-flow size-exclusion chromatography, these effects can be removed via universal calibration methods.[23]

Table 2. Parameters returned from fitting Eqn (1) to the data in Fig. 2

Sample	a_0	$a_1/10^{10}$ s m^{-2}	R^2
PMA free	5.02	1.72	0.99
PSS free	5.01	1.57	0.94
PMA + Sephadex G-50	5.18	2.72	0.97
PSS + Sephadex G-50	5.00	1.90	0.97

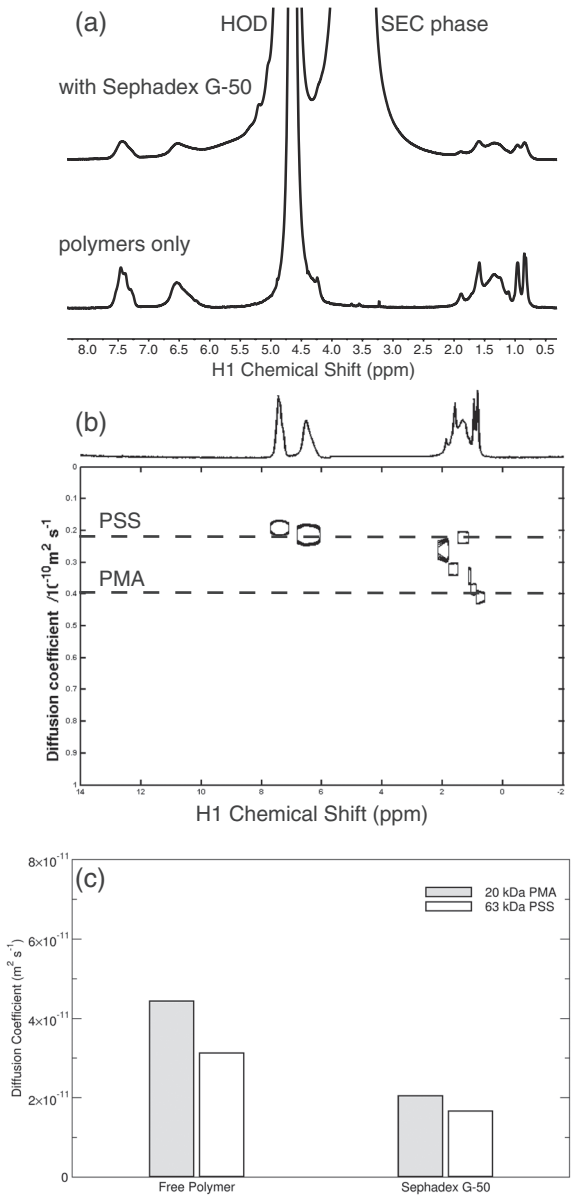

Figure 3. (a) ^{1}H NMR spectra of a mixture of 20.3 kDa PMA and 63.9 kDa PSS in the absence and presence of the Sephadex G-50 stationary phase. (b) DOSY spectrum of the same mixture in the absence of the Sephadex G-50 stationary phase. (c) Diffusion coefficients for the polymer mixture in the presence and absence of Sephadex G-50.

In order to further generalise the results presented, a 'mismatched' sample comprising PMA with a molecular weight of 20.3 kDa and PSS with a molecular weight of 63.9 kDa was prepared in a similar manner to those used above. Figure 3(a) shows the ^{1}H spectra of this mixture in the absence and presence of the stationary phase, demonstrating that the addition of the stationary causes only minor increases in the observed line width. Figure 3(b) shows the DOSY spectrum of the polymer mixture in the absence of Sephadex G-50. There is clearly a separation between the two polymers in the diffusion dimension. The CH_2 region around 1–2 ppm is clearly very crowded and shows extensive overlap of signals from both polymers and the stationary phase dextran support. The methyl groups of the PMA at 0.8 ppm, however, are resolvable and show as a distinct signal in the diffusion dimension, with a larger diffusion coefficient to that of the PSS. The measured diffusion coefficients in the presence and absence of Sephadex G-50 are shown in Fig. 3(c). In the case of the polymers in the absence of the stationary phase, the values are similar to those expected for the individual polymers, although the diffusion coefficient for PSS is slightly larger than observed previously. When the Sephadex G-50 stationary phase is added to the mixture, the observed diffusion coefficients are reduced as expected, broadly in line with the effects seen in Fig. 2. The effect of the stationary phase is greatest for the smaller polymer as its diffusion is hindered more by the pores of the stationary phase than the larger polymer. Overall, similar effects are observed as with the matched-weight polymers; however, the PSS sample used here has a molecular weight above the cut-off of the stationary phase, and hence, its diffusion properties should be unaffected by the addition of the stationary phase. This was observed previously in the case of the single polymers,[15] and in the case of the weight-matched pairs discussed previously. In this case, there is a reduction in the observed diffusion coefficient. This may be the result of some interaction between the PSS and PMA, or due to reduced space for self-diffusion because of the presence of the stationary phase. It is currently unclear as to why this would be observed here, but not previously.

Conclusions

The use of chromatographic stationary phases[3–6,14] or solvent modifiers[7–10,34] to modulate diffusion properties is becoming well established. We have previously demonstrated that size-exclusion media can be used in a similar manner, that is, they can induce a change in the observed diffusion coefficient that is consistent with size-exclusion behaviour.[15] Here, we have demonstrated that

these techniques can be applied to mixtures of polymers with similar results. Modification of the observed diffusion coefficients upon addition of Sephadex G-50 is found whether the polymers are close in molecular weight or not. The size of the modification is again consistent with size-exclusion behaviour occurring in the NMR sample, with the smaller polymers showing a much greater change in diffusion coefficient than the larger polymers. The application of *in situ* size-exclusion chromatographic NMR to other systems, such as biopolymers, is currently under investigation.

Acknowledgements

G. L. A. thanks the School of Life Sciences for a GTA studentship, R. E. J. thanks the EPSRC for a DTA award. The University of Sussex and the EPSRC (EP/H025367/1) are thanked for the financial support.

References

[1] C. S. Johnson. *Prog. NMR. Spec.* **1999**, *34*, 203.
[2] W. S. Price, *NMR Studies of Translational Motion*, Cambridge University Press, Cambridge, **2009**.
[3] S. Viel, F. Ziarelli, S. Caldarelli. *Proc. Natl. Acad. Sci. U. S. A.* **2003**, *100*, 9696.
[4] G. Pages, C. Delaurent, S. Caldarelli. *Angew. Chem. Int. Ed.* **2006**, *45*, 5950.
[5] S. Viel, F. Ziarelli, G. Pages, C. Carrara, S. Caldarelli. *J. Magn. Reson.* **2008**, *190*, 113.
[6] R. E. Hoffman, H. Arzuan, C. Pemberton, A. Aserin, N. Garti. *J. Magn. Reson.* **2008**, *194*, 295.
[7] R. W. Adams, J. A. Aguilar, J. Cassani, G. A. Morris, M. Nilsson. *Org. Bio. Chem.* **2011**, *9*, 7062.
[8] R. Evans, S. Haiber, M. Nilsson, G. A. Morris. *Anal. Chem.* **2009**, *81*, 4548.
[9] C. F. Tormena, R. Evans, S. Haiber, M. Nilsson, G. A. Morris. *Magn. Reson. Chem.* **2010**, *48*, 550.
[10] M. E. Zielinski, K. F. Morris. *Magn. Reson. Chem.* **2008**, *47*, 53.
[11] C. Carrara, G. Pages, C. Delaurent, S. Viel, S. Caldarelli. *J. Phys. Chem. C* **2011**, *115*, 18776.
[12] C. Carrara, S. Caldarelli. *J. Phys. Chem. C* **2012**, *116*, 20030.
[13] C. Carrara, C. Lopez, S. Caldarelli. *J. Chromatogr. A* **2012**, *1257*, 204.
[14] C. Pemberton, R. E. Hoffman, A. Aserin, N. Garti. *J. Magn. Reson.* **2011**, *208*, 262.
[15] R. E. Joyce, I. J. Day. *J. Magn. Reson.* **2012**, *220*, 1.
[16] R. E. Joyce, I. J. Day. *J. Phys. Chem. C* **2013**, *117*, 17503.
[17] GE Healthcare. Gel filtration: principles and methods. **2010**.
[18] G. Paradossi, F. Cavalieri, E. Chiessi, C. Mondelli, M. T. F. Telling. *Chem. Phys.* **2004**, *302*, 143.
[19] M. D. Pelta, G. A. Morris, M. J. Stchedroff, S. J. Hammond. *Magn. Reson. Chem.* **2002**, *40*, S147.
[20] M. Nilsson. *J. Magn. Reson.* **2009**, *200*, 296.
[21] K. F. Morris, C. S. Johnson. *J. Am. Chem. Soc.* **1993**, *115*, 4291.
[22] M. Nilsson, M. A. Connell, A. L. Davis, G. A. Morris. *Anal. Chem.* **2006**, *78*, 3040.
[23] T. Kremmer, L. Boross, *Gel chromatography: theory, methodology and applications*, John Wiley and Sons, Chichester, **1979**.
[24] D. M. W. Anderson, J. F. Stoddart. *Anal. Chim. Acta* **1966**, *34*, 401.
[25] D. M. W. Anderson, J. F. Stoddart. *Carbohyd. Res.* **1966**, *4*, 104.
[26] H. Determann, W. Michel. *J. Chromatogr. A* **1966**, *25*, 303.
[27] S. Auge, P.-O. Schmidt, C. A. Crutchfield, M. T. Islam, D. J. Harris, E. Durand, M. Clemancy, A.-A. Quoineaud, J.-M. Lancelin, Y. Prigent, F. Taulelle, M. A. Delsuc. *J. Phys. Chem. B* **2009**, *113*, 1914.
[28] B. Gelotte. *J. Chromatogr. A* **1960**, *3*, 330.
[29] A. J. W. Brook, S. Housley. *J. Chromatogr. A* **1964**, *41*, 200.
[30] H. Determann. *Nature* **1968**, *219*, 604.
[31] A. J. W. Brook, K. C. Munday. *J. Chromatogr. A* **1970**, *47*, 1.
[32] M. Rubinstein, R. H. Colby, *Polymer Physics*, Oxford University Press, Oxford, **2003**.
[33] I. Teraoka, *Polymer Solutions*, Wiley-Interscience, New York, **2002**.
[34] J. S. Kavakka, I. Kilpelainen, S. Heikkinen. *Org. Lett.* **2009**, *11*, 1349.

Special issue research article

MRC

Received: 3 May 2016 Revised: 17 May 2016 Accepted: 25 May 2016 Published online in Wiley Online Library: 15 June 2016

(wileyonlinelibrary.com) DOI 10.1002/mrc.4464

Size-exclusion chromatographic NMR under HR-MAS

Guillermo Lucena Alcalde, Natalie Anderson and Iain J. Day*

The addition of stationary phases or sample modifiers can be used to modify the separation achievable in the diffusion domain of diffusion NMR experiments or provide information on the nature of the analyte–sample modifier interaction. Unfortunately, the addition of insoluble chromatographic stationary phases can lead to line broadening and degradation in spectral resolution, largely because of differences in magnetic susceptibility between the sample and the stationary phase. High-resolution magic angle spinning (HR-MAS) techniques can be used to remove this broadening. Here, we attempt the application of HR-MAS to size-exclusion chromatographic NMR with limited success. Observed diffusion coefficients for polymer molecular weight reference standards are shown to be larger than those obtained on static samples. Further investigation reveals that under HR-MAS it is possible to obtain reasonably accurate estimates of diffusion coefficients, using either full rotor synchronisation or sophisticated pulse sequences. The requirement for restricting the sample to the centre of the MAS rotor to ensure homogeneous magnetic and RF fields is also tested. Copyright © 2016 John Wiley & Sons, Ltd.

Keywords: diffusion; size exclusion; HR-MAS

Introduction

Nuclear magnetic resonance (NMR) spectroscopy is one of the key analytical techniques for the elucidation or verification of molecular structure.[1,2] There are a huge number of experiments available in the spectroscopic toolbox allowing an atomic level of detail to be obtained.[1,2] However, the vast majority of these experiments are best performed on pure samples, as the presence of impurities or mixtures can lead to ambiguity in the analysis and interpretation. This spectral complexity can be overcome by separating the mixture, either using traditional chromatographic methods, whether online or offline,[3,4] or by pseudoseparation using some molecular parameters such as diffusion coefficient[5] or the generation of a maximum-quantum spectrum.[6] The use of diffusion coefficient to separate mixtures is well documented,[5,7] with the ability to resolve molecules with reasonably small differences in diffusion coefficient under favourable conditions; however, the technique is limited in cases of spectral overlap.[5,7] In 2003, Caldarelli and co-workers proposed a method to improve resolution in the diffusion dimension by the addition of a silica stationary phase normally used in HPLC.[8–10] They showed that separation was improved and correlated with the degree of interaction between the analyte and stationary phase as predicted by traditional chromatographic models.[11,12] The idea of adding a sample modifier has been proposed and utilised by a number of groups and is known as chromatographic NMR[9] or matrix-assisted DOSY.[13,14] Typical sample modifiers include bare and functionalised silica,[8–10,15,16] polymers,[17–19] nanoparticles,[20,21] surfactant micelles[13,22,23] and chiral shift reagents.[14]

Recently, we have extended the concept of chromatographic NMR to the use of size-exclusion stationary phases.[24–26] These phases comprise a porous material, typically based on cross-linked dextran, with pore sizes on the order of 10–100 nm. Chromatographic separation depends on the time different analytes spend exploring the pores, with smaller molecules typically spending longer inside the pores than larger molecules.[27,28] While size-exclusion phases do not offer an improvement in diffusion resolution, as smaller molecules are retarded to a greater degree than larger molecules,[27] the interaction between the analyte and stationary phase, and therefore the change in observed diffusion coefficient upon addition of the stationary phase, can be interpreted in terms of size-exclusion effects[24,26] and provide information on the nature of the interaction between the stationary phase and the analyte.

Several of the common sample modifiers proposed for a chromatographic NMR result in additional line broadening being observed, limiting the spectral resolution. This line broadening arises as a result of magnetic susceptibility differences between the particles of the stationary phase and the bulk solvent.[8,9,15,29] Two approaches have been proposed to alleviate this line broadening and restore high resolution in the spectral dimension, in addition to the improved resolution in the diffusion dimension. The first is magic angle spinning, typically only moderate speeds of around 2–4 kHz are required.[8–10] Under these conditions, liquid-like line shapes are restored at the cost of the appearance of spinning side bands and some concern over the accuracy of the measured diffusion coefficient due to effects such as sample vortexing.[10,30] The second approach to reducing the susceptibility-induced line broadening is to match the magnetic susceptibility of the solvent to that of the stationary phase.[15] This

* Correspondence to: Iain J. Day, School of Life Sciences, University of Sussex, Falmer, Brighton, BN1 9QJ, UK. E-mail: i.j.day@sussex.ac.uk

School of Life Sciences, University of Sussex, Brighton, UK

is typically performed in an empirical manner, adjusting the solvent composition to minimise the spectral line width.[15] This approach is, however, limited as the stationary phase must remain stable in the solvent mixture used. This is possible for silica stationary phases, which are able to tolerate a wide range of solvents, but more of a challenge for dextran, poly(acrylamide) or other cross-linked polymer-based stationary phases and impractical for sample modifiers based on surfactants.

In order to improve the spectral resolution in size-exclusion chromatographic NMR, in this paper, we therefore employ high-resolution magic angle spinning (HR-MAS). We present some preliminary measurements of diffusion coefficients under HR-MAS with size-exclusion stationary phases, which reveal some issues with this technique. Further investigation into the role of pulse sequence design and timings, including the unreliable measurement of the diffusion coefficient under certain conditions,[10,30] demonstrates that it is possible to obtain reliable diffusion measurements under HR-MAS conditions. We note in passing a bug in the vendor-supplied pulse sequences, which hindered our analysis.

Materials and Methods

Sample preparation

Poly(styrene sulfate) (PSS) molecular weight reference standards (polydispersity index < 1.20) were purchased from Kromatek (Essex, UK) and used as obtained. Deuterium oxide and benzene-d_6 were purchased from either Sigma-Aldrich (Dorset, UK) or Goss Scientific (Cheshire, UK). All other chemicals were purchased from Sigma-Aldrich. The polymers, with weight-averaged molecule weights of 10.6, 14.9, 20.7, 32.9 and 63.9 kDa, were prepared as 0.2 mM solutions in a buffer system comprising 150 mM sodium chloride and 50 mM sodium phosphate at pH 9. Sephadex G-50 stationary phase was swelled at a concentration of 60 mg ml^{-1} in the polymer solution for a minimum of 3 h. The stationary-phase suspension was then shaken, and 80 µl were transferred to a 4-mm OD zirconia rotor. The rotor was held vertically, and the suspension was left to settle under gravity. The supernatant (40 µl) was then removed before closing the rotor with the cap and drive ring.

NMR spectroscopy

All NMR experiments were performed using a Varian VNMRS600 (Agilent Technologies, Yarnton, UK) operating at a ^{1}H frequency of 599.6 MHz. HR-MAS spectra were collected using a 4-mm gHX-Nano probe equipped with a magic angle gradient coil capable of producing gradients of approximately 1.66 T m^{-1} along the sample rotation axis. The sample temperature was regulated to be 298 K as measured by the VT controller. The actual sample temperature under HR-MAS conditions ($\nu_r = 2$ kHz) was 305 K, measured using an ethylene glycol thermometer. Non-spinning spectra were recorded using a 5-mm X{^{1}H} probe with an actively shielded z-gradient coil capable of approximately 0.7 T m^{-1}. For these spectra, the temperature was regulated at 298 K.

Diffusion measurements were principally performed using the gradient compensated stimulated echo (GCSTE), bipolar pulse stimulated echo (BPPSTE)[31] or Oneshot[32] sequences as provided in the Agilent DOSY tools package. Typical parameters were as follows: a diffusion labelling period of 50–100 ms; diffusion labelling gradients were 1–3 ms in duration and comprised 15 intensity points equally spaced in g^2 from 0.0457 to 0.8129 T m^{-1}. Spectra were acquired over a spectral window of 9615.4 Hz using 9615 complex data points. All spectra were processed using the NMR plugin of Mestrenova (Santiago de Compostela, Spain) or DOSY Toolbox[33] as appropriate, with 5-Hz exponential line broadening prior to Fourier transformation and subsequent baseline correction with a second-order polynomial. Diffusion data were fitted using a single exponential function to the Stejskal–Tanner equation, suitably modified for the appropriate pulse sequence.[31,32]

Results and Discussion

To demonstrate the effect addition of a stationary phase has on spectral quality and the improvement under HR-MAS conditions,

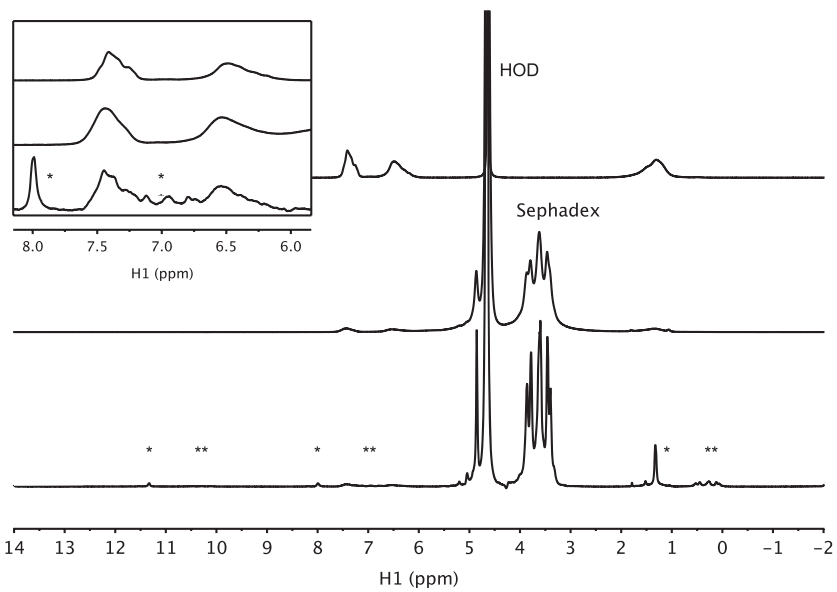

Figure 1. ^{1}H NMR spectra of 63.9-kDa poly(styrene sulfonate). The upper trace is poly(styrene sulfonate) only, middle trace is in the presence of Sephadex G-50 and the lower trace is under 2 kHz high-resolution MAS. * and ** mark spinning sidebands arising from the HOD and Sephadex G-50 signals, respectively.

Figure 1 shows the ^{1}H NMR of a 63.9-kDa sample of poly(styrene sulfonate). Addition of the stationary phase causes an increase in the observed line width, along with a degradation in spectral resolution, and the appearance of signals in the 3–4 ppm range arising from the dextran backbone of the stationary phase. Repeating the experiment under HR-MAS at a spin rate of 2 kHz results in a return to the liquid-like line shape observed in the absence of the stationary phase, but with the added complication of spinning sidebands, indicated by * and ** for the solvent and stationary phase, respectively. Given the relatively slow spinning speeds used in HR-MAS, these sidebands will always occur within the spectral window; however, they can be moved away from signals of interest by small adjustments of the spinning rate.

Previous work has utilised size-exclusion stationary phases in standard 5-mm NMR tubes under static conditions, with the associated reduction in spectral resolution.[24,26] Performing similar experiments using polymer molecular weight reference standards under HR-MAS with and without a Sephadex G-50 stationary phase results in the measured diffusion coefficients presented in Fig. 2. The error bars show that there is an uncertainty of 10–25% in the measured diffusion coefficient, partially as a result of low signal-to-noise ratio in the experiment and the potential overlap of spinning sidebands arising from the Sephadex stationary phase. For comparison, the same measurements performed on static samples (in a 5-mm tube) are also shown.[24] There are clearly alarming differences between the measurements recorded under magic angle spinning compared with those reported previously. In the absence of the stationary phase, the measured diffusion coefficients obtained under HR-MAS appear to be approximately a factor of 2 larger than those obtained in the static samples. Differences in observed diffusion coefficient between spinning and static samples have been reported previously in the case of low-viscosity solvents.[10] A possible initial explanation is that the act of spinning the sample generates bulk sample motion, such as vortexing, resulting in erroneous diffusion coefficients being returned by the analysis. The trends in the measured diffusion coefficients are, however, similar between the spinning and static cases. Fitting these data to the phenomenological equation, similar to that obtained by Anderson and Stoddart[34,35] and Determann and Michel,[36] used previously,[24,26]

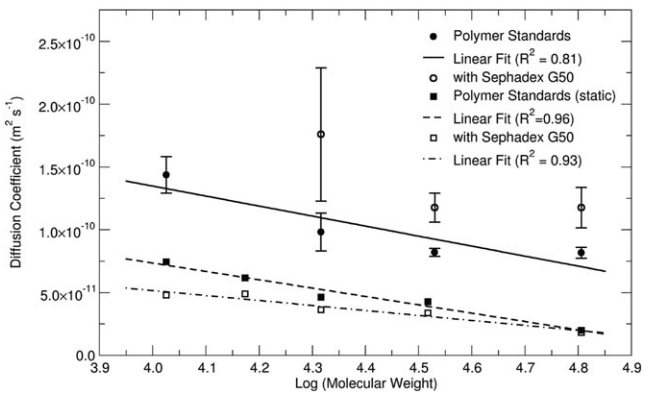

Figure 2. Measured diffusion coefficient as a function of log(molecular weight) for the poly(styrene sulfonate) reference standards under high-resolution MAS conditions ($\nu_r = 2$ kHz) with and without Sephadex G-50. For comparison, diffusion coefficients for the same poly(styrene sulfonate) samples under static conditions, in the absence of stationary phase,[24] are also shown.

Table 1. Parameters returned from fitting Eq. (1) to the diffusion coefficient data presented in Fig. 2

Sample	a_0	$a_1/10^{10}$ s m^{-2}	R^2
PSS standards – static[24]	5.11	1.50	0.96
PSS standards – static + Sephadex G50[24]	5.30	2.52	0.93
PSS standards – 2 kHz MAS	5.69	1.25	0.81

$$\log M = a_0 - a_1 D \quad (1)$$

results in the parameters given in Table 1. The similarity of the parameters for the spinning and static samples suggests that the polymer reference standards are behaving in a comparable manner under both sets of experimental conditions albeit with different measured diffusion coefficients.

On addition of the Sephadex G-50 stationary phase, there is a further marked changed in the measured diffusion coefficients. This change is an unexpected increase in the diffusion coefficient. Previous experiments with size-exclusion phases[25,26] resulted in a decrease in measured diffusion coefficient due to molecules entering the pores of the stationary phase and being retarded, with the degree of retardation being dependent on both the molecular weight and pore size.[27] Chromatographic NMR of benzene and silica stationary phases has shown an increase in diffusion coefficient upon addition of the stationary phase. This was rationalised by including the vapour phase of the benzene in a condensation–evaporation equilibrium between the solvent and stationary phase.[37] This mechanism is unlikely to be operative in the case of the polymers reported here because of their low vapour pressure. The results shown in Fig. 2 clearly indicate that in its current form the simple transfer of the size-exclusion chromatographic NMR method to HR-MAS is not possible. There are clearly factors arising both from the application of magic angle spinning and combination with the stationary phase that require further investigation.

In order to further understand the influence of MAS on the diffusion experiments, a series of measurements were performed using three diffusion experiments of increasing sophistication: the GCSTE, the BPPSTE[31] and the Oneshot experiment,[32] monitoring the residual HOD signal of a D_2O sample. Diffusion measurements were performed as a function of spin rate, and with varying lengths of diffusion encoding gradient (δ). The results are shown in Fig. 3(a, c and e) for the three pulse sequences considered. It is immediately clear that for the GCSTE and BPPSTE sequences there is strong variation on the observed diffusion coefficient with spin rate and the duration of the diffusion encoding gradient. For example, with the GCSTE experiment shown in Fig. 3(a), there is wild variation in the observed diffusion coefficient over an order of magnitude. A similar pattern, although less severe, is seen for the BPPSTE sequence in Fig. 3 (c). The Oneshot sequence shows broadly similar diffusion coefficients across all experimental parameters tested, with a variation of only around 10% of the true diffusion coefficient for D_2O ($D = 2.3 \times 10^{-9}$ m^2 s^{-1}).[38] To ensure the best possible accuracy in the measured diffusion coefficient, it is important that the gradient pulses used for diffusion encoding and decoding excite the same spin packet and therefore should be synchronised to the rotor period, in both their duration and interpulse timing.[30,39,40] Viel *et al*. suggest, however, that

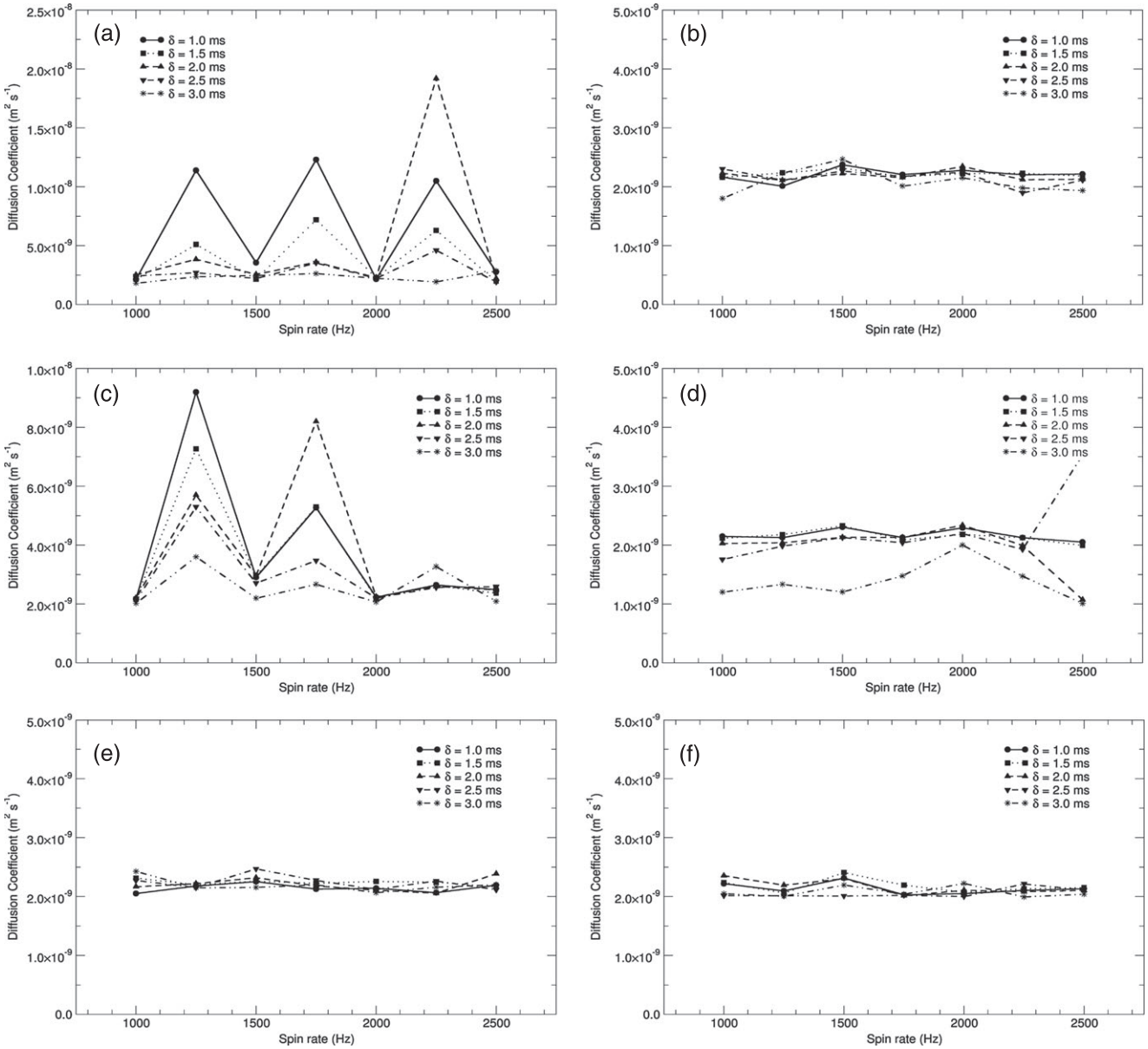

Figure 3. Observed variation in the measured diffusion coefficient of HOD with spin rate using a diffusion encoding time of Δ of 100 ms. (a and b) For the gradient compensated stimulated echo; (c and d) for the bipolar pulse stimulated echo; and (e and f) for the Oneshot sequence. Panels a, c and e are the pulse sequences as supplied in the Agilent library, while panels b, d and f utilise complete rotor synchronisation of the RF pulses, gradient durations and delays.

this may not be necessary, reporting that no such synchronisation was employed in their measurements.[10] In the standard implementation in the Agilent library, the total area of the diffusion encoding gradients is rotor synchronised, but other parameters, including the interpulse spacing Δ, are not synchronised with the sample rotation. Therefore, the diffusion decoding gradient can end up being applied at a different point of the rotor cycle compared with the corresponding diffusion encoding gradient. Figure 3(b, d and f) shows the results of repeating the experiments in Fig. 3(a, c and e), ensuring that the timings of all RF pulses, gradient durations and delays are synchronised with the sample rotation. Clearly, differences with and without rotor synchronisation are apparent for the GCSTE [Fig. 3(a and b)] and BPPSTE sequences [Fig. 3(c and d)], but not for the Oneshot experiment [Fig. 3(e and f)]. Rotor synchronisation of the gradient pulses and delays appears to be imperative for the GCSTE and BPPSTE sequences, but less important for the Oneshot experiment. There are clearly some issues with the BPPSTE sequence, especially with long gradient pulses; however, the performance is clearly improved compared with no rotor synchronisation. The BPPSTE sequence incorporates bipolar gradient pulses, which significantly reduce the impact of any gradient-induced eddy currents.[31] The Oneshot sequence includes an unbalancing factor to allow unwanted coherences to be destroyed by the diffusion encoding gradients, negating the need for extensive phase cycling.[32] The Oneshot sequence is an improved version of the BPPSTE sequence, and therefore, it is unsurprising that the two sequences produce similar results. The similarity in the results obtained between the rotor-synchronised BPPSTE and Oneshot sequences, with or without rotor synchronisation,

suggests that the improvements in the Oneshot sequence over the BPPSTE remove some of the additional complications that are partially ameliorated by the rotor synchronisation. We note that there is a bug in the original Agilent-supplied versions of the GCSTE, BPPSTE and Oneshot sequences. Data obtained from these sequences, when processed with VnmrJ or DOSYToolbox, resulted in diffusion coefficients that are a function of both spin rate and gradient duration. Further details are in the supporting information.

A previous demonstration of chromatographic NMR under HR-MAS by Caldarelli and co-workers also showed that there were differences in the observed diffusion coefficient between static and spinning samples.[10] In this case, the differences were attributed to mechanical mixing and vortexing effects, with the influence of sample geometry also an important factor: restricting the sample volume to the regions of high gradient linearity leads to diffusion coefficients for small molecules, in good agreement with literature data.[10] Small intensity fluctuations in the echo attenuation curve have also been reported in experiments performed with similar sample geometry to that used here.[30] These fluctuations are reported to arise from vortexing of the sample and can be mostly removed by extensive signal averaging.[30] The effect of linear (coherent) motions can also be reduced by the use of convection-compensated sequences[41]; however, for the systems reported here little improvement is seen (data not shown), likely because of the increased pulse sequence complexity. Restricting the sample diameter has the added benefit of reducing the exposure to radial variation in the B_1 RF field, which will be modulated by the MAS because of the lack of cylindrical symmetry in a solenoid coil.[42] This modulation of the B_1 RF field has been shown to be the source of signal loss in TOCSY experiments performed under HR-MAS conditions.[42,43] Slow sample spinning (~20 Hz) has also been suggested as a method for mitigating against the effects of sample convection in diffusion NMR experiments[44]; however, convection effects have recently been reported to be more insidious than previously thought.[45] Bakhmutov has also shown that MAS can lead to changes in observed signal behaviour for spin–lattice relaxation measurements in liquid samples. A change from single to biexponential behaviour was observed as a function of spin rate and attributed to the formation of an air bubble, held concentrically along the rotor axis by centrifugal forces, causing increased paramagnetic relaxation at the interface.[46]

Following the arguments of Viel *et al.*[10] and restricting the sample volume should reduce the dependence of the measured diffusion coefficient on spin rate by restricting the active volume to the centre of the sample rotor. Two sample restriction modalities were employed; the first was designed to restrict the sample geometry radially, i.e. closer to the rotation axis, and reduce the effects of radial field inhomogeneities[39] and vortexing of the sample,[10,30] while the second restricted the sample dimensions axially to regions of greater gradient linearity.[10] To achieve radial restriction, a cylindrical Teflon spacer was introduced into the rotor to reduce the sample to a diameter of 1.5 mm, a reduction of 53%. The measured diffusion coefficient of HOD as a function of spin rate under these conditions for the Oneshot sequence are shown in Fig. 4(a). These data show almost identical trends to those in Fig. 3(c), with slight overestimations of the diffusion coefficient at slow spinning rates. Axial restriction was performed by including a 1-mm-thick Teflon disc (3.1-mm diameter) at the top and bottom

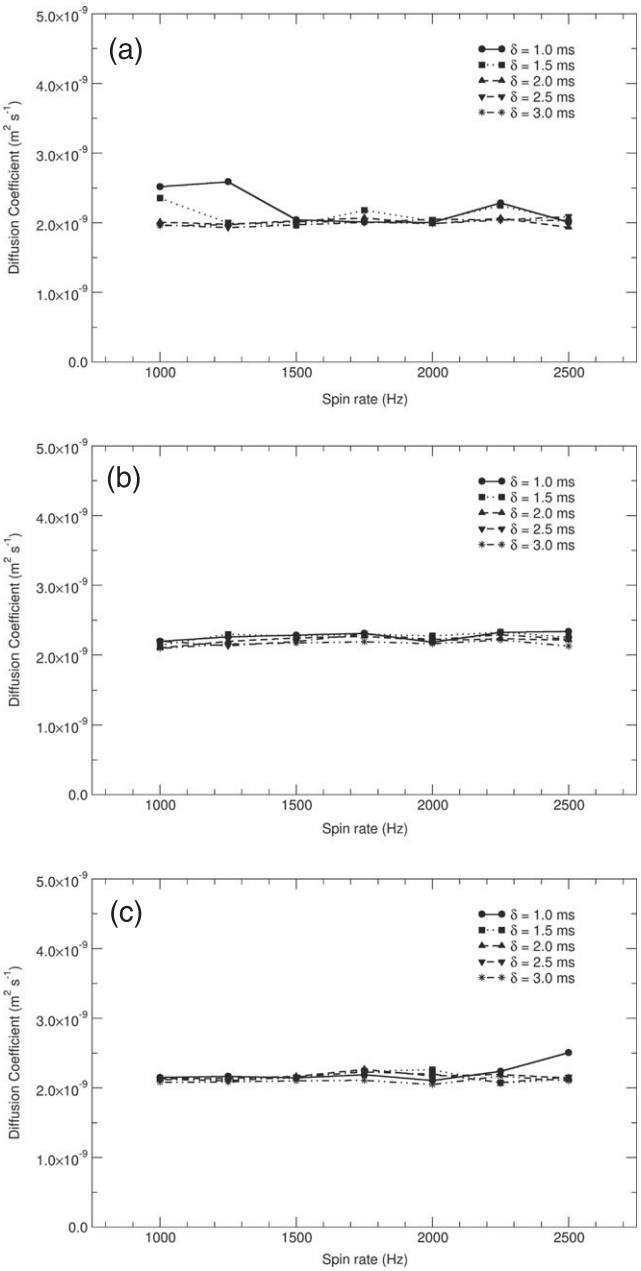

Figure 4. Observed variation in the measured diffusion coefficient of HOD with spin rate recorded using the Oneshot sequence and a diffusion encoding time Δ of 100 ms. (a) The sample was confined to a diameter of 1.5 mm by the inclusion of a Teflon spacer, and (b) the sample was restricted to a height of 2.6 mm using a pair of 1-mm Teflon discs above and below the sample. (c) Combination of both sample restriction methods.

of the sample volume. This reduces the active sample volume by 43%. The results of these measurements are presented in Fig. 4(b). These again show very similar profiles to those in Figs 3(c) and 4(a). Combining the two approaches, i.e. utilising a sample that is restricted both axially and radially, gives the results shown in Fig. 4(c). In this arrangement, the sample volume is approximately 4.7 μl, restricted to the centre of the rotor. Very similar trends in measured diffusion coefficient as a function of spin rate or duration of the diffusion encoding gradient are seen, with a slight minor deviation for higher spin rates and short gradient pulse duration. Taken together, these results suggest that restricting the sample to the centre

of the rotor, either radially or axially, is not required for solvents of moderate viscosity, such as D_2O, and that minor inconsistencies in the measured diffusion coefficient are likely to arise from vortexing of the sample in the manner described previously.[10]

In addition to providing spectral simplification, spinning a sample at high speed under MAS conditions also has the potential to introduce other physical effects as a result of the large mechanical forces present. The acceleration produced at the inside wall of a MAS rotor can be considerable.[47] Even in the case of the 4-mm rotor used here, with an internal diameter of 3.14 mm, at a moderate speed of 2 kHz, the acceleration at the rotor wall is over $20\,000 \times g$. Bertini and co-workers have demonstrated that under fast spinning rates, large biomolecules can be sedimented to the rotor walls akin to ultracentrifugation.[47–49] Figure 5 shows the concentration profile for the poly(styrene sulfonate) samples used in the 4-mm HR-MAS rotor at a spinning speed of 2 kHz, calculated using the approach of Bertini *et al.*[48–50] While this does not show complete sedimentation of the polymers to the rotor wall, it is clear that there is a non-uniform concentration profile across the rotor, with increased concentration at the rotor edge and a concomitant decrease at the rotor centre. The difference in concentration is as much as a factor of >2 for the larger polymer standards. The size-exclusion stationary phase, when present, will also be exposed to the same physical forces and having a much larger effective molecular weight due to cross-linking, therefore likely to be predominantly found in the outer portions of the rotor. The result of this sedimentation effect is that the loading of the polymer solution into the stationary phase will be considerably different compared with the static case reported previously.[24,26] The loading of the stationary phase, i.e. the ratio of solution to stationary phase, has been shown to have a dramatic effect on the modulation of the diffusion coefficient caused by a given stationary phase.[37] This effect is postulated to depend on whether mass transport is confined just to the intraparticle pores or whether there is sufficient solvent to allow escape into the interparticle space.[11,37]

In the case of the samples used here, the ratio of solution to stationary phase is high; therefore, the polymers are able to explore both the intraparticle and interparticle voids. Under the influence of MAS, sedimentation effects will therefore significantly distort the distribution of both the stationary phase and polymer, and hence the stationary phase loading, radially across the rotor. This spatial variation in the sample under MAS conditions may then lead to a distribution of diffusion modulation effects upon addition of the stationary phase should there be any sample vortexing present.

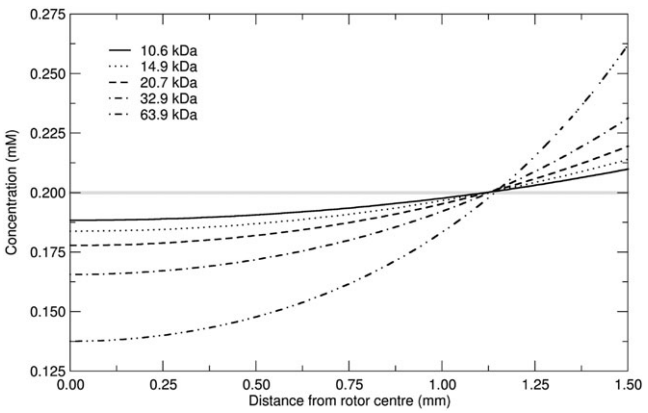

Figure 5. Concentration profiles for various poly(styrene sulfonate) samples in a 4-mm (outer diameter) high-resolution MAS rotor spinning at a speed (ν_r) of 2 kHz. The grey horizontal line indicates the static concentration. The curves were calculated using the method of Bertini *et al.*[48,49] from sedimentation equilibria.[50]

Conclusions

The addition of a chromatographic stationary phase to an NMR sample has the potential for great utility in improving the diffusion resolution[8,9,14,15,23] or providing information on the analyte–stationary phase interaction.[12,37] However, the presence of an insoluble component in the sample can have deleterious effects on the spectral quality.[10,15] The use of HR-MAS methods to reduce these effects[10] has been applied here in the context of size-exclusion chromatographic stationary phases, however, with unexpected results. Using size-exclusion chromatographic stationary phases under HR-MAS yields unexpected results in that the observed diffusion coefficient is larger in the presence of the stationary phase. Evaporation–condensation, postulated previously for benzene–silica systems,[11] is unlikely to be responsible. We confirm that it is possible to obtain reliable estimates of the diffusion coefficient under HR-MAS conditions using either rotor synchronisation of the gradient pulses and delays[30,39,40] or more sophisticated pulse sequences such as Oneshot.[32] The discrepancies in observed diffusion coefficients using size-exclusion chromatography phases are currently under further investigation.

Acknowledgements

The authors thank Rebecca Joyce for collecting preliminary data and helpful discussions. G. L. A. thanks the School of Life Sciences for a GTA studentship. N. A. thanks the late Prof. John Murrell FRS for a summer bursary. The University of Sussex and the EPSRC (EP/H025367/1) are thanked for financial support.

References

[1] T. D. W. Claridge, *High-resolution NMR Techniques in Organic Chemistry*, 2nd edn, Elsevier, Amsterdam, **2009**.
[2] S. A. Richards, J. C. Hollerton, *Essential Practical NMR for Organic Chemistry*, John Wiley and Sons, Chichester, **2011**.
[3] J. C. Lindon, J. K. Nicholson, I. D. Wilson. *Prog. NMR. Spectros.* **1996**, *29*, 1.
[4] M. Cudaj, G. Guthausen, T. Hofe, M. Wilhelm. *Macromol. Rapid Comm.* **2011**, *32*, 665.
[5] C. S. Johnson. *Prog. NMR. Spectros.* **1999**, *34*, 203.
[6] G. N. Reddy, S. Caldarelli. *Chem. Commun.* **2011**, *47*, 4297.
[7] B. Antalek. *Concepts Magn. Reson.* **2002**, *14A*, 225.
[8] S. Viel, F. Ziarelli, S. Caldarelli. *Proc. Natl. Acad. Sci. U. S. A.* **2003**, *100*, 9696.
[9] G. Pages, C. Delaurent, S. Caldarelli. *Angew. Chem. Int. Ed.* **2006**, *45*, 5950.
[10] S. Viel, F. Ziarelli, G. Pages, C. Carrara, S. Caldarelli. *J. Magn. Reson.* **2008**, *190*, 113.
[11] C. Carrara, G. Pages, C. Delaurent, S. Viel, S. Caldarelli. *J. Phys. Chem. C* **2011**, *115*, 18776.
[12] C. Carrara, C. Lopez, S. Caldarelli. *J. Chromatogr. A* **2012**, *1257*, 204.
[13] C. F. Tormena, R. Evans, S. Haiber, M. Nilsson, G. A. Morris. *Magn. Reson. Chem.* **2010**, *48*, 550.
[14] R. W. Adams, J. A. Aguilar, J. Cassani, G. A. Morris, M. Nilsson. *Org. Bio. Chem.* **2011**, *9*, 7062.
[15] R. E. Hoffman, H. Arzuan, C. Pemberton, A. Aserin, N. Garti. *J. Magn. Reson.* **2008**, *194*, 295.
[16] C. Pemberton, R. E. Hoffman, A. Aserin, N. Garti. *J. Magn. Reson.* **2011**, *208*, 262.
[17] J. S. Kavakka, I. Kilpelainen, S. Heikkinen. *Org. Lett.* **2009**, *11*, 1349.

[18] S. Huang, R. Wu, Z. Bai, Y. Yang, S. Li, X. Dou. *Magn. Reson. Chem.* **2014**, *52*, 486.
[19] S. Huang, J. Gao, R. Wu, S. Li, Z. Bai. *Angew. Chem. Int. Ed.* **2014**, *126*, 11776.
[20] T. Gonzalez-Garcia, T. Margola, A. Silvagni, F. Mancin, F. Rastrelli. *Angew. Chem. Int. Ed.* **2016**, *55*, 2733.
[21] M.-V. Salvia, F. Ramadori, S. Springhetti, M. Diez-Castellnou, B. Perrone, F. Rastrelli, F. Mancin. *J. Am. Chem. Soc.* **2015**, *137*, 886.
[22] M. E. Zielinski, K. F. Morris. *Magn. Reson. Chem.* **2008**, *47*, 53.
[23] R. Evans, S. Haiber, M. Nilsson, G. A. Morris. *Anal. Chem.* **2009**, *81*, 4548.
[24] R. E. Joyce, I. J. Day. *J. Magn. Reson.* **2012**, *220*, 1.
[25] R. E. Joyce, I. J. Day. *J. Phys. Chem. C* **2013**, *117*, 17503.
[26] G. Lucena Alcalde, R. E. Joyce, I. J. Day. *Magn. Reson. Chem.* **2014**, *52*, 760.
[27] T. Kremmer, L. Boross, *Gel Chromatography: Theory, Methodology and Applications*, John Wiley and Sons, Chichester, **1979**.
[28] W. W. Yau, J. J. Kirkland, D. D. Bly, *Modern Size Exclusion Chromatography: Practice of Gel Permeation and Gel Filtration Chromatography*, Wiley Interscience, Chichester, **1979**.
[29] J. Z. Hu, R. A. Wind. *J. Magn. Reson.* **2002**, *159*, 92.
[30] S. A. Bradley, J. Paschal, P. Kulanthaivel. *Magn. Reson. Chem.* **2005**, *43*, 31.
[31] D. H. Wu, A. D. Chen, C. S. Johnson. *J. Magn. Reson. A* **1995**, *115*, 260.
[32] M. D. Pelta, G. A. Morris, M. J. Stchedroff, S. J. Hammond. *Magn. Reson. Chem.* **2002**, *40*, S147.
[33] M. Nilsson. *J. Magn. Reson.* **2009**, *200*, 296.
[34] D. M. W. Anderson, J. F. Stoddart. *Anal. Chim. Acta* **1966**, *34*, 401.
[35] D. M. W. Anderson, J. F. Stoddart. *Carbohydr. Res.* **1966**, *4*, 104.
[36] H. Determann, W. Michel. *J. Chromatogr. A* **1966**, *25*, 303.
[37] C. Carrara, S. Caldarelli. *J. Phys. Chem. C* **2012**, *116*, 20030.
[38] H. Weingartner. *Z. Phys. Chem.* **1982**, *132*, 129.
[39] K. Elbayed, B. Dillmann, J. Raya, M. Piotto, F. Engelke. *J. Magn. Reson.* **2005**, *174*, 2.
[40] J.-M. Wieruszeski, G. Montagne, G. Chessari, P. Rousselot-Pailley, G. Lippens. *J. Magn. Reson.* **2001**, *152*, 95.
[41] A. Jerschow, N. Muller. *J. Magn. Reson.* **1997**, *125*, 372.
[42] M. Piotto, M. Bourdonneau, J. Furrer, A. Bianco, J. Raya, K. Elbayed. *J. Magn. Reson.* **2001**, *149*, 114.
[43] E. Kupce, P. A. Keifer, M. Delepierre. *J. Magn. Reson.* **2001**, *148*, 115.
[44] N. Esturau, F. Sanchez-Ferrando, J. A. Gavin, C. Roumestand, M. A. Delsuc, T. Parella. *J. Magn. Reson.* **2001**, *153*, 48.
[45] I. Swan, M. Ried, P. W. A. Howe, M. A. Connell, M. Nilsson, M. A. Moore, G. A. Morris. *J. Magn. Reson.* **2015**, *252*, 120.
[46] I. Bakhmutov. *Concepts Magn. Reson.* **2012**, *40A*, 186.
[47] I. Bertini, C. Luchinat, G. Parigi, E. Ravera, B. Reif, P. Turano. *Proc. Natl. Acad. Sci. U. S. A.* **2011**, *108*, 10396.
[48] I. Bertini, F. Engelke, C. Luchinat, G. Parigi, E. Ravera, C. Rosa, P. Turano. *Phys. Chem. Chem. Phys.* **2012**, *14*, 439.
[49] I. Bertini, C. Luchinat, G. Parigi, E. Ravera. *Acc. Chem. Res.* **2013**, *46*, 2059.
[50] K. E. van Holde, R. L. Baldwin. *J. Phys. Chem.* **1958**, *62*, 734.

Supporting information

Additional supporting information may be found in the online version of this article at the publisher's web site.